Agronomic and Nitrate Leaching Impacts of Pelletized versus Granular Urea

by

Sanjay B. Shah

Dissertation submitted to the Faculty of the

Virginia Polytechnic Institute and State University

in partial fulfillment of the requirements for the degree of

Doctor of Philosophy

in

Biological Systems Engineering

APPROVED:

Mary Leigh Wolfe, Chair	Marcus M. Alley
Jeffrey T. Borggaard	Theo A. Dillaha, III
Saied Mostaghimi	Naraine Persaud

John V. Perumpral, Department Head

August 2, 2000

Blacksburg, Virginia

Keywords: pellet, tension lysimeter, subsurface banding, corn silage yield, mathematical modeling

Agronomic and Nitrate Leaching Impacts of Pelletized versus Granular Urea

by

Sanjay B. Shah

Mary Leigh Wolfe, Chair

Biological Systems Engineering

(ABSTRACT)

Agronomic and water quality impacts of urea particle size were evaluated through field and laboratory experiments and mathematical modeling. In a two-year field study, corn silage yield, corn nitrogen (N) removal, and nitrate-N (NO_3^--N) leaching from urea pellets (1.5 g each) and granules (0.01-0.02 g each) applied at 184 kg-N/ha were compared. A control treatment (no N) and two other N application rates (110 and 258 kg-N/ha) were also included. Urea particle size impact on dissolution rate, dissolved urea movement, mineralization, and NO_3^--N leaching were evaluated in the laboratory. A two-dimensional (2-D) mathematical model was developed to simulate the fate of subsurface-banded urea and its transformation products, ammonium (NH_4^+) and NO_3^-.

With 184 kg-N/ha, corn silage yield was 15% higher ($p = 0.02$) and corn N removal was 19% higher ($p = 0.07$) with pellets than granules in the second year of the field study. In the absence of yield response at 110 kg-N/ha, reason for higher yield at 184 kg-N/ha with pellets was unclear. Greater N removal reduced NO_3^--N leaching potential from pellets compared to granules during the over-winter period. No urea form response to yield or corn N removal was observed in the first year. In 23 of 27 sampling events, granules had higher NO_3^--N concentration in the root zone than pellets, with average NO_3^--N concentrations of 2.6 and 2.2 mg-N/L, respectively. However, statistically, NO_3^--N leaching from the root zone was unaffected by urea form, probably due to high variability within treatments masking the treatment effects. In October 1997, pellets retained 16% more ($p = 0.04$) inorganic-N in the top half of the root zone than granules, due to slower nitrification in pellets as was determined in the mineralization study. Slower NO_3^--N leaching allowed for greater N extraction by

plants. Pellets had lower dissolution, urea hydrolysis, and nitrification rates than granules; however, nitrification inhibition was the dominant mechanism controlling N fate.

The model took into account high substrate concentration effects on N transformations, important for simulating the fate of band-applied N. The model exhibited good mass conservative properties, robustness, and expected moisture and N distribution profiles. Differences in measured field data and model outputs were likely due to uncertainties and errors in measured data and input parameters. Model calibration results indicated that moisture-related parameters greatly affected N fate simulation. Sensitivity analyses indicated the importance of nitrification-related parameters in N simulation, particularly, their possible multiplicative effects. Need for extensive model testing and validation was recognized. The validated 2-D N model could be incorporated into a management model for better management of subsurface-banded granular N. However, the 2-D model is not appropriate for simulating the three dimensional N movement from pellets.

ACKNOWLEDGEMENTS

I would like to express my sincere gratitude to Dr. Mary Leigh Wolfe, Chair of the Dissertation Committee, for providing me with all the professional and personal support to complete my dissertation work, and even more, in helping me develop as a professional. Other members of my Committee were equally supportive. Dr. Mostaghimi provided with substantial advice and funds to purchase the urea pellets. Dr. Jeff Borggaard helped me with my modeling, even on weekends. Dr. Theo Dillaha, Dr. Mark Alley, and Dr. Naraine Persaud helped me with reference letters, advice, logistical, and equipment support, without which, I could not have accomplished what I set out to do. Dr John Perumpral supported many years of my stay over here with a generous Departmental assistantship, an open door, and plenty of advice.

Many faculty members from BSE and Statistics (Dr. M. Reynolds, Dr. K. Hinkelmann, and Dr. C. Coakley) were generous with their advice and support. I owe my gratitude to the staff of BSE, particularly Donnie Wingo, Jan Carr, Jackie Davis, Julie Jordan, Caroll Newell, Dexter Davis, and Leon Alley. My special thanks are due to Jon Wooge and his team in Kentland Farm for help with the field experiment.

I could not have completed my fieldwork without help from my graduate student friends, namely (in no particular order), Jim Kern, Tamie Veith, Tone Nordberg, Sharon Buck, Steve Kirkup, Shuchi and Sanjay Shukla, Erik Lee, Vicky Barone, Byron Petrauskas, Sudha Radhakrishnan, Patcharee Hensirisak, Solos Jivanuwong, Sharla Lovern, Phil O' Regan, Shawn Guyer, Youtong Fu, Mohammad Al-Smadi, Tina Jeoh, Sebastian Zacharais, and many others. My gratitude is also due to Mahadev and Yamuna Sharma, my compatriots in Blacksburg.

My gratitude goes to my mother and father-in-law, both of whom are in Nepal with our families, praying and waiting for our return. And finally, my long-suffering family - wife Banu, son Shashant, and daughter Shivani who allowed me to pursue my dream, always providing the support that was not always deserved. With my dissertation behind me, hopefully, I will be able to fulfill the role of the husband and father that I always wished to be.

TABLE OF CONTENTS

LIST OF FIGURES

LIST OF TABLES

1. INTRODUCTION

1.1. Background

Not too long ago, it had been predicted that the earth could not sustain a human population in excess of 4 billion. Thankfully, those predictions proved to be incorrect; the world population, as of mid-2000 stands at more than 6 billion (U.S. Census Bureau, 2000). Even though there is great disparity in the availability of food, there are no signs that widespread famine is imminent. To feed the increasing world population, even as late as the early decades of the 20^{th} century, people increased cultivated area, an approach that was hampered by the fact that land is finite. Even worse, areas such as wetlands that helped maintain the earth's ecological balance were cultivated with adverse impacts on the environment.

However, at the dawn of the 21^{st} century, humankind has been able to use the fruits of scientific research to meet the demands of the ever-increasing world population for food and fiber. Widespread availability of cheaper and better synthetic fertilizers have fueled the agricultural revolution as have other factors, such as the introduction of high yield varieties. It is estimated that 20 to 25% of the food production is directly attributable to synthetic fertilizers (Harre and White, 1985).

Of all nutrients in fertilizers that are used to supplement the soil's nutrient status, nitrogen (N) is the most heavily applied. In 1995-1996 crop year, world N consumption was 78.7 million MT, 51% more than the combined total for phosphate (P_2O_5) and potash (K_2O), the two most widely used macronutrients after N (FAO, 1997). However, N remains the nutrient that is most frequently deficient (Tisdale et al., 1993) since plants require N in large quantities. In plants, N is not only required for protein synthesis but is also a component of chlorophyll; thus plants contain 1 to 5% N by weight (Tisdale et al., 1993). Additionally, N deficiency results from lower applied-N recovery by the crop which seldom exceeds 70% (Tisdale et al., 1993). Hence, the possibility for significant N losses into the environment from applied-N is real.

Nitrogen fertilizers undergo transformations into plant-available N forms, either as ammonium-N (NH_4^+-N) or nitrate-N (NO_3^--N). Ammonium-N, being held tightly on the negatively-charged surfaces of clay complexes and organic matter (OM), is not readily lost through leaching, except in very sandy soils. By contrast, the highly water-soluble NO_3^--N, which is held rather weakly by the soil and OM, moves freely with soil water and can be lost through leaching readily. Ammonium-N adsorbed on soil and OM can be lost in surface runoff with eroded soil. Eventually, while some of the NH_4^+-N could reach the receiving waters, the remainder would have been converted to NO_3^--N en-route. Inorganic-N contamination, particularly as NO_3^--N, of ground or surface water, has important health and environmental implications.

Nitrate reduces to nitrite (NO_2^-) in the gastrointestinal tract of animals and humans. Nitrite reacts with hemoglobin to reduce the capacity of blood to transport O_2, leading to a condition known as *methemoglobinemia* or blue-baby syndrome which can be fatal in infants. Hence, 10 mg/L NO_3^--N (44 mg/L NO_3^-) is considered the maximum safe level for drinking water (USEPA, 1986). The presence of inorganic-N and inorganic-phosphorus (P) concentrations in excess of 0.3 and 0.001 mg/L, respectively, generally results in eutrophication of surface water bodies (Novotny and Olem, 1994). As ground water aquifers recharge streams, high N concentrations in ground water can result in eutrophication of receiving waters. Apart from deterioration in esthetic quality, eutrophication adversely impacts aquatic life and limits the use of affected water bodies.

In the US, over 97% of the rural population and 40% of the public water supplies use ground water as the primary water source (USGS, 1999). Agricultural chemicals including N are used on 147 million ha in 44 states (USGS, 1999); hence, there is potential for NO_3^--N leaching on a large scale. Ritter et al. (1993) caution that the Coastal Plains are the most vulnerable areas in the US to ground water contamination. In Virginia, in addition to the Coastal Plains, the Valley and Ridge aquifers are the most affected by NO_3^--N contamination from agricultural sources (USGS, 1999).

Compared to conventional tillage (CVT), conservation tillage (CST) yields better surface water quality by reducing soil and chemical losses, with generally comparable crop yields. Even though surface application of fertilizer is widely practiced in CST, it is widely recognized that sub-surface fertilizer application give higher crop yield (Tisdale et al., 1993) and better runoff water quality (Mostaghimi et al., 1991). Given its economic and surface water quality benefits, sub-surface fertilizer application will likely become more popular in CST. However, due to greater percolation in CST, there are concerns of greater leaching of NO_3^--N into ground water when the fertilizer is sub-surface applied (Mostaghimi et al., 1991).

The need to reduce NO_3^--N leaching from corn is particularly important, perhaps the most important cereal planted in CST systems. In 2000, corn has the largest crop acreage in the U.S. (USDA - NASS, 2000). In Virginia, corn was second in acreage, behind hay in 1999 (VASS, 1999). Corn has high N requirements which can exceed 200 kg-N/ha under Virginia conditions (VASS, 1999). During the crop season, due to warm and moist soil conditions, fertilizer N can rapidly transform into NO_3^--N, which, if not removed by the plants, can be lost into the environment.

Hence, there is need to investigate options that can be used to reduce NO_3^--N leaching from sub-surface applied N fertilizer in CST. There is increased emphasis on split N application, especially in soils with high leaching potentials, and site-specific assessment of N requirements based on crop, soil, and environmental conditions (VDCR, 1993; Tisdale et al., 1993). Nitrogen-loss inhibitors (NLIs) which inhibit the conversion of synthetic N to plant-available N forms, have been successful under certain circumstances. However, in addition to the high cost, phytotoxicity and poor efficacy of NLIs under field conditions limit their applicability (Singh et al., 1994). Economic considerations also limit the appeal of slow-release fertilizers, such as sulfur-coated urea (Singh et al., 1994).

There is potential for reducing NO_3^--N leaching by substituting commercial urea granules (1-2 mm diameter, 0.02 g) with larger granules, also known as pellets. Given its high analysis (46% N), urea ($CO(NH_2)$) is a popular N source. Urea pellets, which can weigh up to 3 g, are mainly used in forestry (Singh et al., 1994). By virtue of its large size, and hence lower specific surface area (SSA), a pellet (compared to the same weight of granules) is in contact with a smaller mass of soil. Due to its contact with less soil, a pellet is likely to dissolve and transform into plant-available N forms, primarily NO_3^--N, slower than granules, thus possibly improving N removal by plants by reducing N losses.

Hence, there is a need to evaluate the performance of urea pellets versus granules with respect to crop yield and water quality. There is also a need to understand the mechanisms that impact N transformations and movement from urea pellets versus granules such that N transformations, movement, and N removal can be simulated for both urea forms.

1.2. Objectives

The overall objective of this study was to evaluate the potential impacts of urea granule size on crop yield and nitrate-N leaching from the root zone. The specific objectives were as follow.

1. Evaluate the agronomic and NO_3^--N leaching impacts of subsurface-applied urea pellets versus granules on no-till silage corn.
2. Quantify the rates of dissolution, diffusion, mineralization, and NO_3^--N movement from subsurface-applied urea pellets versus granules.
3. Improve computer-based tools for better management of subsurface-applied urea-N.

2. LITERATURE REVIEW

In this chapter, important N sources are presented, with emphasis on urea, the N source selected for this study. Urea transformations as well as N-loss pathways are discussed, with emphasis on the urea particle size impacts. The quantification and scope of NO_3^--N leaching are briefly discussed. The use of slowly available N sources for improving N removal by plants and reducing N losses are presented. Past studies to evaluate urea pellets with regard to their potential to improve crop yield and N removal by reducing N losses are summarized. Finally, selected N transformation and movement models are discussed.

2.1. Synthetic Fertilizer N Sources

Plants may acquire N either from natural or synthetic sources. Natural sources, such as atmospheric N obtained through N-fixation (by legumes) or animal waste, though important, are not discussed here. There are many synthetic fertilizer N sources varying in N content, state (liquid versus solid), and N form (NO_3^--N versus NH_4^+-N). Sources that are of importance in the U.S. in particular and the world in general are briefly discussed below.

1. Anhydrous ammonia (NH_3)

Anhydrous ammonia is comprised of a mixture of NH_3 in liquid and vapor form. With 82% N, anhydrous NH_3 is the highest analysis N source. Specialized equipment is needed for storage and application of anhydrous NH_3; further, due to its toxic nature, precautions are required. Ammonia is reduced to NH_4^+ by H^+ from the soil water rather rapidly; however, deep application and proper furrow covering are required to reduce NH_3 volatilization (Tisdale et al., 1993).

2. Urea ammonium nitrate (UAN) solution

The aqueous solution of urea and ammonium nitrate is known as UAN solution. Nitrogen content may vary between 28 to 32% N with the lower N content UAN being preferred in colder climates where the dissolved salts may start to precipitate out sooner.

Ease of transportation, application, and compatibility with other chemicals and nutrients combined with a relatively high N analysis have made UAN solutions increasingly popular in the US (Tisdale et al., 1993).

3. Ammonium nitrate (NH_4NO_3)

With 33-34% N, the granular N source, NH_4NO_3 ranks fourth in terms of usage in the US. For topdressing, NH_4NO_3 offers certain advantages as NO_3^--N is readily available to the crops. However, due to storage problems associated with caking and fire hazards, as well as greater N losses due to leaching and denitrification compared to NH_4^+-N sources, its use has declined (Tisdale et al., 1993).

4. Urea ($CO(NH_2)$)

An organic compound, urea has the highest N content (46%) among all solid N sources. Urea's high analysis results in savings in transportation, storage, handling, and application. Further, compared with NH_4NO_3, urea has less tendency to cake and poses no fire hazard. Hence the economics of using urea when combined with lower losses due to denitrification and leaching as compared to NH_4NO_3 make it an attractive alternative to NH_4NO_3.

Other synthetic N sources include potassium nitrate, calcium nitrate, ammonium sulfate, and ammonium phosphate (Tisdale et al., 1993). The decline in use of many N sources could be attributed to their low analyses. However, in niche markets, some of the lesser-used N sources are still important.

2.2. Urea Particle Size Effects on N Transformations

Considering the advantages of urea as an N source, urea was selected as the N source in this study. Between application to the soil and its complete conversion into NO_3^--N, urea undergoes dissolution, hydrolysis, and nitrification. At each transformation stage, applied-N can be lost into the environment through one or more N-loss pathways (fig. 2.1). The rate of transformation and the amount of applied-N lost through a particular N-loss pathway depend on soil and environmental factors as well as the size of the urea particle, i.e., pellet versus granule, and how the urea is applied.

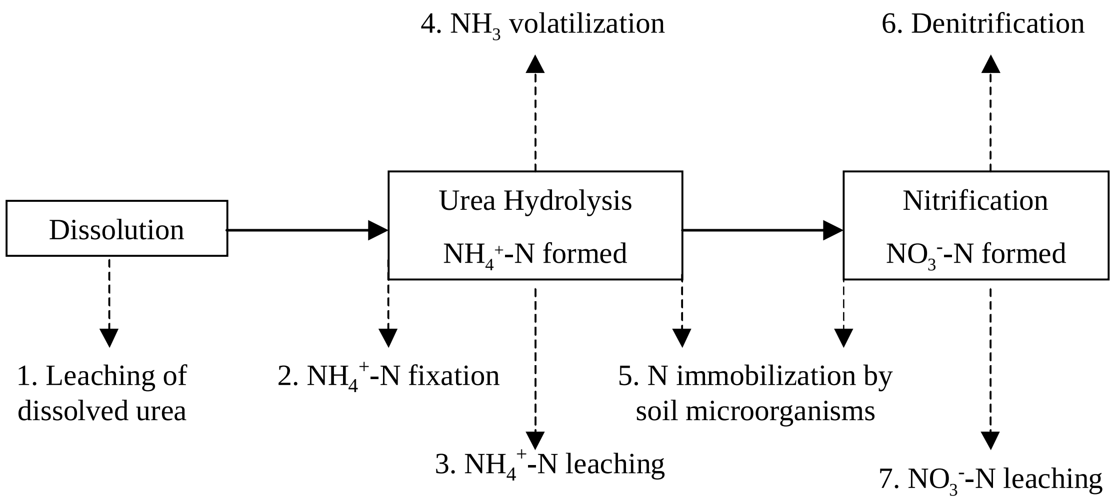

Figure 2.1. Urea transformation stages and N-loss pathways

2.2.1. Dissolution

Description of the dissolution of subsurface-applied urea could not be obtained from published literature. The following account was developed based on urea properties and accepted theories of solute and vapor transport in soil. Urea exhibits hygroscopicity when relative humidity (RH) exceeds 70% (Chao, 1975). Since soil air is close to saturation with water vapor (Hillel, 1971), the subsurface-applied urea particle surface is likely covered with a layer of moisture in a very short period of time. The urea solution thus formed at the urea particle surface diffuses into the surrounding soil; simultaneously, the urea solution exerts an osmotic potential on the surrounding soil causing movement of water vapor towards the urea particle (Marshall et al., 1996), providing continuity to the dissolution process.

Urea particle properties that affect dissolution rate are particle density (PD), specific surface area (SSA, cm^2/g), and particle shape. As particle SSA increases (or particle size decreases), urea will be in contact with a larger soil surface area, and, hence, a larger soil volume, allowing for faster transfer of moisture to urea and transport of dissolved urea into the soil, likely resulting in faster dissolution. Urea particle shape not only affects SSA but also the presence or absence of edges. For example, a tablet-shaped pellet will likely dissolve faster initially (due to edges) than a spherical pellet of the same weight and comparable SSA (G. Sanzoni, personal communication, Blacksburg, Va., 16 September, 1997).

However, it is likely that SSA will have the most significant impact on dissolution due to the large difference in SSA between pellets and granules. For example, while the SSA of granules is 4.8 times higher than 1-g pellets, PD of granules is only 5.4% lower than 1-g pellets (Singh et al., 1994). Surface-applied urea powder dissolved within 2 min. (Sadeghi et al., 1989) and within 10 min. (Singh and Nye, 1984), while a 1-g pellet required more than 20 h to dissolve in soil at field capacity (Wetselaar, 1985). Given the differences in SSA, it is likely that dissolution of pellets (1.5 g) will take much longer than granules. However, it is unclear if the dissolution trend of the urea particle is affected by the particle size. The interactions of soil moisture content with urea particle size and soil particle size distribution with urea particle size on dissolution rate are unknown. The possibility of such higher level interactions also cannot be discounted.

Movement of the dissolved urea is another important aspect related to dissolution and may be treated as part of the dissolution process. The mechanism of dissolved urea movement is not clearly understood. Singh and Nye (1984) suggested that diffusion was the sole transport mechanism for surface-applied urea powder. Based on observations obtained with subsurface-applied sodium chloride, Scotter and Raats (1970) suggested that mass flow was responsible for solute movement in soil. Hence, it is unclear whether molecular diffusion or mass flow is the dominant transport mechanism in subsurface-applied urea. It is also likely that soil moisture content and soil texture may affect the mechanism of dissolved urea movement.

Urease can only hydrolyze dissolved urea. Given the toxic effect of high urea concentration on urease (Wetselaar, 1985), urea dissolution influences the subsequent transformation processes. Hence, subsequent transformation processes and N-losses will more likely be affected in pellets due to their longer dissolution periods than granules.

To simulate dissolution, it is necessary to determine the rate controlling mechanism. In liquid media, Snoeyink and Jenkins (1980) suggested that dissolution was controlled by the rate of diffusion of the species away from the solid. Scotter and Raats (1970) suggested that when NaCl was subsurface-applied to soil, diffusive movement of moisture to the salt was the rate controlling mechanism. Given the soil tortuosity effects and vapor being the dominant constituent of moisture movement, diffusive moisture movement could be the rate controlling mechanism.

Simulation of moisture movement from the surrounding soil to the subsurface-applied solute particle is affected by osmotic and capillary tensions. Osmotic tension is due to the presence of dissolved solute and is continuously changing in time and space. Assuming uniform moisture distribution in the soil, initial moisture movement in vapor form is induced purely by osmotic tension. However, increase in moisture content close to the solute particle is likely to result in capillary tension with a moisture gradient that is opposite in direction to the osmotic tension. Hence, over the entire duration of dissolution, the direction of moisture movement will be affected by both the osmotic and capillary tensions. However, it is difficult to determine total moisture gradient at different points in time and space to estimate moisture fluxes at intermediate dissolution stages.

2.2.2. Urea Hydrolysis

Dissolved urea ($CO(NH_2)_2$) is hydrolyzed by the urease enzyme into ammoniacal-N forms. A simplified urea hydrolysis reaction is (Bremner and Mulvaney, 1978):

$$CO(NH_2)_2 + H_2O \xrightarrow{\text{Urease}} H_2CO_3 + 2NH_3 \qquad [2.1a]$$

$$H^+ + NH_3 \rightarrow NH_4^+ \qquad [2.1b]$$

Urease is present in abundance in the root zone (Tisdale et al., 1993). Urease activity is temperature-dependent with activity increasing in the 10 to 40°C range (Bremner and Mulvaney, 1978). Urease activity seems to be unaffected at tensions less than 30 bars (Singh et al., 1994); however, at lower tensions, urea concentrations could affect urease activity. Bremner and Mulvaney (1978), citing published research, reported that urease activity was unaffected at urea concentrations up to 4 348 µg-urea/g-soil. However, Wetselaar (1985) reported that irrespective of the soil type, urea hydrolysis occurred slowly at one-quarter saturation with no hydrolysis occurring at one-half saturation. Even though Bremner and Mulvaney (1978) and Wetselaar (1985) reported urea concentrations in different units, it is likely that urea concentrations used by Wetselaar (1985) were significantly higher since the researcher worked with urea pellets. Other soil factors such as pH and oxygen do not seem to affect urease activity (Bremner and Mulvaney, 1978).

The rate of reduction of NH_3 to NH_4^+ (Eq. [2.1b]) depends on moisture and pH conditions. Under high moisture conditions, presence of large amounts of H^+ (from water) allows for rapid reduction of NH_3 to NH_4^+. Low pH conditions results in greater H^+ availability from other sources in addition to water thus allowing for rapid formation of NH_4^+. Hence, under warm and moist conditions, urea is completely hydrolyzed into NH_4^+ in several days (Tisdale et al., 1993). However, under dry and high pH conditions, substantial NH_3 can be volatilized if urea-N is surface-applied.

Singh and Beauchamp (1987) reported that urea hydrolysis rate decreased with increasing pellet size (decreasing SSA) in a laboratory experiment. Malhi and Nyborg (1979) also reported that compared to granules, pellets (0.21 g) had a 12% lower urea hydrolysis rate after 114 h. Due to slower dissolution of urea pellets compared with granules, urea concentration will be higher close to the site of application in pellets. Since high localized urea concentrations associated with urea pellets adversely affects the urease enzyme, urea hydrolysis rate will be lower in pellets than granules (Wetselaar, 1985). When urea undergoes hydrolysis, OH^- ions are produced, resulting in a rise in pH. Hence, localized pH values will likely be greater in pellets than granules. Since high pH and the concomitant high NH_3 concentration adversely affect urease activity, urea hydrolysis is further retarded.

2.2.3. Nitrification

Under aerobic conditions, the autotrophic bacterium *Nitrosomonas* oxidizes NH_4^+ into NO_2^-; two other genera, *Nitrosolobus* and *Nitrosospira,* are also active NH_4^+ oxidizers (Schmidt and Belser, 1982). Again under aerobic conditions, the autotrophic bacterium *Nitrobacter* oxidizes NO_2^- to NO_3^-. The two-stage nitrification can be shown as (Tisdale et al., 1993):

$$2NH_4^+ + 3O_2 \xrightarrow[\text{Nitrosomonas}]{} 2NO_2^- + 2H_2O + 4H^+ \qquad [2.2a]$$

$$2NO_2^- + O_2 \xrightarrow[\text{Nitrobacter}]{} 2NO_3^- \qquad [2.2b]$$

Since the conversion of NO_2^- to NO_3^- is faster than NH_4^+ to NO_2^-, generally there is no accumulation of NO_2^- which is toxic to plant roots (Tisdale et al., 1993). Factors that affect nitrification include population of nitrifying organisms, NH_4^+ supply, soil pH, soil temperature, soil aeration, and soil moisture content (Tisdale et al., 1993).

Under similar environmental conditions, soils differ in their ability to nitrify NH_4^+ due to differing populations of nitrifying organisms (Tisdale et al., 1993). Quantification of a population of nitrifiers in a given soil sample is very difficult (Schmidt and Belser, 1982). Further, establishing a relationship between the nitrifying population and nitrification rate is complicated because neither the diversity of nitrifiers within a given population nor the contribution of each genus to the nitrification process is known (Schmidt and Belser, 1982).

Since NH_4^+ is the substrate for nitrification, its availability is paramount to nitrification. However, high NH_4^+-N concentrations (>3000 μg/g-soil) adversely affect the nitrifier population, retarding nitrification (Wetselaar, 1985). Due to the greater localization of NH_4^+ in pellets than granules, nitrification could be delayed in pellets. The likelihood of encountering such high NH_4^+-N concentrations is more likely in pellets than granules.

Nitrification occurs in a pH range of 4.5 to 10, with the optimum pH being 8.5 (Tisdale et al., 1993). Increase in pH due to urea hydrolysis not only affects urea hydrolysis but also nitrification, with reduction in nitrification rate being stronger in pellets than granules. Higher pH results in higher NH_3 concentration in pellets compared to granules leading to a reduction in the nitrification rate due to the toxic effect of NH_3 on nitrifiers.

Singh and Beauchamp (1987) observed that nitrification rate decreased with increasing urea granule size. In 35 d, at 15°C, while 89% of point-applied urea granules (0.02 g) had been nitrified, only 16% of 3-g pellets had been nitrified. The 1-g and 2-g pellets had nitrification rates between granules and 3-g pellets (Singh and Beauchamp, 1987). Comparison among the various treatments was probably affected to some degree by the use of different urea concentrations, for example, 84 and 624 μg-N/g-soil for granules and 3-g pellets, respectively (Singh and Beauchamp, 1987). Based on a review of published research, Singh et al. (1994) reported that nitrification rate decreased with increasing urea particle size. However, factors such as the method of application (e.g., mixing in soil versus band application) should be taken into account while comparing nitrification rates of pellets and granules.

2.3. Nitrogen-loss Pathways as Affected by Urea Particle Size

The various N-loss pathways that affect urea and its transformation products, NH_4^+ and NO_3^-, are shown in figure 2.1. Potential urea particle size impacts on the N-loss pathways are discussed below.

1. Leaching of dissolved urea

In coarse-textured, flooded soils, urea leaching from pellets can be a problem (Singh et al., 1994) though that is unlikely under non-flooded conditions. Since granules are spread over a larger area, they will come in contact with more percolating water than pellets resulting in possibly higher urea leaching from granules. However, factors such as moisture conditions and time elapsed between fertilizer application and precipitation will also affect urea leaching from pellets versus granules.

2. Ammonium fixation

In soils containing hydroxy interlayered vermiculite, vermiculite, and mica clay minerals, NH_4^+ ions can be trapped in the clay interlayers (Tisdale et al., 1993). Ammonium fixation is greater under dry soil conditions. Since some of the fixed NH_4^+ becomes available for plant removal, NH_4^+ fixation represents only a partial loss. Ammonium fixation seems to decrease with increasing particle size due to reduced soil contact (Singh et al., 1994).

3. Ammonium leaching

Due to its affinity to the negatively-charged soil complex, the positively-charged NH_4^+ tends to remain adsorbed to soil particles with only a small fraction present in soil solution. Hence, NH_4^+ leaching concerns are slight except in sandy soils with low cation exchange capacities (CEC) (Singh et al., 1994).

4. Ammonia volatilization

Under high pH conditions in the soil, more of the ammoniacal-N will be present as NH_3. When urea applied in furrows is not properly covered with soil, there is risk of NH_3 loss through volatilization, especially under dry conditions. Hence, given the possibility of higher pH in pellets, there is risk of greater NH_3 availability and hence, NH_3 volatilization. However, NH_3 volatilization decreases with increasing pellet size (Nommik, 1976).

5. Nitrogen immobilization by organic matter

Inorganic-N as NH_4^+ or NO_3^- is converted to the organic-N form by soil microbes when the soil carbon (C): N ratio is more than 8:1. Hence, when the soil C:N ratio is higher than 8:1, applied-N is immobilized by microbes resulting in inorganic-N deficiency. However, N immobilization process is reversible and the immobilized N later becomes available as mineral N (Tisdale et al., 1993). Singh et al. (1994) suggested that N immobilization decreased with increasing particle size due to reduced soil contact.

6. Denitrification

High soil moisture content can result in low O_2 concentrations. When O_2 concentrations fall below 10%, facultative bacteria can reduce NO_3^- and NO_2^- to gaseous forms such as N_2 and N_2O (Tisdale et al., 1993); oxygen obtained through the reduction reaction is used for metabolism by the bacteria. However, for denitrification to occur, there has to be an abundant supply of decomposable organic matter (OM), in addition to suitable temperature and pH conditions (Tisdale et al., 1993). Inorganic C obtained through breakdown of OM is essential for biomass synthesis by the bacteria. As compared to granules, Singh et al. (1994) suggested that reduced nitrification resulted in lower over-winter denitrification and N immobilization in urea pellets applied in late-fall to winter and spring crops (Singh et al., 1994).

7. Nitrate leaching

Since the negatively-charged NO_3^- ion is held weakly by the soil complex and NO_3^--N is highly water-soluble, most of the NO_3^- is in soil solution. When there is sufficient moisture available in the soil profile to permit percolation, NO_3^--N leaching will occur. Nitrate leaching is an important N-loss pathway, especially in humid areas where as much as nearly half of the applied-N can be lost through leaching (Tisdale et al., 1993). Singh et al. (1994) suggested that compared to granules, late-fall pellet application was likely to reduce NO_3^--N leaching. No field studies that compared urea particle size impact on NO_3^--N leaching could be found in the published literature.

2.4. Quantification of Nitrate Leaching

Given the potential adverse health and environmental implications of NO_3^--N leaching from applied-N, considerable attention has been given to develop techniques and tools to quantify NO_3^--N leaching into ground water. Comparison of NO_3^--N leaching between two or more treatments can be achieved using water or soil samples. Both methods for quantifying NO_3^--N leaching are briefly discussed below.

1. Water samples

To trace the fate of pollutants, it is necessary to take observations at multiple points in time. Such observations also allow for comparisons among treatments at a point in time. Soil cores can be obtained at certain intervals in time and analyzed for NO_3^--N; however, the process is labor intensive, and more importantly, affects the hydrologic integrity of the plots. Sampling wells have been used extensively for monitoring NO_3^--N concentration; however, such data represent a cumulative effect. More importantly, sampling wells cannot be used in the vadose zone, which remains largely unsaturated.

Comparison of NO_3^--N in leachate among N fertilizer treatments can be made using tension lysimeters (TLs) or ceramic cup samplers. Tension lysimeters can be used to collect leachate samples under both saturated conditions and within a certain range of unsaturated conditions at any desired depth in the vadose zone. Since TLs can be used to collect leachate samples of percolating water, the “first flush” effect of a storm event on a fertilizer treatment can be better understood.

There is some debate regarding the suitability of TLs for collecting leachate samples for NO_3^--N analysis. Ballestero et al. (1991) reported that TLs changed the chemical composition of samples rendering the samples unrepresentative of the soil solution. However, Poss et al. (1995) demonstrated that TLs were reliable and accurate in monitoring NO_3^--N leaching in a soil that was fairly homogeneous, containing a moderate amount of clay. While there are problems with sampling cationic pollutants that can adsorb to the ceramic cup, an anion like NO_3^--N poses no such problems as it neither adsorbs nor reacts with the ceramic cup (Angle et al., 1990). Angle et al. (1990) reported that TLs had been used in hundreds of studies involving NO_3^--N analysis of leachate samples. Hence, TLs can be used to compare treatments with respect to their NO_3^--N concentrations at any point in time. However, leachate NO_3^--N concentrations obtained using TLs may not be suitable for estimating NO_3^--N loadings since TLs cannot sample the entire range of soil water pressures.

2. Soil samples

Nitrate-N loadings are widely estimated using soil cores (Ritter et al., 1993; Hubbard et al., 1991; Kanwar et al., 1985). Soil cores are obtained from the required depths in sufficient number to account for soil variability and analyzed for NO_3^--N. If the percolation rate below the root zone or any depth of interest is known, percolation volume multiplied by the NO_3^--N concentration yields the NO_3^--N loading. However, repeated soil sampling can affect the hydrologic integrity of the plots.

Inorganic-N amounts in different layers of the root zone or the entire root zone can be used as an indicator to compare treatment impact on NO_3^--N leaching from the root zone or within the root zone. Even though such a method allows for comparison of inorganic-N amounts among treatments, it cannot be used to estimate NO_3^--N loading.

2.5. Past Studies on Nitrate Leaching

Given its health and environmental impacts, NO_3^--N leaching has been studied in a wide range of soil and environmental conditions, in both conservation and conventional tillage systems. In Kansas, Jones and Schwab (1993) reported that more than 25% of drinking water wells in rural areas (mainly with fine-textured soil) contained NO_3^--N concentrations greater than 10 mg/L, the maximum safe drinking water standard. Based on an N balance of a brome meadow, of the 224 kg-N/ha applied as NH_4NO_3, nearly 44% was available for leaching into ground water (Jones and Schwab, 1993).

Ritter et al. (1993) evaluated the impact of split-N application (168 kg-N/ha) on corn grown on loamy sand, both under conventional- and no-till systems in Delaware.

The method of N application was not mentioned. Greater NO_3^--N leaching losses were observed during fall and winter with NO_3^--N concentrations generally exceeding 10 mg-N/L. Nitrate loadings were 57.1 to 94.0 and 55.0 to 78.8 kg/ha-yr from conventional- and no-till plots, respectively (Ritter et al., 1993).

In the Georgia Coastal Plain, Hubbard et al. (1991) applied 369 kg-N/ha to a sweet corn-pearl millet-sweet corn rotation grown on loamy sand over a 15-month period. Neither the N application method nor tillage system was mentioned. Most NO_3^--N from the upper 30-cm of the root zone was leached out in 1.5 months, with irrigation plus precipitation exceeding 20 cm. During the corn season, NO_3^--N concentrations in shallow ground water (0.9-1.8 m) ranged between 11 and 19 mg/L. Even in the deeper well (6 m), despite the presence of restrictive horizons, an average of 10.6 mg/L of NO_3^--N was observed. Hubbard et al. (1991) agreed that concerns about the long-term effects of NO_3^--N leaching were well founded.

Menelik et al. (1990) evaluated the impact of different N application rates and N sources (sewage sludge versus inorganic-N) on a corn-wheat-soybean rotation on sandy loam and continuous corn on silt loam in Virginia. Also evaluated were the impact of no-till versus conventional tillage. Irrespective of treatment differences, N leaching increased with greater residual N in the soil profile at the end of the growing season. The finer-textured soil stored more residual N without incurring significant N leaching losses. While the fine-textured soil lost little N through leaching during the growing season, the coarse-textured soil incurred N leaching losses even during the growing season. Despite higher moisture contents, N leaching was lower in the no-till plots than the conventional tillage plots due to higher yield and N removal from the no-till plots (Menelik et al., 1990).

Kanwar et al. (1985) evaluated the impact of conventional tillage versus no-till on NO_3^--N leaching on bare plots with loam soil in Iowa. Fertilizer-N, as KNO_3 solution at 150 kg-N/ha, was surface-applied to no-till plots; the same amount was surface-applied in the same N form either before or after tillage to the plots under conventional tillage. Simulated rainfall was applied. In both, the 30- and 150-cm soil profiles, the no-till plots retained more NO_3^--N than the plots under conventional tillage. With 12.7 cm rainfall, NO_3^--N loadings from the no-till and conventional tillage plots were 29 and 122 kg-N/ha, respectively (Kanwar et al., 1985). Even though initial soil moisture contents were not reported, 122 kg-N/ha leaching from a 150-cm soil profile with 12.7 cm of rainfall, applied at 2.3 cm/h, 18 h after N application seemed excessively high.

Nitrate-N leaching remains a concern under both conventional and conservation tillage under surplus moisture conditions for a wide range of soil textures in large areas of the US. No studies that compared surface N application with subsurface-N application could be obtained. However, there are concerns that subsurface N application, while improving surface water quality in conservation tillage, have the potential to cause greater NO_3^--N leaching (Mostaghimi et al., 1991). Given the higher soil moisture status and the greater presence of macropores under conservation tillage, the possibility of greater NO_3^--N leaching remains a concern whether N is applied on the surface or beneath the surface.

Given the magnitude of NO_3^--N leaching and its potential adverse impacts, there is greater emphasis on better estimation of N removal by plants by taking into account plant, soil, and environmental factors. In regions with high rainfall and coarse-textured soils, split application of N is emphasized so that NO_3^--N leaching can be reduced and N removal by plants can be improved (VDCR, 1993). Some innovative methods that could be used to reduce NO_3^--N leaching losses, mainly by increasing plant N removal are discussed in the following section.

2.6. Slowly Available N Sources

Plant N removal can be improved by employing management practices discussed above, or, using N sources that release small amounts of plant-available N over an extended period of time to more-or-less match crop N requirement. Such N sources not only have the potential to reduce N losses into the environment but can also eliminate the need for repeated N application or salt injury associated with high N application rates of some N sources close to the seed. Slow N availability can be induced through passive or active inhibition.

1. Passive inhibition

Plant-N availability is inhibited by reducing or delaying the availability of synthetic N by using low solubility N compounds or a barrier; such N sources are also known as slow release N fertilizers. A low solubility N source has only a fraction of its N in cold water-soluble form which transforms into plant-available N form rapidly. The remainder of the N (hot water soluble and hot water insoluble) is released over a longer period of time through biochemical reactions. Examples of such N sources include ureaform (38% N) and isobutylidene diurea (IBDU, 30% N) (Tisdale et al., 1993).

Availability of an N source may be passively delayed by using a less soluble barrier around the N particle, such as sulfur (S). Sulfur-coated urea (SCU) consists of a urea particle coated with S. Urea from an SCU particle will be released when the S layer is oxidized by soil microbes. Urea release rates can be controlled, in theory, by varying the S layer thickness. Use of slow release N fertilizers is limited due to the difficulty in synchronizing N release and removal by plants, and more importantly due to the high cost of such N sources (Singh et al., 1994).

2. Active inhibition

In some N sources, formation of plant-available N is retarded chemically by reducing either the urea hydrolysis rate (urease inhibition) or the nitrification rate (nitrifier inhibition). Urease inhibitors (UIs) inhibit the activity of the urease enzyme thus delaying conversion of urea to NH_4^+ (Tisdale et al., 1993). Even though effective UIs such as phenylphosphorodiamidate (PPD) (Tisdale et al., 1993) exist, urease inhibition does not usually result in yield responses (Scharf and Alley, 1988). Tisdale et al. (1993) preferred direct urease inhibition using urea pellets or point placement to UIs.

Nitrification inhibitors (NIs) temporarily inhibit *Nitrosomonas* activity to prevent conversion of NH_4^+ to NO_3^-; ideally, NIs should not interfere with *Nitrobacter* activity or else NO_2^- buildup and toxicity can result (Tisdale et al., 1993). Nitrapyrin and diacyandiamide (DCD) are regarded as effective NIs. Use of nitrapyrin with solid urea is limited due to loss in inhibition effectiveness during processing, storage, and handling (Singh et al., 1994). Based on review of published literature, nitrapyrin seems to be effective under water surplus (>30.5 cm/yr) or under irrigated conditions (Scharf and Alley, 1988). As NI, DCD seems to be preferable to nitrapyrin; effectiveness of DCD can be further increased by incorporating it with urea pellets (Singh and Beauchamp, 1988). Effectiveness of NIs is affected by factors such as soil texture, pH, and organic matter content (Scharf and Alley, 1988). In addition to effectiveness and phytotoxicity, high cost of NIs limits their usage (Singh et al., 1994).

2.6. Agronomic Impacts of N Pellets Versus Granules - Past Studies

Due to the limited effectiveness and high cost associated with UIs and NIs, some researchers evaluated the urea pellet with regard to its ability to reduce N losses and improve crop yield and N removal compared with granules. However, no information was available on environmental impacts of urea pellets and granules. Studies on the agronomic impact of urea pellets and granules are summarized below.

Winter wheat (Singh and Beauchamp, 1988): Guelph, Ontario, Canada

During 1983-85, crop yield and crop N removal from urea granules (0.01 g) and urea pellets (1-, 2-, and 3-g) applied at different times to winter wheat were compared. While both granules and pellets were applied at planting, additional treatments involved the application of pellets 1 mo. after planting and only granules in spring. Also, a nitrification inhibitor, diacyandiamide (DCD) was applied to 2-g pellets as a separate treatment. Hence, the discussion below is limited to fertilizer treatments (80 kg-N/ha) without DCD, applied at planting only. While granules were incorporated, pellets were applied mid-way between rows at 8 cm depth.

During 1983-84, while the grain yield values were not significantly different between granules and 1-g pellets, the 2- and 3-g pellets significantly outperformed granules and 1-g pellets at α equal to 0.05. Crop removal of applied-N followed the same pattern with wheat fertilized with the 2- and 3-g pellets removing 6 and 9% more N than wheat fertilized with 1-g pellets and granules, respectively. The superior performance of the larger pellets was attributed to lower N losses during winter. In 1984-85, while grain yields were not significantly different between granules and 2-g pellets (other pellets were not used), pellets removed 8% more applied-N than granules. Higher applied-N removal in the pellet treatment was attributed to higher-than-normal precipitation (as rainfall) and temperatures resulting in possibly greater nitrification and more N losses from granules. Greater N losses from granules did not significantly impact grain yield. Yield comparisons between granules and pellets were confounded since granules were not subsurface-banded. Nitrification in surface-banded granules could be lower than surface broadcast or incorporated granules.

Spring barley (Nyborg and Malhi, 1992): Edmonton, Alberta, Canada

During 1980-82, granules (0.01 and 0.1 g) and pellets (0.62 and 2.5 g) were applied at 56 kg-N/ha in fall or spring (granules were also applied in spring) in a total of six experiments. Granules were either mixed (0.01 g at 4 and 12 cm) or banded (0.1 g at 4 cm); 0.62- and 2.5-g pellets were subsurface applied in 22.5×22.5 cm (4 cm depth) and 45×45 cm (4 and 15 cm depth) grids, respectively. Grain yield and N removal comparisons for only those treatments that were applied at the same time are discussed.

In 1980-81, 2.5-g pellets applied at 15 cm produced the greatest grain yield and N removal of all treatments. Averaged over two experiments, grain yield from the 0.01-g granules (mixed) was inferior to the other treatments ($\alpha = 0.05$) while the 0.1-g granules (banded) was inferior only to the 2.5-g pellet applied at 15 cm; the pellet treatments were not significantly different from each other. Nitrogen removal from 0.01-g granule and 2.5-g pellet (15-cm depth) treatments were the lowest and highest, respectively; the remaining three treatments were not significantly different.

In 1981-82, averaged over three experiments, neither grain yields nor N removal values were significantly different ($\alpha = 0.05$) for any of the treatments. While the 2.5-g pellet and 0.1-g granules applied at 15 cm had slightly higher yields and N removal values, the other treatments had comparable values; 0.62-g pellets were not used. Again in 1981-82, in one experiment, 0.01-g granules (mixed 12 cm deep) and 2.5-g pellets (45×45 cm grid, 15-cm depth) were applied 2 weeks before or at sowing (in spring); 0.62-g pellets (22.5×22.55 cm grid, 15-cm depth) were applied only at sowing. While the time of application did not affect grain yield or N removal, granules performed better than both pellet sizes in grain yield. In terms of N removal, granules (before sowing), 2.5-g pellets (before sowing), and 0.62-g pellets were not different. In spring, poor performance of pellets was attributed to slow diffusion of N to plant roots.

Nyborg and Malhi (1992) concluded that effectiveness of fall-applied N was greater with 2.5-g pellets applied at 15-cm depth. Higher grain yield and N removal were attributed to reduced nitrification resulting in decreased denitrification and possibly less immobilization of applied-N. As in the case of the winter wheat study, direct comparison between 0.01-g granules and pellets could not be made since granules were mixed with soil while the pellets were banded (the inter-row and intra-row distances were equal).

Corn (Zhang, 1990): Guelph, Ontario, Canada

Urea prills (0.000 2 g) were point-banded (applied in subsurface pockets to simulate pellets) to no-till corn (on one side of the seed) at 50, 100, 150, and 200 kg-N/ha at distances of 5, 10, and 15-cm spacings. A separate treatment included point banding on both sides (5 cm) at 200 kg-N/ha. Urea prills were also subsurface-banded at 50, 100, 150, and 200 kg-N/ha 5 cm from the seed. Surface broadcast to no-till and broadcast-mixing to conventional tillage were other treatments.

Corn grain yields with point-banded (simulated pellet) and banded treatments were not compared directly. At 5-cm spacing and 200 kg-N/ha, point-banding resulted in zero corn yield while at 150 kg-N/ha, yield was significantly lower than at 10- and 15-cm spacing (Zhang, 1990). High urea concentrations due to point-banding at 150 and 200 kg-N/ha application rates adversely affected crop growth (Zhang, 1990).

The agronomic impacts of urea pellets versus prills were investigated on flooded rice in India and the Philippines (Savant et al., 1992). Urea pellets outperformed prills in yield in both studies; however, the reasons for the superior performance of pellets were not discussed.

Summary

Studies by Singh and Beauchamp (1988) and Nyborg and Malhi (1992) focused on reducing over-winter N losses from fall-applied N. However, in the southeastern US, where rainfall distribution is substantial during the summer crop season, NO_3^--N leaching losses are a concern throughout the year (Hubbard et al., 1991). Even in drier regions where irrigation is used to supplement rainfall, there are concerns about NO_3^--N leaching. Under such conditions, the potential to improve crop yield and N removal by substituting urea granules with pellets to reduce N losses exists. The use of pellets could result in direct reduction in NO_3^--N leaching by keeping the applied-N longer in the less-mobile NH_4^+-N form. Also, indirect reduction in NO_3^--N leaching could be achieved by ensuring greater N removal by the crop, leaving less inorganic-N in the soil for leaching during the winter months.

2.7. Modeling Nitrogen Fate in the Soil

Fate of applied-N is governed by a combination of soil, crop, and environmental parameters. Hence, to maximize plant N removal and minimize N losses into the environment, mathematical models are utilized to make management decisions regarding the form, amount, and timing of N application. Some N management models are briefly discussed below.

1. NFLUX

The model NFLUX is a one-dimensional, field scale model that simulates the fate of urea, NH_4^+, and NO_3^- when N is surface-applied (Wagenet, 1981). Urea hydrolysis, nitrification, denitrification, NH_3 volatilization, and plant N removal are modeled; however, transformation of organic-N is not modeled (Wagenet, 1981). Moisture flux is modeled using the Richards' equation while N fate is modeled using the convective-dispersive equation (CDE) (Wagenet, 1981).

2. CREAMS (Chemicals, Runoff, and Erosion from Agricultural Management Systems)

The model CREAMS is a one-dimensional, field scale management model which simulates hydrology, erosion, and chemistry, including N fate (Knisel, 1980). Nitrogen processes that are simulated include mineralization, denitrification, and plant N removal. The model considers both inorganic and organic-N forms when N is surface-applied. Greater reliance on empirical coefficients rather than physically-based parameters to model N-loss pathways affects the ability to simulate N fate accurately under a wide range of conditions.

3. DAISY

The DAISY model is a one-dimensional, field scale model that simulates N fate of both organic and inorganic-N pools, taking into account mineralization, denitrification, and plant N removal using the convective-dispersive equation (CDE) (Hansen et al., 1990). Given the rapidity of urea hydrolysis, the model neglects urea hydrolysis. Moisture movement is modeled using the Richards' equation (Hansen et al., 1990).

4. OMNI (Organic Matter/NItrogen)

The one-dimensional (1-D) model, OMNI was developed as a component sub-model of the Root Zone Water Quality Model (RZWQM) (Shaffer et al., 1992). The model takes into account the interconnectedness of the C and N cycles, simulating both organic and inorganic-N. Processes simulated include urea hydrolysis, nitrification, immobilization by organic matter, denitrification, and NH_3 volatilization (Shaffer et al., 1992).

5. DRAINMOD-N

The quasi two-dimensional model DRAINMOD-N uses the hydrology component of DRAINMOD to simulate N fate in shallow water table soils with artificial drainage (Breve et al., 1997). Nitrogen processes simulated include mineralization, denitrification, and plant removal. In the unsaturated zone, N fate is simulated in the vertical direction while in the saturated zone N fate is simulated in vertical and lateral directions using the CDE (Breve et al., 1997). The model simulates fertilizer dissolution using a zero-order function based on a threshold moisture content value (Breve et al., 1997).

6. Two-dimensional finite element model for N (Kaluarachchi and Parker, 1988)

Kaluarachchi and Parker (1988) proposed a 2-D finite element model for N (NH_4^+ and NO_3^-) transformation and transport under unsaturated conditions. The model uses Richards' equation and CDE to simulate moisture redistribution and N fate. The model does not simulate the fate of urea. Compared to the analytic solution, the model overpredicted solute concentrations and showed excessive apparent dispersion with one solute specie, surface-applied in a 2-D domain (Kaluarachchi and Parker, 1988). There is no information on the application of the model for simulating subsurface band-applied N.

A majority of the above models are intended for use in a one-dimensional situation and are suitable for simulating the fate of broadcast or incorporated N. While undergoing transformations to plant-available forms, subsurface-banded fertilizer-N moves laterally and vertically with respect to the band. Consequently, crop N removal and N leaching losses from subsurface-banded N are likely to differ from broadcast application or incorporation. Given the two-directional movement of N applied in bands, compared to a 1-D N model, a 2-D model could be expected to simulate N fate from subsurface-banded N more accurately, thereby, improving N management of banded-N. Even with banded pellets, a 2-D model could be expected to simulate N fate better than 1-D models even though N movement from pellets is likely to be three-dimensional.

Further, compared with broadcast or incorporated N application, subsurface-banding is likely to result in higher localized urea and NH_4^+ concentrations. Given that high urea and NH_4^+ concentrations inhibit urease and nitrifier activities, respectively (Wetselaar, 1985), selecting the reaction order (e.g., first order versus zero order) based on substrate concentration may be more appropriate than using a reaction order for all values of substrate concentration. It is unclear if any currently used model considers both urea and NH_4^+ concentrations in selecting reaction orders. Hence, for banded-N, a model that selects the reaction order (for both urea and NH_4^+ transformation) based on substrate concentration is likely to simulate N fate more accurately compared with the current models.

With the exception of DRAINMOD-N, none of the N models discussed above simulate the dissolution process prior to the initiation of the transformation processes. Even DRAINMOD-N does not account for fertilizer particle size effects on N transformation. Given that a 1.5-g urea pellet may take many hours to dissolve, it is likely that dissolution rate may affect both urea hydrolysis and nitrification, at least in the initial stage. Hence, a model that accounts for dissolution rate of the urea particle based on the SSA of the particle can be said to represent the physical process more accurately.

2.8. Rationale for a New Nitrogen Model

From the preceding discussion it is clear that currently available N models, including the 2-D models (Kaluarachchi and Parker, 1988; Breve et al., 1997), are not completely suited to simulate the fate of subsurface-banded urea-N. Modifying a current N model to simulate the fate of banded-N is difficult not only because of problems in understanding the numerical code but also because permission required from its authors if the model code is not available in the public domain. Hence, it may be more appropriate to create a model to simulate the fate of subusrface-banded urea-N with respect to plant N removal and NO_3^- leaching. Apart from being physically-based, such a model should have the following attributes.

2.8.1. Moisture sub-model (1-D)

Solute transport and transformation in porous media is driven by moisture flux. Hence, a robust moisture sub-model for simulating moisture movement in the soil is required. For application at the field scale, it is adequate for the moisture sub-model to simulate moisture movement in one direction. Even though simpler methods, such as the tipping bucket method can be used to simulate moisture redistribution, the Richards' equation (Richards, 1931) has been widely used in simulating moisture redistribution (Skaggs and Khaleel, 1982).

Apart from being physically-based, the Richards' equation can be readily discretized in time and space; the resulting algebraic equations can be solved to calculate moisture content or pressure head values at any time and at any point in space in the model domain. The Richards' equation can be discretized using either the simpler finite difference (FD) method or the more complex finite element (FE) method. While the FE is more suited to complex flow geometry associated with irregular modeling domains and/or multi-directional flows, FD schemes generally give better mass balance (Celia et al, 1990), when the flow regime is simpler. Hence, for a rectangular or square modeling domain in the root zone (crop row spacing times the root depth) with one-directional moisture movement, the FD scheme is preferable to FE methods.

2.8.2. Evapotranspiration component

Evapotranspiration (ET) is usually the biggest component of water balance during the crop season. Older moisture models usually relied on empirical ET methods that considered only a few weather parameters (that affected ET) in simulating ET, such as air temperature and radiation. However, due to the increase in computing power and instrumentation for weather data collection, as well as advancement in the science of ET, the physically-based combination equations have gained widespread acceptance in estimating ET. Combination equations take into account both the energy and transport (wind) components that drive ET. Hence, to accurately simulate plant N removal as well as N-loss pathways, a widely-used combination equation such as the Penman-Monteith method (Allen et al., 1990) could be appropriate.

If there is no moisture deficit, combination equations can be directly applied to calculate crop ET (E_{tc}) or reference crop ET (E_{tr}) for grass or alfalfa. Using E_{tr} and crop coefficient (K_c), E_{tc} can be calculated. While E_{tc} values calculated with combination equations are likely to be more accurate, they require non-standard crop observations (that vary with both the crop type and stage of growth) (Jensen and Rahman, 1985). Hence, it is preferable to use E_{tr} and K_c to calculate E_{tc}.

Under dry soil conditions, E_{tc} has to be adjusted to account for the reduced availability of moisture for plant removal. Adjustment of E_{tc} to account for soil moisture conditions can be done readily if the evaporation and transpiration components are separated. Soil surface evaporation can be calculated using an evaporation equation such as the Priestley-Taylor method (Allen et al., 1990) while actual transpiration can be calculated to account for soil moisture conditions using a method described by Feddes et al. (1978).

Using experimental data, Danielson (1967) reported that plant roots removed 40, 30, 20, and 10% moisture from the top, second, third, and bottom quarters, respectively, of the root zone. Since N movement to roots is mainly through mass flow (Tisdale et al., 1993), N removal is likely to follow a pattern similar to moisture uptake with respect to the root depth. Hence, if plant transpiration can be calculated as a function of root depth, as reported by Danielson (1967), both transpiration and N removal estimations can be improved. Improved transpiration and N removal simulations will improve simulations of moisture redistribution and N fate.

2.8.3. Nitrogen sub-model (2-D)

Given the lateral and vertical movement of N from subsurface-banded urea, a 2-D N model is likely to simulate the fate of banded-N more accurately than a 1-D N model. The convective-dispersive equation (CDE) can be applied to simulate N transport and transformation in two directions (Selim, 1994). For field scale models, since moisture movement is considered only in the vertical direction, lateral N movement in the CDE is simulated solely through molecular diffusion. In the vertical direction, both dispersive (both due to molecular diffusion and hydrodynamic dispersion) and convective components are considered. Discretization of the CDE in both time and space (2-D) can be achieved through the use of the alternating direction implicit (ADI) method (Anderson, 1995), an FD scheme which can be readily implemented. Separate CDEs are required for urea, NH_4^+, and NO_3^-. Each N form has its own source and sink terms to account for additions and removals from the soil solution.

2.8.4. Simulation of urea particle dissolution

With increase in urea particle size, time required for particle dissolution will increase, thereby impacting the subsequent N transformation processes. Most current models assume that the fertilizer-N is dissolved instantaneously, and is hence, available for immediate transformation. Modeling the dissolution process is made difficult by the need to simulate vapor transport towards the urea particle and dissolved urea transport away from the urea particle in multiple directions. Physically-based models that account for solute particle size, soil moisture content, and soil properties that could affect dissolution, could not be found. Even empirical equations that account for urea particle size in simulating the dissolution process would represent the physical process more accurately compared with assuming instantaneous dissolution of fertilizer-N.

2.8.5. Substrate concentration effects on transformation rates

Wetselaar (1985) reported that very high urea concentrations proved toxic to the urease enzyme resulting in inhibition of urea hydrolysis. Since subsurface-banding of urea granules and pellets is likely to cause higher localized urea concentrations than urea incorporation or surface broadcast, it is necessary to incorporate urea concentration effect on urea hydrolysis. Being an enzymatic reaction, urea hydrolysis rate can be modeled up to certain urea concentrations using the Michaelis-Menten reaction (Tabatabai, 1982). It is unclear how urea hydrolysis is simulated at urea concentrations between the Michaelis-Menten threshold and half saturation, when urea hydrolysis ceases (Wetselaar, 1985). It is likely that a relationship would have to be assumed to simulate urea hydrolysis rate for urea concentrations between the Michaelis-Menten threshold and half saturation. Similarly, nitrification can be simulated using a zero-order or first-order reaction, depending on NH_4^+ concentration. At very high NH_4^+ concentrations, nitrification ceases due to the toxic effects of NH_4^+ on the bacteria *Nitrosomonas* (Wetselaar, 1985), which convert NH_4^+ into NO_2^- (Eq. [2-2a]). Hence, a 2-D N model for simulating the fate of banded N needs to account for substrate concentration effects on both urea hydrolysis and nitrification.

2.8.6. Modular design

The envisaged model would be used to simulate the fate of subsurface-banded-N; it would not account for background N or other nutrients. To be of use to managers, a model should be comprehensive, i.e., it should have the capability of simulating the fate of multiple nutrients as well as multiple forms of a nutrient. Hence, the model should be modular in construction so that it can be readily incorporated into existing research or management models.

In order for the model to serve a wider clientele, it should be able to simulate additional N-loss pathways such as NH_4^+ fixation by clay minerals. A model that is modular in construction will be more amenable to modifications in future. Application of urea pellets in subsurface-bands results in N movement in three directions. However, simulating N movement in 3-D is much more difficult than a 2-D situation. Further, when pellets are applied close to one another, it is unclear if a 3-D model will enhance the simulation of N fate as compared with a 2-D model.

3. MATERIALS AND METHODS

The stated objectives were achieved by conducting a field experiment (Objective 1), laboratory experiments (Objective 2), and mathematical simulations (Objective 3). In the field experiment, corn silage yield, corn nitrogen (N) content, nitrate-N (NO_3^--N) concentration in leachate samples, and inorganic-N content in soil samples were measured to evaluate the agronomic and NO_3^--N leaching impacts of urea pellets and granules. In the laboratory, dissolution, incubation, and leaching column studies were conducted to study the impact of urea particle size on dissolution, mineralization, and N transport. In the field and laboratory studies, tablet-shaped 1.5-g urea pellets and commercial urea granules (0.01-0.02 g each) were used. In the laboratory experiments, tablet-shaped 0.5, 1.0, and 2.0-g urea pellets were also used. The urea pellets were obtained from the International Fertilizer Development Center (IFDC), Muscle Shoals, Alabama. The mathematical model is presented in Chapter 5.

3.1. Statistical Methods

Outputs were measured and hypotheses were tested relative to various aspects of the agronomic and NO_3^--N leaching impacts of urea pellets versus granules using both statistical and graphical methods. For testing hypotheses, parametric statistical analyses were used where the data sets complied with the assumptions required for parametric statistical tests; otherwise, non-parametric tests were used. The parametric tests used were Student-t test, Analysis of Variance (ANOVA) or General Linear Model (GLM), and Fisher's Least Significance Difference (LSD) (Ott, 1992). The non-parametric tests used were Wilcoxon Rank Sums two-sample test, Kruskal-Wallis (K-W) (chi-square approximation) (Siegel, 1956), and Bonferroni's one-way multiple comparison test (Daniel, 1990). The level of significance was 10% ($\alpha = 0.1$) in all statistical analyses. Since rejection of the null hypothesis even when it were to be true would have less adverse impact in this study than in drug trial studies (where smaller α values would be used), a comparatively large α value equal to 0.1 was selected. Graphical methods were used to augment the results of the statistical analyses.

The UNIVARIATE procedure in SAS (1996) was used to test normality of the data based on one of three procedures, namely, raw data, log distribution of raw data, and the residuals of the raw data. If the data set was found to be normally distributed based on one of the three procedures, parametric methods were used for the data analyses. For comparing two independent samples to determine if they were from the same population, the Student t-test was performed using PROC TTEST (SAS, 1996). Depending on whether the statistical test of equality in variance was satisfied or not, the p-value corresponding to the equal or unequal variance was used. Since SAS reported the critical p value for a two-tailed hypothesis, for one-tailed hypotheses, the critical p-value was obtained by dividing the reported value by two (SAS, 1996).

For comparing more than two independent data sets, ANOVA was performed using PROC ANOVA; for unbalanced data sets, GLM was performed using PROC GLM (SAS, 1996). Both the Wilcoxon two-sample and K-W tests were applied using PROC NPAR1WAY in SAS (SAS, 1996) for data sets that could not be analyzed with parametric statistical methods. The Bonferroni's one-way multiple comparison test was performed manually using the rank sums obtained from the K-W test to compare treatment means.

3.2. Field Experiment

Objective 1: Evaluate the agronomic and NO_3^--N leaching impacts of subsurface-applied urea pellets versus granules on no-till silage corn.

To achieve Objective 1, a field experiment was conducted to evaluate the agronomic and NO_3^--N leaching impacts of subsurface-applied urea forms (pellets and granules) on no-till silage corn from May 1997 through March 1999. Two urea forms were compared with respect to their impacts on corn silage yield and corn N content. Crop data were obtained for the silage corn crops grown during the 1997 and 1998 seasons. The site was left fallow during the winter of 1997-1998. Nitrate-N leaching from urea pellets versus granules was investigated using residual soil inorganic-N, NO_3^--N concentration in leachate, and N removal by crop. Data on NO_3^--N leaching were collected from July 1997 through March 1999.

3.2.1. Field Selection and Description

The field experiment was conducted at Virginia Tech's Kentland Farm, located about 16 km from the main campus in Blacksburg. The field was located in the lower bottom of Kentland Farm on the banks of the New River, separated from the main farm compound by railway tracks. The field, which formed part of a larger tract, has a rolling topography. In order to select a site that was flat, a portion of the tract that appeared relatively flat measuring about 60 m (east-west) by 45 m (north-south), was surveyed on February 28, 1997. Care was taken to keep a minimum distance of 30 m from a line of trees on the banks of the New River that bordered the southern edge of the tract. A detailed contour map of the area was prepared using the Surfer software (Golden Software, 1995).

Using the contour map, the field measuring 45 m $\times$ 25.5 m (1147.5 m^2) was demarcated with stakes at the four corners. There were production plots on three sides of the field; on the eastern side, there was a grassed area about 6 m wide that served as a farm road. The long axis of the field was roughly east-west. The field had the highest elevation in the middle (along the long axis), with a gentle slope of about 1.5 % on both sides, i.e. along the north-south axis. The field did not have a significant cross slope. During May 1997, the edge of the field was observed to be about 50 m from the banks of the New River. The field was about 2-3 m higher than the river during May 1997. The water table was at a depth greater than 1.80 m during mid-June, 1997. The soil series in the field was Ross (SCS, 1985).

The field had been planted to soybean (in conventional tillage) in the summer of 1996 and had been left fallow during the following winter. It was reported by technicians working at Kentland Farm that the field had serious infestation of common ragweed (*Ambrosia artemisiifolia*), giant ragweed (*Ambrosia trifida*), and johnson grass (*Sorghum halpense*). During the early months of 1997, the field had substantial residue cover. The crop residue was removed with a landscape rake to avoid interference with field operations. The landscape rake caused only minimal soil disturbance. However, due to the removal of the crop residue, the soil developed a hard crust due to raindrop impact. As the soil warmed, substantial weed growth followed.

3.2.2. Soil Description

Ross soils (fine-loamy, mixed, mesic, Cumulic Hapludolls) are deep and well-drained with moderate permeability (SCS, 1985). The soil hydrologic group of this soil series is B (SCS, 1985) with a leaching index of nine for Montgomery County (VDCR, 1993), indicating a possibility of leaching below the root zone (VDCR, 1993). Ross soils comprise a combination of soil textural classes that include sandy loam, loam, silt loam, and silty clay loam. Reactions range from slightly acidic through moderately alkaline (SCS, 1985). The Ross soil series are included in the Soil Productivity Group Ia, with the highest productivity potential (VDCR, 1993). The productivity potential of the Ross soil series for corn silage is 47.6 Mg/ha (21.2 t/acre) at 35% dry matter (DM) (VDCR, 1993).

3.2.3. Field Layout

Three rows of seven experimental plots each were established with the rows running east-west (fig. 3.1). Each of the 21 plots measured 4.5 m $\times$ 4.5 m and had an area of 20.25 m^2. The three rows were separated by 3-m wide access roads; within a row, the plots were separated by 1-m buffers. To isolate the field from the surrounding area, a 3-m wide buffer was maintained on three sides; on the western side, the width of the buffer strip was increased to 4.5 m to provide for adequate turning space for tractors. Nine of the 21 experimental plots were instrumented with tension lysimeters (for leachate sample collection) and access tubes for neutron count measurement to calculate soil moisture content. The layout of the instrumentation is shown in figure 3.2. The details of the instruments are presented in Section. 3.2.7.

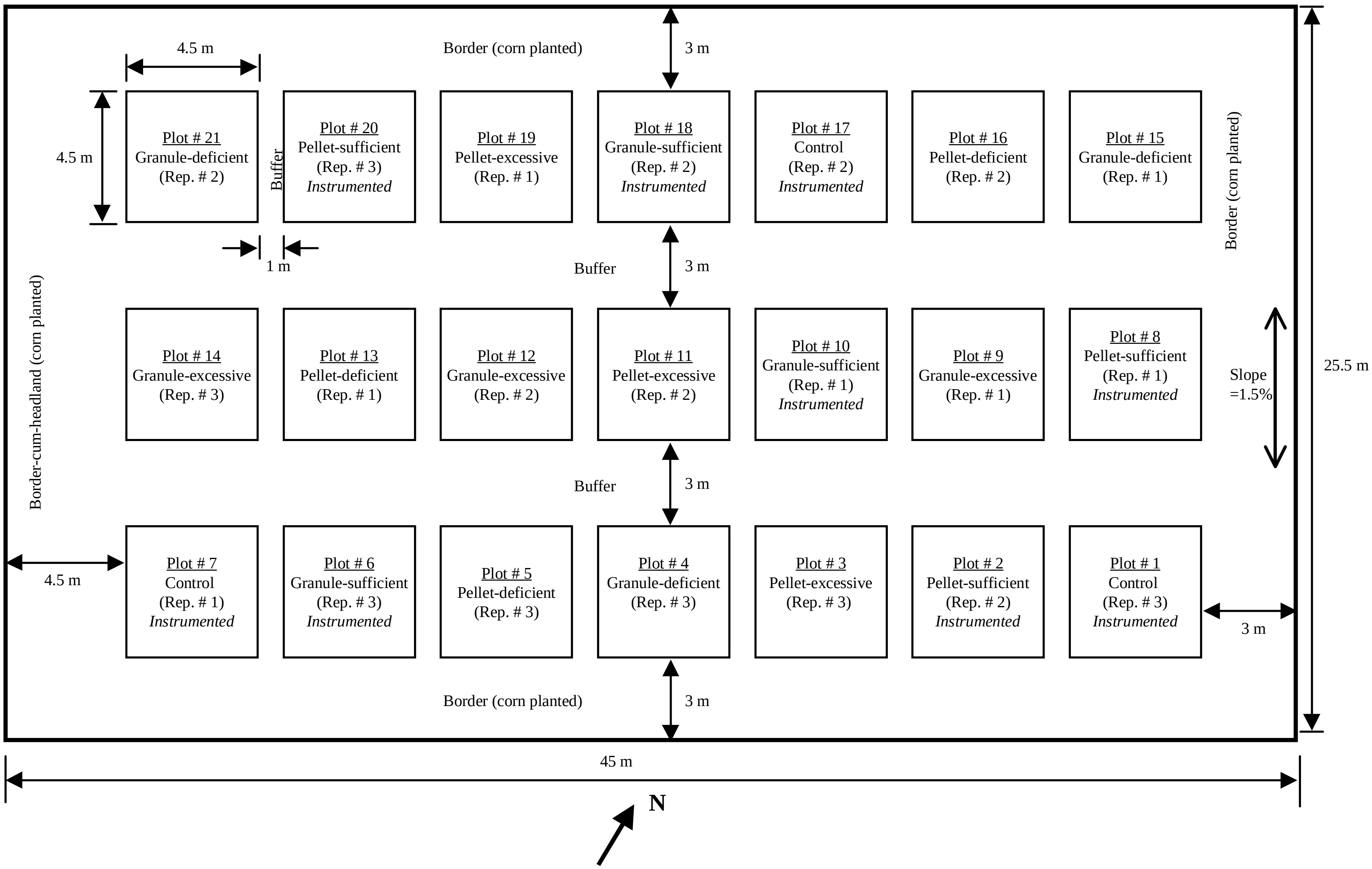

Figure 3.1. Layout of the Field Experiment

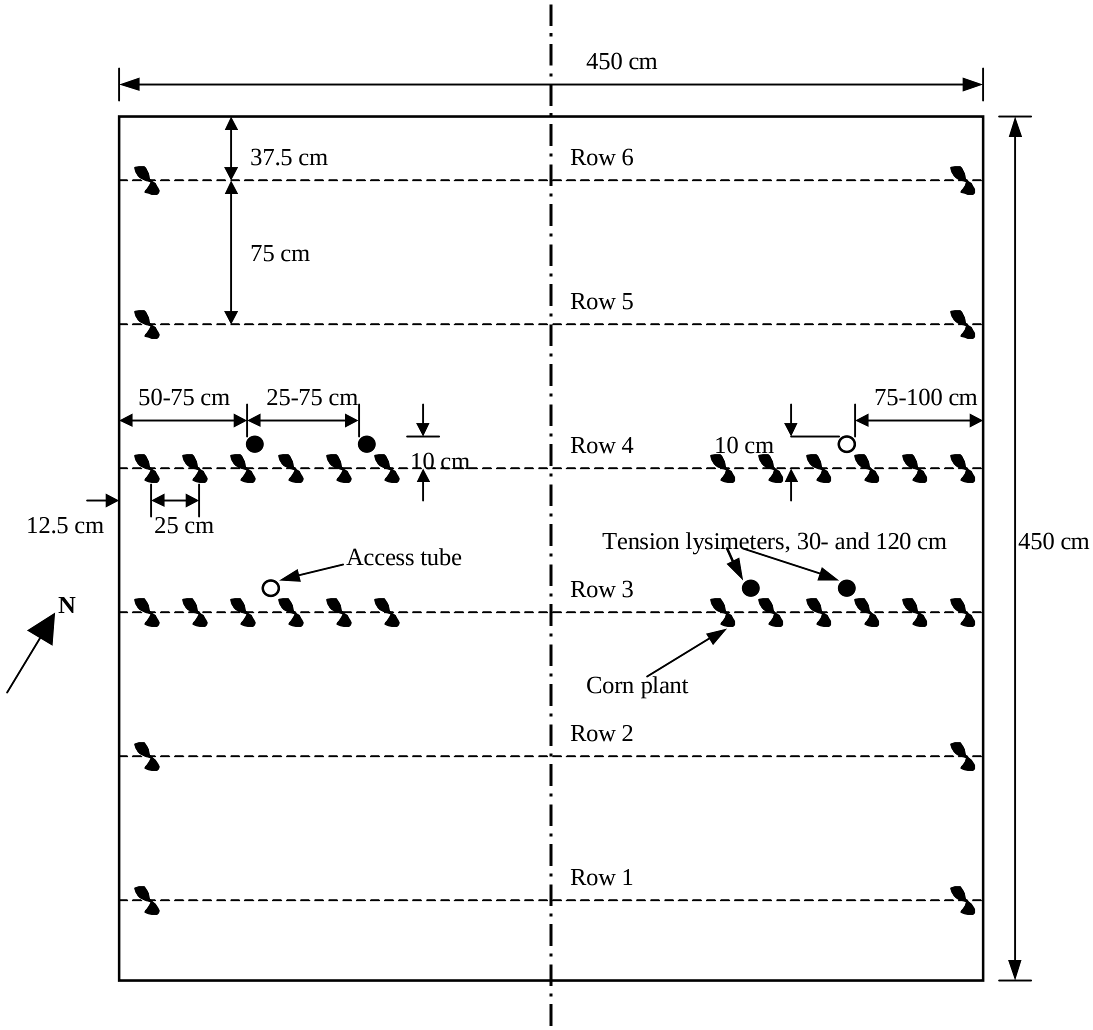

Figure 3.2. Location of tension lysimeters and access tubes in a plot. There are 18 corn plants per row; not all corn plants are shown.

3.2.4. Experimental Design

Two aspects of the experimental design were error-reduction and treatment designs. Two error-reduction design alternatives were considered, the Completely Randomized Design (CRD) and the Randomized Block Design (RBD) (Hinkelmann and Kempthorne, 1993). Both designs allot treatments through randomization to minimize the impact of systematic differences due to factors beyond the control of the experimenter (Hinkelmann and Kempthorne, 1993), for example, the presence of a soil nutrient trend.

Soil NO_3^--N concentration among the three rows of plots was investigated using soil samples to test for the presence of a NO_3^--N concentration gradient. In each row, four soil samples were obtained at approximately equal intervals from within the 1-m wide buffer areas for a total of 12 samples from the field. As recommended for residual NO_3^--N determination by Tisdale et al. (1993), soil cores were obtained from a depth of 65-75 cm using a soil core sampler. The samples were extracted with copper sulfate and analyzed for NO_3^--N using the reference electrode method with a precision of 0.1 mg-N/L (Donohue and Heckendorn, 1994) in the Soil Testing (ST) Laboratory of the Crop and Soil Environmental Sciences (CSES) Department at Virginia Tech. The results indicated that there was no systematic difference in NO_3^--N concentration between the rows, ruling out the need to use RBD. Hence CRD was chosen as the error-reduction design. Potential differences in soil properties were not considered in the experimental design since the plots were small (20.25 m^2 per plot) and the field site was located well inside the region demarcated as Ross soil in the soils map (SCS, 1985).

3.2.5. Treatment Design

Based on the productivity potential of corn silage on the Ross soil series, the sufficient N application level was 184 kg-N/ha (VDCR, 1993). The deficient and excessive N application rates represented a 40% reduction and 40% increase compared to the sufficient level, respectively. A large difference between the sufficient and deficient or excessive application rate permitted the detection of possible N application rate and urea form interaction effect on corn silage yield and corn N content. Hence, the treatment design required six experimental treatments (table 3.1), as a 2×3

treatment design in CRD. A control treatment was added to measure crop yield, crop N removal, and background NO_3^--N leaching under zero N application. Each treatment was replicated three times.

Table 3.1. Treatment description: urea form and application rate

Treatment	Urea form	Application rate, kg-urea/ha* (kg-N/ha)
Control (C)	none	0
Pellet-sufficient (PS)	1.5 g pellets	400 (184)
Pellet-deficient (PD)	1.5 g pellets	239 (110)
Pellet-excessive (PE)	1.5 g pellets	561 (258)
Granule-sufficient (GS)	granules	400 (184)
Granule-deficient (GD)	granules	239 (110)
Granule-excessive (GE)	granules	561 (258)

* 1 kg-urea ≡ 0.46 kg-N

3.2.6. Outputs Measured and Hypotheses Tested

The field experiment outputs were used to compare the agronomic and NO_3^--N leaching impacts of urea pellets versus granules. The agronomic outputs were corn silage yield and corn N content. The NO_3^--N leaching-related outputs included residual inorganic-N in the soil, NO_3^--N concentration in leachate, and N removal by the crop. For each output, multiple hypotheses were tested.

A. Agronomic Component

The impacts of the urea forms, 1.5-g pellets and granules, on corn silage yield and corn N removal were examined. The urea form and N application rate interaction effects on yield and N removal were also examined.

1. **Corn silage yield**

The following hypotheses were tested:

1.1. **Null Hypothesis: Corn silage yield is unaffected by the treatment applied.**

Alternative Hypothesis: Corn silage yield is affected by the treatment applied.

1.2. **Null Hypothesis: Corn silage yield is unaffected by the urea form at the sufficient application rate (184 kg-N/ha).**

Alternative Hypothesis: Corn silage yield is higher with pellets than granules.

1.3. **Null Hypothesis: There is no urea form × N application rate interaction effect on corn silage yield.**

Alternative Hypothesis: There is urea form × N application rate interaction effect on corn silage yield.

1.4. **Null Hypothesis: There is no urea form × year interaction effect on corn silage yield.**

Alternative Hypothesis: There is urea form × year interaction effect on corn silage yield.

1.5. **Null Hypothesis: There is no N application rate × year interaction effect on corn silage yield.**

Alternative Hypothesis: There is N application rate × year interaction effect on corn silage yield.

Using Hypothesis 1.1, all treatments were compared to see if the experimental treatments were different than the control treatment with regard to corn silage yield at 35% DM. If the experimental treatments were found to be different, pellet-sufficient (PS) and granule-sufficient (GS) treatments were compared using Hypothesis 1.2.

Zhang (1990) reported that urea prills applied in pockets (at one pocket per plant), to simulate pellets, at 150-200 kg-N/ha had adversely affected corn yield. Hence, urea form × N application rate interaction effect was tested with Hypothesis 1.3 to determine if there were any potential adverse effects on corn silage yields of applying pellets (1.5 g) and granules within a range of 110 to 258 kg-N/ha.

Due to possible change in soil (e.g., residual-N) and environmental (e.g. precipitation) conditions from 1997 to 1998, urea form impact on corn silage could likely vary. Hence, Hypothesis 1.4 was included to test urea form × year interaction effect on corn silage yield. Similarly, N application rate impact on corn silage yield was likely to change from 1997 to 1998 given changes in environmental conditions and soil nutrient conditions. Hence, Hypothesis 1.5 was tested for N application rate × year interaction effect on corn silage yield.

2. Nitrogen content in corn

The following hypotheses were tested relative to N content in the above-ground corn plant at the time of harvest:

2.1 Null Hypothesis: N content in corn is unaffected by the treatment applied.

Alternative Hypothesis: N content in corn is affected by the treatment applied.

2.2. Null Hypothesis: N content in corn is unaffected by the urea form at the sufficient application rate (184 kg-N/ha).

Alternative Hypothesis: N content in corn is higher with pellets than granules.

2.3. Null Hypothesis: There is no urea form × N application rate interaction effect on N content in corn.

Alternative Hypothesis: There is urea form × application rate interaction effect on N content in corn.

2.4. Null Hypothesis: There is no urea form × year interaction effect on N content in corn.

Alternative Hypothesis: There is urea form × year interaction effect on N content in corn.

2.5. Null Hypothesis: There is no N application rate × year interaction effect on N content in corn.

Alternative Hypothesis: There is N application rate × year interaction effect on N content in corn.

Hypothesis 2.1 allowed for comparison of plant N content among different treatments to ascertain if the experimental treatments were different than the control treatment. If Null Hypothesis 2.1 was rejected, Hypothesis 2.2 was used to test whether N content in corn was affected by the urea form at the sufficient application rate. Higher N content is indicative of a more nutritious silage since protein content increases with N. Further, greater N removal by the crop has the potential to reduce N losses into the environment.

Hypotheses 2.3, 2.4, and 2.5 were included to test effects of factor-level interactions on corn N content. The reasons for including those hypotheses were the same as those that applied to the corn silage yield, i.e., Hypotheses 1.3, 1.4, and 1.5.

B. Nitrate-N Leaching Component

This aspect of the field experiment focused on comparing the potential for NO_3^--N losses from the root zone from the two urea forms, 1.5-g pellets and granules. The urea forms were compared with respect to residual inorganic-N in different layers of the root zone, NO_3^--N concentration in leachate, and crop N removal.

3. Residual inorganic-N in the soil

In mineral soils, less than 1% of the N present in the inorganic form contributes to NO_3^--N leaching (Tisdale et al, 1993). Hence, finding evidence of NO_3^--N leaching loss (as affected by the urea form) using N balance was likely to be difficult. Residual inorganic-N as affected by fertilizer form would, however, provide indirect evidence of the impact of fertilizer form on NO_3^--N leaching. Inorganic-N balances were computed for C, PS, and GS treatments for three soil layers of interest. The following hypotheses were tested separately for each layer.

3.1. Null Hypothesis: Estimated amounts of residual inorganic-N are unaffected by the treatments, i.e., C, PS, and GS.

Alternative Hypothesis: Estimated amounts of residual inorganic-N are affected by the treatments.

3.2. Null Hypothesis: Residual inorganic-N amounts are equal in both urea forms at the sufficient application rate (184 kg-N/ha).

Alternative Hypothesis: Residual inorganic-N amounts are higher in PS than GS.

Hypothesis 3.1 was used to test if the fertilizer treatments resulted in different residual inorganic-N than the control treatment in October 1997 (end of first corn season), May 1998 (beginning of second corn season), October 1998 (end of the second corn season), and April 1999. Hypothesis 3.2 was tested to compare residual amounts of inorganic-N in PS versus GS only if Null Hypothesis 3.1 was rejected. A treatment that results in higher inorganic-N amount in the root zone is likely to have lost less NO_3^--N through leaching and have more N available for plant removal than other treatments.

Soil samples used for testing Hypotheses 3.1 and 3.2 were obtained midway between two rows of corn (Sec. 3.2.7). It was likely that such a soil sampling scheme could have underestimated residual inorganic-N amount since the closest sidedress urea band was placed 17.5 cm away from the sampling site (Sec. 3.2.9). Hence, a different sampling scheme was applied only to the fertilizer treatments in April 1999 which involved taking soil samples in the band (SS1) and 8.75 cm to the side of the band (SS2) in addition to sampling midway between the corn rows (SS3). The soil sampling scheme is described in Sec. 3.2.7. The following hypotheses were formulated *post-hoc* to test whether the sampling scheme affected residual inorganic-N recovery in the three layers (top 30-cm, top 60-cm, and root zone).

3.3. Null Hypothesis: Residual inorganic-N amounts in the fertilizer treatments based on inorganic-N concentrations calculated using the SS1 samples are the same as the control treatment.

Alternative Hypothesis: Residual inorganic-N amounts are higher in the fertilizer treatments than in the control treatment.

3.4. Null Hypothesis: For the same fertilizer treatment, residual inorganic-N amounts based on the inorganic-N concentrations at SS1, SS2, and SS3 are not different.

Alternative Hypothesis: Residual inorganic-N amounts based on the inorganic-N concentrations at SS1, SS2, and SS3 are different.

Residual inorganic-N amounts in the fertilizer treatments based on the SS1 samples are most likely to detect differences in inorganic-N amounts between the fertilizer and control treatments, a hypothesis that was tested using Hypothesis 3.3. If Null Hypothesis 3.3 was rejected, Fisher's LSD was used to compare the pellet and granule treatments. Hypothesis 3.4 was used to compare inorganic-N recovery as affected by the sampling location (e.g., SS1 versus SS2) within a fertilizer treatment.

4. Nitrate-N concentration in leachate

The following hypotheses regarding NO_3^--N concentrations in leachate were investigated for both depths (30 cm and 120 cm) for the C, PS, and GS treatments. The control treatment was included to study background NO_3^--N movement.

4.1. Null Hypothesis: NO_3^--N concentration in leachate is unaffected by fertilizer treatment.

Alternative Hypothesis: NO_3^--N concentration in leachate is affected by the fertilizer treatment.

4.2. Null Hypothesis: NO_3^--N concentration in leachate is unaffected by the urea form (pellet versus granule).

Alternative Hypothesis: NO_3^--N concentration in leachate is lower in the pellet treatment than in granules.

Hypothesis 4.1 was tested for each sampling event at both 30- and 120-cm depths. If Null Hypothesis 4.1 was rejected, Hypothesis 4.2 was tested to see if urea form impacted NO_3^--N leaching. Additionally, the time series of NO_3^--N concentrations in the leachate at both depths were compared graphically among the treatments to evaluate treatment impact on NO_3^--N leaching.

5. Nitrogen removal by crop

The following hypotheses relative to N removal by crop were investigated:

5.1. Null Hypothesis: N removal by crop is unaffected by fertilizer treatment.

Alternative Hypothesis: N removal by crop is affected by fertilizer treatment.

5.2. Null Hypothesis: N removal by crop is unaffected by the urea form at the sufficient application rate (184 kg-N/ha).

Alternative Hypothesis: N removal by crop is higher with PS than GS.

Greater N removal by the crop treated with one urea form compared with the other is likely to reduce the amount of applied inorganic-N left in the soil; hence less NO_3^--N will be available in the soil for leaching. Hypothesis 5.1 allowed for comparison of N removal by the crop among all treatments to ascertain the likelihood of a fertilizer effect. If Null Hypothesis 5.1 was rejected, Hypothesis 5.2 was tested to evaluate if one urea form was superior to the other in facilitating N removal via the crop at the sufficient N application rate.

3.2.7. Sampling for Nitrogen

Nitrate-N leaching losses from the C, PS, and GS treatments were evaluated using N content in soil and NO_3^--N concentration in leachate samples. The control treatment was included to estimate N loss under zero-N application rate.

A. Soil nitrogen

Soil N status in the C, PS, and GS treatments was compared in the top 30-cm, top 60-cm, and root zone (120 cm). Comparison of soil N among the treatments was used to estimate N leaching losses through the root zone and evaluate inorganic-N movement in the soil profile as affected by the fertilizer treatment. The N forms considered in the analyses were total N, NO_3^--N concentration in soil solution, and NH_4^+-N concentration in soil solution.

Soil sample preparation and N analysis

Soil samples were collected four times during the study period (discussed below) using a 2-cm diameter soil sampler. The soil samples were taken to the Land and Water (LW) Laboratory in the BSE Department and dried in an oven at 65°C for 4-5 h to about 5% gravimetric moisture content (M. Flock, personal communication, New Knoxville, Ohio, 20 October, 1997) in a natural convection oven. Beginning May 1998, soil samples were dried in a forced convection oven to ensure more uniform drying and at 35-40°C to reduce NH_4^+-N losses (Bates, 1993).

The dried soil was ground and passed through a 0.5 mm sieve; about 25 g of the sieved soil was transferred to a paper bag and sent to Brookside Laboratories, Inc. for analysis of NO_3^--N, NH_4^+-N, and total N. The samples were analyzed using the colorimetric method for NO_3^--N and NH_4^+-N using the Lachat 800 automatic analyzer. The samples were analyzed for total N using the Carlo Erba NA 1500 analyzer using flash combustion (Carlo Erba Instruments, 1988), an automated Dumas procedure with modifications (Bremner and Mulvaney, 1982). The results were reported in ppm or µg-N/g-oven dry soil. The total mass of soil in each layer (adjusted for moisture content) was calculated using the bulk density (ρ_b) of that layer. Finally, the N concentration in the soil (kg-N/kg-soil) was multiplied by the mass of soil (kg/ha) to obtain the N amount (kg/ha) present in a particular layer.

Soil sampling

The field experiment extended from late-May 1997 to early-April 1999. There were four sampling events which are discussed below.

October 1997

This sampling event followed the corn silage growing season as well as irrigation application (Section 3.2.8). The most significant sources of N addition and removal were N fertilizer application to the corn crop and N removal in the harvested crop, respectively. The residual-N status was determined with soil samples taken on 21 October 1997 after applying irrigation during 6-16 October 1997.

Soil samples were collected from 0-15, 15-30, 30-45, 45-60, 60-90, and 90-120 cm layers. The cores were extracted approximately from the middle of two rows of corn stubble. A minimum distance of 60 cm was maintained from the metal borders to reduce edge effects. Care was taken to maintain a minimum distance of 60 cm from the tension lysimeters. Six cores were obtained from each plot for each depth; at least one core was taken from each of the five inter-row spaces. The six soil cores for a depth were crumbled and thoroughly mixed and a single sample of about 100 g of soil was transported to the LW Laboratory for further preparation for analysis of NO_3^--N, NH_4^+-N, and total-N. In all, there were six samples (one for each depth) per plot, and 54 soil samples in all from the nine plots.

May 1998

This sampling event followed the most critical period with regard to NO_3^--N leaching (Menelik et al., 1990). During late fall through early spring, except during the time when the ground is frozen, there is potential for substantial leaching to occur. The initial N status for this period was the final N status for the previous accounting period. The residual-N status was determined through analysis of soil samples obtained on May 13 and 14, 1998 for NO_3^--N, NH_4^+-N, and total-N.

<u>October 1998</u>

The third sampling event followed the second corn silage-growing season. As in the first sampling event, the most significant sources of N addition and removal were fertilizer N application and N removal through crop harvest, respectively. The residual-N status was determined through analysis of soil samples obtained on 14 October 1998 for NO_3^--N, NH_4^+-N, and total-N. Even though corn silage was harvested on 16 Septembe, soil cores could not be extracted immediately because the soil was very dry. After 5.5 cm of precipitation was received during 7-8 October, soil samples were obtained on 14 October 1998.

<u>April 1999</u>

The last sampling event followed the late fall through early spring period, critical with respect to NO_3^--N leaching. The residual-N status was determined through analysis of soil samples obtained on 2 April 1999 for NO_3^--N and NH_4^+-N.

Since lateral N movement is mainly through molecular diffusion under dry soil conditions, it was likely that applied residual-N would be concentrated close to the fertilizer band. In the laboratory, Singh and Beauchamp (1988) reported that NH_4^+ moved only 6 cm in 35 days in silt loam soil in a soil moisture tension range of 0.35 to 1.20 bars. Hence, sampling between crop rows (located 17.5 cm from the closest fertilizer band) could result in underestimation of residual inorganic-N in soil, especially in the top 30-cm of the root zone. Hence, soil samples were collected using the original scheme in the control plots, while a modified scheme was used for the PS and GS treatments. In the modified scheme, additional sampling included three cores obtained over the band (SS1) and three cores mid-way between SS1 and SS3, i.e., SS2 was 8.75 cm away from the band (fig. 3.3). There were three pairs of soil cores, each pair comprised of one SS1 and one SS2, adjacent to each other. For each fertilizer treatment, in two replications, two SS2 cores were obtained from the left side of the band while one core was obtained from the right. In the remaining replication, the order was reversed so that five and four SS2 cores were obtained from the left and right sides of the band. This arrangement minimized the effect of roots present close to the band on the left.

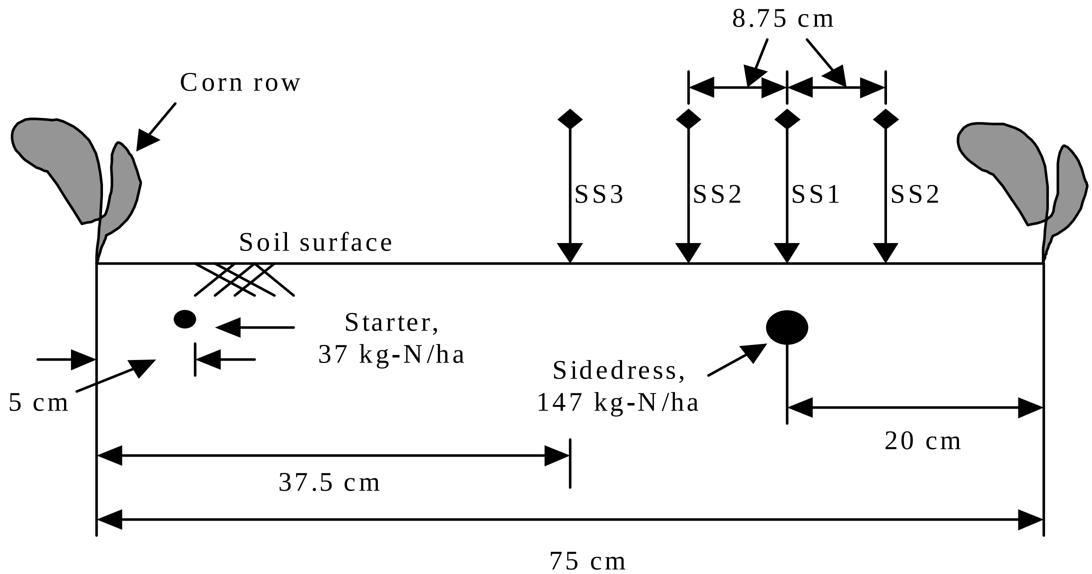

Figure 3.3. Soil sampling scheme design for April 1999. The terms SS1, SS2, and SS3 denote soil sampling sites 1, 2, and 3, respectively.

Soil cores were obtained from 0-15, 15-30, 30-60, 60-90, and 90-120 cm; in the conventional scheme, separate cores had been obtained for 30-45 and 45-60 cm. In each fertilizer treatment plot, for each depth, the three SS1 cores were composited; the same arrangement was applied to the SS2 and SS3 cores. A total of 105 soil samples were analyzed, 15 samples from each of the fertilizer plots and five each from the control plots.

B. Leachate samples

Since tension lysimeters have been widely used in studies involving NO_3^--N in leachate (Angle et al., 1990), in this study, tension lysimeters were used to collect leachate samples for NO_3^--N analysis. Leachate samples extracted from the tension lysimeters were analyzed for NO_3^--N in the Water Quality Laboratory of the BSE Department using the TRAACS 800 automatic water quality analyzer. Comparisons were made between NO_3^--N concentrations in leachate from pellets and granules to see if the urea form affected NO_3^--N losses at a point in time. A control treatment with no N was included to estimate background NO_3^--N leaching.

Tension lysimeters were installed at two depths - 30 cm and 120 cm. The 30-cm depth represents the top quarter of the root zone of the corn plant from which it extracts 40% of its total water supply (Tisdale et al., 1993) and, thus, a substantial portion of NO_3^--N. Further, the top 30-cm of soil represents the most biologically active region where most N transformations occur. The NO_3^--N concentrations in the leachate samples from the 30-cm depth were used as an indicator to compare the fertilizer forms with respect to their NO_3^--N leaching potential. Higher NO_3^--N loss from the top 30-cm was indicative of higher potential for N losses into groundwater.

Tension lysimeters were also installed at the 120-cm depth which can be regarded as the lower limit of corn's root zone from the viewpoint of water management (Schwab and Frevert, 1993). All NO_3^--N moving below this depth was assumed lost to the corn plant and could ultimately pollute the groundwater. Hence, a comparison of NO_3^--N concentrations at the 120-cm depth from pellet versus granule provided a more reliable indicator (than the 30-cm samples) of the impact of urea form on NO_3^--N leaching into groundwater.

Fabrication and testing of tension lysimeters

The tension lysimeters were assembled in the BSE Department from purchased components (fig. 3.4) following the instructions given in Teso et al. (1990). Except for the Class 160 PVC pipe of nominal size 1.5 in. which was procured from a supplier of irrigation pipes in Louisiana, all components for the tension lysimeters were purchased from Soilmoisture Equipment Corporation (SEC). The high-flow ceramic cups (653X01-B.5M2) had a diameter of 4.83 cm and a length of 6.05 cm. The cups had a bubbling pressure of 0.5 bars that permitted faster sample collection compared to cups with higher bubbling pressures.

For the 120- and 30-cm tension lysimeters, the pipes were cut to lengths of 122 and 32 cm, respectively, which allowed 5 cm of the pipe length to stay above the soil surface with the mid-point of the ceramic cup coinciding with the desired depth in the soil. Most ceramic cups did not fit snugly into the PVC pipe due the large tolerances allowed in the manufacture of both the PVC pipe ID and the ceramic cup neck diameter. To provide a better fit, a light coating of epoxy was applied to the neck of the ceramic cup that was then dried for 2-3 h in an oven at 55-65°C (Teso et al., 1990). The ceramic cup was then glued to the pipe by applying epoxy to the neck of the ceramic cup and inserting the cup into the pipe with a slight twist. The glued ceramic cup was then air-dried overnight in a vertical position with the ceramic cup pointing upwards. Epoxy purchased from SEC had a setting time of 1 h, causing the epoxy to drip down the pipe; perhaps an epoxy with a shorter setting time would be more desirable.

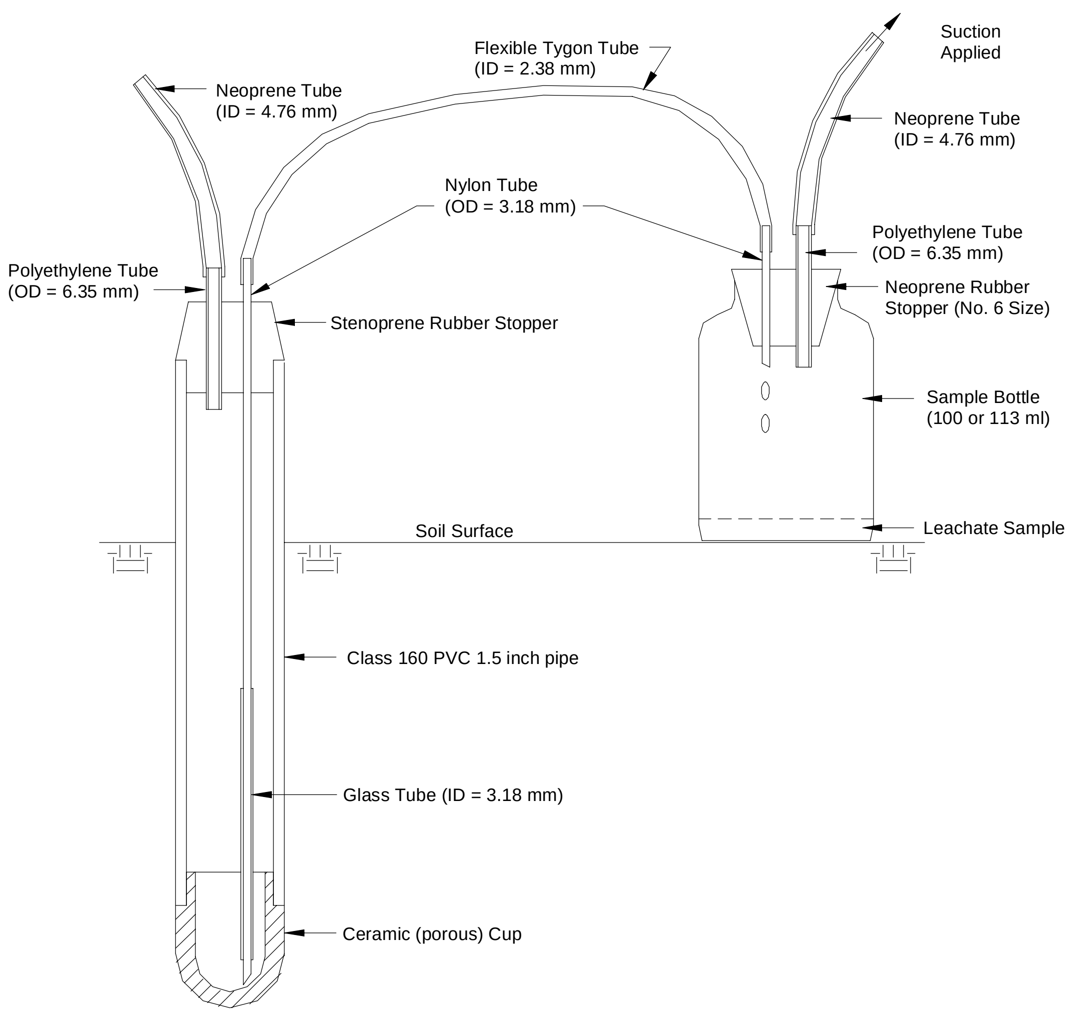

Figure 3.4. Tension lysimeter construction and procedure for leachate sample collection

The stenoprene stopper provided by SEC had a molded neck to fit tightly into the PVC pipe. A neoprene tube (ID = 4.76 mm; wall thickness, WT = 3.18 mm) was attached to the hole provided in the stopper with a polyethylene pipe (OD = 6.35 mm; WT = 1.01 mm). Due to the lack of square ends in some PVC pipes, it was difficult to provide a vacuum seal using the stenoprene rubber stopper that had a slight and short taper. The ordinary neoprene rubber stopper (No. 10 size) provided better sealing since it could be forced down into the PVC pipe to a greater depth.

Suction was to be applied to the tension lysimeter through the neoprene tube using a vacuum pump; the neoprene tube was then closed off with a clamping ring. As per recommendations given by SEC, to collect the sample, a thin nylon tube was to be inserted through the neoprene tube down to the bottom of the tension lysimeter while the other end of the nylon tube was to be connected to a bottle through a two-hole stopper. Suction was to be applied by connecting a vacuum pump to the bottle and stroking the pump. There was the possibility that contaminant adhering to the nylon tube would contaminate the leachate sample. Further, it was cumbersome to carry separate nylon tubes for different depths and treatments. Hence the stopper assembly was modified as discussed below.

A second hole was made in the stopper assembly to insert a nylon tubing (OD = 3.18 mm; WT = 0.4 mm) that reached the bottom of the tension lysimeter (fig. 3.4). The end of the nylon tubing was cut at an angle to prevent a potential seal from forming between the end of the nylon tube and the ceramic cup's wall (Teso et al., 1990). To prevent sample contamination from the previous sample, the end of the nylon tubing was made straight and rigid by providing a glass tube (ID = 3.18 mm), 15-20 cm in length as sheath. The sheath facilitated the placement of the nylon tube at the bottom of the tension lysimeter. The other end of the nylon tubing was connected to flexible Tygon® tubing (ID = 2.38 mm; WT = 0.79 mm). A paper clip was used to clamp the Tygon® tubing when necessary.

The tension lysimeters were tested for leakage using the procedure described by Teso et al. (1990). The tension lysimeters were soaked in water for 6-8 h after which they were pressurized with the ceramic cups submerged in water. Care was taken not to exceed the bubbling pressure (0.5 bar) of the ceramic cups. Tension lysimeters with leaky joints released air bubbles through the leaky spot/s; the leaks were plugged with epoxy. Cracked ceramic cups released air bubbles through the cracks; such tension lysimeters were discarded. Prior to installing the tension lysimeters in the field, each tension lysimeter was flushed with 1 L of deionized water to remove water-soluble contaminants. To ensure that a tension lysimeter was installed in the field at the correct depth, a mark was made with a permanent marker to denote 30- or 120-cm on the PVC pipe measured from the center of the ceramic cup.

Field installation of tension lysimeters

The tension lysimeters were transported to the field site with their ceramic cups covered with strips of sponge to guard against breakage. The ceramic cups were kept soaked in water during transport. Four tension lysimeters (two each of 30- and 120-cm depths) were installed in each of the nine instrumented plots (three each of C, PS, and GS treatments) for a total of 36 tension lysimeters during 28-30 May 1997. Two tension lysimeters were installed in each plot at each depth to obtain a more representative leachate sample. In case of failure of one tension lysimeter, the sample from the other tension lysimeter was used to obtain NO_3^--N concentration for that plot. Each plot was roughly divided into two halves (east-west) and two tension lysimeters, one at 30-cm depth and the other at 120-cm depth were installed in each half (fig. 3.2). In the eastern-half, the tension lysimeters were installed next to the third row of corn while in the western-half, they were installed in the fourth row. The tension lysimeters were installed 10 cm away from the row of plants and midway between two plants. To minimize edge effects, the tension lysimeters were installed at least 50 cm away from the metal border.

For the tension lysimeters installed at 30-cm depth, a 35-cm deep hole was made with an 8.5-cm bucket auger. The soil excavated from each third of the depth was kept separate and passed through a 6.35 mm (0.25 in.) sieve to remove stones and roots. About 300 mL of soil slurry using soil from the lowest segment was poured into the hole and the ceramic cup of the tension lysimeter was submerged in the slurry (Teso et al., 1990). Proper contact between the slurry and the ceramic cup was achieved by raising and lowering the tension lysimeter repeatedly in the slurry. To ensure that the tension lysimeter was installed at the correct depth, the 30-cm mark on the PVC pipe was made level with the soil surface. The remaining excavated soil was poured back into the hole in the reverse sequence in which it was taken out. While pouring the soil back into the hole, the soil was compacted at regular intervals with a blunt 10-mm rod. Finally, at the surface, the soil around the tension lysimeter was slightly raised and firmly compacted to prevent surface water from channeling through the annular space between the tension lysimeter and the hole.

For the 120-cm tension lysimeter, the 8.5-cm bucket auger was used to drill a hole down to a depth of 90 cm, after which, a 7.5-cm screw auger was used to extend the hole down to 125 cm. Due to the greater depth involved in the case of 120-cm tension lysimeter and the smaller diameter of the hole at the bottom, it was more difficult to compact the soil at the bottom. Hence, the bottom 35-cm of the hole was filled with slurry. Otherwise, the 120-cm tension lysimeter was installed the same way as the 30-cm tension lysimeter.

Tension lysimeters in Plot Nos. 1 and 8 were vandalized between 8 and 9 June 1997. In Plot No. 1, an attempt was made to pull out both tension lysimeters at 120-cm depth, failing which, the stopper assemblies on the two tension lysimeters were removed. In Plot No. 8, one tension lysimeter at 30-cm depth was uprooted; no other damage was noted. The repairs on the disturbed tension lysimeters were completed by 12 June 1997. After installation in the field, the tension lysimeters were purged at frequent intervals to prevent algal growth. Regular and frequent purging of the tension lysimeters also helped to stabilize the intake rate of the tension lysimeters (Ballestero et al., 1991). During winter, the freeze-thaw cycle in the top soil layer soil caused the 30-cm tension lysimeters to be heaved upwards by 2-3 cm. Consequently, the tension lysimeter had to be pushed down to the right depth and the soil around it compacted prior to suction application.

Sampling protocol for the tension lysimeters

<u>Sampling interval</u>

Sampling at regular intervals (usually 1-2 weeks) without accounting for individual rainfall events has been widely implemented (Poss et al., 1995; Adams et al., 1994;

Jones and Schwab, 1993). However, such an approach yielded samples that represented "average" conditions; it did not take into account the "first flush" effect (i.e., higher NO_3^--N concentrations) caused by rapidly percolating gravitational water. Stated otherwise, the detection of the "first flush" effect at a certain depth indicates the arrival of the wetting front.

To compare NO_3^--N concentrations in leachate samples (obtained at the same time) from pellet versus granule, it was more pertinent to obtain samples that represented the "first flush" effect. Thus sampling after precipitation provided the best indicator of vertical transport of NO_3^--N by the percolating gravitational water. There were times when there was no precipitation over a 2-week period or more. During such periods, if available, samples were collected at the end of the second week.

Time of sampling

It was necessary to estimate the time required for the wetting front to reach the specified depth since it was desirable to apply suction to the tension lysimeters only around that time. A coarse estimation of the time of arrival of the wetting front was made using the soil's saturated permeability values - 1.5-5.1 cm/h (0.6-2 in./h) (SCS, 1985). Based on the saturated permeability values, the wetting front reached the 30-cm depth in 6-20 h after the start of precipitation; for the 120-cm depth, the wetting front needed 24-79 h.

A more site-specific estimation of the time of arrival of the wetting front was made with the neutron probe (Sec. 3.2.8). A 60-cm diameter infiltration ring was installed around one of the access tubes used for calibration of the neutron probe. The initial moisture content at the depths of interest was measured by taking neutron counts at the specified depths. A known volume of water was ponded inside the infiltration ring and the progress of the wetting front was monitored using the neutron probe. For the soil moisture conditions prevalent at that time, the wetting front took about 30 and 240 min. to reach the 30- and 120-cm depths, respectively. However, the speed of the wetting front is affected by factors such as soil properties (texture and structure), initial soil moisture content, and precipitation intensity. Further, preferential flow as well as flow through the annular space between the access tube and soil could have allowed for such rapid percolation. Given the spatial variability in soil texture, structure, and moisture content, a single time interval needed for the wetting front to reach the specified depths could neither be applied to all plots for a single storm nor to a single plot for different storms.

In view of the uncertainty, an effort was made to collect leachate samples from the percolating water if not the water from the "first flush" effect at least at the 120-cm depth. Suction was applied to the tension lysimeters at both depths 6-18 h after the start of the precipitation event. If the precipitation event was not large enough to produce percolation down to the 120-cm depth, suction was applied to the tension lysimeters at the 120-cm depth later depending on the location of the wetting front as monitored using the neutron probe (Section 3.2.8). In case of another precipitation event during the sample collection stage, a separate set of samples was not collected. However, if the subsequent precipitation event/s caused percolation at the 120-cm depth, samples were collected at the 120-cm depth.

Precipitation data from a rain gage in Pulaski county located about 1 km from the field site were monitored regularly in real time on the National Weather Service website (NWS-NOAA, 1997-1998). Precipitation data observed in Pulaski provided a reliable indicator regarding the depth of precipitation at the field site without traveling to the field site.

Sampling procedure

It was desirable to collect samples by using a low tension value on the tension lysimeters. A lower tension value allowed collection of leachate samples from the percolating water rather than plant-available water. However, it took longer to collect samples of adequate volume using a lower tension value. Hence the tension lysimeters were maintained at 32-40 cbars tension depending on the duration of tension application. Tension was maintained on the tension lysimeters long enough to collect a sample volume of at least 4 mL from each tension lysimeter. Under moist conditions, usually 1-3 h was required to produce the adequate volume of sample; however, under drier conditions, the tension lysimeters were kept under suction overnight. Except during sample collection, the tension lysimeters were maintained at atmospheric pressure.

To ensure that the infiltration characteristics of the plots were not affected by traffic, 3 h were allowed to pass after the end of precipitation, before the plots were entered. Care was taken to minimize disturbance on the soil surface, which could have affected the hydrologic characteristics of the plots.

During July-August 1997 due to lower-than-normal precipitation and high corn ET, the tension lysimeters at the 30-cm depth lost suction as their ceramic cups desiccated. In some sampling events, all plots did not yield samples. For a sampling event, samples were analyzed only when samples from at least two replicates were obtained.

Sample collection, transport, and compositing

Samples were collected in labeled 100-mL plastic bottles or 113-mL (4 oz.) glass bottles, using a 2-hole rubber stopper (No. 6) and vacuum pump as shown in figure 3.4. In one hole of the stopper, a length of neoprene tubing (ID = 4.76 mm) was attached via a piece of polyethylene tubing (OD = 6.35 mm). In the other hole of the stopper, a piece of nylon tubing (OD = 3.18 mm) was inserted. To collect a sample, the stopper was fitted to a bottle and the free end of the flexible Tygon® tubing (ID = 2.38 mm) from the tension lysimeter was connected to the nylon tubing of the stopper and the vacuum pump was connected to the neoprene tubing of the stopper. When vacuum was applied to the bottle, leachate sample from the tension lysimeter was suctioned into the bottle. After emptying the tension lysimeter, the bottle was tightly stoppered. After the two-hole rubber stopper had been used for two tension lysimeters at the same depth in a plot, the stopper was rinsed with distilled water. Distilled water was forced through the nylon tubing in the stopper to prevent any cross contamination of samples. Within the same plot, different two-hole stoppers were used for tension lysimeters at different depths.

After collecting samples, the sample bottles were transported in a cooler to the LW Laboratory immediately. In the LW Laboratory, the sample bottles were stored in the refrigerator at a temperature of less than 4°C prior to compositing. One sample was prepared from each plot by compositing the two samples obtained for each depth. The objective of sample compositing was to obtain a sample that gave equal weight to both tension lysimeters. The volumes of both samples were measured and from the larger sample, an aliquot equal in volume to the smaller sample was obtained. The composite sample was obtained by mixing the aliquot from the larger sample with the smaller sample. If one of the samples was less than 2 mL, a large enough aliquot from the larger sample was mixed with the smaller sample to obtain a composite sample with a volume of 4 mL. In case one tension lysimeter did not yield any leachate from a plot, the available sample was analyzed for NO_3^--N. If the samples contained suspended particles, the samples were filtered using Whatman No. 4 filter paper.

The used sample bottles were scrubbed with soap solution, rinsed with hot water, and immersed in an acid bath, before final rinsing in two distilled water baths. The sample bottles were then allowed to dry at room temperature; the bottles were stoppered after they had dried.

3.2.8. Quantification of Soil Moisture, Precipitation, and Irrigation

Soil moisture was monitored in the C, PS, and GS treatments to monitor the movement of the wetting front. This information was used to decide whether or not to apply tension to the tension lysimeters since sample collection would not be possible under dry soil conditions. The soil moisture data was also used for testing the modeling.

A. Change in soil moisture storage

Neutron probe

In recent years, using the neutron probe for nondestructive soil moisture measurement has become a standard practice in a wide range of hydrologic studies (Grismer et al., 1995). For this study, a neutron probe, Troxler 3332 (Troxler Electronic Laboratories, Inc.) was used to measure soil moisture content because the probe is ideal for measuring soil moisture content at multiple depths with minimum disturbance to the plots. The difference in soil moisture content over a period of time gave the change in soil moisture storage.

The Troxler 3332 has a 10 mCi Americium 241-Beryllium radioactive source of fast neutrons which is lowered into the ground via an access tube of suitable diameter (TEL, 1983). When fast neutrons from the source collide with hydrogen (H) present in the soil as water, the neutrons lose energy resulting in loss of speed. The neutron thus slowed down by collision with H^+ cannot slow down any further and is said to be thermalized.

A counter filled with Helium 3 counts the number of thermalized neutrons which is proportional to the moisture content of the soil (TEL, 1983). However, H^+ will be present in soils also as organic matter, thus requiring the neutron probe to be calibrated on individual soils.

Access tube installation

During the second week of June 1997, aluminum access tubes (ID = 48.3 mm; OD = 50.8 mm), 203 cm long and with rubber stoppers at the bottom were installed in the field. TEL, Inc. (1983) recommends the use of aluminum access tubes because aluminum absorbs fewer thermalized neutrons and is more durable than steel or polyethylene. The ID and OD of the access tube were as per recommendations for the Troxler 3332 (TEL, 1983). A 50.8-mm (2 in.) screw auger was used to drill a hole to a depth of 120 cm after which a bucket auger of the same diameter was used to finish the hole down to 183 cm. The access tube was then inserted into the hole using a wooden mallet. Some water was poured into the hole to ease the insertion of the access tube into the hole. All access tubes were tightly held in the soil.

Two access tubes were installed in each plot for a total of 18 tubes. Each access tube was installed in the row adjacent to the row in which one pair of tension lysimeters (30-cm and 120-cm depth) had been installed (fig. 3.2). Consequently, in each half of the plot, there were one access tube and one pair of tension lysimeters. Each tube was installed 10 cm to the side and in between two corn plants. The access tubes were kept at a minimum distance of 60 cm from the metal border of the plot to minimize edge effects. When the access tubes were installed, 20 cm of tubing protruded above the soil surface. Four of 18 access tubes were shorter in length and thus had shorter lengths of tubing protruding above the soil surface. All access tubes were covered with plastic caps to prevent water entry.

Neutron probe calibration

The neutron probe was calibrated to obtain a relationship between neutron count (independent variable, x) and volumetric moisture content (dependent variable, y) using simple linear regression. To improve calibration regression, change in bulk density (ρ_b) with depth was considered. Volumetric MC (θ_v) was obtained by multiplying the gravimetric MC (θ_m) with ρ_b. Consequently, regressions were developed for different depths.

Three access tubes were installed in the buffer areas to calibrate the neutron probe. Soil samples obtained while excavating to install the access tubes were used for calibration (TEL, 1983). To obtain the soil sample at a particular depth, a 2.5-cm diameter soil core, 10 cm thick (5 cm above and 5 cm below the specified depth) was used. Immediately after installing the access tube, neutron counts were taken at the required depth using a 30-s count. The soil samples were oven-dried at 105°C to constant weight and their θ_m values were determined.

Since the data based on soil samples obtained from within the access tubes were limited, soil cores were taken from the vicinity of the access tubes to obtain more data points for calibration. Care was taken to extract cores at least 25 cm away from the access tubes (TEL, 1983). To obtain more representative samples, three 5-cm cores (2.5 cm above and 2.5 cm below the specified depth) were extracted from around each access tube at each depth; the three cores were then composited to obtain one sample. In order to reduce the error due to neutron count variability, 30-s counts were taken in duplicate. An effort was made to obtain a large number of data points and a wide range of moisture content values.

The ρ_b measurements made for conducting the N balance (Sec. 3.2.7) were used to estimate ρ_b at the specified depths for the neutron probe calibration. The cores were obtained using a ρ_b sampler consisting of a sharpened steel cylinder that accommodates sample cylinders with OD = 50.8 mm (2 in.) and height = 101.6 mm (4 in.). The sharpened steel cylinder screws underneath a steel rod that carries a sliding weight. In order to obtain a core, the sliding weight is raised up to the height of the steel rod and released to drive the sharpened cylinder into the soil.

To extract cores, a 76.2-mm (3-in.) bucket auger was first used to make a hole a little above the desired depth. After deepening and cleaning the holes to the necessary depth, the ρ_b sampler was used to extract a core from the required depth. The soil cores were 48.3 mm in diameter and 50.8 mm in height. The ρ_b values of the cores were determined by the core method using the procedures described by Blake and Hartge (1986a). Blake and Hartge (1986a) recommend a minimum core diameter of 75 mm;

however, since the available ρ_b sampler did not accommodate larger sample cylinders, sample cylinders 50.8 mm in diameter were used for ρ_b determination.

From the vicinity of each access tube installed for calibration, one core sample was extracted from a depth of 5 cm which was representative of the top 15-cm soil layer. Similarly, core samples were extracted from 20-, 35-, 50-, 72.5-, and 102.5-cm depths, which were representative of the 15-30, 30-45, 45-60, 60-90, and 90-120 cm soil layers, respectively. Hence, for each soil layer, there were three soil samples, one from each access tube. The ρ_b values of these samples were determined following the procedures described by Blake and Hartge (1986a). The ρ_b for the 30-cm depth was estimated to be 1.45 g/cm^3 by taking into account the ρ_b values at the 20- and 35-cm depths. Similarly, the ρ_b values at 45, 60, and 90 cm depths were estimated at 1.31, 1.28, and 1.38 g/cm^3, respectively, by taking into account the ρ_b values above and below the specified depths. It was assumed that ρ_b values at 120- and 150-cm depths were equal to the ρ_b at 90-cm depth, i.e. 1.38 g/cm^3.

For each depth, a linear regression was developed (SAS, 1996) to correlate neutron counts with the volumetric moisture content (θ_v) of the soil at that depth:

$$\theta_v = m \times N + c \qquad [3\text{-}1]$$

where m is the slope of the line and c is the intercept. The regression coefficients (m and c) and R^2 for each depth are given in table 3.2.

Table 3.2. Neutron probe calibration curve characteristics by depth

Depth, d (cm)	Number of samples used	R^2* (%)	Slope, m	Intercept, c
30	15	82.3	0.034	5.668
45	13	75.4	0.029	6.418
60	15	39.2	0.018	15.231
90	12	66.6	0.051	-11.920
120, 150	7	80.4	0.049	-10.897

* Coefficient of correlation

Neutron probe operation

The distance of the center of the radioactive source from the bottom face of the neutron probe was 12 cm (A. Gilbert, personal communication, Research Triangle Park, N.C., 3 July 1997). This information was used to position the radioactive source at the specified depth, ensuring that the neutron count corresponded closely to the desired depth.

The neutron probe was used beginning August 1997, after replacing its replaceable battery pack. During 1997, neutron counts were taken whenever the tension lysimeters were placed under tension to collect leachate samples; beginning in 1998, neutron counts were taken once every month during sample collection. Initially, soil moisture contents were to be measured at 15-, 30-, 45, 60-, 90-, 120-, and 150-cm depths. Since neutrons escape through the soil surface at shallower depths resulting in loss of accuracy (Marshall et al., 1996), neutron count measurement at 15-cm depth was discontinued beginning in mid-August 1997.

Neutron count at each depth was taken over a 30-s period. Before taking measurements at the specified depth, a standard count was taken once each day using a 4-min. count period (TEL, 1983). Standard count values were always within the acceptable range of counts as specified by TEL (TEL, 1983) indicating that the neutron probe was operating normally. Safety procedures as specified in Virginia Tech's Radiation Safety Handbook (Department of Health and Safety, 1991) were followed. Radiation from the neutron probe was monitored with a Geiger counter and personal exposure was monitored with a thermoluminescent dosimeter (TLD) badge.

B. Precipitation

There was a precipitation gage in Kentland Farm located 1.5 km from the field site. However, to obtain a more accurate measurement of precipitation for the field site, a weighing-type rain gage was installed on 17 June 1997, on the other side of the railway tracks, about 150 m from the plots. The rain gage could measure precipitation in increments of 1.27 mm (0.05 in.) and used a weekly recording chart. Installation of a rain gage at the field site was ruled out because of interference in collection from the surrounding crop and trees.

C. Irrigation

Irrigation application to supplement precipitation to meet the crop water requirement had not been envisaged. The corn silage season, mid-May to mid-September 1997, was dry with a precipitation deficit of 7.3 cm (2.87 in.) compared to the 30-yr annual average of 37.9 cm during the same period (SERCC, 2000). In order to collect more leachate samples, irrigation was applied using a solid set sprinkler with impact-rotor heads mounted on 91.4-cm (3-ft) risers. The sprinkler configuration was rectangular with sprinkler spacing of 18.3 m (60 ft) and mainline spacing of 9.2 m (30 ft). The resulting precipitation rate was nearly 10 mm/h. A 7.3-kw (10 hp) self-priming gasoline pump was used to pump water from the New River. In order to monitor the application rate, one clear plastic rain gage (non-recording type) was installed in the center of each plot.

During 6-16 October 1997, a total of 17.8 cm (7 in.) of irrigation was applied in six events. To incorporate irrigation into the water balance, the total depth of irrigation was calculated separately for each treatment. As the New River was the source of irrigation water, irrigation also affected the N balance since the river water contained inorganic- and organic-N. Hence, during each irrigation event, water samples were collected in duplicate at the beginning, in the middle, and at the end of the run. The six water samples thus obtained, were composited to obtain a single water sample; the sample was analyzed for NO_3^--N, NH_4^+-N, and total Kjeldahl-N (TKN) in the WQ laboratory using the TRAACS 800 automatic water quality analyzer. The concentrations of various N forms were converted into corresponding N loading rates (kg/ha) for each treatment separately since the precipitation rates varied between plots.

3.2.9. Field Operations

No-till corn (*Zea mays*) silage was grown at the field site for two years, 1997 and 1998. The plots were left fallow during the winter of 1997-1998. The field operations for each of the two seasons are described below.

1997 corn season

Soil samples were obtained from the field for a routine soil analysis to ascertain the nutrient status (except N) and liming requirement of the field. From each row of seven plots, four soil samples were obtained from a depth of 0-20 cm using a soil sampler for a total of 12 samples from the three rows of plots. At each of the 12 sites, two 20-cm long cores extracted within close proximity of each other were mixed. All twelve soil samples thus obtained were thoroughly mixed to obtain a composite sample. The composite sample was analyzed for nutrients and pH in the ST Laboratory of the CSES Department.

Based on the soil test results, application rates for phosphorus (P) and potassium (K) of 84 kg-P_2O_5/ha and 185 kg-K_2O/ha, respectively, were determined (VDCR, 1993). The soil analysis indicated that the field did not require any addition of calcium (Ca), magnesium (Mg), zinc (Zn), or manganese (Mn) (VDCR, 1993). Since the pH of the soil was 6.2, no liming was necessary since the optimum pH for corn is 5.5-6.5 (Tisdale et al., 1993). The corn variety chosen was Southern States 943 because of its resistance to gray leaf spot and maize dwarf mosaic, recurring problems at Kentland Farm (E. Bender, personal communication, Virginia Tech, Blacksburg, Va., 6 March 1997).

The plots had substantial weed growth, primarily ragweed. On 19 May, the field was sprayed with metalochlor 2.2 kg/ha a.i. (2 lb/ac), atrazine 1.8 kg/ha a.i. (1.6 lb/ac), and glyphosate 2.2 kg/ha a.i. (2 lb/ac) to control the weeds. On 21 May, the entire K requirement was applied as muriate of potash (MOP) at 308 kg/ha (624 g/plot) to supply 185 kg-K_2O/ha. To improve uniformity of application, each plot was divided into quarters and 156 g of MOP (metered volumetrically) was broadcast over each quarter.

To apply N and P below the surface, a furrow opener was assembled using components available at Kentland Farm and the BSE Department. The furrow opener consisted of a rippled coulter followed by a narrow chisel (about 2.5 cm wide). The chisel was equipped with wings to prevent the soil clods from falling back into the newly created furrow. Three sets of furrow openers were assembled on a tool bar at a spacing of 75 cm. A wooden plank was provided on top of the implement to add 136 kg of ballast weight to increase the depth of penetration of the furrow openers. The furrows created were about 7.5-8.5 cm deep and about 3.2 cm wide at the base. A furrow depth of 10 cm had been intended; however, the design of the implement proved to be a constraint in creating deeper furrows.

During 22-23 May, the plots were planted to corn. Simultaneously with the corn seeds, the starter N dose (37 kg/ha) as urea (80 kg/ha or 162 g/plot) and the entire P dose (84 kg-P_2O_5/ha) as triple super phosphate (TSP) at 183 kg/ha (390 g/plot) were applied subsurface. To apply the starter N and P, six rows of furrows were created in each plot at 75-cm spacing; this required two passes with the furrow-opening implement.

In the control plots, 3.6 g of TSP (1.2 g-TSP/plant), metered volumetrically, was spread uniformly over a 75 cm long aluminum angle and tipped into the furrow; hence TSP was applied for three corn plants at a time. In other plots with granule-N treatment, 3.6 g of TSP was mixed with 4.5 g of urea granules (1.5 g/plant) and applied uniformly with the angle for three plants at a time. In the plots with pellet treatment, TSP was applied with the angle and urea pellets (1.5 g/ea.) were applied using a wooden template that had markings at 25 cm, thus ensuring a 25-cm pellet spacing.

A soil sampler was used to plant corn 5 cm to the side of the centerline of the fertilizer furrow and at a depth of 5 cm; the spacing between successive hills was 25 cm. Two seeds were planted per hill in order to obtain the required and uniform plant population. In the pellet treatments, the corn seeds were placed adjacent to the pellet such that one pellet was dedicated to a hill. After planting the corn, the seeds and the fertilizer furrow were covered and compacted with the foot. On May 30, widespread germination was observed.

Most plots needed some replanting (less than 4.5% of the required plant population) which was completed on 10 June. To minimize edge effects and deer damage, corn was planted in the border areas on 10 June. During mid-June, sporadic insect damage was observed. To minimize insect damage esfenvalerate solution (700 mL/ha) was applied on June 20 with a backpack sprayer. On 28 June, the plots were thinned manually to one plant per hill to obtain a desired plant population of 53 333 plants/ha at a plant spacing of 25 cm and a row spacing of 75 cm. Each plot had 18 plants per row and six rows for a total of 108 plants.

Nitrogen fertilizer was sidedressed on 8 July. No N was applied to the control plots while 147, 73, and 221 kg-N/ha was subsurface-applied to the sufficient, deficient, and excessive treatments, respectively, as pellets or granules. Since the corn had already grown more than 1 m high, the tractor-drawn furrow opener could not be used. Hence, a push-type cultivator was used to make furrows for subsurface-fertilizer application. Earlier, inspection of the rooting pattern of corn of the same age in a production plot had revealed that making furrows 20 cm away from the plants would not damage the roots. Hence, the furrow for sidedress fertilizer application was made 20 cm away from the line of plants. The furrows were 3.5-5 cm deep and 3.2 cm wide. Since the furrows were made manually, it was difficult to maintain uniform depth and distance from the plants. The furrows were then cleaned with a hand hoe.

Urea granules were applied at 6, 3, and 9 g per plant to the sufficient, deficient, and excessive treatments, respectively, using the aluminum angle used for starter application. As in the starter application, the granular N dose was applied in a solid band, to three plants at a time. Four, two, and six 1.5-g urea pellets were applied per plant to the sufficient, deficient, and excessive pellet treatments, respectively, using suitable templates. Hence, the center distances between pellets in the sufficient, deficient, and excessive application rates were 6.25, 12.5, and 4.17 cm, respectively. After fertilizer application, the furrows were covered and compacted with the foot.

Despite herbicide application prior to planting, ragweed infestation became a serious problem during July. Hence, the herbicide dicamba (584 mL/ha a.i.) was applied with a backpack sprayer on 18 July with particular attention given to the weeds inside the plots. The weeds in the border and buffer areas were mowed on August 18.

To maximize silage yield, the crop was harvested between 30-40% dry matter. To ascertain crop dry matter, on 12 September, 12 whole stalks of corn from the two border rows as well as plants at the ends of the other rows were harvested at random from among the 21 plots. The corn stalks were run through the thresher of a combine. The pulverized mass of corn stalk was thoroughly mixed and about 200 g of the material was analyzed on a Koster® Crop Tester at Virginia Tech's College Farm. The dry matter content of the crop was determined to be 31% indicating that the crop was ready for harvest.

Corn silage was harvested manually with machetes on 18 September. In each plot, the two outermost rows of plants as well as one plant each at the start and end of each of the remaining four rows were removed. Only the 64 remaining plants from each plot were considered for yield and N content analysis. The plants were weighed on a spring scale with a capacity of 27.2 kg and readability of 45 g.

For analysis of N content of crop, one healthy plant was picked at random from each one of the four rows of plants. These plants were shredded in a chipper-shredder and about 1 kg of the shredded sample was stored in a pre-dried and weighed cloth sack. After crop samples were obtained from all the plots, the shredded samples were transported the same day to Virginia Tech's Agronomy Farm for drying.

The moist weights of the shredded samples were obtained by weighing them on a weighing scale with a readability of 1 g. The shredded samples were then dried to constant weight at a temperature of 43-49°C (110-120°F) in a drying chamber. The dried samples were weighed and their moisture contents were calculated on wet weight basis. Each dried sample was thoroughly mixed and a small portion of the mixed sample was ground in a laboratory mill and made to pass through a 1-mm screen and stored in a clean glass bottles. The 21 crop samples were analyzed for N content using the Kjeltech 1030 automatic analyzer at the Forage Testing (FT) Laboratory at Virginia Tech.

1998 corn season

Since the 1997-1998 winter had been warm and wet, heavy weed infestation occurred during the spring of 1998. On 25 April, the field was sprayed with 4.5 kg/ha a.i. (4 lb/ac) atrazine, 1.7 kg/ha (1.5 lb/ac) simazine, and 2.2 kg/ha a.i. (2 lb/ac) glyphosate.

Since difference in corn silage yields between treatments in 1997 had likely resulted in varying residual nutrient contents, prior to planting corn in 1998, nutrient (except N) and lime application rates were determined separately for each treatment. Two soil cores from the top 15-cm were obtained from each plot. For each treatment, the six cores thus obtained were composited to obtain one soil sample which was analyzed for nutrients and pH in the ST Laboratory of the CSES Department. No lime application was required since pH in all treatments ranged between 5.5 and 6.5 (Tisdale et al., 1993).

Since residual-K status varied in a very narrow range, a single application rate of 224 kg-K_2O/ha was determined (VDCR, 1993). The P application rate was determined at 50 kg-P_2O_5/ha for the control, pellet-excessive (PE) and pellet-sufficient (PS) treatments. For the remaining four treatments, the P application rate was 34 kg-P_2O_5/ha. As in 1997, supplemental Ca, Mg, Zn, and Mn were not required for any treatment. The N application rate remained unchanged from 1997.

As in 1997, K was surface-broadcast as MOP at 758 g/plot (374 kg/ha) on 15 May 1998. On 18 May, corn (Southern States 943) was planted using the same procedure employed in 1997. Nitrogen starter (37 kg-N/ha) as urea and the total P dose as TSP were subsurface-banded in a furrow 5 cm to the side of the corn seeds the same day. A push-type cultivator was used to create furrows, 4.5-6.5 cm deep and 2.5 cm wide. The fertilizers were applied using the same techniques employed in 1997.

Widespread germination was observed 1 week after planting. Missing hills (1.7%) were replanted on 1 June to obtain the desired plant population. Due to resurgence of weeds, primarily ragweed and johnson grass, dicamba 365 mL/ha a.i. was applied on 22 June. The plots were thinned to one plant per hill (108 plants/plot) on 24 June. Nitrogen fertilizer was sidedressed on June 29 using the same procedure employed in applying sidedress fertilizer in the 1997 corn season. Again, sidedress N was applied 20 cm away from the corn plants. Due to heavy weed growth, the buffer and border areas were mowed on 12 August.

After determining dry matter content of the crop (using the procedure followed in 1997), the crop was manually harvested on 16 September. As in 1997, the two outermost rows of plants as well as one plant each at the start and end of each of the remaining four rows in each plot were removed. Only the 64 remaining plants from each plot were considered for yield and N content analysis. However, due to weed infestation (primarily of johnson grass) and retarded germination, a few weak plants were observed in all plots except Plot Nos. 18 (granule-sufficient) and 19 (pellet-excessive). In two plots, Nos. 8 (pellet-sufficient) and 13 (pellet-deficient), one row in each plot had to be discarded; hence in these plots, only 48 plants were considered in calculating yield per unit area. In the remaining plots, in lieu of the weak or broken plants, plants at the ends of the rows were considered. Hence, in all other plots, except Plot Nos. 8 and 13, 64 plants/plot were considered in calculating the yield.

For analysis of corn N removal, the procedure used in 1997 was followed with regard to shredding, drying, and sample preparation. As in 1997, the prepared crop samples were analyzed for their N contents using the Kjeltech 1030 automatic analyzer at the FT Laboratory at Virginia Tech.

3.3. Laboratory Experiments

Objective 2: Quantify the dissolution, mineralization, and NO_3-N^- movement of subsurface-applied N pellets versus granules

To achieve Objective 2, laboratory experiments were conducted. The laboratory experiments that were conducted, included, dissolution, incubation, and leaching column studies. The dissolution experiment was conducted to study the impacts of specific surface area (L^2/M) on dissolution rate. The incubation experiment was conducted to study the mineralization (urea hydrolysis + nitrification) rates of pellets versus granules. The leaching column experiment was conducted to compare NO_3^--N movement from pellets and granules. Soil physical and chemical properties were required for the laboratory experiments and modeling.

Soil required for the laboratory experiments was obtained from the site of the field experiment. On 24 October 1997, crop residues were removed from three locations in the border areas. About 250 L of soil from the top 5-10 cm was removed with a front-end loader. The soil was transported to Virginia Tech's Prices Fork Farm and passed through a 6.35-mm sieve. The sieved soil was spread on a tarpaulin in a 10-15 cm layer to air-dry in a covered area. The soil was occasionally stirred and mixed with a rake. The soil was air-dried for one month after which it was passed through a 2-mm sieve. After thorough mixing, the sieved soil was air-dried for one week. The moisture content of the air-dried soil was determined gravimetrically using eight samples drawn from different locations and representative of the entire depth. The air-dried soil was then stored in containers with lids or packed into leaching columns to prevent change in moisture content.

3.3.1. Soil Physical and Chemical Properties

Some soil properties were measured using air-dried and sieved soil brought from the site of the field experiment. Other soil properties were measured using undisturbed soil samples brought from the plots. Selected soil properties are given in Table 3.3.

Table 3.3. Selected properties of the Ross soil series (top 10-cm) at the field site

Properties	Values	Method of analysis
Saturated hydraulic conductivity (K_s)*	0.92 cm/h	Constant head
Bulk density (ρ_b)*	1.34 g/cm^3	Core
Particle density (ρ_p)*	2.66 g/cm^3	Pycnometer
Porosity (f)*	49.6%	Calculated
Textural class	Loam	Calculated
Particle size distribution (%)†		Pipette method
Sand	35.7	
Silt	48.3	
Clay	16.0	
Soil solution pH (1:1)*	6.1	Glass electrode
Organic matter content†	7.6%	Walkley-Black
Cation exchange capacity (pH = 7)†	32.95 cmol$^+$/kg-soil	ICP spectrograph
Urease activity‡	183.46 μg-urea·g^{-1}-soil·5 h^{-1}	Determination of urea remaining

* average of four samples
† average of two samples
‡ average of three samples obtained from the soil used for the dissolution experiment

Physical properties

1. Saturated hydraulic conductivity (K_S)

Vertical K_S of undisturbed samples was measured in the LW Laboratory. Lateral K_S was considered to be negligible assuming that precipitation was uniform. The K_S was used to estimate unsaturated hydraulic conductivity (K_{US}) and simulate NO_3^--N movement in the field under saturated conditions.

Four plots were selected through randomization from among the 21 plots. One undisturbed core sample was obtained from roughly the center of each of these four plots. To extract a core sample, the site from which the sample was to be extracted was cleared of vegetation; stony sites were discarded. Three sample cylinders, two of them 2.54 cm in height and one 5.08 cm in height were inserted into the sleeve of the sampler with the 5.08 cm cylinder in the middle. The ρ_b sampler was driven down into the soil to a depth slightly exceeding 12.7 cm (5 in.). The bottom 2.54-cm portion of the soil core was discarded and the remaining 10.16-cm soil core with a diameter of 4.83 cm was retained. Klute and Dirksen (1986) reported that sample cylinders 2-10 cm in diameter and 5-25 cm in height were reasonably practical for laboratory measurements

The sample cylinders were separated using a sharp knife; care was taken to minimize glazing on the soil faces. The upper and lower 2.54-cm soil cores were discarded while the middle 5.08-cm core was retained for K_S measurement. Hence the soil core represented a soil layer 5.08 cm (2 in.) thick 2.54 cm (1 in.) below the surface. Soil cores that were loose in the sample cylinders, had protruding or visible stones, or were disturbed during separation were discarded. The upper face of the soil core sample was marked. To prevent soil or moisture loss during transport to the LW Laboratory, the soil core samples were covered with parafilm.

In the LW Laboratory, after removing the parafilm covers, the bottom face of the soil core sample was covered with a double layer of cheesecloth and bound with a rubber band to prevent disintegration of the sample during saturation and handling. A circular piece of blotter paper that matched the diameter of the sample cylinder, was placed on the upper face of the soil core sample. The blotter paper was used to prevent erosive loss of soil while applying water on the samples during K_S measurement. The soil core samples were then saturated in a tray with about 4 cm depth of water for 24 h; wetting was from the bottom to reduce air entrapment (Klute and Dirksen, 1986).

A constant head apparatus was used to measure the K_S of the four soil core samples. Volumetric discharge (L^3) was measured for 20-min. durations 2, 6, 24, and 27 h after the start of the experiment. Saturated hydraulic conductivity (L/T) was calculated using the Darcy equation (Klute and Dirksen, 1986):

$$K_S = \frac{V \times L}{A \times t} \Delta H \quad [3\text{-}2]$$

where,

V = volumetric discharge (cm^3),

L = length of the soil column (cm) = 5.08 cm,

A = area of the soil core (cm^2) = 18.32 cm^2,

T = duration for which V was measured (min.) = 20 min., and

ΔH = hydraulic head difference across lower and upper faces of soil column (cm).

The mean K_S value was calculated by averaging the values obtained for the four samples. Mean K_S declined with time, being highest at 2 h and lowest at 24 h and registering a slight increase at 27 h. The change in K_S with time could be due to compaction of the soil column resulting in a reduction of macropores. The mean K_S value at 24 h (0.92 cm/h) was used because the well-drained Ross soil does not stay saturated for long periods of time.

2. Bulk density (ρ_b)

Field ρ_b of the soil was determined to calculate porosity and to pack the leaching columns and incubation pots. Porosity was required for the laboratory experiments as well as modeling. Bulk density was determined by the core method (Blake and Hartge, 1986a) using four undisturbed soil cores.

The soil core samples available after completing the K_S measurement were oven-dried at 105°C to constant weight, for about 60 h. After cooling the samples to room temperature in a desiccator for about 45 min., the weights of the soil cores were determined to the nearest 0.01 g. The weight of oven-dried soil divided by the volume of the cylinder yielded ρ_b. The mean ρ_b (1.34 g/cm^3) was calculated by averaging the ρ_b of the four samples. Bulk density values measured for other depths for neutron probe calibration were not used in the laboratory experiments since the soil from the top 10-cm of the soil profile was used for the laboratory studies.

3. Particle density (ρ_p)

Particle density was required to calculate porosity. The four soil samples that were used for determination of ρ_b were used for calculation of ρ_p using the pycnometer method (Blake and Hartge, 1986b). The oven-dried samples were ground and passed through a 2-mm sieve. The procedures described by Blake and Hartge (1986b) were followed. The experiment was conducted at constant temperature (22°C) and the specific gravity of water was adjusted for the room temperature. The mean ρ_p (2.66 g/cm^3) was obtained by averaging the ρ_p values of the four replications.

4. <u>Porosity (f)</u>

The porosity (49.6%) of the soil was calculated using the expression:

$$f = 100 \times (1 - \frac{\rho_b}{\rho_p}) \qquad [3\text{-}3]$$

5. <u>Soil moisture characteristic curve (SMCC)</u>

The SMCC was used in estimating the soil moisture content (as a function of tension) in the laboratory experiments and in modeling. Gravimetric moisture contents of the soil samples were determined at 5, 7.5, 33, 100, 300, and 1500 cbars (kPa). Thirty-three and 1500 cbars are widely accepted soil moisture tension values for field capacity and permanent wilting point.

Soil moisture contents at 5 and 7.5 cbars were determined using a tension table while moisture content at higher tension values were determined using pressure chambers in the CSES Department. Volumetric moisture contents for the soil samples were determined by multiplying the θ_m values by soil ρ_b (table 3.4). The plot of θ_v values versus corresponding tension values yielded SMCCs for both undisturbed soil core samples and repacked samples (fig. 3.5).

For the undisturbed samples, thirteen plots were selected and from each plot (through randomization), four 2.54-cm thick soil cores (4.83 cm diameter) were extracted at one time using the procedures described for soil core sample extraction and handling for K_S measurement. The top and bottom soil cores were discarded and the two 2.54-cm cores in the middle were retained for moisture content measurement. Hence, 26 soil core samples were transported to the LW Laboratory, two more than were required for the experiment. At each tension value, moisture content was determined on four undisturbed samples.

After removing the parafilm covers, the lower face of the soil core sample was covered with a double layer of cheesecloth. Prior to running the experiments, the samples were saturated from the bottom in about 1.5 cm of water for 24 h. The labeled soil core samples were assigned to different tension values through randomization taking care that no two soil core samples from the same cylinder were used for the same tension.

Table 3.4. Soil moisture contents (%) at different soil moisture tensions

Tension (cbars)	Undisturbed				Repacked			
	θ_m*			θ_v†	θ_m			θ_v
	Max.‡	Min.§	Mean‖		Max.	Min.	Mean#	
0	47.3	31.8	39.0	48.8	46.4	39.9	43.8	58.7
5	34.0	29.1	31.0	37.8	37.8	37.5	37.7	50.5
7.5	34.2	27.7	30.1	37.1	35.2	33.2	34.2	45.8
33	27.5	24.0	25.3	32.6	24.4	24.3	24.3	32.6
100	24.0	22.1	23.1	27.3	21.1	20.9	21.0	28.1
300	19.5	19.3	19.4	25.4	17.3	17.1	17.2	23.0
1500	19.9	13.6	15.6	20.0	10.1	09.9	10.0	13.4

* Gravimetric moisture content

† Volumetric moisture content

‡ Maximum

§ Minimum

‖ θ_m for 0 cbar is a mean of 24 samples while all other θ_m values are mean of four values each

\# θ_m for 0 cbar is a mean of 12 samples while all other θ_m values are mean of two values each

For the repacked samples, two replications were used for each tension value for a total of 12 samples. Compared with four replications for undisturbed samples, only two replications were used for the repacked samples because soil for the repacked samples was obtained from a smaller volume (about 250 L) of air-dried and sieved soil that had been thoroughly stirred.

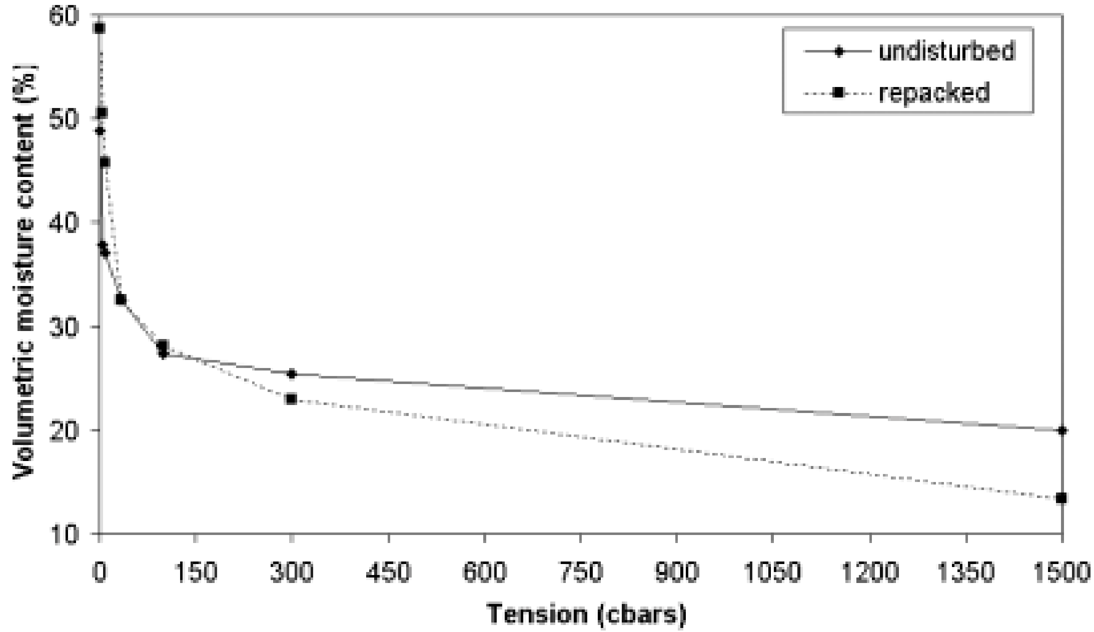

Figure 3.5. Soil moisture characteristic curve. Each data point represents an average of four and two samples for the undisturbed and repacked soil, respectively.

The sample cylinders used for the repacked samples were of the same size as the undisturbed samples. The bottoms of the sample cylinders were covered with a double layer of cheesecloth and retained with a rubber band. To pack the soil to field ρ_b, the amount of oven-dried soil required to fill the cylinder was weighed and poured into the cylinder in thin layers and compacted using a Proctor hammer until the required amount of soil was used to completely fill the cylinder to the top. The samples were saturated from the bottom as in the case of undisturbed samples. To minimize change in soil structure due to slaking of the oven-dried soil, a very shallow depth of water (about 3 mm) was used to wet the samples initially for the first 2-3 h (Klute, 1986). The water level was then raised to 1.5 cm for the remainder of the saturation period.

Tension table

Vomocil (1965) described the theory of operation of the tension table. The tension table was set up and operated following the procedures described by Ess (1994). After removing the cheesecloth bottoms, the saturated soil samples were weighed to the nearest 0.01 g and placed on the tension table. For the 5 cbars (50 cm) tension, six samples (four undisturbed and two repacked) were subjected to tension until drainage from the soil cores ceased. The procedure was repeated at 7.5 cbars (75 cm) tension for a separate set of samples. At both 5- and 7.5-cbar tensions, drainage ceased after 24 h.

The drained samples were removed from the tension table and weighed to determine the weight loss due to drainage. The soil cores were then oven-dried at 105°C to constant weight. Based on the saturated weights, the drained weights, and the oven-dried weights of the soil samples, the moisture contents of the soil samples were determined at saturation as well as at the specified values of tension. The average moisture content at a particular tension was determined separately for the undisturbed and repacked samples.

Pressure chamber

The procedure described by Klute (1986) was followed in measuring water retention at the higher tension values. For the 33- and 100-cbar samples, a single pressure chamber with a ceramic plate of 100 cbars bubbling pressure was used. For the 300- and 1500-cbar samples, separate chambers with ceramic plates with bubbling pressures of 300 and 1500 cbars were used, respectively. Prior to pressurization, the ceramic plates were soaked for at least 6 h. The cheesecloth bottoms were removed from the saturated samples and the samples were weighed to the nearest 0.01 g. The samples were then carefully transferred to the ceramic plates. The ceramic plates and samples were allowed to equilibrate by soaking them overnight.

Pressure was applied to the pressure chambers to produce the required tensions on the soil samples. The pressure was maintained on the chambers until drainage ceased indicating that the soil samples had reached equilibrium at the specified tension. For the 33- and 300-cbar samples, it was observed that 3 d was adequate to reach equilibrium. The 100-cbar samples were under tension for 6 d, for the first 3 d at 33 cbars. The 1500-cbar samples were kept under tension for 6 d.

After removal from the pressure chamber, the soil samples were weighed to the nearest 0.01 g to determine moisture loss while under tension. The soil samples were then oven-dried at 105ºC to constant weight. Based on the weight measurements taken, the saturated as well as the drained moisture contents were calculated. The average moisture content at a particular tension was determined separately for the undisturbed and repacked samples.

6. Particle size distribution

Particle size distribution affects both moisture and solute movement. The particle size distribution of two soil samples obtained from the soil brought from the field site to conduct laboratory experiments were determined in Soil Survey Research (SSR) Laboratory in the CSES Department. Particle sizes were determined using the pipette method (Day, 1982) after removing organic matter. Prior to the pipette analysis, the soil samples were treated with 0.5% (w/w) sodium hexametaphosphate (Na HMP) solution, a dispersing agent (Day, 1982) to completely disintegrate the soil flocs. Finally, mean of the particle size distribution of the two samples was used to determine the soil texture for the soil. Harris et al. (1980) obtained their soil sample for Ross soil from a site located within 10 m from the western boundary of the field (Lucian W. Zelazny, personal communication, Blacksburg, Va., 7 August 2000). Values reported by Harris et al. (1980) were 4.9% higher for clay and 6.0% lower for silt than values measured in this study.

Chemical properties

1. Soil solution pH

Soil pH was required to determine if lime application was required in the incubation and leaching column studies. Soil pH was also required for modeling nitrification. Soil pH was determined in duplicate using air-dried and sieved soil brought from the field experiment site. The samples used for pH analysis were composited samples; each sample was obtained by mixing soil obtained from four locations within the volume of the air-dried and sieved soil. These two samples were also used in the determination of organic matter content and cation exchange capacity. The soil samples were analyzed for pH in the SSR Laboratory. The glass electrode-calomel electrode method (McLean, 1982) was to used to measure pH using a soil:water ratio of 1:1.

2. Organic matter (OM) content

Soil OM content was determined to estimate the amount of organic N in the soil. Soil OM content was measured in the SSR Laboratory with the Walkley-Black procedure (Nelson and Sommers, 1982), in duplicate using air-dried and sieved soil.

3. Cation exchange capacity (CEC)

The CEC is an important index about the capacity of the soil to retain NH_4^+-N on the soil complex, which in turn, affects N transformation and N fate. The CEC was measured in the SSR Laboratory in duplicate using air-dried and sieved soil. The soil samples were extracted with 1 Normal ammonium acetate solution (pH = 7) and amount of adsorbed cations was determined using the inductively coupled plasma (ICP) spectrograph (Chapman, 1965).

4. Urease activity

Urease activity is indicative of a soil's ability to hydrolyze urea-N into ammoniacal-N, especially when comparing different soils for their hydrolyzing potentials. Urease activity was determined for three samples obtained from the soil that was used for the dissolution experiment. Five grams (oven-dried basis) of air-dried and sieved (2 mm) soil was pre-incubated for 7 d at 37ºC, the temperature at which urea hydrolysis was eventually measured.

Following 7 d of pre-incubation, the soil sample was mixed with 5 mL urea substrate solution (2 mg-urea/mL) and incubated for 5 h at 37ºC (Tabatabai, 1982). Residual urea concentration in the soil was determined by the colorimetric method using diacetyl monoxime (DAM) described by Tabatabai (1982). Urease activity was expressed as an average of the three sample values as amount of urea hydrolyzed per gram of soil in 5 h.

3.3.2. Dissolution Study

The use of urea pellets could potentially impact the availability of dissolved urea for transformation to plant-available N-forms due to pellets' slower dissolution rates compared with granules. Hence, the dissolution rate, as well as amount of movement of dissolved urea using the center of mass concept (Luis and McLaughlin, 1992), was investigated. Rate of N transformation would likely increase with increased center of mass of dissolved urea from the plane of placement. To study the dissolution rate, in addition to 1.5-g pellets and granules, 0.5-, 1.0-, and 2.0-g pellets were used to obtain a better understanding of the influence of particle size or specific surface area on dissolution rate. The hypotheses tested were as follow:

1. **Null hypothesis: Urea dissolution rate (% weight loss/time) is unaffected by particle size.**

   Alternative hypothesis: Urea dissolution rate decreases as particle size increases (specific surface area decreases).

2. **Null hypothesis: The distance of center of mass of dissolved urea from the plane of placement is unaffected by the urea form (pellet versus granules).**

   Alternative hypothesis: Center of mass of dissolved urea is at a greater distance from the plane of placement in granules than in 1.5-g pellets.

The particle densities (after calculating the particle volume) and specific surface areas of the pellets were calculated from the pellets' dimensions (Table 3.5). For granules, published values (Singh et al., 1994) were used (Table 3.5).

Table 3.5. Specific surface areas, particle volumes, and particle densities of urea particles of different sizes

Particle form/size	Specific surface area (cm^2/g)	Particle volume (cm^3)	Particle density (g/cm^3)
Granule	19.60	0.01*	1.22†
0.5-g pellet	6.31	0.46	1.08
1.0-g pellet	4.33	0.84	1.20
1.5-g pellet	3.77	1.26	1.19
2.0-g pellet	3.68	1.70	1.17

* Based on a particle diameter of 0.25 cm (Singh et al., 1994)

† Based on an average particle weight of 0.01 g (Singh et al., 1994)

Dissolution rate measurement

A dissolution rate experiment was performed to test Hypothesis 1. Complete dissolution times were measured in a preliminary experiment to determine the sampling frequencies and sampling intervals for all treatments. Sample cylinders 2.54 cm high with an ID of 4.8 cm were filled with oven-dried and sieved (2 mm) soil to field ρ_b. The soil was packed to field ρ_b by filling the cylinder in four equal increments with known volumes of soil; each increment was compacted to the required depth using a specified number of strokes of the Proctor Hammer.

The moisture content of the packed soil was raised to 75% of field capacity by applying distilled water on the soil core surface; the amount of water required was calculated using the SMCC (fig. 3.5). During the leaching column study (Sec. 3.3.4), it had been observed that water percolation rate decreased considerably in the 12 - 18-cbar range. Hence, it was assumed that the soil moisture tension corresponding to moisture content at field capacity was 15 cbars. However, even in the field capacity range, the soil (under repacked conditions) was still too wet to allow field operations for fertilizer application. Hence, a lower θ_v (31.4%), corresponding to 75% field capacity moisture content was used; the corresponding soil moisture tension was 30-31 cbars. After applying water, both faces of the soil core were covered with parafilm and the core was stored at 20°C for 48 h to allow uniform distribution of moisture in the soil core.

After 48 h of storage, the treatments were applied to the soil cores in single replication for the preliminary experiment. In the case of pellets, one pellet each was applied between two soil cores. In the case of granules, 1.5 g of granules was applied uniformly in a circle of about 4.5 cm diameter; this application rate corresponded to 147 kg-N/ha as urea in a subsurface band, the sufficient N application rate as sidedress in the field experiment. To ensure contact between the upper and lower soil cores, a weight was placed on the upper core. The pellet or granules was examined at regular intervals by removing the upper soil core to estimate the extent of dissolution. The approximate complete dissolution times for the granules, 0.5-g pellet, 1.0-g pellet, 1.5-g pellet, and 2.0-g pellet were 8.5, 23.5, 45.0, 60.0, and 73.0 h, respectively.

The procedure for preparing the soil cores and applying the treatments in the dissolution rate experiment was identical to the preliminary experiment, with three replications per treatment. The selected pellets were within ±0.01 g of the nominal pellet weight. After application of treatment to the pair of soil cores, the interface of the soil cores was pressed together to ensure proper contact and sealed with electric insulation tape to prevent moisture loss.

The sampling interval was based on the approximate complete dissolution time obtained from the preliminary experiment for a total of five sampling events in each treatment. The sampling intervals were spaced apart in multiples of 1.5 h except for the time of last sampling when the time interval was selected so as to sample very close to the time of complete dissolution without exceeding it. The sampling intervals for the various treatments were:

granules – 1.5, 3.0, 4.5, 6.0, and 7.5 h,

0.5-g pellet – 3, 6, 9, 15, and 22 h,

1.0-g pellet – 3, 6, 12, 24, and 43 h,

1.5-g pellet – 6, 12, 24, 48, and 57 h, and

2.0-g pellet – 6, 12, 24, 48, and 72 h.

Due to a more rapid initial dissolution rate (as observed during the preliminary experiment) the treatments were sampled at shorter intervals in the beginning. Faster dissolution in the initial stages was likely due to the rapid dissolution of the edges on the pellets. Sampling at 1.5-h multiples allowed for comparison between treatments; for example, at 6 h, percent weight loss for all treatments could be compared.

For the pellet treatments, at each sampling event, soil particles adhering to the pellet were carefully brushed off. The moist pellet was weighed (±0.01 g) and dried in a forced convection oven at 105-110°C for 0.5 h to obtain the net weight of pellet. In the case of granules, soil clung to the particles making it difficult to separate the soil without risking the loss of smaller urea particles. To determine the weight of soil adhering to the granules, the oven-dried urea particles and soil were mixed with distilled water and the resulting solution-suspension filtered through a pre-weighed Whatman No. 42 filter paper (ashless). Additional distilled water was poured over the filter paper to wash out any urea that could have been retained on the filter paper. The filtrate was discarded and the filter paper and soil was oven-dried at 105°C for 24 h. The weight of soil retained on the filter paper was determined by subtracting the weight of the filter paper from the weight of soil plus filter paper.

Titration using the Karl Fisher (KF) autotitrator was likely the most accurate method for determining moisture content of urea samples (F. Agblevor, personal communication, Blacksburg, Va., 24 February 1997). However, since a KF autotitrator was unavailable in the BSE Dept. and only a few samples needed to be analyzed at odd hours, the titration method was not used. The possibility of using infrared (IR) drying was also examined. Even though the IR method is an accepted method of determining moisture content of urea, this method was not used since it required a sample size in the range of 1-1.5 g (D. Kopec, personal communication, Arvada, Colo., 1 March 1998).

Hence, the oven-drying method was examined for its feasibility in removing moisture from urea in a preliminary experiment. It was observed that when a urea particle was placed in unsaturated soil (without hydrostatic pressure on the particle surface), moisture penetrated into the particle, probably as vapor to a rather shallow depth. Consequently, the urea particle remained intact and firm with very little urea paste on the surface. When such pre-weighed particles were oven-dried at 105-110°C for 0.5 h, no volatilization loss of NH_3 was detected.

Center of mass measurement

A center of mass experiment was conducted to test Hypothesis 2. The experiment involved estimation of dissolved urea distribution in the soil after a certain time. Moisture distribution in the soil core as a function of its distance from the plane of fertilizer application was also studied. The urea form (pellet versus granule) would likely affect moisture distribution due to differences in local osmotic potential, thereby, impacting urea movement.

In this experiment, the treatments were1.5-g pellet and granules, with each treatment being applied in triplicate. The air-dried and sieved (2 mm) soil used in this experiment was oven-dried at 110°C for 48 h to destroy all urease enzymes to prevent urea hydrolysis during the experiment. Citing published research, Bremner and Mulvaney (1978) reported that oven-drying soil at 105°C completely eliminated urease activity. Sadeghi et al. (1989) dried soil samples at 110°C for 48 h to eliminate urease activity though some soils required additional chemical treatment. To ensure that urease had been completely destroyed, one soil sample obtained from about 1.5 kg of oven-dried soil was analyzed for urease activity using the method of Tabatabai (1982). Oven-drying Ross soil at 110°C completely eliminated urease activity.

The sample cylinders used in this experiment had an ID of 4.8 cm and were 5.1 cm high. After weighing out the amount of soil required to pack one cylinder (124 g), 29 mL of DDI water was thoroughly mixed to raise the θ_v of the soil to 31.4%, or 75% of field capacity (30-31 cbars). Moist soil was poured into the cylinder using a sterilized scoop and then packed with a glass rod. After pouring all of the moist soil, the Procter Hammer was used to compact the soil with four strokes. A cylinder of the same ID was taped to the top of the sample cylinder to prevent soil from spilling out during compaction.

The treatment was then applied between two soil cores ensuring that the pellet (or granules) was embedded to equal depth in both soil cores. Otherwise, the treatment application was performed in a manner similar to the dissolution rate experiment. After 60 h, the time required for complete dissolution of the 1.5-g pellet, the experiment was terminated for both treatments. The 5-cm soil core was sectioned into five 1-cm segments taking care to note the location of each segment within the soil core. Urea-N concentrations in the soil segments were determined with the modified colorimetric method using diacetyl monoxime (Bremner, 1982).

All colorimetric methods require a calibration graph of light absorbance versus known urea-N concentrations in a wide range of strengths. Care must be taken to ensure that urea-N concentration in the soil sample remains within the range or close to the calibration plot values. To avoid extrapolation, the amount of soil used for the sample as well as volume of the extracted filtered aliquot was adjusted by segment through trial and error. The two outermost segments required 10 g of soil each, the remaining three segments required 5, 2.5, and 1.25 g with progressively smaller soil samples required for the segments closer to the plane of urea application. Similarly, the aliquots used were 10 mL for the two outermost segments while for the remaining segments, 1-mL aliquots were used. Such an approach ensured that urea-N concentrations were determined with the calibration plot, with a minimum of extrapolation. The remaining soil was oven-dried at 105°C to constant weight to determine its moisture content. Hence, 60 soil samples were analyzed for urea and moisture contents in the experiment.

After determining urea amounts in each of the ten 1-cm sections, urea amounts in the top and bottom 1-cm sections, second and ninth 1-cm sections, and so on, were added, yielding five urea amounts, each corresponding to an imaginary 1-cm segment. Urea amount in each segment was expressed as percent of the total urea recovered.

The total urea recovery was 101.2 and 98.9%, respectively, in granules and pellets. More than 100% urea recovery in granules could have been due to the use of the calibration plot for determining urea concentrations in samples. Percent urea in each segment was assumed to be analogous to an imaginary force acting through the center of its segment. Using the principle of moments, the five imaginary forces (F_1, F_2, .., F_5) were replaced by an imaginary resultant force (R) acting a certain distance away from the reference plane (O-O) (fig. 3.6). The distance thus calculated was the center of mass (D) for the treatment (fig. 3.6).

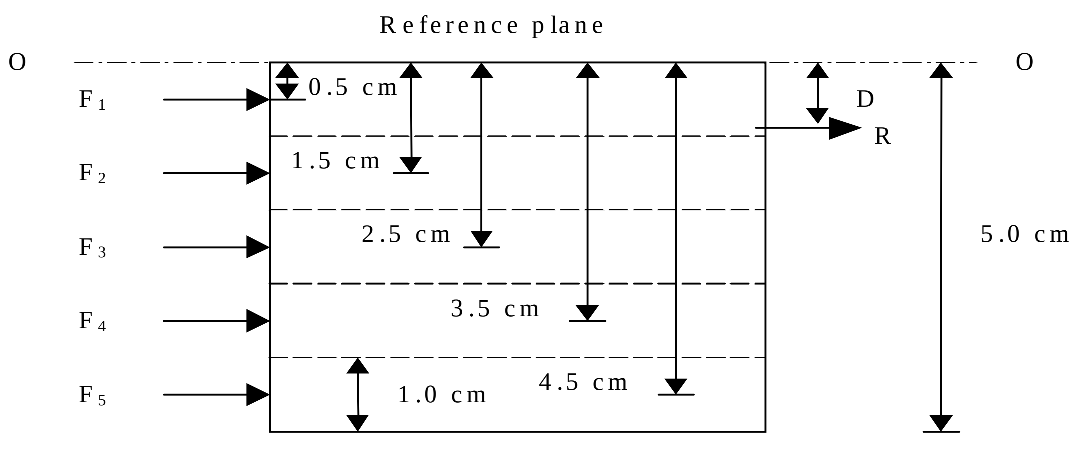

Figure 3.6. Analogy of resolution of forces applied to a soil core to calculate the center of mass of dissolved urea.

Under equilibrium conditions, the equation of the summation of moments (assuming counter-clockwise moments to be positive) can be written as follows:

$$M = F_1 \cdot d_1 + F_2 \cdot d_2 + F_3 \cdot d_3 + F_4 \cdot d_4 + F_5 \cdot d_5 - R \cdot D = 0 \qquad [3\text{-}4]$$

or,

$$D = (F_1 \cdot d_1 + F_2 \cdot d2 + F_3 \cdot d_3 + F_4 \cdot d_4 + F_5 \cdot d_5) / R \qquad [3\text{-}5]$$

where,

M = moment (percent urea·cm),

F = percent urea in segment,

D = force arm (cm) (d_1 = 0.5 cm, d_2 = 1.5 cm, …. d_5 = 4.5 cm), and

R = resultant (100%).

Using Eq. [3-5], the centers of mass were calculated separately for each of the three replications in the pellet and granule treatments. After ensuring that the data set was normally distributed, the data set was subjected to the Student t-test.

3.3.3. Incubation Study

An incubation study was conducted to evaluate the impact of urea particle specific surface area (SSA) on N mineralization processes, namely, urea hydrolysis and nitrification. Further, pH changes were also monitored since nitrification results in acidification. There were four treatments, control (no N), granules (1.5 g), 0.5-g pellet, and 1.5-g pellet, with each treatment being applied in triplicate.

The control treatment was included to monitor background nitrification rate. The primary focus of the study was the comparison of mineralization and acidification between granules and 1.5-g pellets. The 0.5-g pellet was included to obtain more information regarding the role of SSA in mineralization and acidification. The hypotheses tested in this study were as follow:

1. **Null Hypothesis: Rate of urea hydrolysis (percent urea hydrolyzed in 7 d) is unaffected by the fertilizer treatment.**

   Alternative Hypothesis: Rate of urea hydrolysis is affected by the fertilizer treatment.

2. **Null Hypothesis: Rate of urea hydrolysis (percent urea hydrolyzed in 7 d) is unaffected by the urea form (1.5-g pellet and granules).**

   Alternative Hypothesis: Rate of urea hydrolysis is higher in granules than in 1.5-g pellets.

3. **Null Hypothesis: Nitrification rate (amount of NO3--N recovered after 35 d) is unaffected by the treatment applied.**

Alternative Hypothesis: Nitrification rate is affected by the treatment applied.

4. **Null Hypothesis: Nitrification rate (amount of NO3--N recovered after 35 d) is unaffected by the urea form (1.5-g pellets and granules).**

   Alternative Hypothesis: Nitrification rate is higher in granules than in 1.5-g pellets.

5. **Null Hypothesis: pH is unaffected by the fertilizer treatment applied.**

   Alternative Hypothesis: pH is affected by the fertilizer treatment applied.

6. **Null Hypothesis: pH is unaffected by the urea form (1.5-g pellets and granules).**

   Alternative Hypothesis: pH is lower in granules than in 1.5-g pellets.

Hypothesis 1 compared the urea hydrolysis rates of 0.5-g pellets, 1.5-g pellets, and granules. Granules and 1.5-g pellets were compared with respect to their urea hydrolysis rates using Hypothesis 2 only if Hypothesis 1 was rejected. The nitrification rates of all treatments were compared using Hypothesis 3. The nitrification rates of granules and 1.5-g pellets were compared with Hypothesis 4 only if Hypothesis 3 was rejected. The pH values of all treatments were compared using Hypothesis 5. Hypothesis 6 compared pH values between granules and 1.5-g pellets only if Hypothesis 5 was rejected.

Moisture content, inorganic-N, and total-N status of the soil were determined in duplicate for the experiment. The soil samples were analyzed for NO_3^--N, NH_4^+-N, and total-N at Brookside Laboratories, Inc. using the procedure described in Sec. 3.2.7. The experiment was conducted in plastic containers with a square cross-section and a slightly increasing taper towards the mouth; the average dimensions of the container were 9.25 cm $\times$ 9.25 cm $\times$ 8.8 cm (L $\times$ W $\times$ H).

Air-dried and sieved (2 mm) soil was packed to field ρ_b up to half-depth of the container using a fixed number of strokes of the Proctor Hammer applied over a wooden block with dimensions of 8.5 cm $\times$ 8.5 cm $\times$ 4 cm. After adjusting for residual moisture content, enough DDI water was sprinkled on the soil surface to raise θ_v to 31.4% (75% of field capacity corresponding to a soil moisture tension of 30-31 cbars). The granules were sprinkled uniformly over the soil surface taking care not to apply granules close to the edges. The 1.5-g pellet was applied at the center of the square soil surface. The 0.5-g pellets were applied in a triangular configuration with the pellets being applied approximately at the corners of an equilateral triangle having sides equal to 6 cm. After applying the treatments, the remaining soil was added to the container and compacted to field ρ_b. Again, DDI water was sprinkled on the soil surface to raise θ_v to 31.4% in the entire soil volume. In the fertilizer treatments, the urea-N concentration was 686.6 µg-N/g-oven dry soil.

The incubation experiment was conducted in the LW Laboratory's Environmental Chamber at a constant temperature of 20°C and relative humidity of 85%. Seventy-two plastic pots were incubated with 18 pots per treatment. The pots were covered to reduce moisture loss; however, holes were made in the lids to allow for air exchange. There were six sampling events: 7-, 14-, 21-, 35-, 49-, and 63-d after starting the experiment. The first three sampling events were spaced 7 d apart while the remaining events were spaced 14 d apart because it was expected that N transformations would be more rapid in the early stages. At each sampling event, 12 pots (three per treatment) were removed for sampling.

For the first sampling event (7 d), a thin layer of soil in the vicinity of fertilizer application was scraped and used for pH analysis. For analysis of urea-N, NH_4^+-N, NO_3^--N, total-N, and moisture content, the entire soil mass was thoroughly mixed and about 100 g of soil was set aside for the analyses. The fertilizer treatments were immediately analyzed for urea by the colorimetric method using DAM (Bremner, 1982). The results of the urea analysis were reported as µg-urea/g-oven dry soil, after adjusting for soil moisture content. Ten grams of the moist soil was used for pH analysis (soil:water ratio of 1:1) using the glass electrode-calomel electrode method (McLean, 1982). Soil for NH_4^+-N, NO_3^--N, and total-N analyses was dried at 65°C and analyzed at Brookside Laboratories, Inc. using the procedure described in Sec. 3.2.7.

During the first sampling event, free NH_3 was detected in all fertilizer treatments though it was stronger in the 1.5-g pellet treatment. Hence, for the next two batches of samples, the entire soil mass was transferred to an air-tight plastic container. The soil was thoroughly mixed inside the container and allowed to sit for 10-15 min. to allow for the reduction of NH_3 to NH_4^+ (R. Reneau, personal communication, Blacksburg, Va., 15 March 1998). No NH_3 was detected in the remaining batches.

Sampling of the remaining batches was performed in a similar manner with some modifications. Since urea recovery was less than 5% in the first batch of samples, no urea analyses were performed on the subsequent batches. For pH analysis, 10 g of moist soil obtained after thorough mixing of the entire soil mass was used. Further, soil samples for the analyses of NH_4^+-N, NO_3^--N, and total-N were dried at 35-40°C (Bates, 1993) in a forced convection oven since it was likely that higher drying temperature had contributed to greater loss of NH_4^+-N.

3.3.4. Leaching Column Study

The leaching column (LC) study was conducted to investigate the impact of urea form (pellet versus granule) on NO_3^--N leaching under controlled conditions in the laboratory. Compared to the field study, a laboratory study could reduce random error (e.g. local variations in soil properties). Further, since the study was conducted at constant temperature (20°C), the possibility of temperature × fertilizer form interaction effect on N transformation, as mentioned by Singh and Beauchamp (1987) was avoided.

The LC study was designed to investigate not only the NO_3^--N concentration in leachate from the two fertilizer treatments (at a point in time) but also the possible existence of different trends of NO_3^--N leaching as affected by urea form. The existence of different trends in NO_3^--N leaching from pellets and granules would also corroborate the results of the incubation study since the LCs also allowed for incubation. Residual inorganic-N amounts in different layers in the LCs were also compared for the different treatments after the experiment was concluded.

There were three treatments in the LC study, three 1.5-g pellets, 4.5 g granules, and control (no N), with three replications per treatment for a total of nine columns. The control treatment was included to observe background NO_3^--N movement under zero-N application. Inorganic-N and total-N status of the soil used in the experiment were determined in duplicate. The soil samples were analyzed for NO_3^--N, NH_4^+-N, and total-N at Brookside Laboratories, Inc. using the procedures described in Sec. 3.2.7. The study was conducted for 2 months.

One objective of the leaching column study was to compare the time series of NO_3^--N concentration in leachate among the different treatments. The NO_3^--N leaching trends were compared graphically for all treatments to determine if the trend of NO_3^--N leaching was affected by the treatment applied.

The second objective of this study was to compare residual soil inorganic-N in different layers of the column among treatments. The following hypotheses were tested to achieve this objective:

1. **Null Hypothesis: Inorganic-N concentration is unaffected by the treatment.**
   Alternative Hypothesis: Inorganic-N concentration is affected by the treatment.
2. **Null Hypothesis: Inorganic-N concentration is unaffected by the fertilizer treatment.**
   Alternative Hypothesis: Inorganic-N concentration is higher in the pellet treatment than granules.

Hypothesis 1 allowed for comparison of inorganic-N among all treatments in the top-third, middle-third, and bottom-third of the leaching column, as well as for the entire column. If Null Hypothesis 1 was rejected, Hypothesis 2 was tested.

Leaching column construction

The leaching column (fig. 3.7) was constructed using a 91.4-cm (36 in.) long Schedule 40 PVC pipe of 20.3-cm (8 in.) nominal diameter. Three pieces of 7.6 × 7.6 × 0.6 cm (3 × 3 × 3/16 in.) mild steel (MS) angle, each about 2.5 cm wide, were bolted radially (at 120° displacement) on the inside of the PVC pipe. The angles were bolted flush with one end of the PVC pipe. A circular plexiglass (1.0 cm thick) plate of diameter 20.1 cm (equal to the ID of the PVC pipe) comprised the LC base. In the center of the plate, a hole of suitable size was drilled and threaded with a suitable tap to accommodate a 3.2-mm (0.l25-in.) hose connector. A 0.6-cm (0.25-in.) ID Tygon® tubing about 10 cm in length, was attached to the hose connector to drain the column.

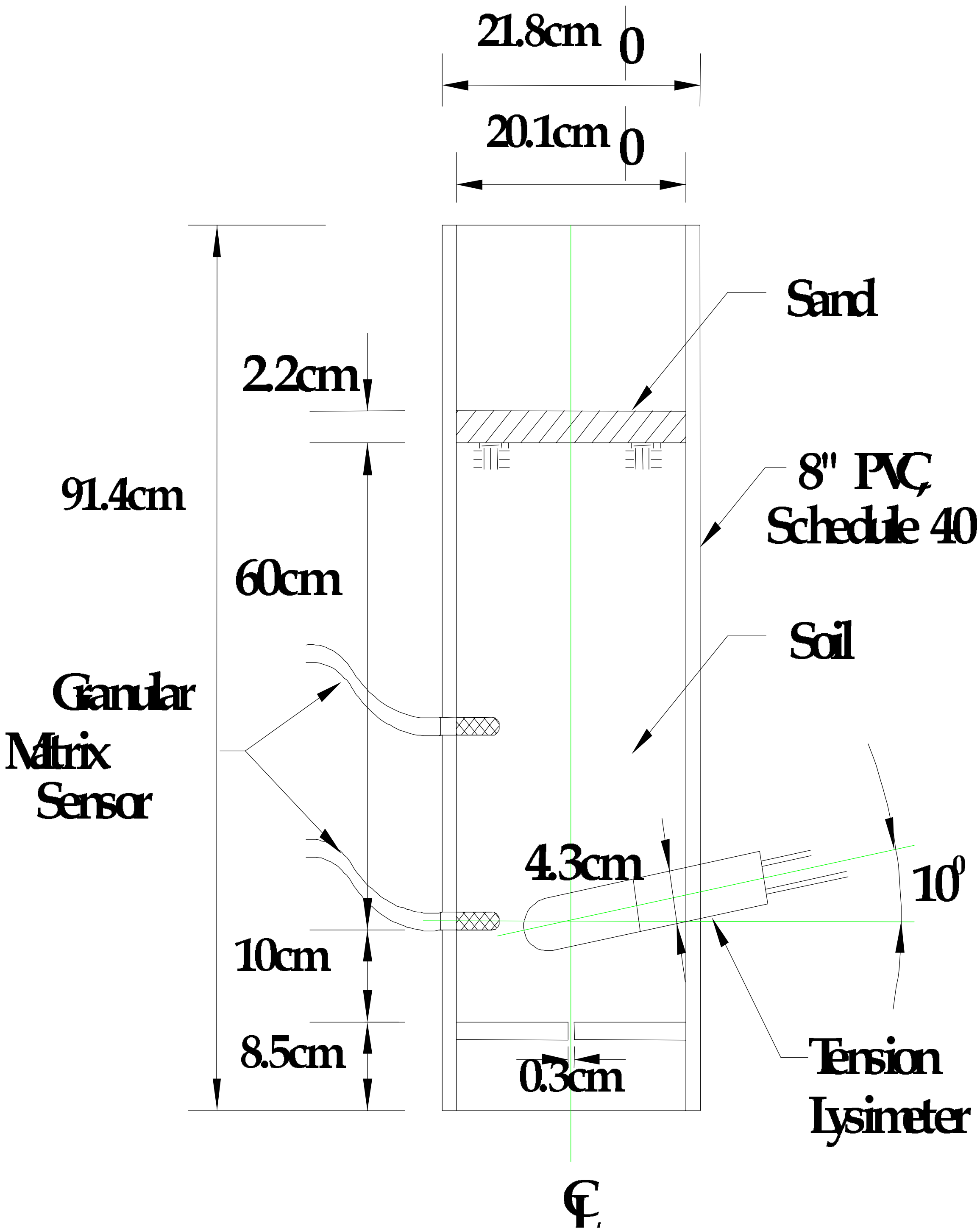

Figure 3.7. Schematic of leaching column

The plexiglass plate was bolted on the three MS angles using 0.8 cm (5/16 in.) countersunk bolts. Hence the surface of the plexiglass plate was located 82.9 cm from the top of the pipe. Silicon grease was smeared over the bolt heads to prevent leakage. The gap between the plexiglass plate and PVC pipe was sealed with silicone caulk to prevent leakage through the interface. The other end of the Tygon® tubing attached to the hose connector was run outside the PVC pipe through a hole in the pipe wall.

Leaching column packing and instrumentation

A fine nylon screen having a diameter that matched the ID of the PVC pipe was placed at the bottom of the LC. Two 185-mm diameter Whatman No. 4 filter papers were placed over the screen to prevent the soil from blocking the hose connector hole at the bottom. The moisture content of the air-dried and sieved soil used for packing the LCs was determined by the gravimetric method. After adjusting for the residual moisture content, 2.36 kg of air-dried soil was required to pack 5 cm of the column depth to a field ρ_b of 1.34 g/cm^3. After pouring the soil into the PVC pipe, the soil was leveled by shaking the pipe and tamping with a 12.7-mm thick steel plate with a diameter of 19.8 cm. The soil surface was compacted uniformly with a Proctor Hammer with a 2.5-kg (5.5-lb) mass and a diameter of 5.1 cm (2 in.). A 75-cm long 10 × 10-cm wooden beam was used to remove the ridges and achieve the final compaction. A steel tamping plate with the same ID as the leaching column was used to level the soil surface. Before pouring the next batch of soil, the compacted soil surface was scratched with a sharp piece of wood to reduce layering (N. Persaud, personal communication, Blacksburg, Va., 20 November 1997). After packing to a depth of 55 cm, the LCs were transported to the LW Laboratory.

The circumference of the soil surface was grooved with a wooden wedge and bentonite slurry was poured into the groove. Care was taken to ensure that bentonite slurry was confined to the periphery of the soil surface. Bentonite slurry was used to eliminate preferential flow between the soil column and the pipe wall. Azevado et al. (1996) used molten paraffin wax while Li and Ghodrati (1994) used silicone sealant in 5- cm increments to prevent preferential flow. Under moist soil conditions prevalent in the column, bentonite slurry would likely provide a more flexible and effective sealing medium than either wax or silicone because moist bentonite adhered well to both the soil and the PVC pipe.

To minimize soil dispersion, the LCs were saturated with 0.005 M calcium sulfate ($CaSO_4$) solution (Azevado et al., 1996). One pore volume equivalent of 0.005 M $CaSO_4$ (after adjusting for the residual moisture content) or 6.13 L was applied to each of the LCs. To prevent surface sealing and compaction due to the action of falling water, the soil surface was covered with a double layer of 185-mm diameter Whatman No. 4 filter paper. A plastic bucket with an OD slightly smaller than the ID of the PVC pipe was used for applying the $CaSO_4$ solution. Holes (0.5-1 mm) were made on the bottom of the plastic bucket and the bucket was then inserted into the LC. The bottom of the bucket was about 10 cm above the soil surface. The $CaSO_4$ solution was poured into the bucket in 2-L installments.

It took more than 48 h for the entire volume of $CaSO_4$ solution to infiltrate. The slow infiltration rate witnessed in the LCs was due to the absence of preferential flow pathways present in natural systems and the lack of an effective mechanism to remove the entrapped air. A larger hose connector at the base of the LC could have been more useful in expelling air. While the LCs were soaking with $CaSO_4$ solution, holes for installing granular matrix sensors (GMSs) and tension lysimeters were made in the columns using 2.54-cm (for GMS) and 5.72-cm (for tension lysimeter) cutters mounted on a hand drill.

In each column, two GMSs were installed, one at 30 cm below the soil surface (after the LC had been packed to a depth of 60 cm) and the other at 50 cm below the soil surface (fig. 3.7). The GMSs used in this study were suitable for monitoring soil moisture tension in the range of 0-2 bars. The GMSs were installed perpendicular to the LC about 6.7 cm inside the soil using the native soil slurry. Soil tension readings in the upper GMS (installed at mid-depth) was assumed to be representative of the entire soil column. The soil moisture tension in the lower GMS was used to decide on the time to apply suction to the tension lysimeter.

One tension lysimeter was installed in each LC at an angle of 10° above the horizontal, 50 cm below the soil surface. Hence, the center of the ceramic cup of the tension lysimeter was at the same depth as the GMS, but diametrically opposite to it.

The tension lysimeter protruded 10 cm inside the PVC pipe; hence, there was a distance of 3.4 cm between the tension lysimeter and the GMS. As in the field, the tension lysimeters were installed using native soil slurry. The tension lysimeters were used to collect leachate samples and to drain the LC to prevent anaerobic conditions developing within the column. When the LCs needed draining, the Tygon® tubing from one or two tension lysimeters were connected to a larger volumetric flask fitted with a neoprene stopper. Tension was applied to the volumetric flask via the neoprene tube fitted to the neoprene stopper.

It was observed that the 10° inclination of the tension lysimeter with the horizontal did not permit the tension lysimeters from being completely purged since the tip of the nylon tubing was not at the lowest point in the ceramic cup. In order to purge the tension lysimeters completely to avoid contamination, a length of straight nylon tubing (stiffened internally with a length of stainless steel wire) was inserted through the neoprene tube on the tension lysimeter stopper. The tension lysimeter was purged by applying suction to the nylon tubing while the nylon tubing was being slowly rotated inside the ceramic cup. Alternatively, when there was no standing water on the surface of the LC, the column was tilted backward (10-15° with the vertical) to purge the tension lysimeter.

Leaching column operation

It was proposed to apply the fertilizer treatments when the LCs reached field capacity, i.e. at a tension of 30-35 cbars. For this purpose, soil moisture tensions were measured daily and to expedite moisture removal, the tension lysimeters were kept under suction for the first few days. However, 8 d after applying $CaSO_4$ solution to the columns, it was noted that columns had reached an average tension of only 15 cbars (12-18 cbars). The slow rate of drainage indicated that the columns were in the field capacity range. At field capacity, Cuenca (1989) reported that tensions varied from 10 cbars for sandy soils to 33 cbars for fine silty or clay soils. Hence, it was assumed that the loamy soil used for the study had a tension in the range of 12-18 cbars at field capacity.

The LCs were drained for 2 weeks before the fertilizer treatments were applied. The circumference of the soil surface was depressed with the fingertips, and more bentonite slurry was applied to the depressions thus formed; to confine the bentonite to the edges, soil slurry was applied over the bentonite. In addition to the slow drainage, the low temperature in the LW Laboratory (the heating system was not working) impeded the drying of the LCs. Further, the soil surface developed cracks in all LCs as the soil began to dry. The cracks were removed by roughing the surface by a knife to a depth of about 2.5 cm, followed by an application of a small amount of air-dried soil. Prior to the treatment application, the soil surfaces were compacted lightly with the steel tamping plate which eliminated all cracks.

The three treatments were assigned randomly to the nine LCs. No fertilizer was applied to the control treatment. Granules were applied using a doughnut-shaped paper template (OD = 20 cm, ID = 15 cm). The template was placed on the soil surface of the LC and 4.5 g of urea granules were spread manually inside the 15-cm diameter circle. Such an arrangement ensured that the urea granules were not applied close to the edge of the soil surface, thus reducing the possibility of short-circuiting. The pellets (three 1.5 g pellets/LC) were applied using a paper template with an OD of 20 cm and having three 14-mm holes displaced at 60°.

After application of the treatments, 2.3 kg of air-dried and sieved soil (enough to pack the column to a depth of 60 cm at field ρ_b) was poured into each LC. Care was taken not to dislodge the pellets or granules while the soil was being poured into the column. After leveling the soil with the hand, the soil was lightly compacted with the steel tamping plate. The freshly added soil was saturated with 0.005 M $CaSO_4$ solution at 0.56 L/LC. To prevent surface sealing, a double layer of cheesecloth was spread on the soil surface. However, the cheesecloth was not very effective in protecting the soil surface. The circumference of the soil surface was again depressed with the fingertips and bentonite and soil slurries were poured into the depression in succession to reduce the possibility of short-circuiting.

The first leaching event was applied 4 d after fertilizer application. The tensions in the columns were recorded and the θ_v corresponding to the average tension was read from the SMCC (fig. 3.3). The volume of distilled water required to raise the MC to saturation was calculated and the same volume of water was applied to all LCs. The leaching was applied in 1-L increments at short intervals using the water application system described earlier. To protect the soil surface from sealing and compaction, a circular-shaped absorbent fabric 2 mm thick was placed on the soil surface before applying water.

The tension in the columns was monitored at regular intervals. Tension (32-34 cbars) was applied to the tension lysimeters 48 h after application of water after all the columns had become saturated. Samples were collected 1.25 h later following the procedures used in the field experiment. It was noted that even under saturated conditions, the columns still retained a substantial depth of ponded water indicating that use of the saturated volumetric moisture content likely overestimated the amount of water required to saturate the columns. Small amounts of water leached from the bottom of most columns. However, since water infiltrated into the columns very slowly, suction had to be applied to the tension lysimeters to hasten moisture movement. Ultimately, 5 d after applying irrigation, 1.3 L of ponded water was removed from each of the LCs taking care not to disturb the soil surface.

Six days after the first leaching event, it was noted that the soil surfaces developed cracks as they dried. After filling the cracks with air-dried and sieved soil, a 2.2-cm thick layer of sieved and air-dried silica sand was applied over the soil surface to prevent the surface from drying rapidly and developing cracks. Further, the sand allowed for more uniform leaching application (Shani et al., 1992) and protected the surface from compaction during application of water.

The second leaching event was applied 9 d after the first leaching event since it took longer for the LCs to reach field capacity. All other leaching events were applied at 7-d intervals. When all the moisture sensors at the lower depth in the LCs indicated soil moisture tensions close to saturation (0 cbar), suction (40 cbars) was applied to the tension lysimeters for 0.5 h. The leachate thus collected was discarded to prevent contamination of the sample by leachate from the previous leaching events retained in the ceramic cup. The tension lysimeters were then subjected to 40 cbars of suction for 1-1.5 h. The samples thus collected were used for analysis of NO_3^--N and urea (first event). Nitrate analysis on the leachate samples was performed in the WQ Laboratory using the TRAACS 800 automatic water quality analyzer. Urea analysis was performed by the colorimetric method using DAM (Bremner, 1982) in the LW Laboratory. Since no urea was detected in the first set of samples, no urea analyses were performed on samples from the subsequent events.

After sample collection, the tension lysimeters were subjected to 38-40 cbars of suction for the remaining duration to reduce the moisture content in the columns to field capacity. Efforts were made to ensure uniform moisture contents in all LCs by changing the level and/or duration of suction applied to each LC. After collecting the last set of leachate samples, soil core samples were obtained from the LCs to analyze for residual N. From each LC, three soil cores were obtained from the top third of the column using a core sampler. The three soil cores were thoroughly mixed to obtain a single soil sample. Soil samples were also obtained from the middle third and bottom third of the column using the same procedure used for the top third. The 27 soil samples (three samples per LC) were dried at 65°C and analyzed at Brookside Laboratories, Inc. for NO_3^--N, NH_4^+-N, and total-N using procedures described earlier.

4. RESULTS AND DISCUSSION

Objective 1 was achieved by conducting a field experiment that was comprised of two components - agronomic and NO_3^--N leaching. Multiple hypotheses were tested for each component. To achieve Objective 2, three laboratory experiments, namely, dissolution, incubation, and leaching column experiments were conducted; multiple hypotheses were tested for each experiment. Within an objective, for each component or experiment, the results are presented which are followed by the discussion on individual hypotheses.

4.1. Field Experiment

Objective 1: Evaluate the agronomic and NO_3^--N leaching impacts of subsurface-applied urea pellets versus granules on no-till silage corn.

A field experiment was conducted to evaluate agronomic and NO_3^--N leaching impacts of urea pellets versus granules on no-till corn from May 1997 until April 1999. The agronomic impacts of the two urea forms were evaluated with respect to corn silage yield and corn N content. The NO_3^--N leaching component involved evaluation of the two urea forms with respect to residual soil inorganic-N, NO_3^--N concentration in leachate, and N removal by crop.

4.1.1. Agronomic Component

The impacts of the two urea forms on corn silage yield and corn N content were compared. Interaction effects of urea form, N application rate, and year on corn silage yield and corn N content were also evaluated. Corn silage yield response and corn N content response curves as well as the plot of corn silage yield versus N content are presented and discussed.

1. Corn silage yield

Corn silage yields adjusted to 35% DM are presented in figure 4.1, categorized by year and treatment. During 1997, while the yield difference between the fertilizer treatments and control treatment exceeded 10 Mg/ha, yield difference among the fertilizer treatments was low, with yields ranging from 55.1-56.7 Mg/ha. Corn silage yield from the control treatment was slightly lower than the corn silage productivity potential of 47.6 Mg/ha for Ross soil (VDCR, 1993). In 1998, yield difference between the fertilizer treatments and control exceeded 17 Mg/ha; also, greater variations in yield were observed among the fertilizer treatments. Compared to 1997, yield declined by 33% in the control treatment while in the fertilizer treatments, yield declines ranged between 10.9 and 14.1% for pellet-deficient (PD), granule-deficient (GD), and granule-sufficient (GS) treatments. For the pellet-sufficient (PS), pellet-excess (PE), and granule-excess (GE) treatments, yield levels changed little between 1997 and 1998.

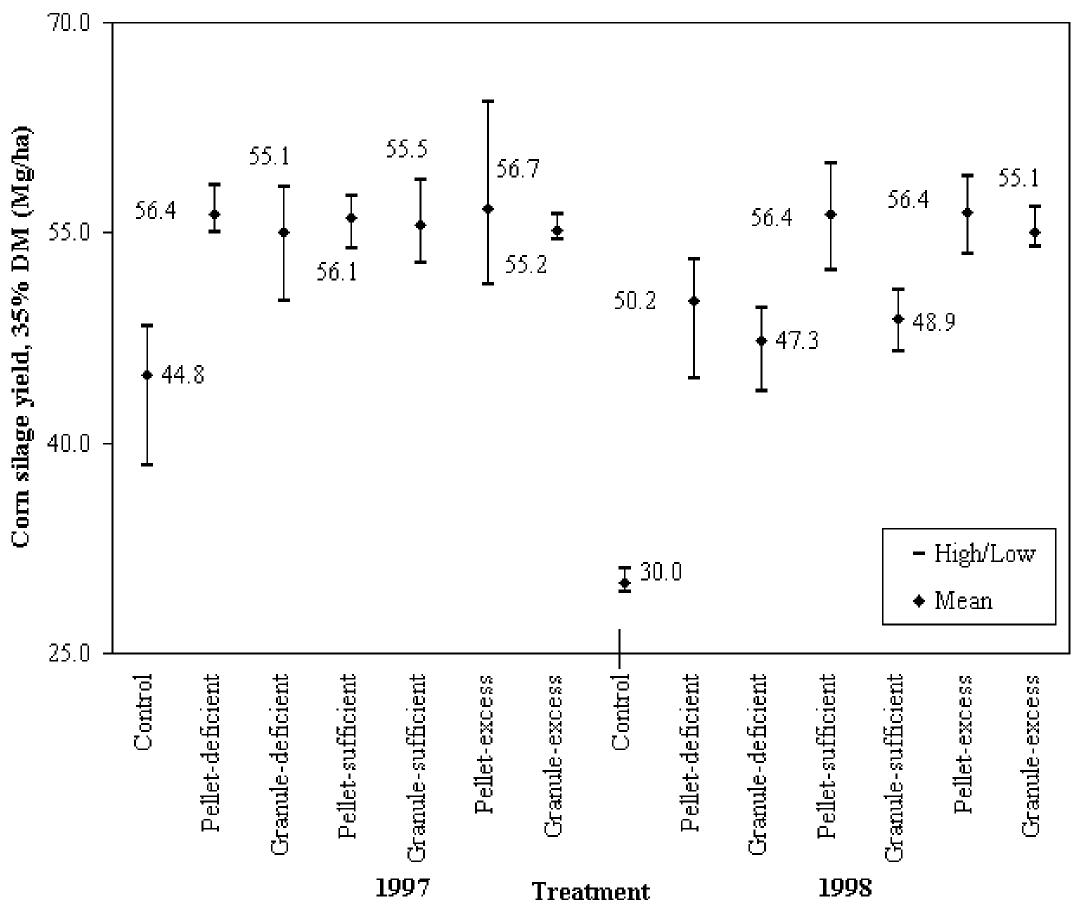

Figure 4.1. Corn silage yields in 1997 and 1998. Each mean yield value represents the mean of three replications.

1.1. Null Hypothesis: Corn silage yield is unaffected by the treatment applied.

Alternative Hypothesis: Corn silage yield is affected by the treatment applied.

Treatment effect (including control) on corn silage yield (35% DM) was investigated for 1997 and 1998. The data set for the two years were not combined into a single data set since corn silage yield was significantly ($p < 0.01$) affected by the year. Since yield residuals for both data sets were found to be normally distributed, the data were subjected to ANOVA and Fisher's LSD at $\alpha = 0.1$ (table 4.1).

Table 4.1. Treatment effect on corn silage yield (1997 and 1998): results of the statistical analyses at $\alpha = 0.1$

Treatment	1997		1998	
	Mean*	SD†	Mean	SD
	-------------------------Mg/ha (35% DM)-----------------------			
Control	44.8b‡	5.6	30.0c	0.9
Pellet-deficient	56.4a	1.74	50.2b	4.8
Granule-deficient	55.1a	4.4	47.3b	3.2
Pellet-sufficient	56.1a	2.0	56.4a	3.8
Granule-sufficient	55.5a	3.0	48.9b	2.2
Pellet-excess	56.7a	6.8	56.4a	2.8
Granule-excess	55.2a	1.0	55.1a	1.5
LSD§	4.4		3.3	

* Average of three replications

† Standard deviation

‡ Treatment means in the same column, followed by the same letter are not significantly different at $\alpha = 0.1$ using Fisher's LSD.

§ Fisher's Least Significant Difference

Null Hypothesis 1.1 was rejected for 1997 ($p = 0.03$); hence, the treatments affected corn silage yield. The Fisher's LSD results indicated that while the control treatment differed significantly from the fertilizer treatments, the fertilizer treatments were not significantly different from one another. All fertilizer treatments gave substantially greater corn silage yields than the corn silage productivity potential of 47.6 Mg/ha for the Ross soil (VDCR, 1993).

For 1998, Null Hypothesis 1.1 was again rejected ($p < 0.01$); hence, the treatments affected corn silage yield. However, in contrast to 1997, some fertilizer treatments gave higher corn silage yields than other fertilizer treatments. The PS, PE, and GE treatments produced significantly higher yields than PD, GD, and GS treatments (table 4.1).

Except for the PS, PE, and GE treatments, all other treatments registered large yield declines from 1997 to 1998. Weed infestation was ruled out as a factor in yield decline since a qualitative evaluation indicated that all treatments had been more-or-less equally affected. Two potential reasons for yield decline, precipitation and soil inorganic-N, were evaluated for their impacts.

1. Precipitation

Scharf and Alley (1988) reported that nitrification inhibitors (NIs) performed better under irrigated conditions or in areas with annual water surplus of more than 30.5 cm as the NIs reduced N leaching and denitrification losses compared to conventional fertilizers. Since pellets inhibit nitrification and urea hydrolysis (Singh and Beauchamp, 1987), pellets can be regarded as NIs. Hence, pellets might be expected to give higher yields than granules under moist conditions, because lower N leaching losses from pellets (than granules) can increase plant-N availability. Hence, precipitation amounts and/or distribution between two crop seasons can affect the performance of pellets versus granules.

Normal precipitation (30-yr average) during the corn season (mid-May to mid-September) is 37.9 cm as shown in figure A(a), Appendix A (SERCC, 2000). Compared with the normal precipitation, during the 1997 and 1998 corn seasons, precipitation deficits were 7.3 and 11.5 cm, respectively (fig. 4.2). Given the precipitation deficit in 1998, impact of N leaching losses in pellets versus granules on corn silage yield is not a reasonable explanation.

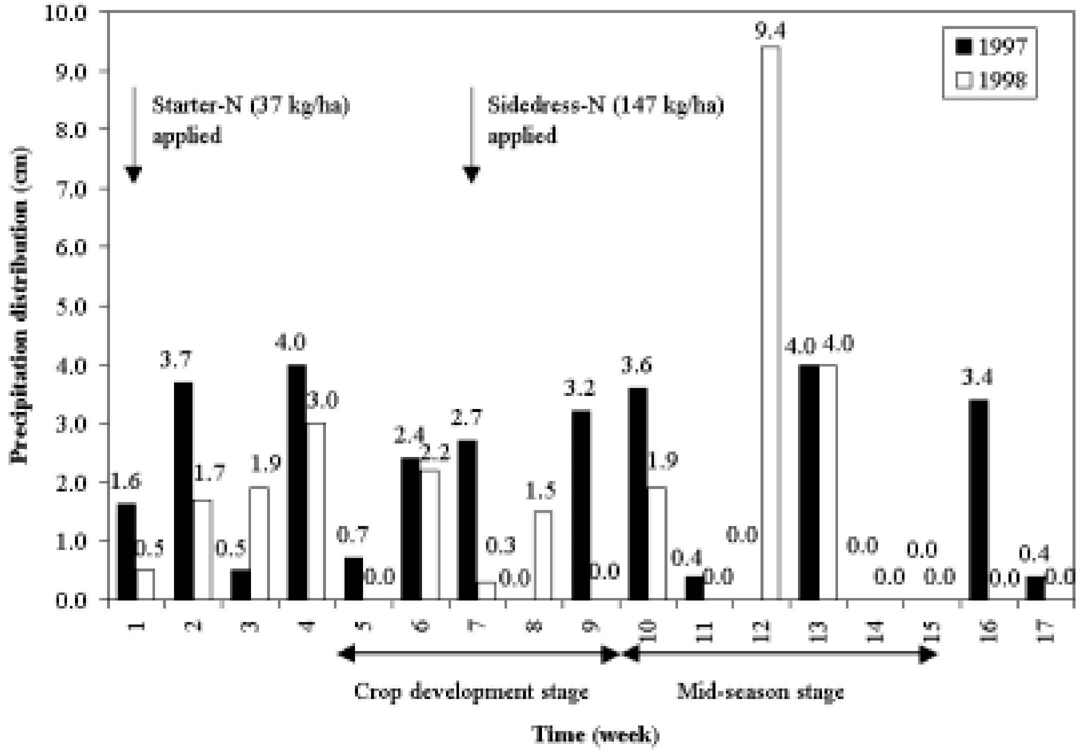

Figure 4.2. **Weekly precipitation distribution during the 1997 and 1998 crop seasons.**

Crop evapotranspiration (ET) requirement rises rapidly during the crop development stage (about 35 d), beginning about 20 d after planting (Doorenbos and Pruitt, 1977). Crop ET then levels off at the highest level for about 40 d corresponding to the mid-season stage. Critical periods of soil water stress also correspond to these two stages for corn (Doorenbos and Pruitt, 1977).

On weekly basis, the crop development stage (week 5 through week 9 after planting) received 9.0 and 4.0 cm of precipitation during 1997 and 1998, respectively (fig. 4.2). The 1997 and 1998 crops received 8.0 and 15.3 cm of precipitation, respectively, during the mid-season stage (week 10 through week 15 after planting) (fig. 4.2). Total precipitation during the two critical stages were similar for both years. Lesser precipitation and a longer dry spell during the crop development stage should have adversely affected vegetative development of the corn during 1998. However, corn silage yields in PS, PE, and GE treatments were unaffected in 1998 compared with 1997. Reduction in yield in some treatments as a result of the adverse effects of high pH and high NH_3 concentrations were unlikely since yield declines did not occur in the PE treatment which had the highest localized urea concentration (and the most likely to be adversely affected) among all treatments. During the mid-season stage, there was more precipitation in 1998 than in 1997 but precipitation distribution was more uniform in 1997. Hence, it was unlikely that precipitation distribution during the mid-season stage affected yield.

2. Soil inorganic-N

At the same N application rate, depending on the amount of soil inorganic-N, crop yield could vary greatly. Citing published research, Tisdale et al. (1993) reported on wheat grain yield response to applied-N for different soil-N (NO_3^- concentration in the profile) levels. In medium and low soil-N, wheat grain yields were 70 and 135% higher, respectively, compared to yield at high soil-N when N was applied at 67 kg/ha (at >67 kg/ha, yields declined at all soil-N levels) (Tisdale et al, 1993). Hence, varying amounts of soil inorganic-N over the two crop seasons had the potential to impact crop response since applied-N remained unchanged over the two years.

Since soil inorganic-N data were not available for May 1997, comparisons could not be made between inorganic-N values at planting, i.e., in May 1997 and May 1998. However, there was evidence that soil-N amount in May 1997 was higher than in May 1998. The field site had been planted to soybean in the summer of 1996. Typically, soybean fixes 112 kg-N/ha-year (Tisdale et al., 1993) which likely resulted in a high soil-N status. During October 1996 through April 1997, a precipitation deficit (as compared to normal precipitation) of 6.2 cm (J. Wooge, personal communication, Blacksburg, Va., 27 September 2000) was observed at Kentland Farm. Hence, it was unlikely that a substantial amount of soil-N (due to the soybean crop) was lost due to leaching as compared to an over-winter period with normal precipitation. In addition to crop N removal in 1997, environmental conditions during the over-winter period of 1997-1998 also provided favorable conditions for N loss. Between the time of corn silage harvesting in September 1997 and corn planting in May 1998, 89.7 cm of precipitation and irrigation was received compared to a 30-year average precipitation of 66.0 cm (SERCC, 2000).

Hence, the wet soil conditions combined with warmer-than-normal conditions (fig. A(b), Appendix A) to increase mineralization and N losses through leaching and denitrification. High background inorganic-N in 1997 resulted in raising the plant-N availability in the fertilizer treatments to sufficiently high levels that crop yield response to fertilizer treatments was not observed.

A 33% decline in corn silage yield in the control treatment from 1997 to 1998 also indicated that depleted soil inorganic-N affected yield. By contrast, GD, the fertilizer treatment with the largest reduction in yield only experienced a 14% decline. Compared to 1997, corn silage yields were comparable at higher N application rates (except GS) in 1998, indicating that despite a reduced soil inorganic-N, greater N availability provided a greater crop response.

An attempt was made to explain the performance of pellets and granules in view of their performances at different application rates. Given the possibility of reduced N losses from pellets versus granules (Nyborg and Malhi, 1992) and a greater yield response at a lower N application rate, corn silage yield should have been significantly higher with PD than GD. The lack of a significant difference in yield between the PE and GE treatments from 1997 to 1998 despite decline in soil inorganic-N could be attributed to the abundance of applied-N. Even with increased N losses from the GE treatment, it was likely that the remaining applied-N sufficed to produce corn silage yield comparable to the PE treatment.

It was unclear why pellets outperformed granules at the sufficient N application rate but not at the deficient N application rate. The N loss pathways that could have affected N loss based on urea form were NO_3^--N leaching, denitrification, immobilization of inorganic-N by OM, and NH_4^+-N fixation by certain clays. Since both crop seasons were drier-than-normal (fig. A(a), Appendix A), it was unlikely that substantial NO_3^--N leaching occurred from either urea form. Nyborg and Malhi (1992) attributed higher spring-barley yield and N removal from 2-3 g urea pellets (compared with commercial granules) to lower denitrification and possibly lower immobilization of applied-N. Even though the 1998 crop season was drier-than-normal (fig. A(a), Appendix A) with 7.2 cm of precipitation was received on 8 August 1998. Given the high organic carbon content of the soil (the soil had an organic matter content of 7.6%, table 3.3) and moist conditions, there could have been higher denitrification losses in granules than pellets. Immobilization of applied-N by OM was likely to have been minor since the urea forms were subsurface-applied.

Since NH_4^+-N fixation decreases with increasing urea particle size (Singh et al., 1994), possibility of NH_4^+-N fixation affecting corn silage yield in pellets versus granules was considered. The clay mineralogy for the same soil was studied by Harris et al. (1980) for a site located within 10 m from the western boundary of the field site (Lucian W. Zelazny, personal communication, Blacksburg, Va., 7 August 2000). Presence of substantial amounts of NH_4^+-N fixing clay minerals such as vermiculite (20%), mica (10%), and hydroxy interlayered vermiculite (25%) in the clay fraction of the Ross soil (Harris et al., 1980) indicated that the clay fraction had substantial NH_4^+-N fixing capacity. Nommik and Vahtras (1982) reported that clayey silt and fine sand were capable of considerable NH_4^+-N fixation. Mica constituted 8 and 25% of the total clay minerals in the silt and sand fractions, respectively. Since the silt fraction contained 21% fine silt and the sand fraction contained 95% fine sand, the silt and sand fractions could have contributed to the NH_4^+-N fixation capacity of the soil. In 1998, during the four-week period following sidedress application, only 3.7 cm of precipitation was received (fig. 4.2). The combination of NH_4^+-N fixing clay minerals and dry conditions could have resulted in increased NH_4^+-N fixation during the 1998 season. In eastern Canada, as much as 70% of fertilizer NH_4^+ was fixed in the subsurface soil (Tisdale et al., 1993).

Hence, there was a possibility that there were greater denitrification and NH_4^+-N fixation losses from granules than pellets in 1998. However, it seemed unlikely that possibly higher N losses in granules resulted in reduced corn silage yield as compared to pellets in 1998. Lack of difference in yield between the PD and GD treatments in 1998 indicated that possible reduced N losses due to denitrification and NH_4^+-N fixation in pellets as compared to granules, probably did not explain the difference in corn silage yield between PS and GS in 1998.

Corn silage yield response curve

Corn silage yield response curves for N were developed for urea pellets and granules at different N application rates for 1997 (fig. 4.3) and 1998 (fig. 4.4). Due to the limited data (only four data points), the responses would be applicable only to soil and environmental conditions similar to this study. Nevertheless, the response curves provided general trends on the response of corn silage yield to N application as urea pellets and granules.

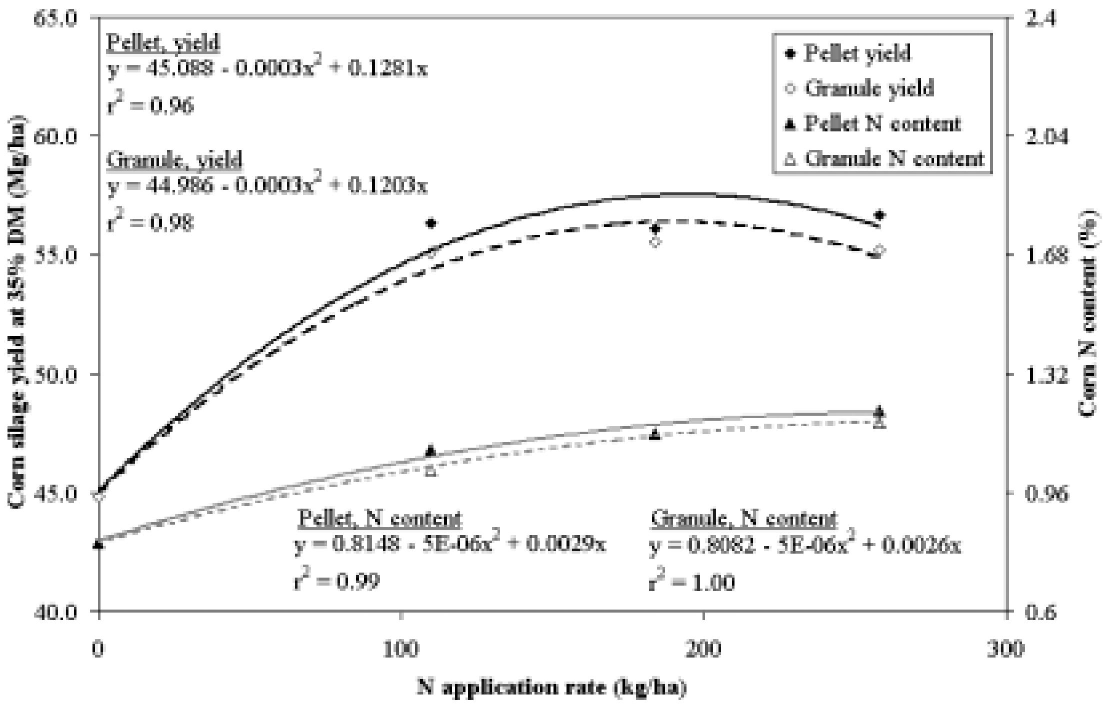

Figure 4.3. Corn silage yield and corn N content response curves for urea pellets and granules in Ross loam in 1997 at control (0 kg-N/ha), deficient (110 kg-N/ha), sufficient (184 kg-N/ha), and excessive (258 kg-N/ha) application rates. There were no separate control treatments for pellets and granules. Each data point represents the mean of three replications.

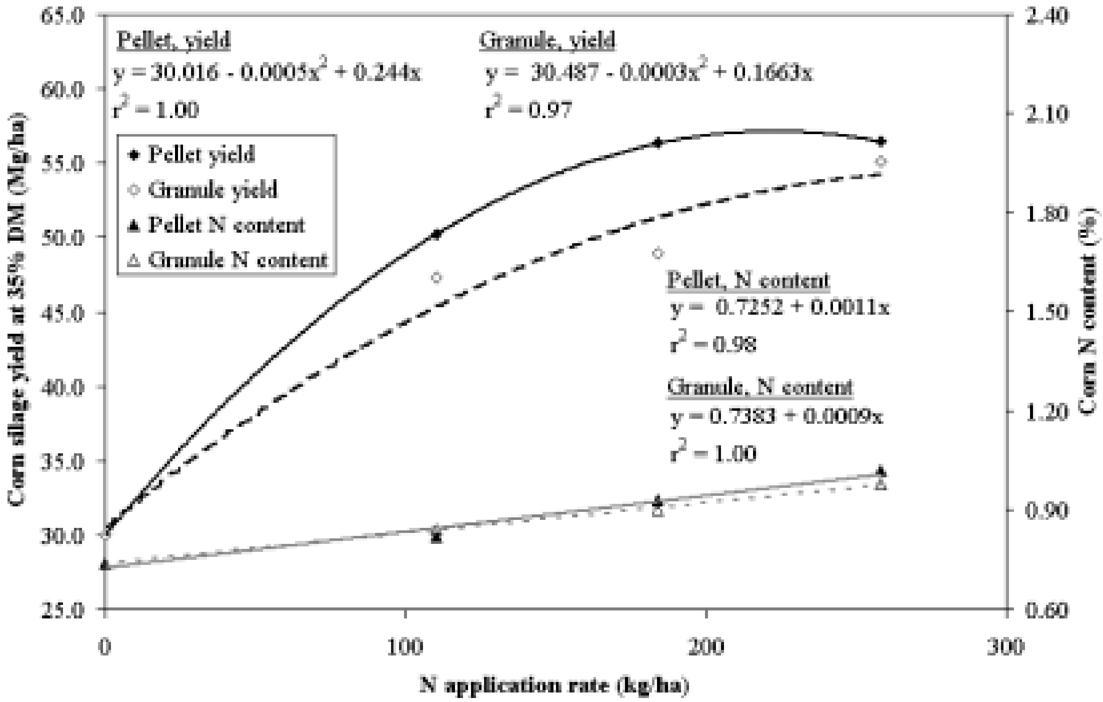

Figure 4.4. Corn silage yield and corn N content response curves for urea pellets and granules in Ross loam in 1998 at control (0 kg-N/ha), deficient (110 kg-N/ha), sufficient (184 kg-N/ha), and excessive (258 kg-N/ha) application rates. There were no separate control treatments for pellets and granules. Each data point represents the mean of three replications.

For corn silage yield response (both pellets and granules), second-order polynomials provided good fit to the observed data in both 1997 (fig. 4.3) and 1998 (fig. 4.4). Use of second-order polynomial explains the increase in yield with N application rate until a certain N application rate threshold, after which, N toxicity and suppression of removal of other nutrients will result in decline in yield (Tisdale et al., 1993). Even though the regression equations in both years for both urea forms show good correlation as indicated by high r^2 values (fig. 4.3; fig. 4.4), the regressions are based on four data points only.

1.2. Null Hypothesis: Corn silage yield is unaffected by the urea form at the sufficient application rate (184 kg-N/ha).

Alternative Hypothesis: Corn silage yield is higher with pellets than granules.

Corn silage yield data for the PS and GS treatments were analyzed for 1997 and 1998. Since both data sets were normally distributed with respect to their yields, they were statistically analyzed using Student t-test (table 4.2).

Table 4.2. Corn silage yields (35% DM) for pellet-sufficient (PS) vs. granule-sufficient (GS) treatments (1997 and 1998): results of statistical analyses at $\alpha = 0.1$

Data set	PS		GS		Student t-test	Significant
	Mean†	SD‡	Mean	SD	p-value*	
	-----------Mg/ha (35% DM)---------					
1997	56.10	1.96	55.52	3.01	0.40	Fail to reject
1998	56.35	3.81	48.91	2.20	0.02	Reject

* One-tailed probability

† Mean of three replications

‡ Standard deviation

The evidence failed to reject Null Hypothesis 1.2 in 1997 (p = 0.40); hence, at 184 kg-N/ha, neither urea form produced greater corn silage yield. However, in 1998, Null Hypothesis 1.2 was rejected (p = 0.02); PS gave greater corn silage yield than GS. Despite likely differences in N losses as affected by the urea form, high soil inorganic-N status in 1997 likely resulted in failure to reject Null Hypothesis 1.2 in 1997. In 1998, despite rejection of Null Hypothesis 1.2, it was unclear if greater N losses in granules resulted in decreased corn silage yield as compared to pellets.

In 1998, at 184 kg-N/ha, corn silage yield was 15.2% higher with pellets than granules. Overall, the yield increase obtained in this study was lower than those obtained in winter wheat (Singh and Beauchamp, 1988) and spring barley (Nyborg and Malhi, 1992). The studies on winter wheat and spring barley compared broadcast-incorporated urea granules with subsurface-banded pellets; hence, the higher yield differences in those studies could be partly attributed to more rapid nitrification from broadcast-incorporated granules than from subsurface-banded granules as was used in this study. Further, possible N loss pathways in this study were different from the N loss pathways in studies on winter wheat and spring barley.

Yield results obtained in this study were different compared to results obtained by Zhang (1990). Even though both studies were conducted on no-till corn, the methods used were very different. Zhang (1990) applied the entire N in a single application with the 150 and 200 kg-N/ha treatments receiving 4.9 and 6.5 g-urea/plant, respectively, at distances of 5, 10, and 15 cm. In this study, the N application was split with 37 kg-N/ha being applied as starter with one 1.5-g urea pellet being applied 5 cm from the seed. The remaining N, 147 kg-N/ha in the sufficient application rate, was applied as sidedress, in a line 20 cm away from the plants at a pellet-to-pellet distance of 6.25 cm at 6 g-urea/plant. Hence, conditions that caused yield decline associated with large urea concentrations in the Zhang (1990) study did not apply to the present study resulting in dissimilar results.

1.3. Null Hypothesis: There is no urea form × N application rate interaction effect on corn silage yield.

Alternative Hypothesis: There is urea form × N application rate interaction effect on corn silage yield.

Since the yield data sets for the fertilizer treatments for both years were found to be normally distributed, ANOVA was applied to test for interaction at $\alpha = 0.1$ (table 4.3). The control treatment was excluded in this analysis. The evidence failed to reject Null Hypothesis 1.3 in both 1997 ($p = 0.98$) and 1998 ($p = 0.27$); hence, there was no urea form × N application rate interaction on corn silage yield in either year of the study.

Table 4.3. Urea form × N application rate interaction effects on corn silage yield at $\alpha = 0.1$

Source	1997		1998	
	ANOVA* p-value	Significant	ANOVA p-value	Significant
Urea form	0.54		0.03	
N application rate	1.00		0.01	
Urea form × N application rate	0.98	Fail to reject	0.27	Fail to reject

* Analysis of Variance

1.4. Null Hypothesis: There is no urea form × year interaction effect on corn silage yield.

Alternative Hypothesis: There is urea form × year interaction effect on corn silage yield.

Since the data set was normally distributed, ANOVA was applied to test for interaction on yield data (the control treatment was excluded) for both years at $\alpha = 0.1$ (table 4.4). The evidence failed to reject Null Hypothesis 1.4 ($p = 0.28$); hence, there was no urea form × year interaction. The failure to reject Null Hypothesis 1.4 indicated that corn silage yield decreased from 1997 to 1998, irrespective of the urea form. The magnitude of yield decrease for pellets and granules, averaged over all application rates, was 2.05 and 4.84 Mg/ha, respectively.

Table 4.4. Urea form × year and N application rate × year interaction effects on corn silage yield at $\alpha = 0.1$

Source	ANOVA* p-value	Significant
Hypothesis 1.4		
Urea form	0.06	
Year	0.01	
Urea form × year	0.28	Fail to reject
Hypothesis 1.5		
N application rate	<0.01	
Year	<0.01	
N application rate × year	<0.01	Reject

* Analysis of Variance

1.5. Null Hypothesis: There is no N application rate × year interaction effect on corn silage yield.

Alternative Hypothesis: There is N application rate × year interaction effect on corn silage yield.

Since the yield data were normally distributed, ANOVA procedure was applied to test for interaction at $\alpha = 0.1$ (table 4.4). In this case, the control treatment was included in the statistical analysis since it represented an N application rate. The evidence rejected the Null Hypothesis 1.5 ($p < 0.01$); hence, there was N application rate × year interaction. Rejection of Null Hypothesis 1.5 indicated that corn silage yield responded better to an increasing N application rate in 1998 than in 1997. As was discussed in Hypothesis 1.1, the depleted soil inorganic-N status in 1998 compared with 1997 resulted in better yield response to an increasing N application rate.

2. Corn nitrogen content

Corn N content data are presented in figure 4.5, categorized by year and treatment. During 1997, the fertilizer treatments had N contents in the range of 1.03 to 1.21%, 27.2 to 49.4% more N than control; N content increased with N application rate. In 1998, N contents declined in all treatments; however, the decline was higher in the fertilizer treatments than in the control treatment.

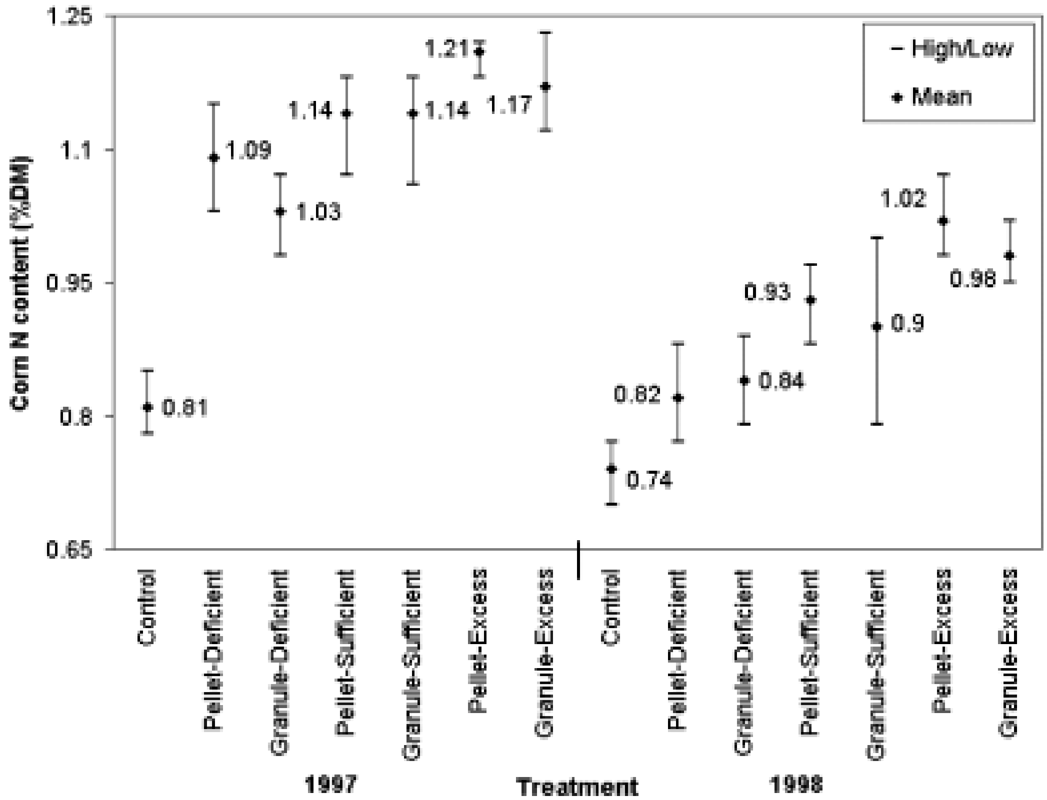

Figure 4.5. Corn N content in 1997 and 1998. Each mean N content value represents the average of three replications.

2.1. Null Hypothesis: N content in corn is unaffected by the treatment applied.

Alternative Hypothesis: N content in corn is affected by the treatment applied.

Treatment effect (including control) on corn N content (% dry matter) was investigated for 1997 and 1998. The data sets for the two years were not combined into a single data set since corn N content was significantly ($p < 0.01$) affected by the year.

Since both data sets were normally distributed, ANOVA and Fisher's LSD at $\alpha = 0.1$ were used in their analyses (table 4.5).

Table 4.5. Treatment effect on corn N content (1997 and 1998): results of the statistical analyses at α = 0.1

Treatment	1997		1998	
	Mean*	SD†	Mean	SD
	----------------------N content as % of DM----------------------			
Control	0.81e‡	0.04	0.74f	0.04
Pellet-deficient	1.09cd	0.06	0.82e	0.06
Granule-deficient	1.03d	0.05	0.84de	0.05
Pellet-sufficient	1.14bc	0.06	0.93bc	0.05
Granule-sufficient	1.14bc	0.07	0.90cd	0.11
Pellet-excess	1.21a	0.02	1.02a	0.05
Granule-excess	1.17ab	0.06	0.98ab	0.04
LSD§	0.06		0.06	

* Average of three replications

† Standard deviation

‡ Treatment means in the same column, followed by the same letter are not significantly different at $\alpha = 0.1$ using Fisher's LSD.

§ Fisher's Least Significant Difference

For 1997, Null Hypothesis 2.1 was rejected ($p < 0.01$); hence, the treatments applied affected corn N content. Null Hypothesis 2.1 was rejected for 1998 ($p < 0.01$) indicating that corn N content was affected by the treatments applied. Based on mean values, in both years, corn N contents generally increased with N application rates (table 4.5). The urea form did not affect corn N content in either year.

Compared with 1997, large declines (8.6-24.8%) in corn N content were observed in all treatments in 1998. The least affected was the control treatment while the most affected was PD. Since larger N content declines were observed in the lower N application rates, it was likely that the decreased soil inorganic-N (that reduced corn silage yields for most treatments in 1998 as compared to 1997), also contributed to reduction in corn N content in 1998 for all treatments.

Zhang (1990) did not report crop N content values from urea pellet versus granules in corn. Hence, the results from this study could not be compared with published values of crop N content as affected by the urea form in corn. In studies on the impact of urea pellet versus granules in winter wheat (Singh and Beauchamp, 1988) and spring barley (Nyborg and Malhi, 1992), crop N contents and DM were not reported. Consequently, comparisons based on percent improvements in crop N removal with pellets versus granules were not possible.

Goodrich and Meiske (1985) reported that corn silage contained 1.33% N (8.3% crude protein) on DM basis. In this study, corn N contents obtained even from the excessive N application treatments were substantially lower than 1.33% N. Split application of N in subsurface-bands should have resulted in higher N removal by the crop. Further, the lower-than-normal precipitation in both seasons should have increased crop protein content (Tisdale et al., 1993), and hence N content. It was unclear if the corn variety affected corn N content adversely.

<u>Corn N content response curves</u>

Corn N content curves for urea pellets and granules at different N application rates are presented in figure 4.3 for 1997 and figure 4.4 for 1998. As with corn silage yield response curves, N content response curves would be applicable to soil and environmental conditions specific to this study. In keeping with decline in corn N content at extremely high N application rates, in 1997 (fig. 4.3), a quadratic regression model provided good fit for both urea forms and was also appropriate for the data. In 1998 (fig. 4.4), a linear model provided a better fit to the data indicating that within the range of N application rates used in this study, corn N content did not decline with higher N application rates. This was likely due to the depleted soil inorganic-N status in the study in 1998, which did not adversely impact N content. Even though the regression equations for both urea forms showed good correlation as indicated by high coefficient of determination (r^2) values in both years (fig. 4.3; fig. 4.4), only four points were used to develop the regressions.

2.2. Null Hypothesis: N content in corn is unaffected by the urea form at the sufficient application rate (184 kg-N/ha).

Alternative Hypothesis: N content in corn is higher with PS than GS.

The 1997 corn N content data set was not normally distributed and was analyzed with Wilcoxon Rank Sums 2-sample test (table 4.6). The 1998 data set was normally distributed and was analyzed with the Student t-test (table 4.6).

Table 4.6. Corn N contents for pellet-sufficient (PS) vs. granule-sufficient (GS) treatments (1997 and 1998): results of the statistical analyses at α = 0.1

Data set	PS		GS		Student t-test p-value*	Wilcoxon p-value*	Significant
	Mean†	SD‡	Mean	SD			
	---N content as % of DM-----						
1997	1.14	0.06	1.14	0.07	-	0.50	Fail to reject
1998	0.93	0.05	0.90	0.11	0.34	-	Fail to reject

* One-tailed probability
† Mean of three replications
‡ Standard deviation

The evidence failed to reject Null Hypothesis 2.2 in 1997 (Wilcoxon p = 0.50). In 1998, the evidence failed to reject Null Hypothesis 2.2 (Student t-test p = 0.34). Hence, in both years, at sufficient N application rate (184 kg/ha), no urea form had higher corn N content.

2.3. Null Hypothesis: There is no urea form $\times$ N application rate interaction effect on N content in corn.

Alternative Hypothesis: There is urea form $\times$ N application rate interaction effect on N content in corn.

Since the corn N content data sets for both years were normally distributed with respect to the residuals, ANOVA was used to test for interaction at α = 0.1 (table 4.7). The control treatment was excluded in this analysis. The evidence failed to reject Null Hypothesis 2.3 in both 1997 (p = 0.69) and 1998 (p = 0.64); hence, there was no urea form $\times$ N application rate interaction on corn N content in either year.

Table 4.7. Urea form $\times$N application rate interaction effects on corn N content at α = 0.1

Source	1997		1998	
	ANOVA* p-value	Significant	ANOVA p-value	Significant
Urea form	0.26		0.60	
N application rate	<0.01		<0.01	
Urea form $\times$ N application rate	0.69	Fail to reject	0.64	Fail to reject

* Analysis of Variance

2.4. Null Hypothesis: There is no urea form $\times$ year interaction effect on N content in corn.

Alternative Hypothesis: There is urea form $\times$ year interaction effect on N content in corn.

Since the combined data set for both years was normally distributed, ANOVA was applied to test for interaction at α = 0.1 (table 4.8). The evidence failed to reject the null hypothesis (p = 0.79); hence, no urea form $\times$ year interaction effect was observed on corn N content.

Table 4.8. Urea form × year and N application rate × year interaction effects on corn N content at $\alpha = 0.1$

Source	ANOVA* p-value	Significant
Hypothesis 2.4		
Urea form	0.41	
Year	<0.01	
Urea form × year	0.79	Fail to reject
Hypothesis 2.5		
N application rate	<0.01	
Year	<0.01	
N application rate × year	0.03	Reject

* Analysis of Variance

2.5. Null Hypothesis: There is no N application rate × year interaction effect on N content in corn.

Alternative Hypothesis: There is N application rate × year interaction effect on N content in corn.

Since the data set (including control) was normally distributed, ANOVA was applied to test for interaction at $\alpha = 0.1$ (table 4.8). The null hypothesis was rejected ($p = 0.03$) indicating that there was N application rate × year interaction on corn N content. Decline in corn N content was only 8.6% from 1997 to 1998 in the control treatment (zero N). In the fertilizer treatments, based on the mean corn N content values for both urea forms at the same application rate, corn N content decreased with increasing application rate between 1997 and 1998. Between 1997 and 1998, decline in corn N content in the deficient, sufficient, and excessive N application rates were 21.7, 19.8, and 16.0%, respectively.

Discussion summary: agronomic impacts

In 1997, corn silage yield was unaffected by both urea form and N application rate which was likely due to the high soil inorganic-N status. In 1997, while all fertilizer treatments had comparable corn silage yields, yield from the control treatment was significantly lower than the fertilizer treatments. Combined with at least 110 kg/ha of applied N, high soil inorganic-N status due to the soybean crop in 1996 ensured abundant N supply for plant removal, irrespective of the application rate or the possible impact of urea form on N losses.

In 1998, there was possibility of N losses due to denitrification and NH_4^+-N fixation by clay minerals. Singh et al. (1994) and Nyborg and Malhi (1992) suggested that N losses due to denitrification and NH_4^+-N fixation by clay minerals were higher with granules than pellets. However, reduced N losses from PS was unlikely to have resulted in higher corn silage yield as compared to GS since no response was observed between PD and GD, the application rate most likely to indicate a yield response. Corn N content was unaffected by the urea form applied at any N application rate.

Singh and Beauchamp (1988) and Nyborg and Malhi (1992) suggested that higher yields from pellets were due to reduced N losses primarily through denitrification and NO_3^--N leaching, N losses that result from surplus moisture conditions. However, in this study, in both years, the deficit moisture conditions during the crop season minimized NO_3^--N leaching losses.

4.1.2. Nitrate-N Leaching Component

Statistical and graphical methods were used to evaluate if urea form affected NO_3^--N leaching. Residual soil inorganic-N (NO_3^--N + NH_4^+-N) amounts in the PS, GS, and control treatments were compared at each sampling event. Nitrate-N concentrations in leachate samples from PS, GS, and control treatments were compared. Crop removal of N was also compared among all treatments to see if urea form affected N removal. Greater N removal by the crop ensured that lesser NO_3^--N would be available for leaching in the over-winter period.

3. Residual Inorganic-N in the soil

Soil inorganic-N (NH_4^+-N and NO_3^--N) amounts were determined from soil cores obtained on 21 October 1997, 14 May 1998, 14 October 1998, 2 April 1999. Distribution of soil inorganic-N amounts within the root zone provides information on potential for NO_3^--N leaching as well as N availability for plant removal. A treatment that results in higher inorganic-N amount in the upper half of the root zone is likely to have less NO_3^--N for leaching and more N available for plant removal than other treatments. Soil inorganic-N amounts in the top 30-, top 60-, and 120-cm (root zone) layers at each sampling event are presented in figure 4.6.

The general trend of inorganic-N amounts during the study indicated that sharp declines occurred between October 1997 and May 1998 for all layers in the pellet and granule treatments. For pellets, inorganic-N levels did not change substantially between May and October 1998 in any layer. In granules, inorganic-N levels showed a decline for all layers between May and October 1998. However, between October 1998 and April 1999, inorganic-N amounts increased sharply in all layers in both pellets and granules; the increase was particularly large for the root zone in granules. Inorganic-N amounts in the control treatment decreased, stagnated, and increased in the top 30-cm, top 60-cm, and root zone layers, respectively, during October 1997 and October 1998. However, between October 1998 and April 1999, inorganic-N amounts increased sharply in all three layers in the control treatment.

For each sampling event, Hypotheses 3.1 and 3.2 were tested in succession; each hypothesis was tested for all three layers. Where there was no evidence for rejecting Null Hypothesis 3.1 for a particular layer, Null Hypothesis 3.2 was not tested. The failure to reject Null Hypothesis 3.1 indicated that there was insufficient evidence that applied-N contributed to the inorganic-N in the layer.

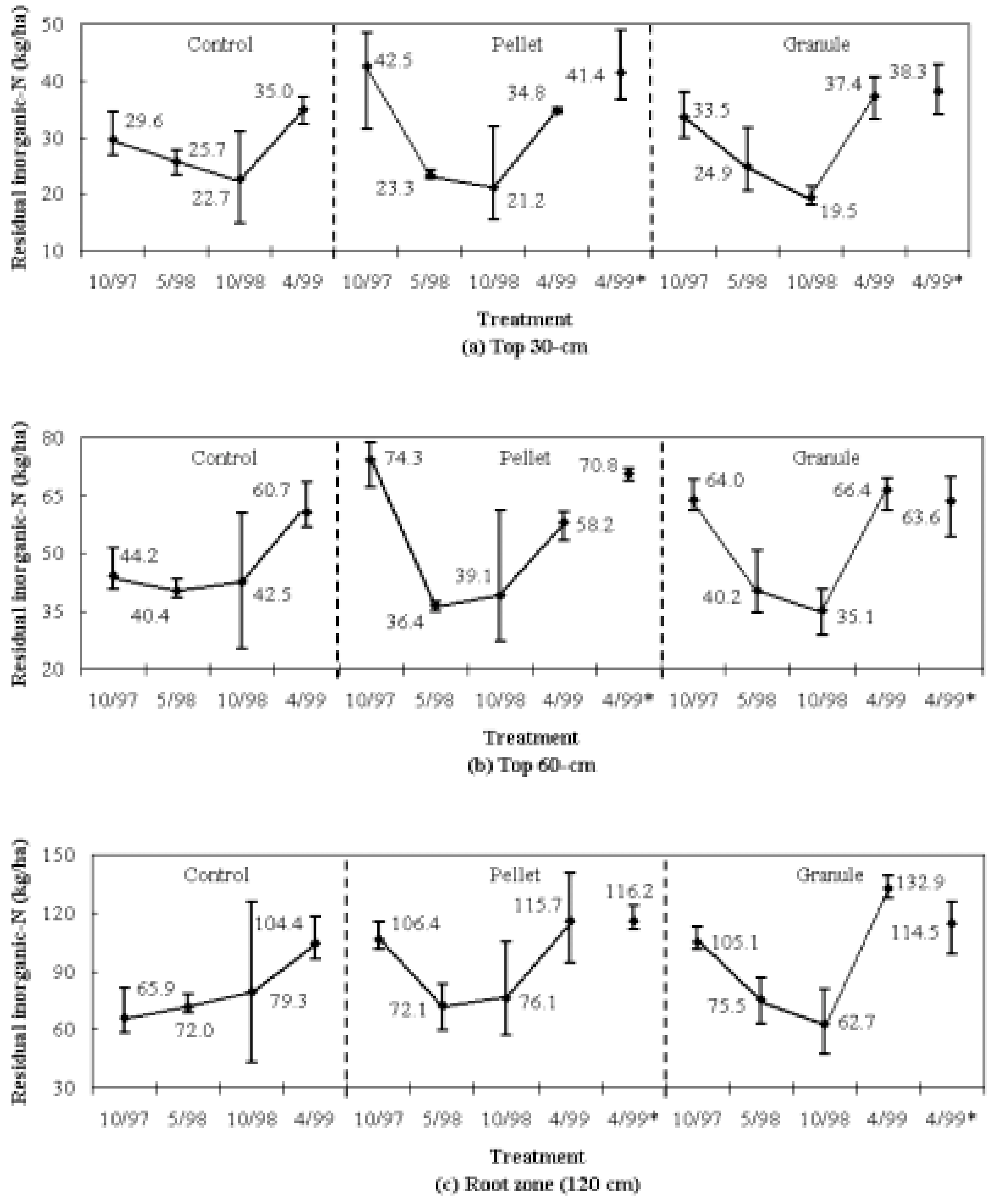

Figure 4.6. **Soil residual inorganic-N (kg/ha) among treatments by layer, (a) top 30 cm, (b) top 60 cm, and (c) root zone, and by sampling time. Mean (♦) values are the average of three replications obtained midway between crop rows; the mean value corresponding to 4/99* represents the average of three replications obtained in the fertilizer band. Mean values are joined by a line to indicate the trend. Maximum and minimum values are indicated.**

3.1. Null Hypothesis: Estimated amounts of residual inorganic-N are unaffected by the treatments, i.e., C, PS, and GS.

Alternative Hypothesis: Estimated amounts of residual inorganic-N are affected by the treatments.

The inorganic-N amounts in the three layers are compared among the treatments in figure 4.6. While the inorganic-N content data (nine data points per layer) for the top 30- and 60-cm layers were normally distributed with respect to residuals, data for the root zone were not normally distributed. While parametric statistical methods were used for the 30- and 60-cm layers, non-parametric methods were used for the root zone.

The evidence failed to reject Null Hypothesis 3.1 (ANOVA $p = 0.12$) in the top 30-cm layer indicating that the control and fertilizer treatments did not significantly differ in inorganic-N contents. Consequently, Hypothesis 3.2 was not tested for the top 30-cm layer.

For the top 60-cm layer, Null Hypothesis 3.1 was rejected (ANOVA $p < 0.01$) indicating that at least one treatment had a significantly lower residual inorganic-N amount (fig. 4.6). That the null hypothesis was rejected in the top 60-cm layer but not in the top 30-cm layer was likely due to leaching of the NO_3^--N from the top 30-cm layer and its accumulation in the lower half of the top 60-cm layer due to irrigation. The residual inorganic-N (from the applied-N) in the PS and GS treatments was 30.1 and 19.8 kg/ha, respectively, in the top 60-cm layer.

Null Hypothesis 3.1 was rejected for the root zone (fig. 4.6) using the K-W test ($p = 0.07$) indicating that at least one treatment had a significantly lower residual inorganic-N amount. After adjusting for background inorganic-N, the PS and GS treatments had 40.5 and 39.2 kg-N/ha as residual inorganic-N (from the applied-N), respectively, in the root zone.

3.2. Null Hypothesis: Residual inorganic-N amounts are equal in both urea forms at the sufficient application rate (184 kg-N/ha).

Alternative Hypothesis: Residual inorganic-N amounts are higher in PS than GS.

In the top 60-cm layer, Null Hypothesis 3.2 was rejected with the Student t-test ($p = 0.04$, equal variance) indicating that pellets conserved more inorganic-N in the top 60-cm layer than granules. For the root zone, the evidence failed to reject Null Hypothesis 3.2 with the Wilcoxon Rank Sums two-sample test ($p = 0.50$). Hence, the urea form did not impact residual inorganic-N amounts in the root zone.

With 39.8 cm of rainfall and irrigation, 3.5 months after sidedress N application (147 kg-N/ha), pellets contained 16% (10.3 kg-N/ha) more soil inorganic-N (t-test $p = 0.04$) than granules in the top 60-cm layer (fig. 4.6). Hence, NO_3^--N leaching was slower from pellets than granules, possibly due to slower nitrification. Even though the two urea forms did not differ in residual inorganic-N amount in the top 30-cm, the difference in the amounts of inorganic-N in pellets and granules, 27% (9.0 kg/ha), in half the soil volume of the top 60-cm layer was of practical significance. Increased inorganic-N amount in the top 30-cm layer could lower N requirement for the winter crop and reduce NO_3^--N leaching.

<u>May 1998</u>

3.1. Null Hypothesis: Estimated amounts of residual inorganic-N are unaffected by the treatments, i.e., C, PS, and GS.

Alternative Hypothesis: Estimated amounts of residual inorganic-N are affected by the treatments.

The inorganic-N amounts in the three layers are compared among the treatments in figure 4.6. For all three layers, the data were found to be normally distributed; hence, ANOVA was used for data analysis. In the top 30-cm layer, top 60-cm layer, and root zone, the evidence failed to reject Null Hypothesis 3.1 with ANOVA p-values of 0.73, 0.63, and 0.90, respectively. Hence, the treatments did not impact residual inorganic-N amounts in any of the three layers indicating that all applied-N had leached out of the root zone during the over-winter period. During this period, 67.5 cm of precipitation was received compared with normal precipitation of 54.8 cm (fig. A(a), Appendix A). Precipitation on moist soil (due to irrigation applied prior to the October 1997 sampling) and warm conditions (fig. A(b), Appendix A) combined to create conditions that were conducive to rapid mineralization as well as NO_3^--N leaching and denitrification. Since inorganic-N was not affected in any layer by the treatments, Hypothesis 3.2 was not tested for any layer to see if urea form affected residual inorganic-N retention.

<u>October 1998</u>

3.1. Null Hypothesis: Estimated amounts of residual inorganic-N are unaffected by the treatments, i.e., C, PS, and GS.

Alternative Hypothesis: Estimated amounts of residual inorganic-N are affected by the treatments.

The inorganic-N amounts in the three layers are compared among the treatments in figure 4.6. In the top 30-cm layer, top 60-cm layer, and root zone, the evidence failed to reject Null Hypothesis 3.1 with ANOVA p-values of 0.86, 0.84, and 0.79, respectively. Hence, the treatments did not impact residual inorganic-N amounts in any of the three layers indicating that there was no treatment effect on residual inorganic-N amount in any layer. Consequently, Hypothesis 3.2 was not tested to compare the urea forms.

Since all treatments had comparable inorganic-N amounts in all layers in May 1998, lack of difference in October 1998 in inorganic-N amounts in any layer among the treatments was unexpected given that the fertilizer treatments received 184 kg-N/ha during the crop season. Large N losses from the fertilizer treatments due to NO_3^--N leaching or denitrification seemed unlikely since only 17.1 cm of precipitation fell between sidedress N application and crop harvest (fig. 4.2). During a one-month period between harvest (mid-September) and soil sampling, there was 7.9 cm of precipitation (fig. A(a), Appendix A) which is likely to have caused very little leaching since there had been no precipitation for four weeks prior to harvest (fig. 4.2). Applied-N losses through denitrification and NH_4^+-N fixation by clay minerals were likely of minor importance in explaining why the control and fertilizer treatments had similar inorganic-N amounts.

Failure of the soil sampling scheme to account for the residual applied-N was likely a major factor. Soil sampling in October 1997 and May 1998 was performed under moist conditions that allowed for substantial movement of inorganic-N both laterally and vertically. The dry soil conditions preceding the October 1998 sampling likely resulted in the applied-N remaining in the vicinity of the band. Consequently, soil sampling 17.5 cm away from the band likely resulted in underestimation of applied inorganic-N in the October 1998 sampling, thereby requiring a modified sampling scheme for the last sampling event.

April 1999

3.1. Null Hypothesis: Estimated amounts of residual inorganic-N are unaffected by the treatments, i.e., C, PS, and GS.

Alternative Hypothesis: Estimated amounts of residual inorganic-N are affected by the treatments.

The inorganic-N amounts in the three layers are compared among the treatments in figure 4.6. Based on the sampling procedure (between the rows) followed earlier, the three treatments were not significantly different with p values of 0.45, 0.23, and 0.16, in the top 30-cm, top 60-cm, and root zone, respectively. Inorganic-N amounts were higher in all treatments and in all layers in April 1999 than in October 1998.

A warmer-than-normal fall-through-spring of 1998-1999 (fig. A(b), Appendix A) was conducive to mineralization of background-N. However, during that period, only 27.4 cm of precipitation was received compared to a normal precipitation of 42.6 cm (fig. A(a), Appendix A). The combination of warm and dry conditions probably resulted in accumulation of mineralized inorganic-N in the root zone leading to higher inorganic-N in all layers in all treatments in April 1999 as compared with October 1998. Given the absence of treatment effect on residual inorganic-N amount in any layer, Hypothesis 3.2 was not tested to compare between the urea forms.

3.3. Null Hypothesis: Residual inorganic-N amounts in the fertilizer treatments based on inorganic-N concentrations calculated using the SS1 samples are the same as the control treatment.

Alternative Hypothesis: Residual inorganic-N amounts are higher in the fertilizer treatments than in the control treatment.

Inorganic-N amounts in the two fertilizer treatments are compared for the two sampling schemes in figure 4.6. In pellets, using the t-test, in the top 60-cm layer, there was significantly greater ($p = 0.01$) inorganic-N amount in the fertilizer band than midway between crop rows, while there were no significant differences in the top 30-cm ($p = 0.16$) and root zone ($p = 0.98$). Both sampling schemes gave comparable soil inorganic-N amounts in the top 30-cm, top-60 cm, and root zone of the granule treatment with t-test p-values of 0.82, 0.64, and 0.11, respectively.

Greater inorganic-N recovery in the fertilizer band in the top 60-cm layer in the pellet treatment indicated that soil sampling on the fertilizer band in October 1998 could have provided a more accurate estimate of soil inorganic-N amounts in the fertilizer treatments. It is unclear if such a sampling scheme could have affected the results in October 1997 and May 1998. Both sampling events were preceded by wet periods where substantial N movement in the downward direction as well as laterally (due to diffusion) would be expected. Even though the inorganic-N amounts in the two sampling schemes were not significantly different in the root zone of the granule treatment, inorganic-N recovery in the fertilizer band was 14% lower than midway between the rows which was unexpected.

3.4. Null Hypothesis: For the same fertilizer treatment, residual inorganic-N amounts based on the inorganic-N concentrations at SS1, SS2, and SS3 are not different.

Alternative Hypothesis: Residual inorganic-N amounts based on the inorganic-N concentrations at SS1, SS2, and SS3 are different.

Comparison of inorganic-N amounts in each layer using data from three sampling locations (SS1, SS2, and SS3) for each treatment are presented in table 4.9. Except for the top 60-cm layer in the granule treatment which was analyzed using K-W test, all other data sets were normally distributed and were analyzed using ANOVA. When the null hypothesis was rejected, Fisher's LSD or the Bonferroni test was used to compare between treatments.

In the pellet treatment, based on the p-values shown in table 4.9, the sampling location did not affect inorganic-N estimation in any layer. However, lower p-values in the top 30-cm and top 60-cm layers compared to the root zone indicated that, compared to sampling between rows, sampling on the fertilizer band in October 1998 would have given a more accurate estimate of residual inorganic-N.

In granules, the sampling location did not affect inorganic-N estimation in the top 30-cm and top 60-cm layers (table 4.9). However, greater inorganic-N recovery in the root zone from SS3 than from SS1 or SS2 (table 4.9) was unexpected. Since the solute plume would be more concentrated directly below the point of application (SS1) as compared to a point 17.5 cm away (SS3), the unexpected result could be attributed to one or a combination of uncertainties associated with sampling, inorganic-N analysis, or solute transport in macropores. However, relatively low variability in the SS3 results in the root zone (table 4.9) raises the possibility of greater lateral dispersion of applied-N, primarily as NO_3^- in granules than pellets. It was unclear if the less effective root interception of applied-N in granules than in pellets resulted in greater lateral dispersion of applied-N in granules.

Table 4.9. Comparison of soil inorganic-N amounts in three sampling locations for each fertilizer treatment in different layers in April 1999

Treatment	Location*	Top 30-cm layer		Top 60-cm layer		Root zone	
		Mean†	SD‡	Mean	SD	Mean	SD
		---------------------------kg-N/ha--------------------------					
Pellet	SS1	41.4	6.6	70.8	1.9	116.2	6.8
	SS2	35.9	3.4	63.8	9.3	109.1	6.2
	SS3	34.8	0.4	58.2	4.2	115.7	23.3
	p-value	0.21		0.11		0.80	
Granule	SS1	38.3	4.4	63.6	8.3	114.5b§	14.2
	SS2	41.4	6.9	65.1	5.0	112.3b	9.5
	SS3	37.4	3.9	66.4	4.8	132.9a	5.7
	p-value	0.64		0.79‖		0.10	

* SS1 – sampling on the fertilizer band; SS2 – sampling 8.75 cm on the side of SS1; and SS3 – sampling mid-way between crop rows (17.5 cm from SS1)

† Average of three replications

‡ Standard deviation

§ Treatment means in the same column, followed by the same letter are not significantly different at $\alpha = 0.1$ using Fisher's LSD.

‖ Kruskal-Wallis p-value

4. Nitrate-N concentration in leachate

To evaluate treatment impact on NO_3^--N leaching, NO_3^--N concentrations in leachate at 30- and 120-cm depths were compared among the three treatments. During the leachate sampling period, 31 and 27 sets of samples were collected at 30-cm and 120-cm depths, respectively (table 4.10). Given the dry conditions during the 1997 corn season, only one set of leachate samples was collected at each depth. Irrigation (17.8 cm over 11 days) was applied at 1.0 cm/h to collect leachate samples after harvesting corn silage in 1997. Nitrate-N concentrations at 30- and 120-cm are presented in figures 4.7 and 4.8, respectively.

Table 4.10. Schedule of leachate sample collection

Time period	Precipitation during period (cm)	Number of sample sets collected	
		30-cm depth	120-cm depth
July 24 – September 18, 1997	34.1	1	1
September 19, 1997 – May 17, 1998	89.7*	16	14
May 18 – August 31, 1998	31.8	6	6
September 1 – December 31, 1998	14.4	0	0
January 1 – April 2, 1999	20.7	8	6
Total	190.7	31	27

* Includes 17.8 cm of irrigation

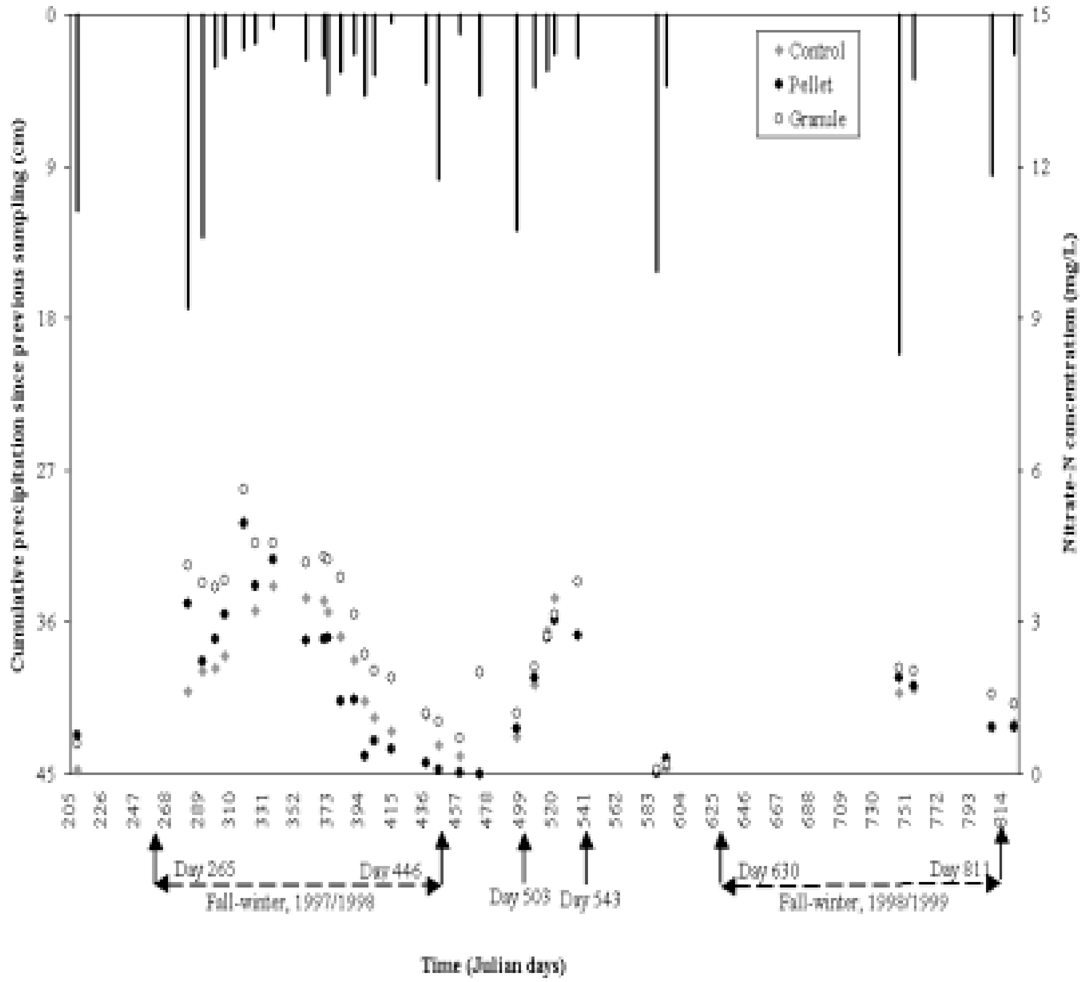

Figure 4.7. **Nitrate-N concentration in leachate samples at 30-cm depth from control, pellet, and granule treatments from July 29, 1997 (day 210) through April 2, 1999 (day 822). Each data point is the average of three replications. On days 503 and 543, starter- and sidedress-N were applied to the 1998 corn crop. For days 438 and 595, data for one replication of the control treatment was unavailable; for days 306 and 374, data for one replication of the pellet treatment and for day 210, data for one replication of the granule treatment were unavailable. For day 589, one replication each were unavailable for the control and granule treatments.**

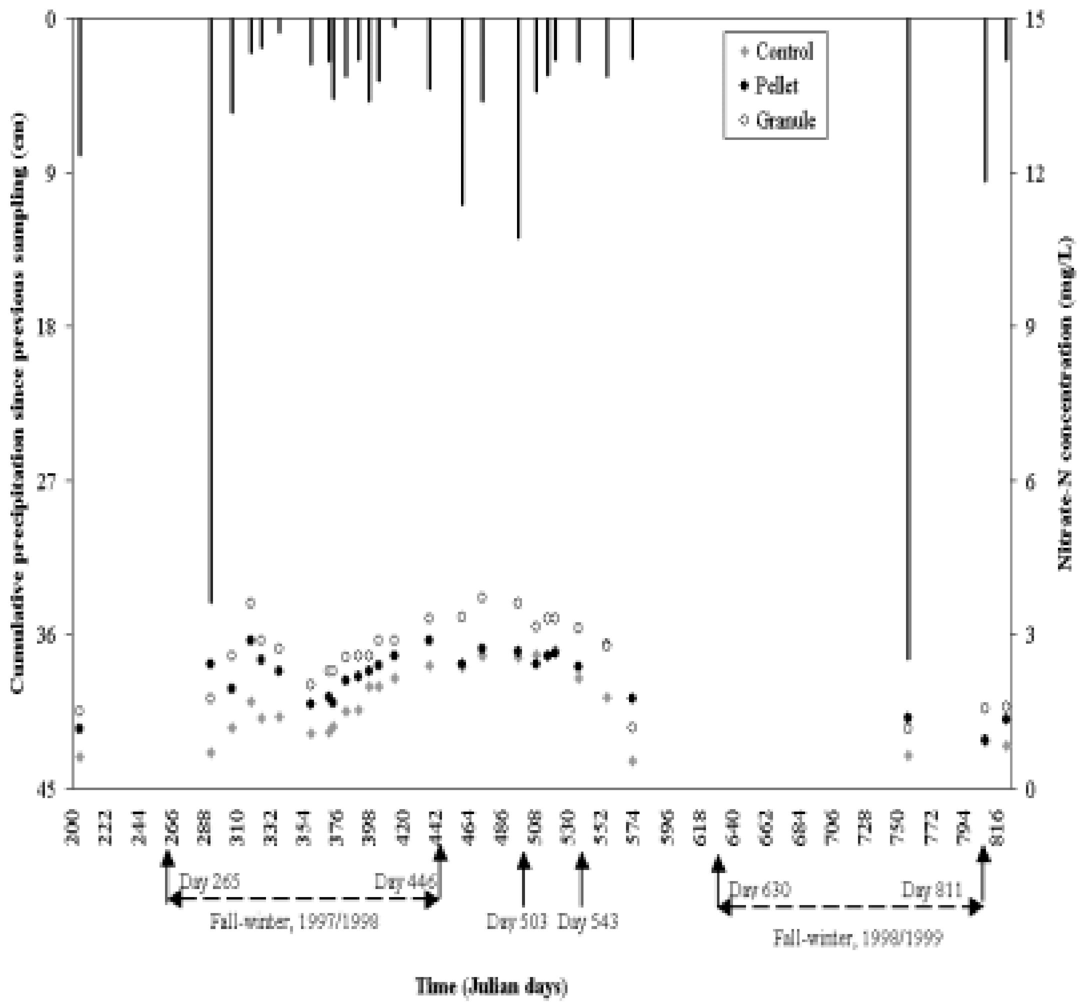

Figure 4.8. Nitrate-N concentration in leachate samples at 120-cm depth from control, pellet, and granule treatments during July 24, 1997 (day 205) to April 2, 1999 (day 822). Each data point is the average of three replications. On days 503 and 543, starter- and sidedress-N were applied to the 1998 corn crop. For days 306 and 374, data for one replication of the pellet treatment and for day 205, data for one replication of the granule treatment were unavailable. One data set collected on day 452 was discarded because the tension lysimeters were submerged.

For each depth, samples obtained for a sampling event were compared statistically using GLM or K-W. If the GLM or K-W test resulted in a rejection of Null Hypothesis 4.1, Hypothesis 4.2 was tested using the t-test or Wilcoxon Rank Sums test. Time series of the three treatments were compared at both depths.

4.1. Null Hypothesis: NO_3^--N concentration in leachate is unaffected by fertilizer treatment.

Alternative Hypothesis: NO_3^--N concentration in leachate is affected by the fertilizer treatment.

4.2. Null Hypothesis: NO_3^--N concentration in leachate is unaffected by the urea form (pellet versus granule).

Alternative Hypothesis: NO_3^--N concentration in leachate is lower in the pellet treatment than in granules.

<u>30-cm depth</u>

In 28 of 31 sampling events, the pellet treatment had lower NO_3^--N concentration than the granule treatment (fig. 4.7, table 4.11). Averaged over the 31 events, NO_3^--N concentrations in the control, pellet, and granule treatments were 1.9, 1.8, and 2.6 mg-N/L, respectively (table 4.11). However, NO_3^--N concentration from the granule treatment was significantly higher than the pellet treatment (Student t-test $p = 0.06$) only on 27 October 1997. High variability in NO_3^--N concentration within treatments may have masked differences. Leachate NO_3^--N concentrations in four of 31 sampling events (table 4.11) showed treatment effects (ANOVA or K-W $p < 0.1$), indicating differences between control and fertilizer treatments.

Increasing NO_3^--N concentration in leachate at the 30-cm depth (fig. 4.7) during 9 October 1997 (Julian day 282) through 15 November 1997 (Julian day 319) was due to the flushing action of the irrigation applied during 6-16 October 1997. Nitrate-N concentration in leachate at the 30-cm depth declined during 22 November 1997 (Julian day 326) through 18 April 1998 (Julian day 473) possibly due to NO_3^--N leaching during the warm and wet fall through spring of 1997-1998. Increasing NO_3^--N concentration in leachate at the 30-cm depth during 12 May 1998 (Julian day 497) through 21 June 1998 (Julian day 537) could be due to the moist and warm conditions (figures A(a) and A(b), Appendix A) which favored rapid mineralization of background N and NO_3^--N leaching. For the remaining period, no trend was evident since there were too few data points because of dry soil conditions.

Table 4.11. Nitrate-N concentration in control (C), pellet (P), and granule (G) treatments at 30-cm depth

Date	Julian day	Control		Pellet		Granule		ANOVA (or K-W)* p-value	T-test[†] p-value	Inference
		Mean[‡]	SD[§]	Mean	SD	Mean	SD			
		---------------NO_3^--N, mg-N/L---------------								
7/29/97	210	0.1	0.1	0.8	0.2	0.6	0.2	0.01	0.31	G=P>C
10/9/97	282	1.6	0.2	3.4	1.5	4.1[‖]	1.0	0.12		G=P=C
10/19/97	292	2.1	0.3	2.2	1.8	3.8	0.2	0.06**	0.28	G=P>C
10/27/97	300	2.1	0.3	2.6	0.9	3.7	0.3	0.03	0.06	G>P>C
11/2/97	306	2.3	0.4	3.1[§]	0.1	3.8	0.4	0.02	0.13	G=P>C
11/15/97	319	5.0	0.8	5.0	1.3	5.6	1.0	0.72		G=P=C
11/22/97	326	3.2	1.0	3.7	0.9	4.6	0.5	0.22		G=P=C
12/4/98	338	3.7	0.9	4.2	0.4	4.5	0.4	0.35		G=P=C
12/25/98	359	3.5	1.2	2.6	0.2	4.2	0.5	0.13		G=P=C
1/6/98	371	3.4	0.9	2.7	0.8	4.3	0.9	0.11**		G=P=C
1/9/98	374	3.2	1.0	2.6[‖]	1.3	4.2	1.7	0.47		G=P=C
1/17/98	382	2.7	1.3	1.4	0.4	3.9	2.6	0.29		G=P=C
1/26/98	391	2.2	1.0	1.4	0.8	3.2	2.6	0.51		G=P=C
2/2/98	398	1.4	0.8	0.4	0.2	2.4	2.6	0.36		G=P=C
2/8/98	404	1.1	0.5	0.6	0.5	2.0	2.3	0.50		G=P=C
2/18/98	415	0.8	0.6	0.5	0.6	1.9	2.4	0.51		G=P=C
3/14/98	438	1.1	0.2	0.2	0.3	1.2	1.8	0.57		G=P=C
3/22/98	446	0.6	0.5	0.1	0.1	1.0	1.7	0.58		G=P=C
4/5/98	460	0.3	0.3	0.0	0.0	0.7	1.2	0.73**		G=P=C
4/18/98	473	0.0	0.0	0.0	0.0	0.4	0.6	0.73**		G=P=C
5/12/98	497	0.7	0.2	0.9	0.1	1.2	0.8	0.50		G=P=C
5/24/98	509	1.7	0.5	1.9	0.1	2.1	0.3	0.51		G=P=C
6/1/98	517	2.8	0.6	2.7	0.6	2.7	0.2	0.94		G=P=C
6/6/98	522	3.5	0.9	3.0	0.5	3.2	0.3	0.71		G=P=C
6/21/98	537	2.7	1.0	2.7	1.2	3.8	0.2	0.30		G=P=C
8/12/98	589	0.1[‖]	0.1	0.0	0.0	0.1[‖]	0.1	0.55		G=P=C
8/18/98	595	0.1[‖]	0.2	0.3	0.2	0.2	0.3	0.76		G=P=C
1/17/99	747	1.6	0.5	1.9	0.5	2.1	0.5	0.49		G=P=C
1/27/99	757	1.7	0.4	1.7	0.9	2.0	0.5	0.79		G=P=C
3/19/99	808	0.9	0.2	0.9	0.6	1.6	0.6	0.29		G=P=C
4/2/99	822	1.0	0.3	0.9	0.7	1.4	0.8	0.63		G=P=C
Mean		1.9	0.6	1.8	0.6	2.6	1.0			

* Analysis of variance or Kruskal-Wallis
† Student t-test
‡ Average of three replications, unless indicated otherwise
§ Standard deviation
‖ Average of two replications
** Kruskal-Wallis p-value

<u>120-cm depth</u>

In 23 of 27 sampling events, the pellet treatment had lower leachate NO_3^--N concentrations than the granule treatment (fig. 4.8, table 4.12). Averaged over 27 events, leachate NO_3^--N concentrations at 120 cm in the control, pellet, and granule treatments were 1.6, 2.2, and 2.6 mg-N/L, respectively (table 4.12).

Table 4.12. Nitrate-N concentration in control (C), pellet (P), and granule (G) treatments at 120-cm depth

Date	Julian day	Control Mean‡	Control SD§	Pellet Mean	Pellet SD	Granule Mean	Granule SD	ANOVA (or K-W)* p-value	T-test (or W-R)† p-value	Inference
		---NO$_3^-$-N, mg-N/L---								
7/24/97	205	0.6	0.3	1.2	1.2	1.5‖	0.8	0.53		G=P=C
10/19/97	292	0.7	0.6	2.4	1.1	1.8	0.2	0.07	0.35	G=P>C
11/2/97	306	1.2	0.2	1.9§	0.8	2.6	0.7	0.08	0.40	G=P>C
11/15/97	319	1.7	0.4	2.9	0.9	3.6	0.6	0.03	0.31	G=P>C
11/22/97	326	1.4	0.3	2.5	0.8	2.9	0.5	0.02	0.44	G=P>C
12/4/98	338	1.4	0.2	2.3	0.8	2.7	0.4	0.06	0.45	G=P>C
12/25/98	359	1.1	0.1	1.6	0.5	2.0	0.1	0.03	0.33**	G=P>C
1/6/98	371	1.1	0.1	1.8	0.6	2.3	0.1	0.03	0.12	G=P>C
1/9/98	374	1.2	0.2	1.7‖	0.7	2.3	0.2	0.04	0.22	G=P>C
1/17/98	382	1.5	0.5	2.1	0.6	2.5	0.2	0.07	0.27	G=P>C
1/26/98	391	1.5	0.3	2.2	0.6	2.6	0.2	0.05	0.34	G=P>C
2/2/98	398	2.0	0.2	2.3	0.5	2.6	0.1	0.18		G=P=C
2/8/98	404	2.0	0.3	2.4	0.5	2.9	0.5	0.11		G=P=C
2/19/98	415	2.1	0.4	2.6	0.5	2.9	0.4	0.19		G=P=C
3/14/98	438	2.4	0.5	2.9	0.5	3.3	0.8	0.30		G=P=C
4/5/98	460	2.4	0.4	2.4	0.6	3.3	1.3	0.36		G=P=C
4/18/98	473	2.6	0.6	2.7	0.7	3.7	1.3	0.30		G=P=C
5/12/98	497	2.5	0.4	2.7	0.9	3.6	1.5	0.45		G=P=C
5/24/98	509	2.6	0.4	2.4	0.9	3.1	1.0	0.58		G=P=C
6/1/98	517	2.6	0.3	2.6	0.6	3.3	1.5	0.59		G=P=C
6/6/98	522	2.7	0.1	2.6	0.3	3.3	1.4	0.60		G=P=C
6/21/98	537	2.2	0.2	2.4	0.4	3.1	1.3	0.37		G=P=C
7/10/98	556	1.8	0.8	2.8	0.6	2.7	0.8	0.23		G=P=C
7/27/98	573	0.6	0.5	1.7	1.4	1.2	0.7	0.38		G=P=C
1/27/99	757	0.6	0.1	1.4	0.4	1.1	0.3	0.06	0.50	G=P>C
3/19/99	808	0.8	0.2	1.2	0.4	1.3	0.2	0.10		G=P=C
4/2/99	822	0.8	0.2	1.3	0.4	1.6	0.3	0.06	0.41	G=P>C
Mean		1.6	0.3	2.2	0.7	2.6	0.7			

* Analysis of variance or Kruskal-Wallis
† Student t-test or Wilcoxon Rank Sums test
‡ Average of three replications, unless indicated otherwise
§ Standard deviation
‖ Average of two replications
** Kruskal-Wallis p-value

In 12 of 27 sampling events (table 4.12), the fertilizer treatments had significantly higher NO_3^--N concentrations (ANOVA or K-W $p < 0.1$) than the control treatment. Ten of the 12 events were sequential, beginning with the set of samples collected after irrigation application (19 October 1997, Julian day 292) and ending with the sample sets collected on 26 January 1998 (Julian day 391). Of the 12 events with treatment effects, no difference in NO_3^--N concentration in pellets and granules were observed in any event. However, comparison of the time series of NO_3^--N concentration indicated that granules had the highest NO_3^--N concentration, followed by the pellet and control treatments, respectively (fig. 4.8). High variability in NO_3^--N concentration within the treatments (table 4.12) may have masked treatment effects on NO_3^--N leaching.

Increased NO_3^--N concentration in leachate in all treatments from 19 October 1997 (Julian day 292) through 15 November 1997 (Julian day 319) indicated the flushing action of the irrigation on NO_3^--N from both applied and background sources (table 4.12, fig. 4.8). The increase and decrease in NO_3^--N concentration between 2 February 1998 (Julian day 398) and 27 July 1998 (Julian day 573) was likely due to mineralization of background N (table 4.12, fig. 4.8). Too few data points were available after July 1998 to identify a trend.

In the early stages of data collection, NO_3^--N concentration at 120 cm was generally lower than NO_3^--N concentration at 30-cm depth. During late-winter through spring of 1998, lower NO_3^--N concentrations at 30 cm than at 120 cm was due to NO_3^--N movement through the soil profile.

Tension lysimeters installed at 30 cm were situated 15 and 30 cm from the nearest starter (37 kg-N/ha) and sidedress (147 kg-N/ha) bands, respectively. In addition to interception by the dense crop rooting in the top 30-cm, low transverse dispersivity (compared with longitudinal dispersivity) probably resulted in very little of the applied-N reaching the 30-cm tension lysimeters under dry conditions or when N movement was mostly due to mass flow. One sampling event (27 October 1997) at 30-cm depth, where leachate from the pellet treatment had lower NO_3^--N concentration than granules, had been preceded by 17.8 cm of irrigation applied in small amounts (3 cm/event, spread over six events) over 11 days. As a result, substantial amounts of applied NO_3^--N could have diffused laterally reaching the tension lysimeters. Compared to the 30-cm depth, larger amounts of NO_3^- from the applied-N reached the 120-cm tension lysimeters, as was indicated by 12 of 27 sampling events showing fertilizer treatment effects.

The tension lysimeter study indicated that when urea was subsurface-applied at 184 kg-N/ha, the maximum NO_3^--N concentration (3.7 mg-N/L) in the percolate leaving the root zone (table 4.12) remained substantially below the maximum safe level of 10 mg-N/L for drinking water. However, for all sampling events, NO_3^--N concentrations from all treatments were in excess of 0.3 mg-N/L, the threshold concentration level that can result in eutrophication in surface waters in the presence of a minimum of 0.001 mg/L of inorganic-P (Novotny and Olem, 1994).

5. Nitrogen removal by crop

Greater N removal by the crop ensures that lower amount of applied-N is available in the soil to be lost through NO_3^- leaching and other N-loss pathways. Nitrogen removal by corn silage (kg-N/ha) was calculated by multiplying DM (Mg/ha) with N content (% of DM) and is displayed by year in figure 4.9.

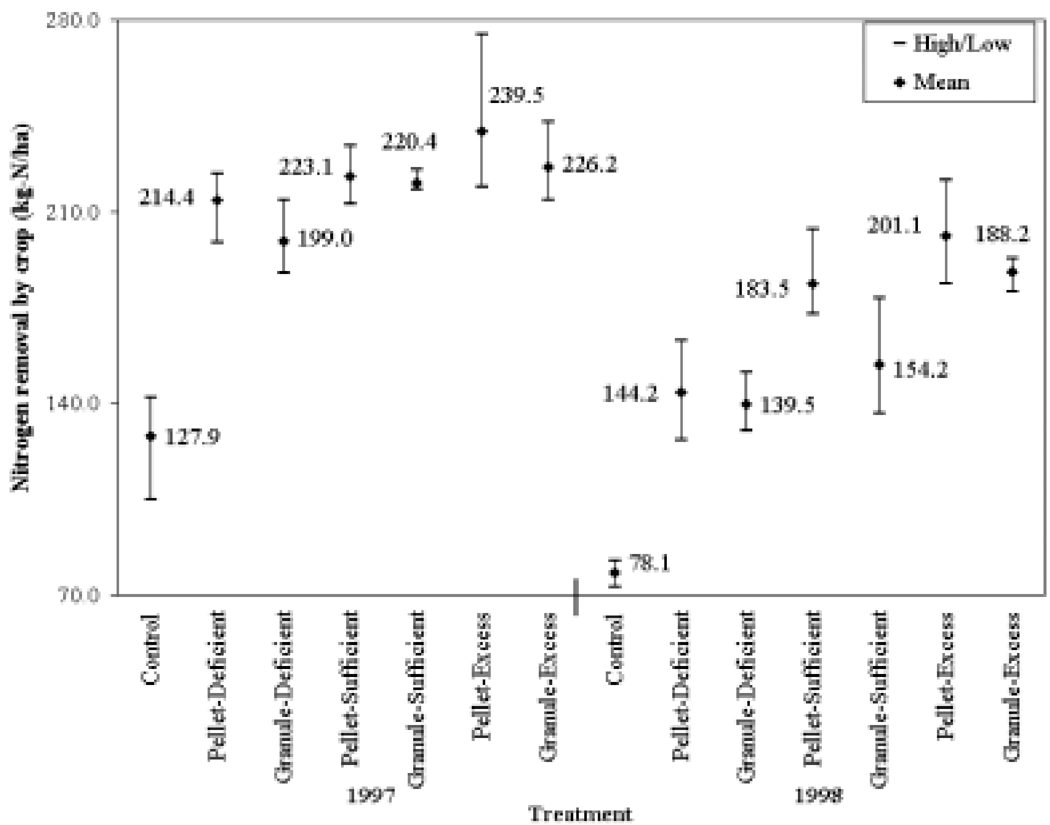

Figure 4.9. Total N removal by corn silage by treatment and year. Mean (♦) values are the average of three replications; maximum and minimum values represent the spread of the data.

5.1. Null Hypothesis: N removal by crop is unaffected by fertilizer treatment.

Alternative Hypothesis: N removal by crop is affected by fertilizer treatment.

Treatment effect (including control) on N removal by crop was investigated separately for 1997 and 1998. Since N removal data for both years were normally distributed, they were analyzed using ANOVA and Fisher's LSD (table 4.13). Even though corn silage yield and corn N content were discussed earlier in Hypotheses 1.1, 1.2, 2.1, and 2.2, N removal by crop will be discussed here in depth since it combines the effects of corn silage yield and corn N content.

Table 4.13. Treatment effect on N removal by crop (1997 and 1998)

Treatment	1997		1998	
	Mean* (kg-N/ha)	η_{Nrem}† (%)	Mean (kg-N/ha)	η_{Nrem} (%)
Control	127.9d‡	-	78.1d	-
Pellet-deficient	214.4bc	78.6	144.2c	60.1
Granule-deficient	199.0c	64.6	139.5c	55.8
Pellet-sufficient	223.1ab	51.7	183.5b	57.3
Granule-sufficient	220.4ab	50.3	154.2c	41.4
Pellet-excess	239.5a	43.3	201.1a	47.7
Granule-excess	226.2ab	38.1	188.2ab	42.7
LSD§	18.9		16.8	

* Average of three replications

† Applied-N removal efficiency

‡ Treatment means in the same column, followed by the same letter are not significantly different at $\alpha = 0.1$ using Fisher's LSD.

§ Fisher's Least Significant Difference

Also presented in table 4.13 is the applied-N removal efficiency, η_{Nrem}, for the fertilizer treatments. The amount of applied-N removed by the fertilizer treatment was calculated by subtracting N amount removed by the control treatment from the fertilizer treatment. The applied-N amount removed by the crop was divided by the total applied-N to the treatment to obtain η_{Nrem}.

Null Hypothesis 5.1 was rejected for 1997 (ANOVA $p < 0.01$); hence, the treatment significantly impacted N removal by crop. As expected, Fisher's LSD results indicated that N removal was lower in the control treatment as compared to the fertilizer treatments (fig. 4.9). Even though high variability within treatments masked differences between the fertilizer treatments, mean N removal values indicated that treatments with higher N application rates removed more N. The urea form did not affect crop N removal.

As expected, η_{Nrem} decreased with increasing N application rate in 1997. Also η_{Nrem} values were generally higher in pellets than granules, particularly at the deficient N application rate. Hence, more efficient applied-N interception by the plant roots in pellets than granules was a possibility.

For 1998, Null Hypothesis 5.1 was again rejected (ANOVA $p < 0.01$); hence, as in 1997, the fertilizer treatments significantly impacted N removal by the crop. As in 1997, Fisher's LSD results indicated that N removal was lower in the control treatment as compared to the fertilizer treatments (fig. 4.9). Fisher's LSD results also indicated that except at the sufficient N application rate, where the use of pellets resulted in greater N removal by crop than granules, the urea forms were not significantly different. Due to the depleted soil inorganic-N, all treatments experienced a decline in N removal by crop from 1997 to 1998. As expected, greater declines were observed in the deficient N application rates with the smallest declines observed in the excessive N application rates. However, at the sufficient N application rate, while the pellets underwent a decline of only 39.6 kg-N/ha, the granule treatment experienced a decline of 66.2 kg-N/ha, second only to PD with 70.2 kg-N/ha. The reason for the large decline in N removal in the GS treatment was unclear. Also unclear was whether decline in N removal adversely affected yield or vice-versa.

In 1998, for pellets, η_{Nrem} values declined with N application rate, remaining higher than corresponding values for granules. However, in granules, the reason for insignificant change in η_{Nrem} between the sufficient and excessive N application rate was unclear. As expected, due to the depleted soil-N status, the PS, PE, and GE treatments performed better than in 1997. However, the sharp decline in η_{Nrem} in the GS treatment in 1998 as compared to 1997 was unclear.

5.2. Null Hypothesis: N removal by crop is unaffected by the urea form at the sufficient application rate (184 kg-N/ha).

Alternative Hypothesis: N removal by crop is higher with PS than GS.

Nitrogen removal by crop was compared for PS and GS treatments for 1997 and 1998. Since both data sets were normally distributed, the Student t-test was applied to the data sets to test Hypothesis 5.2.

In 1997, the evidence failed to reject Null Hypothesis 5.2 ($p = 0.35$, equal variance); hence, urea form did not impact N removal by crop. However, in 1998, the null hypothesis was rejected ($p = 0.07$, equal variance) thus indicating that there was greater N removal by crop in the PS than in the GS treatment. As discussed earlier, compared to 1997, greater N removal by crop in 1998 in PS as compared to GS was unclear since the amounts of N removed by the PD and GD treatments were not significantly different.

4.1.3. Discussion Summary of Field Experiment

In 1997, due to high soil inorganic-N status, no urea form impact was observed on either corn silage yield (table 4.1) or corn N content (table 4.5). In 1998, urea form impact was observed on corn silage yield only at the sufficient application rate (184 kg-N/ha). There could have been greater N losses from granules (due to denitrification and NH_4^+-N fixation) than pellets in 1998. However, given the lack of difference in corn silage yield between PD and GD, higher corn silage yield from PS due to reduced N losses than GS did not seem likely. No urea form impact was observed on corn N content in any year. The PS treatment removed 29.3 kg-N/ha more than the GS treatment in 1998; hence, less N was available in the soil to be lost through leaching or denitrification during the over-winter period.

In October 1997, with 39.8 cm of rainfall and irrigation, over a 3.5-month period, compared to granules, slower nitrification in pellets resulted in greater inorganic-N (10.3 kg/ha) retention in the top 60-cm layer. Higher NO_3^--N concentration in granules than in pellets at 30 cm in the leachate samples (table 4.11) obtained 11 days (27

October 1997) after conclusion of irrigation supported the soil sampling results in October 1997 indicating that NO_3^--N movement was likely slower in pellets than granules. Greater inorganic-N retention in the top 60-cm layer in pellets could potentially enable a winter cover crop to scavenge N more effectively than from granules, resulting in reduced over-winter N losses. The wet and warm over-winter period of 1997-1998 probably resulted in near-complete removal of applied-N from the root zone as evidenced by comparable inorganic-N amounts in all three treatments in all three layers (fig. 4.6) in May 1998.

The October 1998 soil sampling (between crop rows) was preceded by dry conditions which probably limited the lateral movement of applied-N, thereby leading to an underestimation of applied residual-N. Comparison of inorganic-N amounts from different sampling schemes (fig. 3.3) provided evidence that sampling on the fertilizer band could potentially provide a better estimate of residual-N. Location of the 30-cm tension lysimeters with respect to the urea bands likely allowed for very little of the applied-N to reach the tension lysimeters (table 4.11). By comparison, more of the applied-N reached the 120-cm tension lysimeters (table 4.12). High variability in NO_3^--N concentration within the treatment probably masked differences between pellets and granules at 120 cm (table 4.12). However, comparison of time series of NO_3^--N concentration among the treatments, particularly at the 120-cm depth, showed that the NO_3^--N concentration was higher in granules, followed by pellets and control, respectively (table 4.12). This study showed that soil and leachate sampling schemes that apply to broadcast-N applications are not appropriate for determining residual-N concentration when N is banded

Nitrate-N leaching has been observed during the corn season in medium to coarse-textured soils in Georgia (Hubbard et al., 1991) and Virginia (Menelik et al., 1990). Due to deficit moisture conditions in both crop seasons, the impact of urea form on NO_3^--N leaching and its concomitant impact on corn silage yield and corn N content could not be evaluated. This study provided evidence that pellets could reduce NO_3^--N leaching during part of the over-winter period as compared to granules. While the 1997-1998 over-winter period was excessively wet, the 1998-1999 over-winter period was excessively dry. Hence, further evaluation using more intensive soil and leachate sampling is needed to determine if pellets are effective in reducing losses during over-winter periods under normal precipitation conditions.

4.2. Laboratory Experiments

Objective 2: Quantify the dissolution, mineralization, and NO_3^--N movement of subsurface-applied N pellets versus granules.

Laboratory experiments were conducted in the LW Laboratory of the BSE Department to achieve Objective 2. The rates of dissolution and movement of dissolved urea, as affected by urea form (pellet versus granule) were measured in a two-part dissolution study. Mineralization (urea hydrolysis and nitrification) rates of urea pellets and granules were quantified in an incubation study. Movement of NO_3^--N from pellets and granules were investigated using a leaching column study. The results of the laboratory experiments are presented and discussed in the following sections.

4.2.1. Dissolution Study

The dissolution study had two components - comparison of dissolution rate and comparison of center of mass of dissolved urea as affected by urea particle size. Dissolution rates of urea particles were measured by monitoring periodic weight loss of urea granules (1.5 g-urea/soil core) and pellets (0.5, 1.0. 1.5, and 2.0 g), applied between soil cores (fig. 4.10).

Time required for total dissolution increased with particle size. For all treatments, dissolution rate, as indicated by the weight loss versus time relationship, declined with time. Rapid dissolution in the initial stages in larger pellets was likely due to rapid dissolution of the edges since the pellets were tablet-shaped (G. Sanzoni, personal communication, Blacksburg, Va., 16 September 1997). For example, while 30% of the 2.0-g pellet dissolved in 6 h, the remaining 70% required 66 h to dissolve.

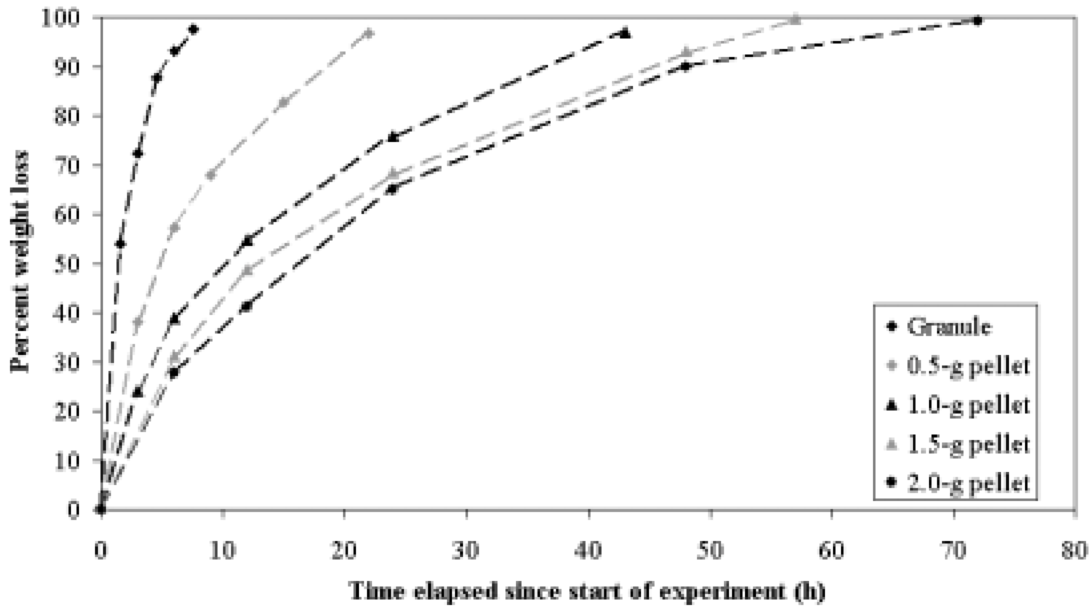

Figure 4.10. Percent weight loss in urea granules and pellets with time. Each data point is the mean of three replications. Data points are connected by dashed lines to show the dissolution trend.

1. **Null hypothesis: Urea dissolution rate (% weight loss/time) is unaffected by particle size.**

   Alternative hypothesis: Urea dissolution rate decreases as particle size increases (specific surface area decreases).

Due to the non-linearity of the percent weight loss versus time relationship (fig. 4.10), a dissolution rate that could be considered representative of the entire duration of dissolution was impossible to define for any of the treatments. A transformed plot of weight loss versus square root of time was used to linearize the relationship (fig. 4.11).

High correlation coefficient (r) values (fig. 4.11) indicated that percent weight loss versus square root of time had strongly linear relationships in all treatments. The regressions indicated that the slopes of the three largest pellets were close in value to each other while the two other treatments were different. A statistical comparison of the slopes using indicator variables in regression could not be performed since not all of the data sets were normally distributed. Based on the graphical comparison (fig. 4.11), it was likely that the granule, 0.5-g pellet and 1.5-g pellet treatments had different dissolution rates. However, the 1.0-g pellet, 1.5-g pellet, and 2.0-g pellet had similar dissolution rates.

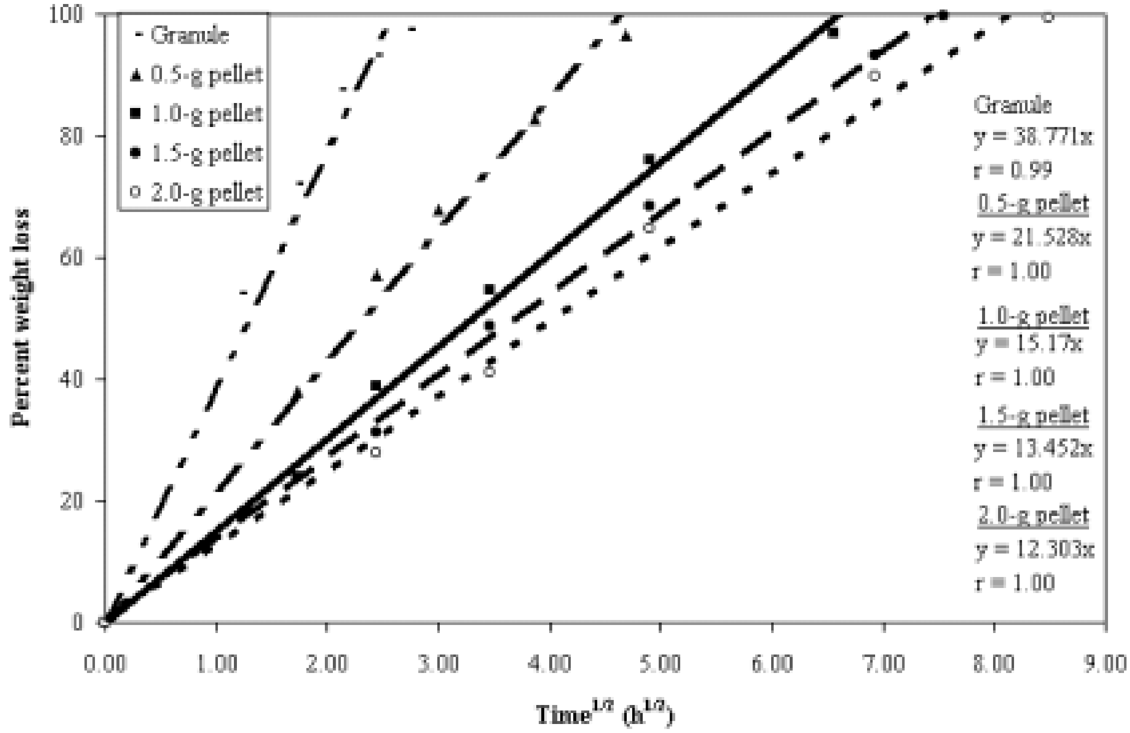

Figure 4.11. Per cent weight loss in urea granules and pellets with square root of time. Each data point is the mean of three replications. Data points for the treatment are connected by lines to show weight loss trend.

Center of mass of dissolved urea in pellets and granules were compared for granules (1.5 g-urea/soil core) and 1.5-g pellets based on dissolved urea (as percent of total urea in the soil core) in 1-cm thick layers, above and below the point of urea application (fig. 4.12). Amount of urea recovered in each 1-cm segment was represented as a point-load applied at the middle of the layer (fig. 3.6). Hence, the distances of point load applications were at 0.5, 1.5, 2.5, and 3.5 cm, as both, positive and negative numbers from the point of urea application. Measurements were made at 4.5 cm also; however, no urea was recovered at that distance in both pellets and granules. In pellets, 55% of the urea was recovered in the lower core compared to 52.1% in granules.

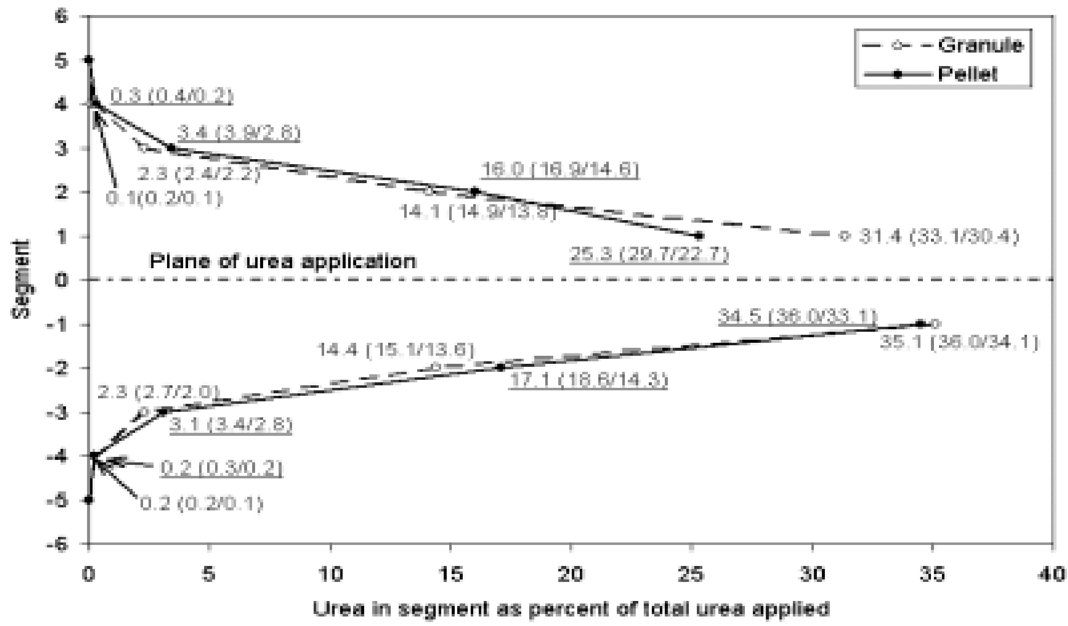

Figure 4.12. Urea distribution by segment in pellet and granules. Each data label is the mean value of three replications; numbers in parentheses represent maximum and minimum values. Segment 1 (or –1) represents a 1-cm soil section closest to the urea application plane. Positive segment markings represent segments above the plane of urea application.

2. Null hypothesis: The distance of center of mass of dissolved urea from the plane of placement is unaffected by the urea form (pellet versus granules). Alternative hypothesis: Center of mass of dissolved urea is at a greater distance from the plane of placement in granules than in 1.5-g pellets.

The center of mass values for the pellet and granule treatments were 0.98 and 0.89 cm, respectively, while the corresponding SD values were 0.04 and 0.03 cm. Null Hypothesis 2 was rejected (t-test p = 0.02, equal variance). Hence, the evidence indicated that center of mass was at greater distance from the plane of urea application in pellets than in granules.

It had been expected that the opposite would be the case, i.e., dissolved urea from granules would have a greater center of mass than pellets. For the experimental conditions, since the 1.5-g pellets dissolved in 60 h versus 7.5 h in granules, it had been expected that dissolved urea from the granules would have more time to move away from the plane of fertilizer placement resulting in a greater center of mass. Further, it had been expected that three-dimensional movement of dissolved urea in pellets compared to a largely one-dimensional movement in granules, would possibly result in slower downward urea movement in pellets than granules.

The reason for the greater dispersal of dissolved urea from pellets than from granules was probably due to greater mass flow in pellets than in granules as was indicated by greater urea recovery in the lower soil core in pellets than granules. Compared to granules, the dissolved urea from the pellet acting on a smaller area of contact probably exerted greater pressure causing greater displacement of dissolved urea from the point of application. However, since nearly half of the applied urea was present above the plane of urea application, molecular diffusion was likely the predominant mode of urea transport. Near-absence of urea in the two outer-most sections in each of the upper and lower cores indicated that volatilization loss from subsurface-applied urea, irrespective of its form would likely not be significant.

Moisture distribution within the soil column was investigated to compare between the two treatments; moisture distributions in the upper and lower cores were also compared to investigate the presence of a moisture gradient (fig. 4.13). Presence of a moisture gradient could provide information on the mode of urea transport.

No moisture gradient was observed in either of the treatments in either of the cores. The absence of a monotonically decreasing moisture gradient (with higher θ_v close to the plane of urea application) supported the earlier inference that urea movement in the soil cores was largely due to molecular diffusion. Singh and Beauchamp (1988) subsurface-applied urea powder at 60.3 mg/cm^2 to silt loam soil packed in a pipe. Up to a distance of 5 cm away from the plane of fertilizer application, at θ_m values ranging from 20 to 24%, moisture content gradients of 0.8%/cm were observed with θ_m increasing with distance (Singh and Beauchamp, 1988). Since a higher urea concentration (82.9 mg/cm^2) was applied in this study (resulting in greater osmotic suction) compared to the study by Singh and Beauchamp (1988), a moisture gradient had been expected in this study. Further, given the fact that silt loam will hold soil moisture with greater tenacity than loam sandy, the presence of a moisture gradient in the Singh and Beauchamp (1988) study and its absence in this study was unclear. Singh and Nye (1984) detected no moisture gradient when urea powder was surface-applied at 4.6 mg/cm^2 to sandy loam soil at θ_m = 20%. Lack of moisture gradient in the Singh and Nye (1984) study could have been due to low solute concentration resulting in low osmotic tension.

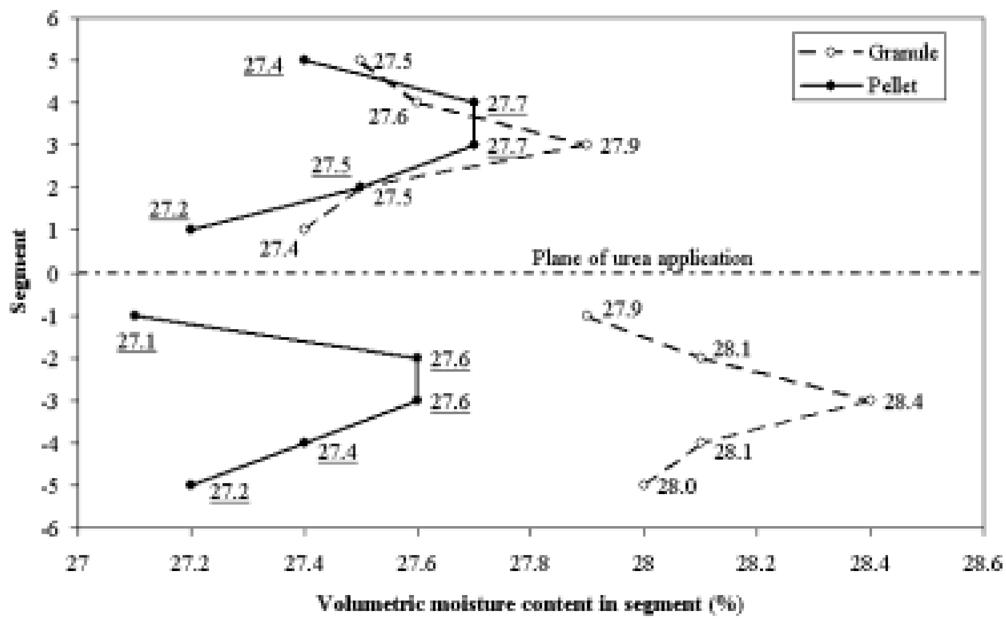

Figure 4.13. **Moisture distribution by segment in pellet and granules. Each data label is the mean value of three replications. The underlined values represent moisture content for the pellet. Segment 1 (or –1) represents a 1-cm soil section closest to the urea application plane. Positive segment markings represent segments above the plane of urea application.**

Moisture distribution in the pellet treatment was nearly identical in the upper and lower cores with average θ_v values of 27.5% and 27.3%, respectively. The granule treatment had average θ_v values of 27.6% and 28.1, respectively, in the upper and lower cores. Hence, in terms of moisture distribution, the pellet and granule treatments were comparable. The highest moisture contents were observed in the central section of each core (sections 3 and -3); thereafter, moisture content gradually tapered off towards the ends. The reason for such moisture distribution was unclear. Over the 60-h experimental period, the pellet and granule treatments lost 3.0 and 2.7% of water, respectively. Since both faces of the soil column were covered with double layers of parafilm (held by rubber band) and the interface between the upper and lower layers was sealed with tape, it was unclear how moisture was lost.

Even though the centers of mass in pellets and granules were statistically different, the actual difference (1 mm) was unlikely to impact mineralization and transport of urea and its transformation products. Further, conducting this experiment in a sterilized soil (to eliminate urease activity) likely reduces the applicability of these results to natural soil conditions with normal urease activity. Under natural soil conditions, urea recovery would have been lower due to conversion of urea to NH_4^+-N starting at the fringes of the dissolved urea front where the urea solution concentration would have been low enough to allow urea hydrolysis to proceed. However, this study indicated that urea movement was mainly through molecular diffusion, with nearly equal amounts moving in the upward and downward directions.

Proposed mechanism of dissolution of urea particles as affected by particle size

Chao (1967) reported that at greater than 70% relative humidity (RH), urea exhibits hygroscopicity. Since soil air is always close to saturation (Hillel, 1971), the dissolution process is initiated by the wetting of the urea particle surface by water in vapor or liquid form. The dissolved urea on the particle surface moves into the surrounding soil throughout the particle surface. The dissolved solute in soil solution exerts an osmotic suction in the surrounding soil resulting in vapor diffusion towards the solute particle (Marshall et al., 1993). However, the additional vapor flux into a region with high RH will result in supersaturation leading to condensation of vapor in pores close to the particle-soil interface. The concomitant increase in moisture content will reduce vapor diffusivity as thicker water films in the soil pores obstruct vapor movement (Marshall et al., 1993). Eventually, depending on the duration of the dissolution process, direct vapor movement from the surrounding soil to the urea particle may be reduced over time. Meanwhile, the dissolved urea will migrate in all directions with diffusion being the primary mode of movement.

However, due to migration of the dissolved urea at the particle surface into the surrounding soil, an annular space is created all around the particle except where the particle rests on the soil. The annular space is likely to prevent dissolved urea movement into the soil except through the area where the particle is still in contact with the soil. Liquid water across the annular space will convert to vapor and migrate to the particle surface due to osmotic suction exerted by the dissolved urea on the particle surface. In granules, due to their larger SSA, more of the dissolved urea will have moved in the upward direction before the annular space stops the upward and lateral transfer of dissolved urea directly from the granules to the soil. An indication of greater upward movement from granules as compared to pellets was provided by the higher urea recovery (of the total) in the upper soil core in granules (47.9%) versus pellets (45.0%).

One likely reason for the decline in dissolution rate (weight loss/unit time) with time (fig. 4.10) is due to faster dissolution of edges in pellets in the early stages; as the edges become smooth, the dissolution rate declines. A second reason for the greater dissolution rate decline in larger particles is perhaps due to the slower movement of the dissolved urea through the contact surface into the soil.

It was observed that both pellets and granules did not retain their tablet or spherical shapes; this was likely due to the downward flow of the dissolved urea to the base of the particle. Especially in pellets, the partly-dissolved particles assumed irregular shapes, sometimes resembling a column with pointed ends. Due to the greatly reduced area of contact between the particle and soil, dissolved urea movement into the soil was retarded, more so in the case of larger pellets than in smaller, more numerous granules.

However, the reduced rate of dissolved urea movement in pellets compared to granules seemed to contradict the results of the center of mass measurement experiment. In that experiment, greater distance of movement of dissolved urea was detected in pellets than granules. In granules, due to more-or-less, uniform application, dissolved urea movement was likely to be along one axis, perpendicular to the plane of urea application, in both upward and downward directions. Dissolved urea movement likely occurred along all three axes, in upward and downward directions in pellets. However, in pellets, due to a greater overburden of dissolved urea acting through a smaller surface area, there was likely greater vertical downward movement, with convective transport playing a more important role than in granules. However, dissolved urea movement parallel to the plane of application as well as in the upward direction was likely governed by molecular diffusion as in granules.

As discussed earlier, the dominant mode of dissolved urea movement seemed to be diffusion, though convection could have contributed to a certain extent, especially in pellets. The dominance of diffusion was supported by the absence of a moisture gradient in the soil core. The absence of monotonic moisture gradient in the soil profile was consistent with the results obtained by Singh and Nye (1984) who attributed diffusive transport to the lack of such a gradient.

4.2.2. Incubation Study

The incubation study was conducted to estimate rates of urea hydrolysis and nitrification of subsurface-applied urea pellets (1.5 g) and granules. The pellets and granules were also compared with respect to pH since nitrification is accompanied by a decline in pH. One-half gram pellets were also included in the study to evaluate the impact of SSA on mineralization and acidification. The control treatment was used to quantify background mineralization and acidification processes; however, it was excluded in the statistical analyses. Results and hypotheses for urea hydrolysis, nitrification, and acidification are presented separately.

<u>Urea Hydrolysis</u>

The first batch (7 d after start of incubation) of incubation pots were sampled and analyzed for urea (fig. 4.14) as described in Section 3.3.3. No urea analysis was performed on the control pots. Since urea recovery did not exceed 5% of the applied amount, assuming that all of the remaining urea would be hydrolyzed within the next 7 d, subsequent batches were not analyzed for urea. Based on urea-N recovered (fig. 4.14), urea hydrolysis rates for the granule, 0.5-g pellet, and 1.5-g pellet were 96.9, 96.4, and 93.8 μg-N/g-soil per day, respectively, over the 7-d period. Using percent urea hydrolyzed as the index of the rate of urea hydrolysis, Hypothesis 1 was tested to compare the three treatments.

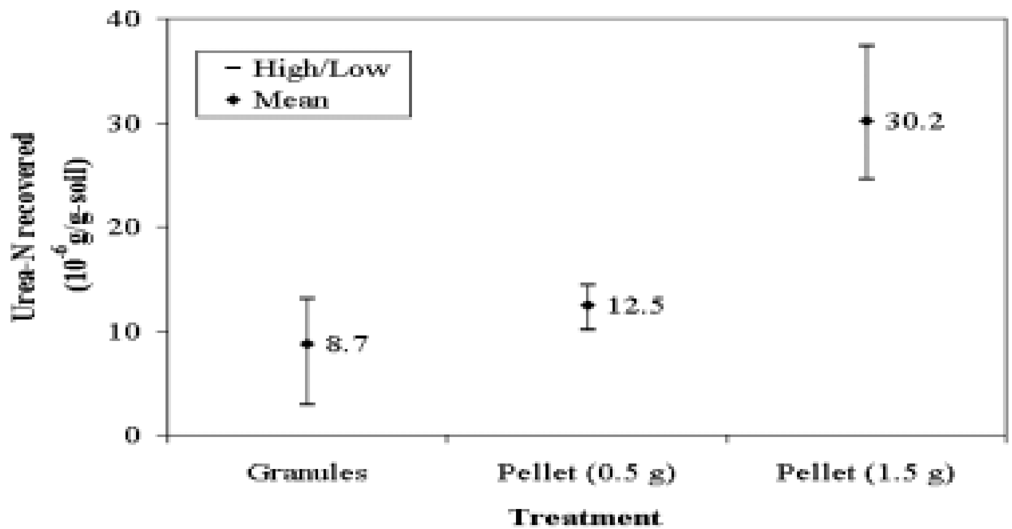

Figure 4.14. Urea-N recovered in the fertilizer treatments 7 d after start of incubation experiment. The mean values represent the average of three replications; the maximum and minimum values are represented by dash marks.

1. **Null Hypothesis: Rate of urea hydrolysis (percent urea hydrolyzed in 7 d) is unaffected by the fertilizer treatment.**

   Alternative Hypothesis: Rate of urea hydrolysis is affected by the fertilizer treatment.

Analysis of variance and Fisher's LSD were used to test the null hypothesis that urea hydrolysis rate was unaffected by the fertilizer treatment. The results are given in table 4.14.

Since the null hypothesis was rejected ($p < 0.01$), urea hydrolysis rate was affected by the treatment applied. Compared to granules and 0.5-g pellets, the 1.5-g pellet had a significantly lower urea hydrolysis rate. Singh and Beauchamp (1987) also reported that rate of urea hydrolysis decreased with increasing pellet size for 1-, 2-, and 3-g urea pellets.

Table 4.14. Incubation study results: urea hydrolyzed (7 d), nitrate recovered (35 d), and pH (35 d) from the control, granule, 0.5-g pellet, and 1.5-g pellet treatments

Treatment	Urea hydrolyzed (%)		Nitrate-N (μg/g-oven dry soil)		pH	
	Mean*	SD†	Mean	SD	Mean	SD
Control	-	-	45.8	-	5.94	-
Granule	98.8a‡	0.8	407.5a	8.1	4.93a	0.03
0.5-g pellet	98.2a	0.3	392.6a	14.4	5.16b	0.07
1.5-g pellet	95.6b	0.9	334.3b	19.9	5.44c	0.08
LSD§	0.8		17.6		0.07	

* Average of three replications in all treatments

† Standard deviation

‡ Treatment means in the same column, followed by the same letter are not significantly different at $\alpha = 0.1$.

§ Fisher's Least Significant Difference

The rate of urea hydrolysis of the 0.5-g pellet (SSA of 6.3 cm^2/g) did not differ significantly from that of granules with a much higher SSA (19.6 cm^2/g). Hence, it was likely that the reduction in SSA in the 0.5-g pellet compared to granules was not adequate to reduce the rate of urea hydrolysis over a 7-d period. It was likely that if the urea analysis had been performed at a shorter interval, say 2 d, the rates of urea hydrolysis of 0.5-g pellets and granules could have been significantly different. Further, spreading out the 0.5-g pellets at 6-cm intervals could have accelerated urea hydrolysis. In 7 d, more than 95% urea had been hydrolyzed in all three treatments; rapid urea hydrolysis observed in this study agreed with the conclusions of Singh and Beauchamp (1987).

Urea hydrolyzes when it is available in the dissolved form to the soil enzyme urease. Even when urea is available in soil in dissolved form, high urea concentrations in soil solutions can be detrimental to urease activity. Irrespective of soil type, urea in excess of half-saturation in soil solution resulted in total urease inhibition while even one-quarter saturation significantly retarded urease activity (Wetselaar, 1985). Slower dissolution of the 1.5-g pellet, as compared to the granules and 0.5-g pellets, resulted in reduced availability of dissolved urea for hydrolysis. Further, higher concentration of dissolved urea in the vicinity of the 1.5-g pellets could have retarded urease activity to a greater degree than in the other treatments.

2. **Null Hypothesis: Rate of urea hydrolysis (percent urea hydrolyzed in 7 d) is unaffected by the urea form (1.5-g pellet and granules).**

   Alternative Hypothesis: Rate of urea hydrolysis is higher in granules than in 1.5-g pellets.

Since the data set was normally distributed, Student t-test was applied to the two treatments. Null Hypothesis 2 was rejected ($p < 0.01$, equal variance); hence, granules had a significantly higher rate of urea hydrolysis than the 1.5-g pellet. Retardation in urea hydrolysis rate in 1.5-g pellets versus granules was likely due to the reasons discussed under Hypothesis 1.

<u>Nitrification</u>

All six batches were analyzed for NO_3^--N using the procedure described in Sec. 3.3.3. Soil NO_3^--N concentrations for all four treatments are presented in table 4.15. Apparent nitrification in the fertilizer treatment was calculated by subtracting the average NO_3^--N concentration in the control treatment from the fertilizer treatment. The plot of apparent nitrification rate (percent urea nitrified over time) is presented in figure 4.15.

Apparent nitrification rates in all treatments were comparable at the first sampling event, perhaps due to the rapid dissolution of pellet edges resulting in rapid nitrification. Apparent nitrification rates of all fertilizer treatments increased approximately linearly up to the fourth sampling event (35 d). However, at the fifth sampling event (49 d), NO_3^--N recovery declined in all fertilizer treatments while it registered a gradual increase in the control treatment (table 4.15). Since the reason for decline in NO_3^--N recovery was unclear, the soil samples for this batch were reanalyzed. The reanalysis confirmed the original results.

Table 4.15. Nitrate-N concentration in the different treatments at the six sampling events

Sampling event	NO_3^--N recovery (µg-N/g-soil)							
	Control		Granules		0.5-g pellet		1.5-g pellet	
	Mean*	SD	Mean	SD	Mean	SD	Mean	SD
7 d	32.2	1.4	47.3	2.7	44.8	3.4	38.5	1.9
14 d	31.3	7.1	121.7	5.8	124.7	3.6	83.2	0.5
21 d	39.2	0.5	210.6	0.8	192.5	37.6	178.9	8.5
35 d	45.8	1.9	407.4	7.8	392.8	14.4	333.8	19.9
49 d	54.7	3.0	291.0	2.6	290.4	5.5	284.6	1.8
63 d	52.1	3.7	366.5	12.5	361.1	6.4	357.6	10.3

* Average of three replications

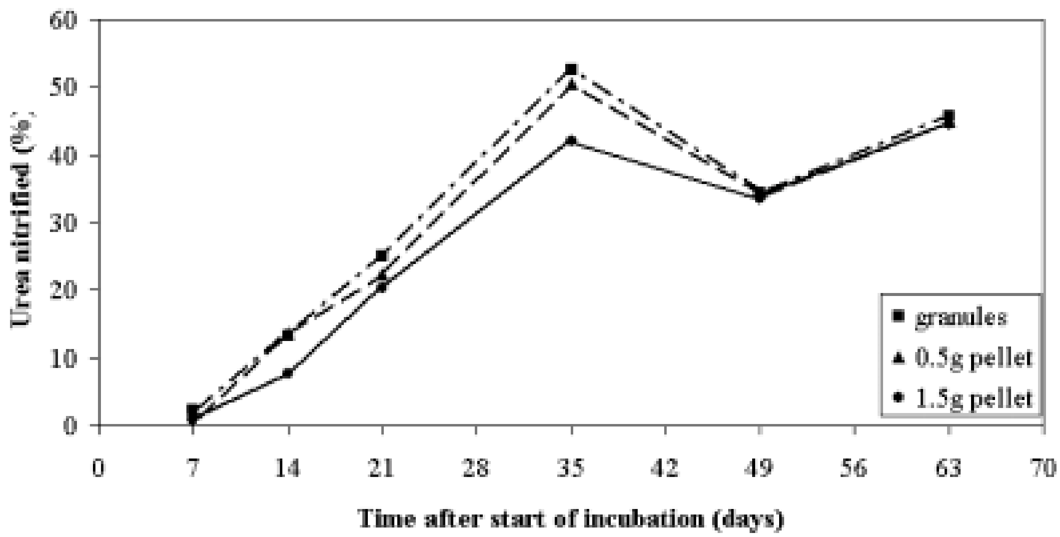

Figure 4.15. Apparent nitrification of urea pellets (0.5 and 1.5 g) and granules during incubation. Each data point is the average of three replications. For each treatment, the data points are connected by a line to indicate the apparent nitrification trend. No samples were collected at 28, 42, and 56 d.

The possibility of poor NO_3^--N recovery in the fifth batch due to substantial immobilization of applied-N by OM was ruled out since it occurred late in the study (R.

Reneau, personal communication, Blacksburg, Va., 15 March 1998). The possibility of significant NH_4^+-N fixation was also considered since the Ross soil contains NH_4^+-N fixing clay minerals, as discussed earlier. Since the soil was continuously maintained at a constant θ_v of 31.4% and since NH_4^+-N fixation increases with drying (Bohn et al., 1985), NH_4^+-N fixation was probably not substantial. Further, it was unlikely that NH_4^+-N fixation could have occurred on such a large scale so late in the study (R. Reneau, personal communication, Blacksburg, Va., 15 March 1998). However, it was likely that applied-N immobilization by OM and NH_4^+ fixation by the soil clay fraction partly affected applied-N recovery.

A likely explanation for the low NO_3^--N recovery in the fifth batch was denitrification. It was likely that moisture evaporated from the soil surface condensing on the inside of the container lid and dripping back to the soil surface created a localized wet layer with anaerobic sites resulting in denitrification (R. Reneau, personal communication, Blacksburg, Va., 15 March 1998). Since denitrification increases with NO_3^--N concentration (Tisdale et al., 1993) and the fertilizer treatments contained at least five times more NO_3^--N than control, conditions were favorable for denitrification (table 4.13). However, given the excellent forced convection in the environmental chamber through the floor (the incubation pots were placed on the floor), it was unclear how denitrification could have occurred on such a large scale.

With the last batch of samples (63 d), NO_3^--N recovery showed a slight improvement over the fifth batch of samples (49 d). The apparent NO_3^--N recovery (or urea-N nitrified) at the last sampling event (63 d) for the granule, 0.5-g pellet, and 1.5-g pellet were 45.8, 45.0, and 44.5% of the urea-N applied, respectively. Over the long term, nitrification rate would not likely be affected by size or form of urea. However, given the decline in NO_3^--N recovery at 49 and 63 d in comparison to 35 d, it was unclear at what stage the urea particle size effects on apparent NO_3^--N recovery would cease.

Since greater NO_3^--N recovery in one treatment versus another is indicative of a reduced nitrification rate, inferences regarding the impact of urea size and form on nitrification rate were based on NO_3^--N recovery. Comparisons were made at 35 d since the overall NO_3^--N recovery was highest (48.4% in granules) at 35 d. Since the

NO_3^--N components from the fertilizer and background sources could not be separated, the amount of NO_3^--N recovered was used to compare treatments with respect to their nitrification rates.

3. **Null Hypothesis: Nitrification rate (amount of NO_3^--N recovered after 35 d) is unaffected by the treatment applied.**

   Alternative Hypothesis: Nitrification rate is affected by the treatment applied.

Since the combined data set for the fertilizer treatments was normally distributed, ANOVA and Fisher's LSD were used to test the null hypothesis that the nitrification rate was unaffected by the fertilizer treatment applied (table 4.14). The null hypothesis was rejected ($p < 0.01$) indicating that at least one treatment differed from the other treatments with regard to NO_3^--N recovery (or nitrification rate). Means comparison using Fisher's LSD indicated that while the 1.5-g pellets had significantly lower NO_3^--N recovery than 0.5-g pellets and granules, the 0.5-g pellets and granules were not significantly different.

Retardation in urea hydrolysis possibly retarded nitrification in the 1.5-g pellets as compared with the other fertilizer treatments. More importantly, higher concentration of NH_4^+-N and, possibly, NH_3, in the vicinity of the 1.5-g pellet (as compared to the two other fertilizer treatments) likely inhibited nitrification. Wetselaar (1985) reported that high concentration of NH_4^+-N and smaller amounts of NH_3 proved toxic to nitrifying bacteria resulting in reduced nitrification. Based on observations during sampling (stronger NH_3 smell from the 1.5-g pellet), there was evidence of higher NH_3 concentrations in the 1.5-g pellets than in the other fertilizer treatments. Compared to granules, higher pH in pellets (see following discussion on pH) provided indirect evidence of higher NH_3 concentrations since NH_3/NH_4^+ ratio increases with pH (Tisdale et al., 1993).

4. **Null Hypothesis: Nitrification rate (amount of NO_3^--N recovered after 35 d) is unaffected by the urea form (1.5-g pellets and granules).**

   Alternative Hypothesis: Nitrification rate is higher in granules than in 1.5-g pellets.

Since the data set was normally distributed, Student t-test was used to compare the nitrification rates of 1.5-g pellets and granules at 35 d. Null Hypothesis 4 was rejected ($p < 0.01$, equal variance) indicating that the nitrification rate in granules was significantly higher than 1.5-g pellets. The likely reasons for the lower nitrification rate in 1.5-g pellets compared to granules are discussed under Hypothesis 3.

pH

Change in soil pH was monitored for all treatments since nitrification, an acid-forming process, is accompanied by a decline in pH. Measured pH values over time are plotted for all treatments in figure 4.16.

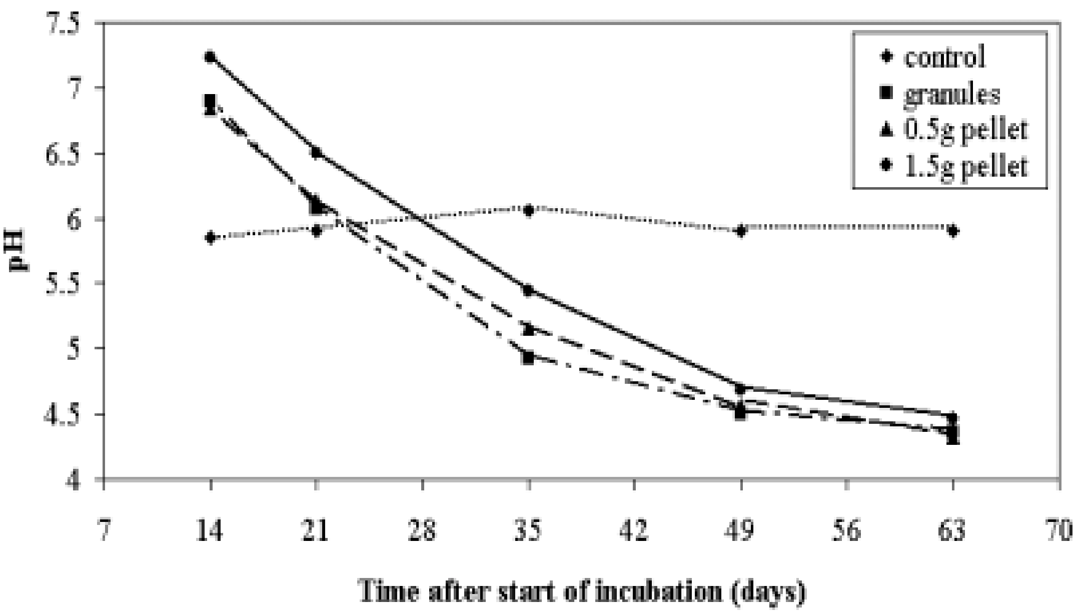

Figure 4.16. Effect of urea pellet (0.5 and 1.5 g) and granule treatments on pH during incubation. Each data point is the average of three replications. The control treatment was included to indicate change in background pH level. For each treatment, the data points are connected by a line to indicate the trend in pH. No samples were collected at 28, 42, and 56 days.

Higher pH values were consistently observed in the 1.5-g pellet treatment compared to the other fertilizer treatments. Generally, the 0.5-g pellet and granules had very close pH values except at 35 d. As expected, decline in pH over time provided evidence of continuing nitrification, unlike NO_3^--N recovery that declined after 35 d. As with the nitrification hypotheses, it had been intended to compare pH among treatments for the last batch (63 d) or the batch with the highest NO_3^--N recovery. Accordingly, the pH hypotheses were tested using data for the 35-d sampling event.

5. Null Hypothesis: pH is unaffected by the fertilizer treatment applied.

Alternative Hypothesis: pH is affected by the fertilizer treatment applied.

The null hypothesis was tested using ANOVA and Fisher's LSD (table 4.14) for the pH data for the fertilizer treatments obtained at 35 d. The null hypothesis was rejected ($p < 0.01$) indicating that at least one treatment differed from the other two with respect to pH. The Fisher's LSD results indicated that all fertilizer treatments differed significantly from one another with pH decreasing with an increase in SSA. More rapid nitrification in smaller urea particles (higher SSA) caused more acid formation, resulting in a decline in pH (Tisdale et al., 1993) compared with larger urea particles (lower SSA). Unlike the urea hydrolysis and nitrification results, pH values of the granules, 0.5-g pellets, and 1.5-g pellets were significantly different. Higher pH in the 0.5-g pellet as compared to granules provided some evidence that nitrification was faster in granules. However, the difference in nitrification rate between 0.5-g pellet and granules was not large enough to be detected.

6. Null Hypothesis: pH is unaffected by the urea form (1.5-g pellets and granules).

Alternative Hypothesis: pH is lower in granules than in 1.5-g pellets.

Student t-test was used to compare the pH at 35 d in granules versus 1.5-g pellets. Since the null hypothesis was rejected ($p < 0.01$, equal variance), the granules had a significantly lower pH than 1.5-g pellets. As discussed in Hypothesis 5, more rapid nitrification in granules resulted in more acid formation lowering pH values compared to 1.5-g pellets. Higher pH in the 1.5-g pellet treatment as compared with the other fertilizer treatments lead to more of the ammoniacal-N remaining as NH_3 (Tisdale et al., 1993) causing greater nitrifier inhibition, potentially resulting in slower nitrification.

Discussion: incubation study

Results of the incubation study indicated that the reduction in nitrification rate was probably more important than urease inhibition in reducing NO_3^--N availability from pellets compared to granules. While urea hydrolysis was significantly faster in granules than 1.5-g pellets at 7 d, the actual difference was only 3.1%. Urea hydrolysis was slower in 1.5-g pellets than granules due to higher urea concentrations in the vicinity of urea application, resulting in greater urease inhibition (Wetselaar, 1985). However, apparent nitrification was 22% faster in granules than 1.5-g pellets 35 d after start of incubation (table 4.14). Although urea hydrolysis was rapid, nitrification was slower as indicated by NO_3^--N recovery as well as pH data (table 4.12). The combination of higher NH_4^+-N concentration and higher NH_3/NH_4^+-N ratio in 1.5-g pellets as compared to the other fertilizer treatments, caused greater nitrifier inhibition, resulting in slower nitrification. Compared to granules, 1.5-g pellets had a smaller amount of applied-N as NO_3^--N; hence, leaching and denitrification losses could be lower from 1.5-g pellets than granules.

4.2.3. Leaching Column Study

The leaching column study was performed to study the impact of urea form on NO_3^--N leaching in the laboratory using both leachate and soil samples. The leachate and soil samples are discussed separately.

Leachate samples

Nitrate-N concentration in leachate from the different treatments was determined over the study duration to investigate both the amount and trend. Time series of NO_3^--N concentrations in the different treatments are compared in figure 4.17.

During the first two leaching events, the control treatment gave the highest NO_3^--N concentrations followed closely by pellets and granules. Even during the third leaching event, the control treatment gave comparatively high NO_3^--N concentration. High NO_3^--N concentrations in the initial stage in all treatments were likely due to background NO_3^--N leaching as the air-dried soil packed into the leaching columns had 25 and 5.3 μg-N/g-oven dry soil as NO_3^- and NH_4^+, respectively. Such high variability in NO_3^--N concentration especially in the first leaching event was unexpected (fig. 4.17).

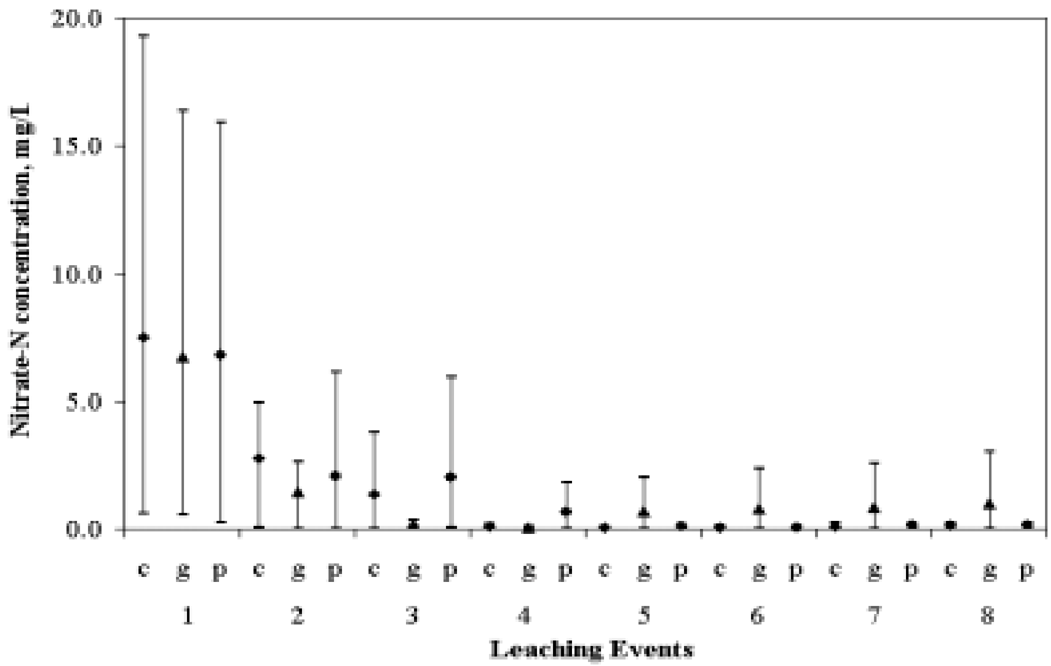

Figure 4.17. NO_3^--N concentrations in the control (c), granule (g), and pellet (p) treatments. Treatment means (♦for control; ▲ for granules; • for pellets) represent the average of three replications; dashes show the high and low values.

Beginning with the fourth leaching event (fig. 4.17), it was unclear why the pellet and control treatments declined to almost negligible NO_3^--N levels while the granule treatment showed a slow and steady rise. Calculated as the average of all leaching events, the mean NO_3^--N concentrations for the control, pellet, and granule treatments were 6.7, 6.6, and 6.6 mg/L, respectively. Comparable NO_3^--N concentrations among the treatments provided further indication that most N in the leachate did not come from applied-N.

Soil samples

Soil residual inorganic-N (NO_3^--N and NH_4^+-N) for the three treatments at different layers as well as for the entire column were compared (fig. 4.18). The fertilizer treatments contained substantially larger amounts of inorganic-N than the control treatment in the top-third layer and in the entire column. The differences in inorganic-N amounts in the middle-third and bottom-third layers between the fertilizer and control treatments were substantially lower than in the top-third of the leaching columns. Inorganic-N concentrations were comparable between the pellet and granule treatments.

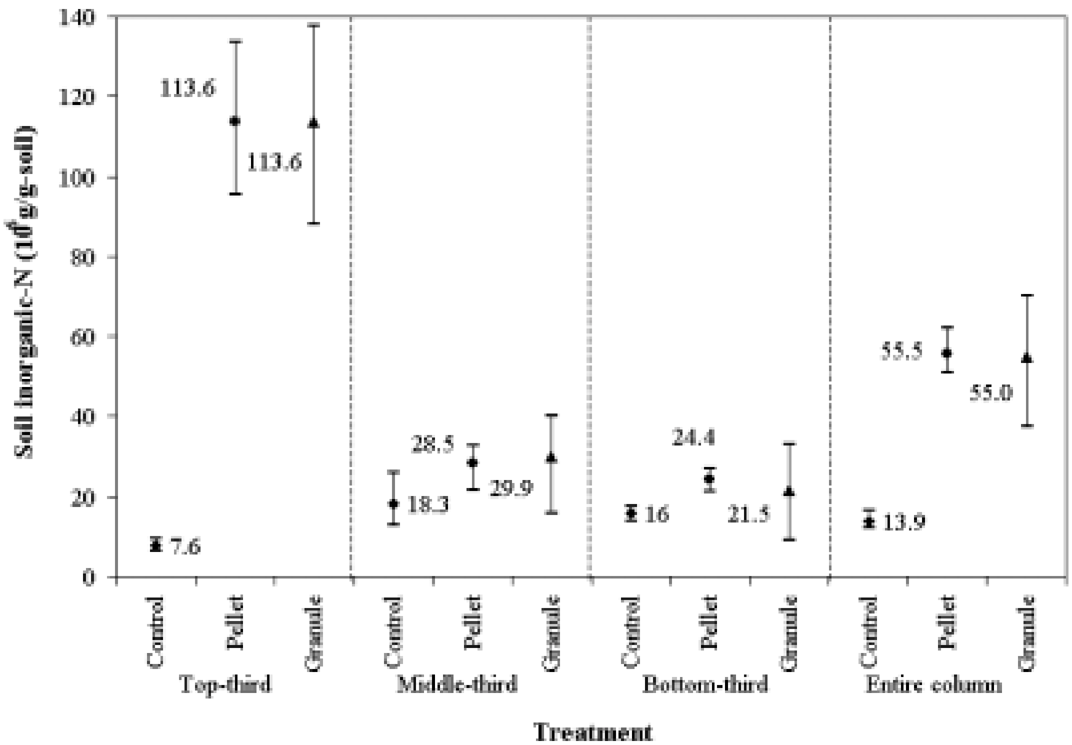

Figure 4.18. Soil inorganic-N for the different treatments shown by layer and for the entire leaching column. Treatment means (♦ for control; ▲ for granules; • for pellets) represent the average of three replications; dashes show the high and low values.

1. **Null Hypothesis: Inorganic-N concentration is unaffected by the treatment applied.**

   Alternative Hypothesis: Inorganic-N concentration is affected by the treatment applied.

Since the data were normally distributed, Hypothesis 1 was tested using ANOVA. Null Hypothesis 1 was rejected for the top-third ($p < 0.01$) as well as for the entire column ($p < 0.01$), indicating that at least one treatment had lower inorganic-N concentration in the top-third of the column as well as in the entire column. However, there was no evidence that the treatments were different in terms of inorganic-N concentrations in the middle-third ($p = 0.30$) and bottom-third ($p = 0.41$) portions of the leaching column. Hence, Hypothesis 2 was tested for the top-third of the leaching column as well as for the entire column.

2. **Null Hypothesis: Inorganic-N concentration is unaffected by the fertilizer treatment applied.**

   Alternative Hypothesis: Inorganic-N concentration is higher in the pellet treatment than granules.

The Student t-test was applied to the pellet and granule treatments after confirming the normality of the data sets on the top layer and entire column (data for all three layers as well as the entire column for the pellet and granule treatments were used to test for normality). The evidence failed to reject Null Hypothesis 2 for both the top-third ($p = 0.5$) as well as the entire column ($p = 0.48$) for the top layer, indicating that the fertilizer form did not affect inorganic-N in the top layer. It is clear from figure 4.18 that a substantial portion of the applied-N remained confined to the top-third of the leaching column in both the pellet and granule treatments.

Discussion: leaching column study

Residual inorganic-N analysis indicated that irrespective of the fertilizer form, the applied fertilizer remained largely confined to the top-third of the soil column. An attempt was made to account for all applied-N in both fertilizer treatments by estimating the contribution of applied-N to the total residual inorganic-N. Based on the residual inorganic-N status of the control treatment (mean of three replications), the apparent residual inorganic-N concentrations were calculated for all layers as well as the entire column for both pellets and granules. Of the 2.07 g-N (as urea), 0.9 g of applied-N was estimated to be present in the top-third of the column in both treatments. In the lower two-thirds of the column, 0.16 and 0.15 g of applied-N remained in the pellet and granule treatments, respectively. Hence, 1.01 and 1.02 g of applied-N could not be accounted for in the pellet and granule treatments, respectively.

It was unlikely that a major portion of the unaccounted, applied-N had been lost through leaching since leachate from all three treatments gave nearly equal mean NO_3^--N concentrations. Even though leachate amounts were not measured, given that equal amounts of water were applied to all the columns, it was unlikely that NO_3^--N loadings varied with treatment. Apart from inorganic-N as NO_3^- and NH_4^+, the soil samples were also analyzed for total-N. Given the large background total-N concentration of 0.14% (1400 μg-N/g-oven dry soil) versus only 81 μg-N/g-oven dry soil applied as urea, it was unclear if the applied-N had been immobilized by organic matter. However, since both fertilizer treatments had 0.14% total-N at the end of the experiment, equal to the initial total-N, it was unlikely that this N-loss pathway affected the two urea forms differently. Given the continuously wet conditions, it was unlikely that N loss through NH_4^+ fixation was a major N-loss pathway (Bohn et al., 1985).

The likely major N-loss pathway was denitrification. Since the soil packed into the leaching columns had a high carbon content (4.6%), it likely contained abundant water-soluble organic carbon. High water-soluble organic carbon content, combined with highly moist conditions (resulting in anoxic conditions) can result in denitrification (Tisdale et al., 1993). The Ross soil is medium-textured (loam) and has only moderate permeability (SCS, 1985). When air-dried and sieved soil was packed into the leaching column at field ρ_b, the permeability of the soil could have been greatly diminished as compared to the field soil in the absence of root and worm holes resulting in slow drainage and possibly, anoxic conditions. Use of air-dried soil in the leaching columns further increased the denitrification rate when anoxic conditions developed (Tisdale et al., 1993). Nitrification was probably inhibited by high NH_4^+-N concentration (NH_4^+-N/total inorganic-N in control, pellet, and granule treatments were 82.4, 97.4, and 98.6%, respectively, more than 2 months after N application) and high moisture content (Tisdale et al., 1993). Hence, denitrification was likely to have been rapid.

Denitrification could have been minimized by improving drainage in the leaching column. Drainage could have been improved by applying suction at the base of the soil column to accelerate percolation; the single tension lysimeter was inadequate in draining the soil column. Operating the leaching columns at a lower soil moisture content would have possibly reduced denitrification. Percolation could also have been improved by using a mixture of native soil and sand.

5. MATHEMATICAL MODELING

Objective 3 of the study was to improve management of subsurface-applied urea-N as pellets or granules through the development of a mathematical model to simulate the fate of band-applied urea-N. The developed model simulated the fate of applied urea-N only. The model utilized data from the laboratory experiments (described in Chapters 3 and 4) and was tested using the field data (described in Chapters 3 and 4). Model development, model evaluation, sensitivity analyses, and model summary are presented in separate sections in this chapter.

5.1. Model Development

Objective 3: Improve computer-based tools for better management of subsurface-applied urea-N.

To achieve Objective 3, a mathematical model was developed to simulate the fate and movement of subsurface-banded urea-N. The model is comprised of a one-dimensional (1-D) moisture redistribution sub-model and a two-dimensional (2-D) N sub-model. The moisture sub-model provides moisture flux (q) and volumetric moisture content (θ) as inputs to the N sub-model for simulating the fate of applied urea-N. Results obtained from the dissolution study in the laboratory were used as input parameters in the model. Model outputs were compared with data from the field experiment data.

The model flowchart is presented in figure 5.1. The physically-based, lumped parameter model was designed for field-scale application to simulate N fate in subsurface-banded urea-N. Other important model features are listed below.

1. The model domain is the root depth $\times$ crop row space.
2. The model uses a variable time step (10^{-6} to 1 h) with the smaller time step being applied to infiltration conditions.
3. Moisture redistribution in the soil profile is simulated using a numerical approximation (finite difference) of the Richards' (1931) equation.

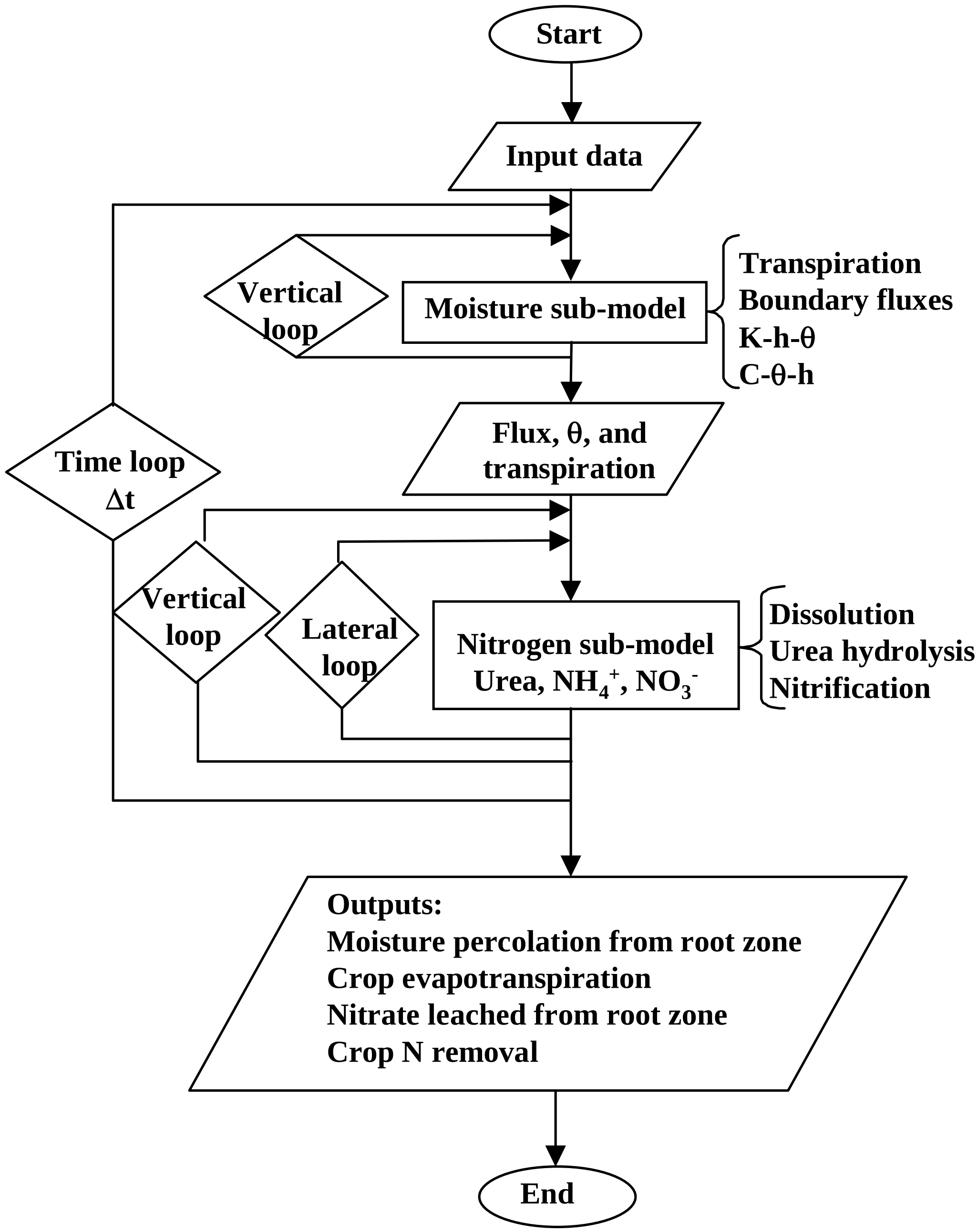

Figure 5.1. Flowchart of two-dimensional nitrogen model

4. Actual crop transpiration is estimated as a function of reference evapotranspiration, soil moisture content, and root depth.
5. The model does not simulate surface runoff; moisture that does not infiltrate into the soil is ignored.
6. The N sub-model uses a numerical approximation (finite difference) of the convective-dispersion equation (CDE) applied in 2-D to subsurface-banded urea-N. Dissolution and movement of dissolved urea, urea hydrolysis, and nitrification are simulated. Substrate concentration effects on N transformation orders and rates are taken into account.
7. Nitrogen removal by plants and NO_3^--N leaching from the root zone are simulated. Other N-loss pathways (ammonia volatilization, N loss in surface runoff, inorganic-N immobilization by organic matter, and NH_4^+ immobilization by clay) are not simulated.
8. The model has been designed to simulate N fate in a corn-fallow rotation; however, the model can be readily modified to simulate other crop rotations.

5.1.1. Moisture Redistribution Sub-model

The moisture redistribution sub-model uses a finite difference approximation of the Richards' equation to simulate moisture redistribution in the root zone in the vertical direction. Components of the hydrologic cycle that are simulated include infiltration through the soil surface, soil surface evaporation, crop transpiration, and percolation from the root zone. Surface runoff routing is not simulated. The sub-model outputs are moisture flux, θ, and transpiration values, which are supplied to the N sub-model as inputs.

Governing Equation

Richards (Richards, 1931) combined the conservation of mass relationship (Eq. [5-1]) with Darcy's Law (Eq. [5-2]) to obtain a partial differential equation (PDE) of the parabolic type (Remson et al., 1971). The resulting equation used in simulating moisture redistribution in the soil profile in this model, is known as the Richards' equation (Eq. [5-3]).

$$\frac{\partial \theta}{\partial t} = -\frac{\partial q}{\partial z} \qquad [5\text{-}1]$$

$$q = -K\frac{\partial H}{\partial z} \qquad [5\text{-}2]$$

$$C(h)\frac{\partial h}{\partial t} = \frac{\partial}{\partial z}\left[K(h)\left(\frac{\partial h}{\partial z} - 1\right)\right] - T(z, h, t) \qquad [5\text{-}3]$$

where,

θ = volumetric moisture content (mL/cm^3),

t = time (h),

q = moisture flux in the z direction (cm/h)

z = distance above the datum plane or the elevation head, positive downward (cm),

K = hydraulic conductivity (cm/h),

H = hydraulic head (cm) = h – z,

h = pressure head, unsaturated values being negative (cm),

C = soil water capacity = $\partial\theta/\partial h$ (cm^{-1}), and

T = transpiration (cm$^3\cdot$h$^{-1}\cdot$cm^{-3}).

Transpiration is applied as a sink term to the Richards' equation (Eq. [5-3]). The hydraulic head, H, takes into account gravitational, capillary, and osmotic forces that govern the energy status of soil water. However, in this model, since the osmotic component is disregarded, H only accounts for gravitational and capillary forces.

While the right side of Eq. [5-1] is expressed in terms of θ, the right side of Eq. [5-3] is expressed in terms of h since h values can be calculated for points in the soil profile for known θ values, assuming a unique θ-h relationship, i.e., for non-hysteretical soils. The θ-based equation cannot be used for saturated conditions, since the diffusivity term D (K/C) approaches infinity as θ approaches saturation (Skaggs and Khaleel, 1982). Hence, the h-based form that is applicable to both saturated and unsaturated conditions was used. If the h values due to capillary forces are known at the initial conditions in the soil profile, Eq. [5-3] can be used to calculate h values at any desired time. In addition, the model requires K-h-θ and C-h-θ relationships which are discussed in the following sections.

K-h-θ relationships

For every time step, K values are required and estimated from h (provided the h(θ) relationship is well-described and unique) using semi-empirical methods. A soil displaying non-unique h(θ) relationship is hysteretical in nature, and will need separate K(h) relationships depending on whether the soil is wetting or drying. Such K(h) methods involve the combination of theoretical pore-size distribution models and soil moisture characteristic curve or desorption curve data (de Jong, 1993) to predict K. A simple and widely used equation suggested by Campbell (1974) is:

$$K = K_s \left(\frac{h_e}{h} \right)^{2+2/b} \qquad [5\text{-}4]$$

where h_e is the air-entry value (L) and b is the slope of the log (h) versus log (θ) expressed as a positive number. Campbell (1974) reported that Eq. [5-4] did not give valid estimates of K when the plot of the log (h) vs. log (θ) was not a straight line. Hence at high moisture content values, the accuracy of K estimation could be adversely affected (Campbell, 1974). Further, Eq. [5-4] is highly sensitive to h_e, a parameter that is difficult to estimate with accuracy.

Hence, the method developed by van Genuchten (1980) was evaluated for estimating K from h. van Genuchten applied the empirical S-shaped moisture retention function to the pore distribution theory suggested by Mualem (1976). Durner (1992) reported that the Mualem-van Genuchten method was the most popular method since it successfully described water retention and K characteristics. The K-h relationship is (van Genuchten, 1980):

$$K(h) = K_s \bullet \Theta^L \left[\int_0^\Theta \frac{1}{h(z)} dz \Big/ \int_0^1 \frac{1}{h(z)} dz \right]^2 \qquad [5\text{-}5]$$

where the dimensionless moisture content (relative saturation) is given as:

$$\Theta = \frac{\theta - \theta_r}{\theta_s - \theta_r} \qquad [5\text{-}6]$$

In Eq. [5-5], the dimensionless parameter, L, though soil-specific, is estimated to be 0.5 for a wide range of soils (de Jong, 1993). In Eq. [5-6], θ_r is the θ corresponding to a very low though finite h value (van Genuchten et al., 1991) and θ_s is saturation θ. van Genuchten (1980) proposed the following $\Theta(h)$ relationship:

$$\Theta = \frac{1}{(1+|\alpha h|^n)^m} \qquad [5\text{-}7]$$

where α is the absolute inverse of the air entry value (cm^{-1}), and m and n are constants (dimensionless) that affect the shape of the $h(\theta)$ relationship. To reduce the number of parameters to be estimated, van Genuchten (1980) assumed that m was a function of n. The simplified method wherein m = 1-1/n was adequate for $1.25 < n < 6$ in approximating K values reasonably well (van Genuchten and Nielsen, 1985); however, the full model (where m and n are independent) estimated K(h) better for a wide range of soils.

Using Equations [5-5]-[5-7], a simplified expression relating K with K_s and h modified from the van Genuchten method is:

$$K(h) = K_s \frac{\left[\left(1+|\alpha h|^n\right)^m - |\alpha h|^{n-1}\right]^2}{\left[1+|\alpha h|^n\right]^{m(L+2)}} \qquad [5\text{-}8]$$

where L is the pore-connectivity parameter. In this study, the software RETC.FOR (van Genuchten et al., 1991) which uses the Mualem-van Genuchten method discussed above, was used to estimate θ_r, α, m, n, and L using non-linear least squares optimization. Using the parameters θ_r, α, m, n, and L estimated using RETC.FOR and measured θ_s, for known values of h, θ was estimated with the following relationship in the model:

$$\theta = \theta_r + \frac{(\theta_s - \theta_r)}{(1+|\alpha h|^n)^m} \qquad [5\text{-}9]$$

Equation [5-9] was obtained by combining Equations [5-6] and [5-7]. Equation [5-9] was modified to calculate h for known values of θ (Eq. [5-10]):

$$h = -\frac{\left(\left(\frac{\theta_s - \theta_r}{\theta - \theta_r}\right)^{1/m} - 1\right)^{1/n}}{\alpha} \qquad [5\text{-}10]$$

C-h-θ relationship

Soil water capacity (C) is the slope of the h-θ relationship; however, given the non-linearity of the h-θ relationship requires that C be evaluated at every combination of h and θ. Hence, C can be written as follows:

$$C = \frac{d}{dh}\left(\theta_r + \frac{(\theta_s - \theta_r)}{(1+|\alpha h|^n)^m}\right) \quad [5\text{-}11]$$

It may be noted that when θ reaches saturation, C becomes zero and since the right hand side of Eq. [5-3] is divided by C, h becomes indeterminate. Hence, a non-zero value of C was calculated based on a very small positive value of h (Section 5.2). Based on the differentiation of Eq. [5-11], the C(h) relationship can be rewritten as:

$$C = \frac{-\alpha \cdot m \cdot n\,(\theta_s - \theta_r)(1+|\alpha h|^{n-1})^{m-1}(|\alpha h|^{n-1})}{(1+|\alpha h|^n)^{2m}} \quad [5\text{-}12]$$

Application of the finite difference method to Richards' equation

In order to be applicable to a wide range of boundary conditions, a numerical approximation, in the form of a finite difference (FD) or finite element method (FEM), is applied to the Richards' equation since analytical solutions exist only for restrictive initial and boundary conditions. The application of the finite element method (FEM) would have been desirable if the flow domain had been complicated. However, since the model simulates moisture redistribution in 1-D, in a rectangular domain, the simpler FD method was used. Application of the FD scheme to the Richards' equation involves discretizing the equation in both time and space domains as discussed below.

<u>Discretization of the time domain</u>

Discretization of the time domain requires the FD form of the Richards' equation to be solved in small time steps (Δt) and the addition of all the time steps sums up to the simulation period. Different discretization schemes of the time domain to obtain FD approximations to Eq. [5-3] were considered. The discretization schemes are discussed in detail, for example, in Remson et al. (1971). The explicit (forward difference) scheme, though simple, was discarded due to stability and convergence problems (Skaggs and Khaleel, 1982). The Crank-Nicolson (C-N) (central difference) scheme with reduced truncation error of $O((\Delta t)^2 + (\Delta z)^2)$ allows for more rapid convergence compared to the explicit scheme with a greater truncation error of $O((\Delta t) + (\Delta z)^2)$ (Remson et al., 1971). Further, the C-N scheme is unconditionally stable. However, the resulting FD equations are difficult to linearize, and thus, difficult to solve (Remson et al., 1971). Finite difference equations can also be quasi-linearized using the Kirchhoff transformation, however, Haverkamp et al. (1977) reported that the Kirchhoff transformation integral changed too drastically with time during infiltration resulting in decreased accuracy of prediction compared to the implicit scheme discussed below.

A third discretization scheme is the implicit method (backward difference scheme). Even though the implicit method has the same truncation error as the explicit method, it is stable (Remson et al., 1971). More importantly, the resulting set of FD equations can be linearized by applying an efficient linearization technique (Remson et al., 1971). Hence, the implicit scheme was used for discretization of the time domain in this model. The method of selection of Δt and the application of the implicit scheme to the Richard's equation are presented later.

Discretization of the space domain

The soil profile was discretized into thin layers (depth increment, Δz) separated by nodes and the h, C, and K values were estimated for each time increment (Δt) for all depth increments before proceeding to the next time step. The discretization of the modeling domain, as applied to the 2-D situation is shown in figure 5.2. Discretization along the y-axis was achieved by dividing the distance between the crop rows into segments spaced at equal distance, Δy. In this model, Δz and Δy were kept equal. The discretization along the y-axis does not apply to the 1-D moisture model. Placement of the first node (i = 1) in the z-axis $\Delta z/2$ below the soil surface permitted the application of Darcy's Law to the first node since Darcy's Law does not apply to the node in the air-soil interface. Hence, the bottom node (i = L) was located $\Delta z/2$ above the root zone boundary.

The central difference operator was applied to the space domain in the Richards' equation, i.e., h values at the nodes above and below the node of interest are considered. The backward difference operator (i and i-1) and the forward difference operator (i+1 and i) were the other possible alternatives. However, since the backward difference operator is more appropriate for percolation and the forward difference operator is more appropriate for evaporation, the central difference operator represents a compromise that works under both percolation and evaporation conditions. Selection of Δz and Δy is presented later.

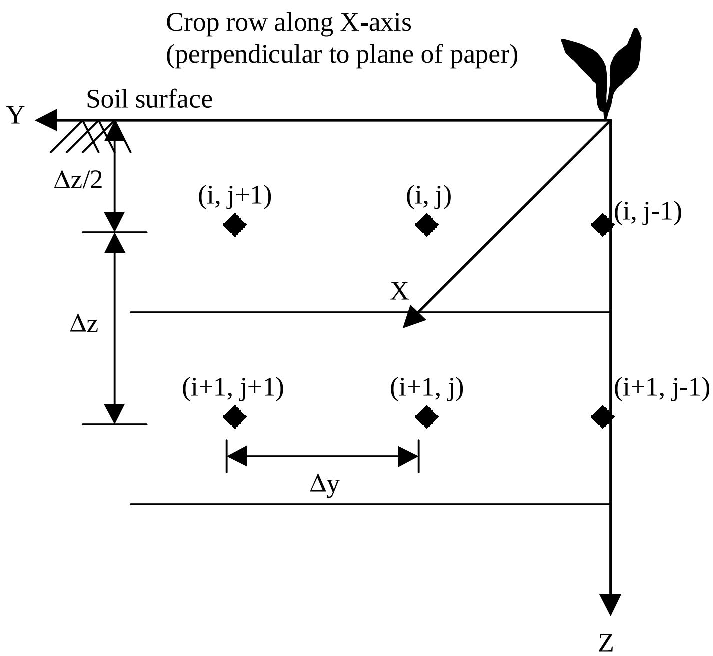

Figure 5.2. Discretization of the 2-D domain

The possibility of applying a two-dimensional FD method was explored for the moisture sub-model. At greater soil depths (say, at 1 m), corn roots are not as evenly distributed in the soil layer as in the top 30-cm. Hence, there could be an advantage in modeling moisture movement in 2-D (laterally toward the roots as well as vertically). Such a model could simulate transpiration more accurately if accurate root distribution information were available. However, due to the lack of reliable root distribution data at lower depths, a one-dimensional FD method was used.

Linearization and solution of FD equations

When finite differencing is applied to the non-linear and parabolic Richards' equation, the resulting set of non-linear algebraic equations are difficult to solve. Such non-linear equations can be linearized using one of various linearization techniques, such as, predictor-corrector, iteration, and extrapolation (Remson et al., 1971). For the 1-D problem in question, Remson et al. (1971) reported that the Douglas-Jones (D-J) predictor-corrector technique, also known as the implicit linearization technique (Haverkamp et al., 1977), was perhaps the best method. The explicit linearization technique, though simpler to program, was less accurate than D-J predictor-corrector (Haverkamp et al., 1977). Accordingly, the D-J predictor-corrector was used in this model to linearize the finite difference equations.

The D-J predictor-corrector requires the FD equations for the entire depth of interest to be solved twice for a time step. For the first half of the time step ($t + \Delta t/2$), predictor equations are solved to obtain values of h; using h values at $t + \Delta t/2$, values of K, C, and T are calculated. Predictor equations can be of the implicit (backward difference) or the C-N (central difference) types. The comparative merits or demerits of the implicit versus C-N predictor are unclear (Remson et al., 1971; Haverkamp et al., 1977; Douglas and Jones, 1963). Since the programming for the C-N type is more involved (Douglas and Jones, 1963), the simpler implicit form of the predictor equation was applied in this model as was done by Haverkamp et al. (1977). For the second half of the time step, the corrector equations (C-N type) were solved (using the C and K values obtained from the predictor equations) to evaluate the pressure distribution. Equation [5-3] is expressed in the D-J predictor-corrector in the following sections.

Both iterative and direct methods for solving a set of linear algebraic equations were considered. Iterative methods such as the Jacobi iteration, Gauss-Seidel, and Successive Over Relaxation (SOR) are desirable for solving elliptic equations while direct methods are preferred for parabolic equations such as the Richards' equation (Remson et al., 1971). Among the direct methods, the most popular method uses the Thomas algorithm for solving a set of tridiagonal equations (Haverkamp et al., 1977; Feddes et al., 1978; Remson et al., 1971). Since the D-J predictor-corrector results in tridiagonal equations, the Thomas algorithm is particularly suited for this situation and was used in this model.

Finite difference equation for the Richards' equation (non-boundary node)

Due to the application of boundary conditions, different FD equations are required for boundary and non-boundary nodes. For the non-boundary nodes 2 < i < L - 1 (i = 1 and L are boundary nodes), the D-J predictor-corrector equations for time step k + 1 (k = 1, …, N) are given below.

Predictor (for $t + \Delta t/2$ ($k + \frac{1}{2}$))

$$C_i^k\left(\frac{h_i^{k+1/2}-h_i^k}{\Delta t/2}\right)=\frac{K_{i+1/2}^k}{\Delta z}\left(\frac{h_{i+1}^{k+1/2}-h_i^{k+1/2}}{\Delta z}-1\right)-\frac{K_{i-1/2}^k}{\Delta z}\left(\frac{h_i^{k+1/2}-h_{i-1}^{k+1/2}}{\Delta z}-1\right)-T_i^k \qquad [5\text{-}13]$$

Since the values of C, K, T, and h were known at the previous time step (k), Eq. [5-13] was used to calculate h values for all nodes at $t + \Delta t/2$ ($k + \frac{1}{2}$) by solving the predictor equations for all nodes. Using the h at the k + ½ time step, the values of C, K, and T were calculated explicitly for the k + ½ time step. The value of $K_{i+1/2}^{k+1/2}$ (K at the internode between nodes i+1 and i), was calculated as the arithmetic mean of $K_{i+1}^{k+1/2}$ and $K_i^{k+1/2}$, K values at the nodes i+1 and i. Hydraulic conductivity values at the nodes were calculated using Eq. [5-8]. The value of $C_i^{k+1/2}$ was calculated using Eq. [5-12]. The actual transpiration T was kept unchanged throughout the time step, as is discussed later under evapotranspiration (ET).

Moisture flux values for the k + ½ time step at the internodes ($q_{i+1/2}^{k+1/2}$) were calculated by substituting $K_{i+1/2}^{k+1/2}$, $h_{i+1}^{k+1/2}$, and $h_i^{k+1/2}$ in Darcy's Law (Eq. [5-2]). Similarly, using $h_i^{k+1/2}$, $\theta_i^{k+1/2}$ values were calculated using Eq. [5-9]. The calculated $q_{i+1/2}^{k+1/2}$ and $\theta_i^{k+1/2}$ values were used as inputs to the first step of the two-step N sub-model (Section 5.1.2). To solve the FD equations with the Thomas algorithm, Eq. [5-13] was rewritten as:

$$AM_i \cdot h_{i-1}^{k+1/2} + BM_i \cdot h_i^{k+1/2} + CM_i \cdot h_{i+1}^{k+1/2} = KM_i \qquad [5\text{-}14]$$

where,

AM_i = sub-diagonal coefficient of the tridiagonal matrix = $-K_{i-1/2}^k/(\Delta z)^2$,

BM_i = diagonal coefficient of the tridiagonal matrix

= $(2C_i^k/\Delta t) + (K_{i-1/2}^k - K_{i+1/2}^k)/(\Delta z)^2$,

CM_i = super-diagonal coefficient of the tridiagonal matrix) = $-K_{i+1/2}^{k}/(\Delta z)^2$, and

KM_i = $(2C_i^k \cdot h_i^k/\Delta t) + (K_{i-1/2}^k - K_{i+1/2}^k)/(\Delta z)^2 - T_i^k$.

When a set of linear equations for all the nodes in the modeling domain is solved simultaneously with the Thomas alogrithm with known values of tridiagonal matrix coefficients, $h^{k+1/2}$ values are calculated for all nodes. Detailed information on the Thomas algorithm was presented by Carnahan et al. (1969).

<u>Corrector(for t + Δt (kj + 1))</u>

The corrector equation (Eq. [5-15]) resembles the predictor equation except for the use of the full time step and the updated C and K values:

$$C_i^{k+1/2}\left(\frac{h_i^{k+1}-h_i^{k}}{\Delta t}\right)=\frac{K_{i+1/2}^{k+1/2}}{\Delta z}\left(\frac{h_{i+1}^{k+1/2}-h_i^{k+1/2}}{\Delta z}-1\right) -\frac{K_{i-1/2}^{k+1/2}}{\Delta z}\left(\frac{h_i^{k+1/2}-h_{i-1}^{k+1/2}}{\Delta z}-1\right)-T_i^k \quad [5\text{-}15]$$

However, the C-N scheme was implemented (as mentioned earlier) to modify the corrector equation as shown in Eq. [5-16]:

$$C_i^{k+1/2}\left(\frac{h_i^{k+1}-h_i^{k}}{\Delta t}\right)=\frac{K_{i+1/2}^{k+1/2}}{\Delta z}\left(\frac{((h_{i+1}^{k+1}+h_{i+1}^{k})/2)-((h_i^{k+1}+h_i^{k})/2)}{\Delta z}-1\right) -\frac{K_{i-1/2}^{k+1/2}}{\Delta z}\left(\frac{((h_i^{k+1}+h_i^{k})/2)-((h_{i-1}^{k+1}+h_{i-1}^{k})/2)}{\Delta z}-1\right)-T_i^k \quad [5\text{-}16]$$

From Eq. [5-16], h values at k + 1 time step were calculated by solving the corrector equations for all nodes. As in the predictor step, h values at the k + 1 time step were used to update C, K, q, and θ values from the k + ½ time step to the k + 1 time step while T was updated from the k time step to the k + 1 time step. The updated C, K, and T values were used as inputs in the predictor equation in the next time step while q and θ values were used as inputs to the second step of the N sub-model. Also, as discussed later, q values were used in calculating the time step. In order for the set of corrector FD equations to be solved using the Thomas algorithm, Eq. [5-16] was written in a form similar to Eq. [5-14] with the pressure head values written at the k + 1 time step.

Initial conditions

The initial volumetric moisture content (θ) at each of the vertical nodes was specified as:

$$\theta_i = \theta_i^{t=0} \qquad [5\text{-}17]$$

Boundary conditions and FD equations for boundary nodes

Boundary conditions were specified for the top (i = 1) and bottom (i = L) nodes. The surface boundary conditions accounted for precipitation and evaporation separately. The boundary conditions and the concomitant FD equations are discussed below.

1. Soil surface

Precipitation condition

Under precipitation conditions, depending on precipitation and soil characteristics, infiltration will be either flux- or profile-controlled. Hence, the Neumann condition was applied to the soil surface which required the specification of downward flux through the soil surface based on precipitation rate, soil moisture conditions, and K_S at the soil surface. The Neumann condition specifies the values of the normal gradient on the boundary (Press et al., 1989) either as flux or as dh/dz. Reduction in infiltration through the soil surface due to surface sealing was not considered. The following steps were implemented in calculating surface flux (q_s) and formulating the FD equation for the top node.

- If the top node was unsaturated, using Darcy's Law, potential infiltration (i_{sur}) through the soil surface was calculated as:

$$i_{sur} = -\frac{(K_s + K_{1+1/2})}{2} \cdot \left(\frac{h_{1+1/2} - h_s}{\Delta z} - 1 \right) \qquad [5\text{-}18]$$

where K_S is the saturated hydraulic conductivity at the soil surface, $K_{1+1/2}$ is the arithmetic mean of K_1 and K_2, $h_{1+1/2}$ is the arithmetic mean of h_1 and h_2, and h_s is the saturation pressure head at the soil surface. It was assumed that under precipitation conditions, the soil surface saturated instantly and, hence, had a hydraulic conductivity value equal to K_S. If i_{sur} was greater than precipitation, q_s was set equal to precipitation rate; otherwise, q_s was set equal to i_{sur}.

- If the top node was saturated, i_{sur} was set equal to K_S. If precipitation rate was greater than i_{sur} (or K_S), q_s was set equal to i_{sur}; otherwise, q_s was set equal to the precipitation rate.

<u>Non-precipitation condition</u>

As under precipitation, the Neumann condition was used as the surface boundary condition for calculating the evaporative flux through the soil surface. The following steps were implemented in calculating q_s and formulating the FD equation for the top node under evaporation conditions.

- Hourly potential evaporation rate (E_{pot}) was calculated using the Priestly-Taylor method (Allen et al., 1990) which is discussed in detail in the evapotranspiration section.
- When moisture availability was limited, it was assumed that evaporative flux was controlled by the moisture flux in the upper soil surface region. Hence, when h_1 was lower than - 48 000.0 cm (van Bavel and Ahmed, 1976), q_s was set equal to $q_{1+1/2}$ provided $q_{1+1/2}$ was negative (i.e., moisture was moving upwards) and the absolute value of $q_{1+1/2}$ was less than or equal to E_{pot}. When moisture availability was adequate, it was assumed that evaporative flux would solely be controlled by environmental conditions. Hence, if h_1 was higher than - 48 000.0 cm, q_s was set equal to $-E_{pot}$.
- Hence, based on the surface boundary condition, for either precipitation or evaporation, the conservation of mass relationship (Eq. [5-1]) was rewritten for the top node as (Simunek et al., 1999):

$$\frac{\partial\theta}{\partial t} = -\frac{q_{i+1/2} - q_s}{\Delta z} \qquad [5\text{-}19]$$

where the left side of the equation is identical to Eq. [5-13] for the predictor and Eq. [5-16] for corrector in the FD form. Application of the FD scheme to the right side of Eq. [5-19] for both predictor and corrector followed logically since $q_{1+1/2}$ was calculated by Darcy's Law and q_s was calculated as described above.

No transpiration component was applied to the top node since it was assumed that root distribution would be scarce in the top layer. Equation [5-19] was written in the following form for the predictor to facilitate solution using the Thomas algorithm:

$$BM_i \cdot h_i^{k+1/2} + CM_i \cdot h_{i+1}^{k+1/2} = KM_i \qquad [5\text{-}20]$$

where the tridiagonal matrix coefficients were defined earlier. The corrector FD equation was also written in a similar manner with the h values at the k + ½ time step replaced by h values at the k + 1 time step.

2. Bottom of the root zone

As at the surface, the Neumann condition was applied at the bottom of the root zone (i = L). However, instead of specifying the bottom flux, it was assumed that the hydrostatic pressure gradient (dh/dz) was zero. Accordingly, the FD equation for the predictor was written as follows:

$$AM_i \cdot h_{i-1}^{k+1/2} + BM_i \cdot h_i^{k+1/2} = KM_i \qquad [5\text{-}21]$$

where AM_i and BM_i are both equal to one and KM_i is equal to zero. The formulation of the corrector equation was also straightforward, with the h values at the k + ½ time step replaced by h values at the k + 1 time step.

Evapotranspiration (ET)

In order to accurately simulate moisture movement, and hence solute transport, it is important to estimate ET accurately since ET is usually the largest component of moisture balance during the crop season. However, ET can be estimated more accurately if the evaporation and transpiration components are estimated separately since currently available ET models tend to underestimate evaporation under partial canopy conditions (Farahani and Bausch, 1985).

As mentioned earlier, the potential evaporation rate (E_{pot}) was estimated as upward flux through the soil surface, and hence, was assumed to occur only through the top node. Transpiration was applied by node and took into account not only atmospheric factors but also soil moisture status and crop phenology. However, transpiration was not calculated using the 'extraction model' approach used by Molz and Remson (1970); rather, transpiration was applied as an abstraction in the Richards' equation as done by

Wagenet (1981). The following procedure was implemented in estimating crop ET and separating the evaporation and transpiration components.

1. Reference ET (E_{tr})

Reference ET is defined as the water loss based on atmospheric demand, when soil moisture supply is not limiting from a reference crop that completely covers the ground and is unaffected by disease or pest (Allen et al., 1990). Given the agroclimatic conditions in Virginia, grass was used as the reference crop.

For estimation of E_{tr}, a physically-based combination equation was used. Combination equations are the most accurate and portable of all ET estimation methods since combination equations are based on physical laws and account for the maximum number of variables that influence the process (Allen et al., 1990). A combination equation applies a radiation balance plus aerodynamic approach for estimating E_{tr}. The energy component is required to convert water to vapor; the wind component transports the vapor. Among 19 ET estimation methods, the grass-based Penman-Monteith method gave the most accurate estimations when compared with lysimeter data in a wide range of climatic conditions (Allen et al., 1990). Unlike the older combination equations (e.g., 1963 Penman), the Penman-Monteith method incorporates the aerodynamic and surface resistances to sensible heat and vapor transfer (Allen et al., 1990):

$$E_{tr} = \frac{\left[\Delta(R_n - G) + \rho \cdot c_p \left(e_z^0 - e_z\right)/ r_a\right]}{\lambda\left(\Delta + \gamma^*\right)} \qquad [5\text{-}22]$$

where,

E_{tr} = reference ET (mm/d),

Δ = slope of the saturation vapor pressure-temperature curve (kPa/°C),

R_n = net radiation ($MJ \cdot m^{-2} \cdot d^{-1}$),

G = soil heat flux ($MJ \cdot m^{-2} \cdot d^{-1}$), sign of G is positive if warming,

ρ = air density (kg/m^3),

c_p = specific heat at constant pressure ($kJ \cdot kg^{-1} \cdot °C^{-1}$),

e^0_z = saturation vapor pressure of air at height z m (kPa),

e_z = vapor pressure of air at height z m (kPa),

r_a = aerodynamic resistance to sensible heat and vapor transfer (s/m),

λ = latent heat of vaporization (2.47 MJ/kg),

$\gamma^* = \gamma(1 + r_c/r_a)$,

γ = psychrometric constant, and

r_c = surface resistance to vapor transfer (s/m).

Penman-Monteith E_{tr} was calculated on an hourly basis using the Reference Evapotranspiration Calculator Ver. 2.0 (REF-ET) (Allen, 1990). Inputs to the REF-ET model included hourly values of air temperature, relative humidity (RH), solar radiation, precipitation, and wind speed. The hourly E_{tr} output was used as input in moisture modeling.

Recent advancements in ET modeling include the introduction of combination models that simulate ET within different layers of the canopy thus providing for better accounting of energy and vapor transfer. Multi-layer models such as the Shuttleworth-Wallace (2-layer) and Choudhary-Monteith (4-layer), though based on the Penman-Monteith type equations are probably capable of better evaporation and transpiration estimation than the parent models (Farahani and Bausch, 1995). Farahani and Bausch (1995) reported that the Shuttleworth-Wallace model outperformed Penman-Monteith on irrigated corn. Farahani and Bausch (1995) reported that evaporation was underestimated by Penman-Monteith under partial canopy conditions; the two models performed satisfactorily under full canopy conditions. However, given the complexity of the multi-layer models and lack of adequate testing, the multi-layer models were not used.

2. Hourly potential crop ET (E_{tc})

Hourly potential crop ET (E_{tc}) is ET from a crop that is well-supplied with moisture and is under no disease or pest stress. Potential crop ET can be measured in lysimeter studies. However, it is more common to estimate E_{tc} using E_{tr} values by introducing an empirical crop coefficient, $K_c = E_{tc}/E_{tr}$. For a specific crop, K_c applies to a given growth stage and a specified soil moisture condition (Allen et al., 1990). Crop coefficient values can be further refined to improve E_{tc} estimates by accounting for available soil moisture in the root zone and soil surface wetness (to adjust evaporation values) (Allen et al., 1990). In this study, no adjustments were made to K_c since E_{sur} and T were adjusted for soil moisture status, as discussed later.

3. <u>Hourly potential evaporation (E_{pot}) and evaporative surface flux (q_s)</u>

Using air temperature and solar radiation as inputs, potential evaporation was estimated with the Priestly-Taylor equation (Allen et al., 1990):

$$E_{pot} = \frac{\Delta}{\Delta + \gamma} \phi_n R_{ns} \qquad [5\text{-}23]$$

$$\phi_n = 0.92 + 0.40(R_{ns}/R_n) \qquad [5\text{-}24]$$

where Δ and γ are as defined earlier and R_{ns} is the net radiation received on the soil surface. The coefficient ϕ_n involves the ratio of R_{ns} to R_n, net solar radiation received on the earth's surface. The net radiation, R_n, can be either measured directly using net radiometers or estimated from solar radiation, R_s (Allen et al., 1990). A relationship for estimating R_n as a function of R_s is given in Section 5.2. The following expression from Uchijima (1976) cited in Farahani and Bausch (1995) relates R_n to R_{ns}:

$$R_{ns} = R_n e^{-C_e \cdot LAI} \qquad [5\text{-}25]$$

where C_e is the extinction coefficient and LAI is the leaf area index. Leaf area index increases with canopy development.

When E_{pot} was greater than E_{tc} or when the field was in fallow, E_{pot} was set equal to E_{tc}. As discussed earlier in the section on boundary conditions, based on soil moisture content, q_s was calculated using E_{pot}.

4. <u>Potential hourly transpiration (T_{pot})</u>

It was assumed that plants began to transpire 5 days after planting and stopped transpiring a certain number of days after planting, depending on the length of the crop season. Hence, T_{pot} was set equal to zero outside of that time period. During the transpiring period, T_{pot}, was calculated by subtracting the evaporative surface flux (q_s) from E_{tc}.

5. <u>Allocation of T_{pot} by node</u>

It is well recognized that roots at all depths are not equally effective in extracting moisture for transpiration; roots in the upper regions extract more water than deep roots. Studies have indicated that crops extract 40, 30, 20, and 10% moisture from the first, second, third, and last quarter, respectively, of the root zone (Danielson, 1967). In this model, a modification of the so-called 40-30-20-10 rule was used in apportioning transpiration in the root zone (fig. 5.3). As indicated in figure 5.3, no transpiration was assumed to occur from the top node (i = 1). By dividing the length of the y-axis in figure 5.3 into R-1 nodes, where R is the number of nodes in the root zone, the area corresponding to that node as a fraction of the total area, gives the fraction of transpiration assumed to occur through that node. The amount of potential transpiration occurring through any node i ($T_{pot(i)}$) in mm/h, was expressed as:

$$T_{pot(i)} = T_{pot} \frac{(0.45R - 0.4i - 0.1)}{0.25(R-1)(R-2)} \quad [5\text{-}26]$$

where $1 < i \leq R$. Equation [5-26] was verified using a spreadsheet to ensure that $T_{pot(i)}$ for all layers added up to T_{pot}.

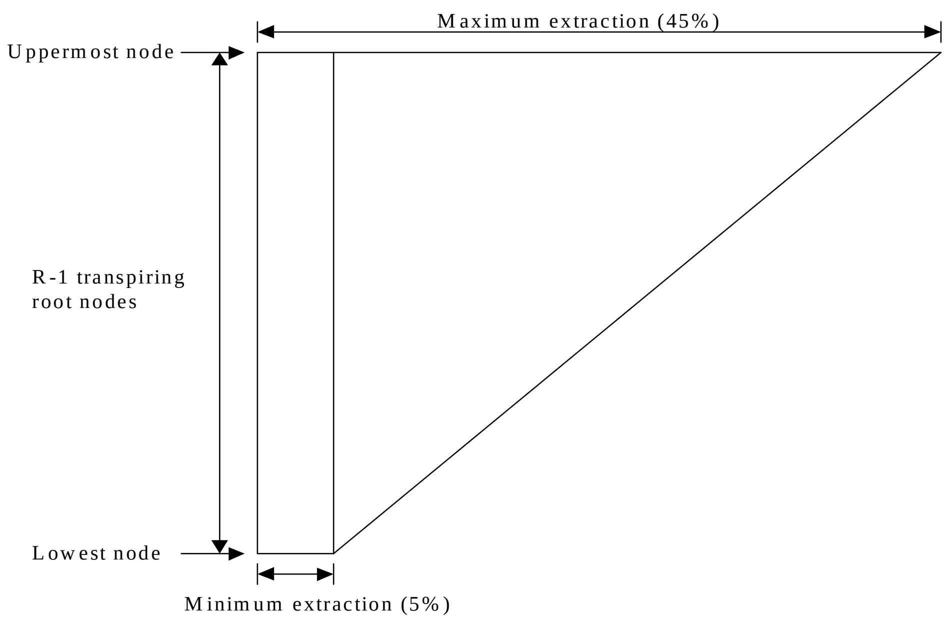

Figure 5.3. Moisture extraction as affected by the location of the node within the root zone. There are R nodes in the rootzone but the top node (i = 1) does not transpire. The maximum and minimum extraction percentages are not the percentages of moisture extracted by the uppermost and lowest nodes but the upper and lower integral limits.

6. Hourly actual transpiration by node ($T_{act(i)}$)

When soil moisture is not limiting, $T_{act(i)}$ will be equal to $T_{pot(i)}$. However, under limited moisture conditions, a modification of the sink term given by Feddes et al. (1978) as used to explain the impact of soil pressure head on transpiration is given in figure 5.4.

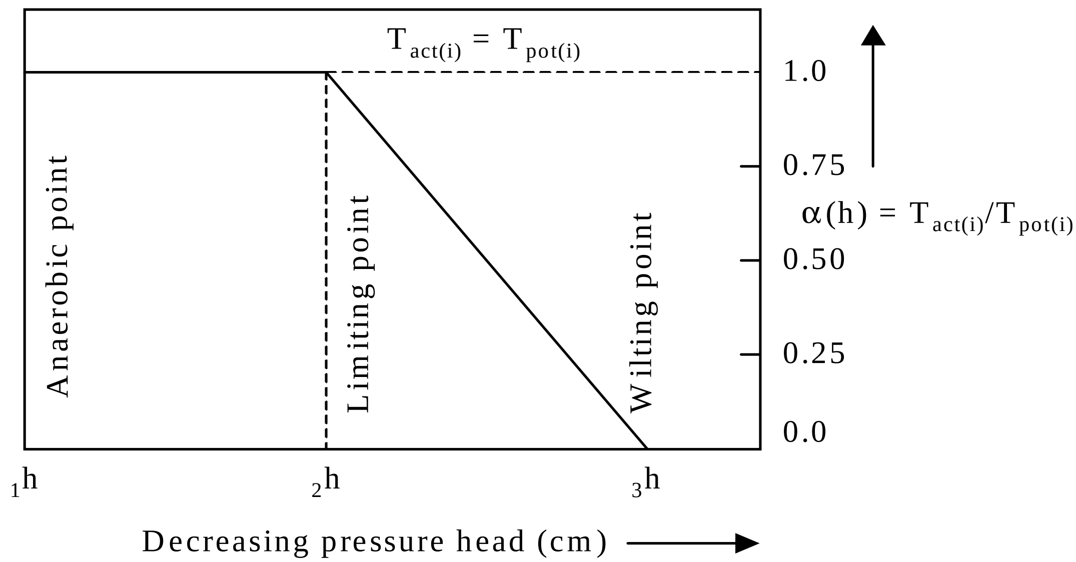

Figure 5.4. Change in actual transpiration with pressure head. For node i, $T_{act(i)}$ and $T_{pot(i)}$ are actual transpiration and potential transpiration, respectively. The pressure heads at the anaerobic, limiting, and wilting points are denoted by $_1h$, $_2h$, and $_3h$, respectively (adapted from Feddes et al., 1978).

Soil moisture content close to saturation will result in anaerobic soil conditions thus denying oxygen to the roots to breathe (Feddes et al., 1978). However, since field soils seldom reach saturation and saturation conditions persist for only short periods, it was assumed there would be no reduction in transpiration under saturation conditions. In the h range of $_1h$ and $_2h$, transpiration was assumed to occur at the potential rate. However, as shown in figure 5.4, under deficit soil moisture conditions, $T_{act(i)}$ was reduced as compared to $T_{pot(i)}$ and was calculated as (Feddes et al., 1978):

$$T_{act(i)} = T_{pot(i)} \frac{h_i - {}_3h}{{}_2h - {}_3h} \qquad [5\text{-}27]$$

where $_2h$ is the pressure head below which there is decline in the transpiration rate. When h_i has a value lower than $_3h$, transpiration ceases. The values of $_2h$ and $_3h$ are dependent on crop phenology (Feddes et al., 1978). Feddes et al. (1978) suggested a range of –500.0 to –1 000.0 cm for $_2h$ and a range of –15 000.0 to –20 000.0 cm for $_3h$. In this model, $T_{act(i)}$ for all nodes is set equal to zero during precipitation events.

Calculation of percolation

Percolation through the root zone for any time step Δt is calculated by multiplying flux at the mid-time step ($q^{k+1/2}_L$) through the bottom node (i = L) by the time step. The lower boundary condition specifies that dh/dz is equal to zero; hence, $q^{k+1/2}_L$ is set equal to $K^{k+1/2}_L$. Percolation amounts at the individual time steps are summed to obtain percolation during the simulation period.

Selection of the time increment or time step (Δt)

Selection of Δt plays an important role in ensuring the stability of the finite difference solution. Implicit time domain discretization methods as applied to linear parabolic systems are always stable; however, the Richards' equation (Eq. [5-3]) is highly nonlinear given the dependence of C and K not only on the independent variables (t and z) but also on the dependent variable, h. Even though the results from linear problems may be used as guidelines to nonlinear problems, frequently the stability of the solution is determined through trial and error. One such procedure, involving the use of an adjustment factor (ς) for calculating Δt used by Feddes et al. (1978) is:

$$\Delta t^{k+1} < \frac{\varsigma \cdot \Delta z}{|q|^k} \tag{5-28}$$

where,

Δt^{k+1} = time step for the new time increment,

ς = time step adjustment factor (0.015-0.035), and

$|q|^k$ = absolute value of flux through the upper or lower boundary at the previous time step.

In Eq. [5-28], lower values of ς are used for high infiltration conditions while higher values are used for soil evaporation under extremely dry soil surface conditions. Stability criteria or expressions for calculating Δt are usually analogous to Eq. [5-28] with Δt increasing with Δz and decreasing with increasing flux. However, in addition to the stability problems associated with the nonlinearity of the Richards' equation, while the selection of Δt may result in a stable solution, mass balance accuracy may be unacceptable. A conservative approach using a very small Δt will result in unacceptably high computing time, especially if the simulation period is long.

Hence, in this study, using a fixed value of Δz (the selection rationale for which is discussed in the following section), the mass balance accuracy of a stable solution for different combinations of Δt and q were determined. Unlike Eq. [5-28] where only the boundary flux was considered, in this study, the maximum flux (upwards or downwards) anywhere in the soil profile was considered to be the governing flux in determining Δt. The mass balance error (ξ, %) was computed as:

$$\xi_{moist} = 100 \frac{\sum_{i=1}^{L} \Delta\theta - (q_{sur} - ET - q_{bot})}{\sum_{i=1}^{L} \Delta\theta} \qquad [5\text{-}29]$$

where $\Sigma_{i=1}^{L}(\Delta\theta)$ is the change in θ (cm^3) and q_{bot} is percolation flux from the root zone (cm^3). The terms q_{sur} and ET are as defined earlier.

Using a maximum ξ of 0.2%, for different values of maximum flux, suitable values of Δt were determined using trial and error. The following empirical relationship was developed using the plot of maximum flux versus Δt:

$$\Delta t = 0.0001 \cdot q_{max}^{-2.4907} / \tau \qquad [5\text{-}30]$$

where q_{max} was the maximum flux anywhere in the soil profile and τ was the margin of safety set equal to 1.25. By using different values of Δz for different combinations of q_{max} and Δt, for a preset value of ξ, it is likely that a relationship analogous to Eq. [5-28] will emerge. However, since the model also has an N sub-model, the Δt value calculated based on the moisture sub-model was compared with the Δt value based on the N sub-model and the lower of the two Δt values was chosen. The criterion for selecting Δt based on the N sub-model is presented in Section 5.1.2. Overall, Δt for the model ranged between 10^{-6} and 1.00 h.

Selection of the space increment (Δz or Δy)

Selection of Δz is affected by factors such as degree of soil heterogeneity, desired accuracy of the modeling results, and the available computing resources. By reducing

Δz, the discretization error can be reduced; however, computation time increases since the number of both nodes and time steps increases (Press et al., 1989). To simulate moisture redistribution in soil columns for a few hours, a small Δz will be required. However, in the field, the simulation time may run into months and such accuracy may not be feasible to obtain; hence, a small Δz may increase computation time without a proportionate increase in accuracy. For example, while Haverkamp et al. (1977) kept Δz equal to 1 cm for a laboratory study, Short et al. (1995) kept Δz equal to 16.7 cm for a field study. For this study, Δz and Δy were both kept equal to 1.25 cm. A choice of 1.25 cm as Δz (or Δy) represented a reasonable compromise between accuracy and simulation time. Selection of equal-sized increments in the z- and y-axes simplified the modeling code.

5.1.2. Nitrogen Sub-model

The two-dimensional N sub-model simulates the fate of subsurface-banded N using the convective-dispersive equation (CDE). Processes that are simulated include dissolution of urea particles, urea hydrolysis, and nitrification. Crop N removal and NO_3^- leaching from the root zone are estimated. In addition to the initial N concentrations in the root zone, moisture redistribution model outputs (moisture flux, θ, and transpiration) are applied as inputs to the N sub-model.

Governing equation

The CDE is used to simulate the fate of urea-N and its transformation products in the 2-D N sub-model. The general form of the CDE applicable to all three N forms, urea, NH_4^+, and NO_3^-, is written as (Selim, 1994):

$$\frac{\partial(\theta c)}{\partial t} + \rho_b \frac{\partial S}{\partial t} = -\left(\frac{\partial J_y}{\partial y} + \frac{\partial J_z}{\partial z}\right) \pm Q \qquad [5\text{-}31]$$

and

$$J_y = -\theta(D_m + D_t)\frac{\partial c}{\partial y} + q_y c \qquad [5\text{-}32]$$

$$J_z = -\theta(D_m + D_l)\frac{\partial c}{\partial z} + q_z c \qquad [5\text{-}33]$$

where c is N-form concentration in soil solution (mg/mL); ρ_b is soil bulk density (g/cm^3); S is the amount of N-form adsorbed on the soil complex (mg/g-soil); J_y and J_z are N-form fluxes in y and z-directions (mg/cm^2·h), respectively; and Q represents both source (positive) and sink (negative) terms. The molecular diffusion coefficient for the N-form is D_m (cm^2/h); D_t and D_l are dispersion coefficients for the soil in the transverse and longitudinal directions (cm^2/h), respectively; and q_y and q_z are moisture fluxes along the y and z axes (cm/h), respectively.

The dispersion coefficients are written as:

$$D_t = \lambda_t \cdot v_y \qquad [5\text{-}34]$$

$$D_l = \lambda_l \cdot v_z \qquad [5\text{-}35]$$

where λ_t and λ_l are dispersivities (cm) in the transverse and longitudinal directions, respectively, and v_y ($=q_y/\theta$) and v_z ($=q_z/\theta$) are pore velocities along the y and z axes. Since the moisture redistribution sub-model is one-dimensional, moisture flux along the y-axis is assumed to be zero. Consequently, Eq. [5-32] simplifies to the following expression.

$$J_y = -\theta D_m \frac{\partial c}{\partial y} \qquad [5\text{-}32a]$$

The molecular diffusion coefficient D_m can be expressed as:

$$D_m = D_0 \cdot b \cdot \theta \qquad [5\text{-}36]$$

where D_0 is the N-form diffusivity in bulk aqueous solution (cm^2/h) and b is the tortuosity (cm/cm). Since physically-based tortuosity models were not available, the empirical Millington and Quirk (MQ) tortuosity model cited in Ryan and Cohen (1990) was used in this study. Using the MQ tortuosity model, b is expressed as:

$$b = \theta^{2.3} / f^2 \qquad [5\text{-}37]$$

where f is soil porosity. Based on the above discussion, Eq. [5-31] was rewritten as follows:

$$\frac{\partial(\theta c)}{\partial t} + \rho_b \frac{\partial S}{\partial t} = \theta\left(\frac{D_0 \theta^{3.3}}{f^2}\right)\frac{\partial^2 c}{\partial y^2} + \frac{\partial}{\partial z}\left[\left(\theta\left(\frac{D_0\theta^{3.3}}{f^2} + \frac{\lambda_l q_z}{\theta}\right)\frac{\partial c}{\partial z}\right) - \frac{\partial (q_z c)}{\partial z}\right] \pm Q \qquad [5\text{-}38]$$

or,

$$\frac{\partial(\theta c)}{\partial t} + \rho_b \frac{\partial S}{\partial t} = (\theta D_y)\frac{\partial^2 c}{\partial y^2} + \frac{\partial}{\partial z}\left((\theta D_z)\frac{\partial c}{\partial z}\right) - \frac{\partial(q_z c)}{\partial z} \pm Q \qquad [5\text{-}39]$$

where D_y (D_m) and D_z ($D_m + D_l$) are the apparent dispersion coefficients (cm^2/h) along the y- and z-axes, respectively. Since q_y was zero, dispersion along the y-axis was solely due to molecular diffusion. However, dispersion along the z-axis was due to both molecular diffusion and longitudinal dispersion. While θ varied with z, it remained constant with y; hence it was treated as constant for the y-axis term in Eq. [5-39].

The D_l component also contains the flux term q_z (Eq. [5-38]). If q_z becomes negative (moisture movement is towards the soil surface), even for small values of upward flux, D_l becomes negative and may cause D_z to become negative, a physical impossibility. Longitudinal dispersion ceases when water flow ceases (Selim, 1994); hence, it was assumed that for negative values of q_z, D_z was equal to D_m.

Application of the finite difference method to the CDE

In view of 2-D N movement in granules, a finite differencing scheme that allowed for two-dimensional discretization in space was required. Due to superior stability characteristic of the implicit method, a finite difference scheme that combined the ability to simulate in 2-D with stability was considered desirable. Accordingly, the alternating-direction-implicit (ADI) technique was applied to the CDE. Further, the use of the ADI technique results in a set of tridiagonal equations that can be solved rapidly using the Thomas algorithm (Anderson, 1995). Briefly, the ADI technique involves a two-step process to solve for the unknowns at time $t + \Delta t$. In the first step, the unknown values of c are estimated at $t + \Delta t/2$ using known values of c at t. In the second step, the unknown values of c at $t + \Delta t$ are solved using the known values at $t + \Delta t/2$. In the first step, one space coordinate is treated implicitly while the other space coordinate is treated explicitly. In the following step, the space coordinate that was previously treated explicitly is treated implicitly and vice-versa, as the name ADI implies.

Space discretization of the dispersive terms in Eq. [5-39] (the first two terms on the right side) was implemented using the central difference scheme. However, since convection is dependent on the magnitude and direction of q_z, a backward difference operator was applied to the convective term when q_z was downwards (positive). For negative q_z, the convective term was implemented as a forward difference operator. The FD equations for the CDE are presented in the following section.

Finite difference equation for the CDE (non-boundary node)

Due to the presence of boundary conditions along both vertical (z) and horizontal (y) axes, different FD equations are required for boundary and non-boundary nodes. For the non-boundary nodes along the y- (2<i<L-1) and z- (2<j<M-1) axes, the ADI finite differencing scheme was applied to the CDE equation as given below.

<u>ADI first step (for t + Δt/2)</u>

In the first ADI step, for each node along the z-axis (vertical), the Thomas algorithm was solved for all nodes along the horizontal y-axis before being moved to the next node along the z-axis. The general FD equation for the non-boundary node, as applied to any N-form for the first step of the ADI is:

$$\begin{aligned}
&\frac{\theta_i^{k+1/2}\cdot c_{i,j}^{k+1/2}-\theta_i^{k}\cdot c_{i,j}^{k}}{\Delta t/2}+\rho_b\frac{S_{i,j}^{k+1/2}-S_{i,j}^{k}}{\Delta t/2} \\
&=(\theta D_y)\frac{(c_{i,j+1}^{k+1/2}-2c_{i,j}^{k+1/2}+c_{i,j-1}^{k+1/2})}{(\Delta y)^2}+\frac{(\theta D_z)_{i+1/2}^{k}(c_{i+1,j}^{k}-c_{i,j}^{k})}{(\Delta z)^2} \\
&-\frac{(\theta D_z)_{i-1/2}^{k}(c_{i,j}^{k}-c_{i-1,j}^{k})}{(\Delta z)^2}-\frac{(q_{i+1/2}^{k}(c_{i,j}^{k})_L-q_{i-1/2}^{k}(c_{i,j}^{k})_U)}{\Delta z}\pm Q
\end{aligned}\qquad [5\text{-}40]$$

where the (θD_z) term was explicitly evaluated with known variables θ_i and q_i as well as constant terms (Eq. [5-36]). The values of $(c_{i,j}^{k})_L$ (concentration in the <u>L</u>ower node) and $(c_{i,j}^{k})_U$ (concentration in the <u>U</u>pper node) in the convective term change depending on the direction of q_i as given below.

$$(c_{i,j}^{k})_L=\begin{cases} c_{i,j}^{k} & q_{i+1/2}^{k}\geq 0 \\ c_{i+1,j}^{k} & q_{i+1/2}^{k}<0\end{cases}\qquad [5\text{-}41a]$$

$$(c_{i,j}^{k})_U=\begin{cases} c_{i-1,j}^{k} & q_{i-1/2}^{k}\geq 0 \\ c_{i,j}^{k} & q_{i-1/2}^{k}<0\end{cases}\qquad [5\text{-}41b]$$

Hence, as discussed in the previous section, the convective term was always evaluated explicitly since the values of $(c_{i,j}^{k})_L$ and $(c_{i,j}^{k})_U$ changed with the direction of moisture flux. In order for the FD equations for the first ADI step to be solved using the Thomas algorithm, Eq. [5-40] was written as:

$$AS_j c_{i,j-1}^{k+1/2} + BS_j c_{i,j}^{k+1/2} + CS_j c_{i,j+1}^{k+1/2} = KS_j \quad [5\text{-}42]$$

where AS_j, BS_j, and CS_j are the sub-diagonal, diagonal, and super diagonal coefficients, respectively, of the tridiagonal matrix while KS_j is comprised of the remaining (known) terms. Hence, using $q_i^{k+1/2}$ and $\theta_i^{k+1/2}$ obtained from the predictor of the moisture sub-model, $c_{i,j}^{k}$ and $c_{i,j}^{k+1/2}$ values are obtained at t + Δt/2. For each node (i,j), Eq. [5-42] was written separately for urea, NH_4^+, and NO_3^- with appropriate source and sink terms, as discussed in the following section.

ADI second step (for t + Δt)

For the second ADI step, for each node along the horizontal y-axis, the Thomas algorithm was solved for all nodes along the z-axis before being moved to the next y-axis node. The general FD equation for the non-boundary node, as applied to any N-form for the first step of the ADI is as follows:

$$\begin{aligned}
&\frac{\theta_i^{k+1}\cdot c_{i,j}^{k+1} - \theta_i^{k+1/2}\cdot c_{i,j}^{k+1/2}}{\Delta t/2} + \rho_b \frac{S_{i,j}^{k+1} - S_{i,j}^{k+1/2}}{\Delta t/2} \\
&= (\theta D_y)\frac{(c_{i,j+1}^{k+1/2} - 2c_{i,j}^{k+1/2} + c_{i,j-1}^{k+1/2})}{(\Delta y)^2} + \frac{(\theta D_z)_{i+1/2}^{k+1}(c_{i+1,j}^{k+1} - c_{i,j}^{k+1})}{(\Delta z)^2} \\
&- \frac{(\theta D_z)_{i-1/2}^{k+1}(c_{i,j}^{k+1} - c_{i-1,j}^{k+1})}{(\Delta z)^2} - \frac{(q_{i+1/2}^{k+1/2}(c_{i,j}^{k+1/2})_L - q_{i-1/2}^{k+1/2}(c_{i,j}^{k+1/2})_U)}{\Delta z} \pm Q
\end{aligned} \quad [5\text{-}43]$$

where the convective term is expressed explicitly, i.e., in terms of t + Δt/2 even though the diffusive component associated with the z-axis is expressed implicitly, i.e., in terms of t + Δt. Evaluation of $(c_{i,j}^{k+1/2})_L$ and $(c_{i,j}^{k+1/2})_U$ were performed based on the signs of $q_{i+1/2}^{k+1/2}$ and $q_{i-1/2}^{k+1/2}$, respectively, following the conditions expressed in Eqs. [5-41a] and [5-41b].

As with the first ADI step, Eq. [5-43] is written in the following form to be solved using the Thomas algorithm:

$$AS_i c_{i-1,j}^{k+1} + BS_i c_{i,j}^{k+1} + CS_i c_{i+1,j}^{k+1} = KS_i \quad [5\text{-}44]$$

where AS_i, BS_i, and CS_i are the sub-diagonal, diagonal, and super diagonal coefficients of the tridiagonal matrix while KS_i is comprised of the remaining (known) terms.

Hence, in the second ADI step, q_i^{k+1} and θ_i^{k+1} from the corrector of the moisture sub-model and $c_{i,j}^{k+1/2}$ from the first step of the ADI are used to calculate $c_{i,j}^{k+1}$ values at t + Δt. As with the first ADI step, for the second ADI step, for each node (i,j), Eq. [5-44] was written separately for urea, NH_4^+, and NO_3^- with appropriate source and sink terms, as discussed later.

Initial conditions

For each of the N-forms, the initial N-form concentrations (mg/mL) were specified for all nodes in the y- and z-axes in the modeling domain as:

$$\begin{aligned} {}_u c_{i,j} &= {}_u c_{i,j}^{t=0} \\ {}_a c_{i,j} &= {}_a c_{i,j}^{t=0} \\ {}_n c_{i,j} &= {}_n c_{i,j}^{t=0} \end{aligned} \qquad [5\text{-}45]$$

where ${}_u c_{i,j}$, ${}_a c_{i,j}$, and ${}_n c_{i,j}$ are urea, NH_4^+, and NO_3^- concentrations, respectively at the node(i,j) at time t = 0.

Modeling the fate of urea, ammonium, and nitrate

The model simulates the fate of urea ($CO(NH_2)_2$) applied as granules or pellets in subsurface bands. With passage of time, urea hydrolyzes to NH_4^+ at a rate that is affected not only by environmental conditions but also by the urea concentration at the site. Unlike urea or NO_3^-, a large fraction of NH_4^+ remains adsorbed to the soil matrix. Ammonium in the soil is depleted as a result of conversion to NO_3^- as well as due to removal by the crop. Nitrification is affected by both environmental factors and by the NH_4^+ concentration at the site. Hence, in addition to having different CDE equations, the three N forms have different source and sink terms as well as different boundary conditions as discussed below.

A. Urea

1. <u>Governing equation for urea</u>

Fate of urea was simulated using the CDE in 2-D as shown in Eq. [5-39] with S, the adsorbed urea component, set equal to zero since urea is only in the dissolved form with no fraction adsorbed to the soil matrix (Singh and Nye, 1984). The source term associated with urea is due to addition of urea to the soil solution as the applied urea dissolves. The urea sink term accounts for the rate of urea hydrolysis. The description of both source and sink terms are presented later in this section.

2. Boundary conditions applicable to urea

Under favorable soil conditions, urea hydrolysis is a rapid process resulting in complete conversion to NH_4^+ in several days (Tisdale et al., 1993). Hence, it was assumed that urea concentration at any boundary node (i = 1 or L; J = 1 or M) was zero. At any time t, boundary conditions for urea were written as:

$$ {}_u c_{i,j} = \begin{cases} 0 & i = 1, 1 \le j \le M, t \ge 0 \\ 0 & i = L, 1 \le j \le M, t \ge 0 \\ 0 & j = 1, 1 \le i \le L, t \ge 0 \\ 0 & j = M, 1 \le i \le L, t \ge 0 \end{cases} \qquad [5\text{-}46] $$

3. Dissolution of applied urea (source term)

When urea granule or pellet dissolves, the rate of increase in urea content per unit soil volume ($mg \cdot cm^{-3} \cdot h^{-1}$) is termed as the urea source term. In the model, the urea source term appears with a positive sign on the right side of Eq. [5-40] (first ADI step) and Eq. [5-43] (second ADI step) in only those nodes which received urea application.

The dissolution rates of urea pellets and granules were determined (Chapter 4) in the laboratory at a θ_v of 31.4%. The amount of urea dissolved in time $\Delta t/2$ in a node was estimated as follows:

$$ U_{dis} = m_g \cdot U_{mass} \cdot (\Delta t / 2)^{0.5} \qquad [5\text{-}47] $$

where U_{dis} is the mass of urea dissolved (mg), m_g is the mass of urea granules dissolved per square root of time ($mg/h^{0.5}$), and U_{mass} is the amount of urea remaining in the node. To simulate the dissolution of pellets, m_g was substituted by m_p which is the mass of urea pellet dissolved per square root of time ($mg/h^{0.5}$). Finally, the urea source term was expressed as:

$$ {}_u Q_{source} = \frac{U_{dis}}{(\Delta t / 2)(\Delta z)^3} \qquad [5\text{-}48] $$

where ${}_u Q_{source}$ is the urea source term ($mg \cdot cm^{-3} \cdot h^{-1}$). The denominator on the right side of Eq. [5-48] was divided by $(\Delta z)^3$ since the amount of urea dissolved was from a single node and it was assumed that node was enclosed in a cube of dimension Δz. It was assumed that Δz and Δy were equal and for simplicity, the space increment along the x-axis (along the fertilizer band) Δx was also assumed equal to Δz.

It was assumed that urea was applied in a band 2.5 cm wide; hence, two nodes along the y-axis received equal amounts of urea. Along the z-axis, it was assumed that all of the urea was confined to a single node. Since the boundary conditions assume that there is no urea concentration in the boundary nodes, the urea source terms were never applied to the two nodes closest to the boundary (i = 1, 2, L-1, and L or j = 1, 2, M-1, and M).

4. Urea hydrolysis rate (sink term)

Urea is hydrolyzed into NH_4^+ by the soil enzyme urease:

$$CO(NH_2)_2 + H^+ + 2H_2O \xrightarrow{\text{urease}} 2NH_4^+ + HCO_3^- \qquad [5\text{-}49]$$

where HCO_3^- is the bicarbonate ion. Urea hydrolysis results in removal of urea from the node and hence, urea hydrolysis rate (${}_uQ_{sink}$) appears with a negative sign on the right side of Eq. [5-40] (first ADI step) and Eq. [5-43] (second ADI step) in all except the boundary nodes.

Being an enzymatic reaction, the ${}_uQ_{sink}$ is best described by a Michaelis-Menten equation (Tabatabai, 1982):

$${}_uQ_{\sin k} = \frac{\rho_b \cdot V_{max} \cdot {}_u c_{i,j}}{(K_{max} + {}_u c_{i,j})} \qquad [5\text{-}50]$$

where V_{max} is the maximum reaction velocity (mg·g^{-1}-soil·h^{-1}), ${}_uc_{i,j}$ is urea concentration (mg/mL) in any node (i,j), and K_{max}, the Michaelis constant, is the urea concentration at half V_{max}. Between urea concentration of zero and, as yet undefined, ${}_uc_2$ (fig. 5.5), ${}_uQ_{sink}$ (or the reaction velocity) follows the rectangular hyperbolic locus.

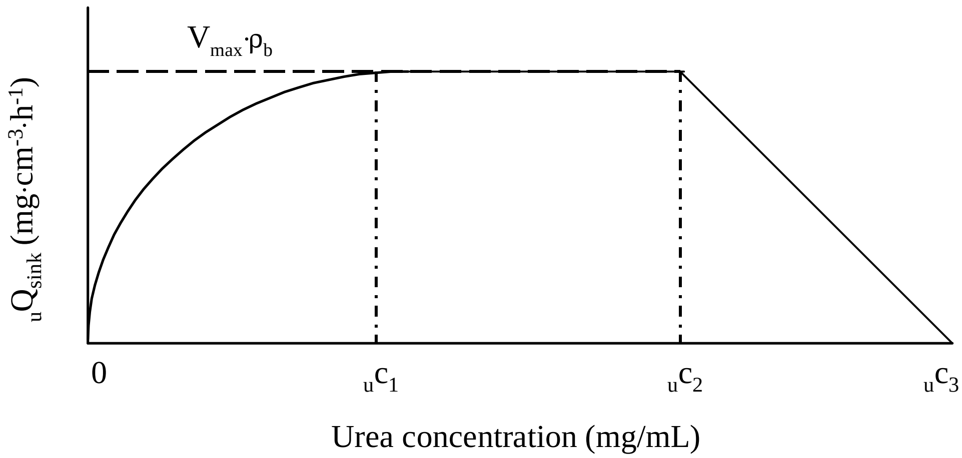

Figure 5.5. Rectangular hyperbola with decreasing reaction velocity with urea concentration between $_uc_2$ and $_uc_3$. V_{max} is the maximum reaction velocity (adapted from Tabatabai, 1982).

Given the likelihood of encountering very high urea concentrations in banded pellets and granules, the inhibitory effects of high urea concentrations on the rate of urea hydrolysis are likely. Wetselaar (1985) reported that urea hydrolysis ceased when urea concentrations equaled half-saturation (535.0 mg/mL-soil solution at 20°C). Hence, in the model, while urea concentration remained at or below $_uc_2$, ${}_uQ_{sink}$ was calculated using the Michaelis-Menten equation (Eq. [5-50]). At urea concentrations in excess of $_uc_2$, ${}_uQ_{sink}$ was assumed to decrease linearly as shown in figure 5.5 and expressed in Eq. [5-51].

$$ {}_uQ_{sink} = -\frac{\rho_b \cdot V_{max}}{({}_uc_3 - {}_uc_2)}\left({}_uc_{i,j} - {}_uc_3\right) \qquad [5\text{-}51] $$

Since K_{max} and V_{max} values, and hence, ${}_uQ_{sink}$ are highest at a temperature of 37°C (Bremner and Mulvaney, 1978), ${}_uQ_{sink}$ was adjusted for a different temperature by multiplying with a urea hydrolysis temperature factor ${}_{uh}f_T$ (0-1). The urea hydrolysis temperature factor ${}_{uh}f_T$ was calculated using the Arrhenius equation (Tabatabai, 1982):

$$ {}_{uh}f_T = {}_{uh}A \cdot \exp(-{}_{uh}E_a / RT) \qquad [5\text{-}52] $$

where ${}_{uh}A$ is the pre-exponential factor for urea; ${}_{uh}E_a$ is the activation energy in Kcal/mole-urea; R is the universal gas constant (1.99×10^{-3} kcal/mole-K); and T is the soil temperature in K.

B. Ammonium

1. Governing equation for NH_4^+

Fate of NH_4^+ was simulated using the CDE in 2-D (Eq. [5-39]). The negative charge on the soil matrix and on organic matter can result in large amounts of NH_4^+ being retained on the soil and organic matter complex. The commonly used Freundlich isotherm is used in the model to express adsorbed NH_4^+ fraction as a function of the dissolved NH_4^+ fraction (Novotny and Olem, 1994; McLaren, 1978):

$$S = K_d \cdot {}_a c_{i,j}^{1/n} \qquad [5\text{-}53]$$

where S is the amount of NH_4^+ retained on the soil (mg/g-soil), K_d is the distribution coefficient (mL/g), ${}_a c_{i,j}$ is the NH_4^+ concentration in the node (i,j), and n is the Freundlich exponent. When n is not equal to one, Eq. [5-39] becomes nonlinear, and hence, cannot be solved using the Thomas algorithm. Hence, following the work of Selim and Iskandar (1981), n was assumed to be one to linearize the isotherm.

The source term associated with NH_4^+ is due to hydrolysis of urea, resulting in the addition of NH_4^+ to the soil N pool. The NH_4^+ sink terms account for nitrification rate as well as NH_4^+ removal rate by plants. The description of both source and sink terms are presented later in this section.

2. Boundary conditions applicable to NH_4^+

Due to its tendency to adsorb to the soil matrix, NH_4^+ movement in soil is largely due to diffusion (Tisdale et al., 1993), which results in limited NH_4^+ movement in soil. Hence, it was assumed that NH_4^+ concentration at any boundary node (i = 1 or L or J = 1 or M) was zero. At any time t, boundary conditions for NH_4^+ were written as:

$$
{}_a c_{i,j} = \begin{cases} 0 & i = 1, 1 \le j \le M,\ t \ge 0 \\ 0 & i = L, 1 \le j \le M,\ t \ge 0 \\ 0 & j = 1, 1 \le i \le L,\ t \ge 0 \\ 0 & j = M, 1 \le i \le L,\ t \ge 0 \end{cases} \qquad [5\text{-}54]
$$

3. Ammonium source term

When urea hydrolysis occurs, urea is consumed and NH_4^+ is produced. For every 60 g (1 mole) of urea hydrolyzed, 36 g (2 moles) of NH_4^+ is produced. Hence, the NH_4^+ source term was calculated as:

$$
{}_a Q_{source} = (36/60) \cdot {}_u Q_{\sin k} \qquad [5\text{-}55]
$$

where ${}_aQ_{source}$ is expressed in mg·cm^{-3}·h^{-1}. The ${}_aQ_{source}$ was written on the right side of the CDE as a positive term for all except the boundary nodes.

4. Nitrification rate (sink term 1)

Ammonium is converted into NO_3^- in a two-stage process with NO_2^- as the intermediate product. While NH_4^+ is converted into NO_2^- by the autotrophic bacteria *Nitrosomonas*, NO_2^- is rapidly converted into NO_3^- by the autotrophic bacteria *Nitrobacter*. For simplicity, the intermediate stage of NO_2^- formation is usually not modeled, with conversion of NH_4^+ to NO_3^- modeled as a one-stage process. Modeling NO_2^- formation is not widespread probably because NO_2^- presence is short lived and it is not removed by plants. Since nitrification is a biological reaction, a biological model is desirable (Prosser, 1986). However, difficulty in quantifying the nitrifier populations and establishing the contribution of each genus to the nitrification process (Schmidt and Belser, 1982), has made simpler physicochemical models popular (Sparks, 1986).

Hence, in this study, the simple physicochemical models, zero- and first-order reactions were used as a one-stage process to quantify nitrification rate (${}_aQ_{sink1}$). Further, due to NH_4^+ toxicity at high concentrations (at or above quarter-saturation) (Wetselaar, 1985), nitrification was halted at high NH_4^+ concentrations (Eq. [5-56]). Ammonium concentration effects on nitrification order in the model is expressed as:

$$
\frac{d({}_a c_{i,j})}{dt} = \begin{cases} {}_{nit}k_1({}_a c_{i,j}) & {}_a c_{i,j} < {}_a c_1 \\ {}_{nit}k_0 & {}_a c_1 \le {}_a c_{i,j} < {}_a c_0 \\ 0 & {}_a c_0 \le {}_a c_{i,j} \end{cases} \qquad [5\text{-}56]
$$

where ${}_{nit}k_1$ (h^{-1}) and ${}_{nit}k_0$ ($mg \cdot mL^{-1} \cdot h^{-1}$) are the first- and zero-order rate constants for nitrification, respectively; ${}_{a}c_{i,j}$ is the NH_4^+ concentration in the node (i,j); and ${}_{a}c_1$ is the threshold NH_4^+ concentration below which the first-order reaction is used. Zero-order reaction governs nitrification when NH_4^+ concentration remains between ${}_{a}c_1$ and ${}_{a}c_0$. Hence ${}_{a}Q_{sink1}$ is expressed as:

$$ {}_{a}Q_{\sin k1} = \theta_i \cdot \frac{d({}_{a}c_{i,j})}{dt} \qquad [5\text{-}57] $$

The nitrification rate as calculated in Eq. [5-56] is true for optimum pH (8.5), temperature (25°C), and soil moisture tension (0.1 bar) values, three environmental factors that significantly affect the nitrification rate. For environmental conditions that are less than optimum, nitrification coefficients were used to reduce ${}_{a}Q_{sink1}$.

A mildly non-linear relationship given in Novotny and Olem (1993) was used to describe pH effects. Accordingly, values of the pH factor for nitrification ${}_{nit}f_{pH}$ (0-1) were calculated as (Novotny and Olem, 1994):

$$ {}_{nit}f_{pH} = \begin{cases} 0.12 & 4.5 \le pH < 6.0 \\ 0.352 \cdot (pH - 6.0) + 0.12 & 6.0 \le pH \le 8.5 \\ 0.40 \cdot (pH - 10.0) + 0.40 & 8.5 < pH \le 10.0 \end{cases} \qquad [5\text{-}58] $$

As with urea hydrolysis, the Arrhenius equation was used to account for temperature effects on nitrification rate. Assuming 25°C as the optimum temperature for nitrification, the temperature factor for nitrification ${}_{nit}f_T$ (0-1) was calculated as:

$$ {}_{nit}f_T = {}_{nit}A \cdot \exp(-{}_{nit}E_a / RT) \qquad [5\text{-}59] $$

where ${}_{nit}A$ is the pre-exponential factor for NH_4^+ and ${}_{nit}E_a$ is the activation energy in Kcal/mole-NH_4^+; R and T are as previously defined.

Raynes (1986) reported that nitrification rate in silt loam incubated at 21°C was highest at –100.0 cm and nitrification rates at 0.0 cm and –15 000.0 cm were 4.8 and 15.1%, respectively of the highest rate (at –100.0 cm). Based on the work of Raynes (1986), assuming that nitrification rate was negligible at 0 cm pressure, the nitrification coefficient for soil moisture tension, ${}_{nit}f_h$ (0-1) was calculated using a linear equation for h values between 0 and -100 cm and a logarithmic equation was used for h values below -100 cm:

$$ {}_{nit}f_h = \begin{cases} 0.01 \cdot |h| & 0 > h \geq -100 \text{ cm} \\ -0.1673 \cdot \ln(|h|) + 1.6864 & -100 > h \geq -15000 \text{ cm} \end{cases} \qquad [5\text{-}60] $$

Hence, ${}_aQ_{sink1}$ was adjusted for pH, soil temperature, and pressure head effects. Oxygen composition in the soil air plays an important role in the nitrification rate; it was assumed that ${}_{nit}f_h$ addressed this issue. No other environmental factors were considered. The adjusted sink term was applied as a negative quantity on the right side of the CDE to all except the boundary nodes.

5. Rate of NH_4^+ removal by plants (sink term 2)

The second sink term in the NH_4^+ CDE, ${}_aQ_{sink2}$ accounted for the rate of NH_4^+ removal by the crop. The following assumptions were applied in estimating ${}_aQ_{sink2}$.

- There was no preferential removal of NH_4^+ over NO_3^- or vice-versa.
- The amount of NH_4^+ removed by the crop from a cell ($1.25 \times 1.25 \times 1.25$ cm^3) was equal to the amount of water removed from the cell multiplied by the dissolved NH_4^+ concentration. Hence, NH_4^+ removal followed a zero-order reaction.
- Equal amounts of water were removed from all cells (j = 1, M) at any vertical node (i).

Hence, based on the amount of water removed by transpiration from each cell, the amount of NH_4^+ from a particular cell was estimated. The sink term, ${}_aQ_{sink2}$ was applied as a negative quantity on the right side of the CDE to all except the boundary nodes

C. Nitrate

1. Governing equation for NO_3^-

Fate of NO_3^- was simulated using the CDE in 2-D as shown in Eq. [5-39] with S, the adsorbed NO_3^- component set equal to zero since NO_3^- remains largely in the dissolved form given its weak anionic charge, and hence, its inability to adsorb to the soil matrix in substantial amounts. The source term associated with NO_3^- is due to addition of NO_3^- to the soil solution as NH_4^+ undergoes nitrification. The NO_3^- sink term accounts for the rate of NO_3^- removal by plants. The description of both source and sink terms are presented later in this section.

2. <u>Boundary conditions applicable to NO_3^-</u>

Four types of boundary conditions were applied at the boundaries along the y- and z-axis as discussed below.

- Top node (i = 1, j = 1, …., M)

Since NO_3^- is highly water soluble, it can move upwards to the soil surface due to capillary action. However, given the suction exerted by the plant roots, NO_3^- concentration in the surface layer was assumed to be negligible, and the Dirichlet boundary condition was expressed as:

$$_{n}c_{i,j} = 0 \qquad i = 1, 1 \leq j \leq M, t \geq 0 \qquad [5\text{-}61]$$

- Bottom node (i = L, j = 2, …, M-1)

Nitrate readily leaches with water percolating through the root zone; consequently, it is unclear what kind of boundary condition best explains the physical situation. Hence, the differential of the NO_3^- concentration gradient with depth (also a Neumann boundary condition) was assumed to be zero (J.T. Borggaard, personal communication, Blacksburg, Va.17 July 2000) at the bottom node. The boundary condition (Eq. [5-62]) and the resulting CDE (obtained by modifying Eq. [5-39]) are:

$$\frac{\partial^2 ({}_{n}c)}{\partial z^2} = 0 \qquad i = L, 2 \leq j \leq M-1, t \geq 0 \qquad [5\text{-}62]$$

$$\frac{\partial(\theta \cdot {}_{n}c)}{\partial t} = (\theta \cdot {}_{n}D_y)\frac{\partial^2 {}_{n}c}{\partial y^2} + \left(\frac{\partial(\theta \cdot {}_{n}D_z)}{\partial z} \cdot \frac{\partial({}_{n}c)}{\partial z}\right) - \frac{\partial(q_z \cdot {}_{n}c)}{\partial z} - Q \qquad [5\text{-}63]$$

where $_{n}D_y$ is D_y for NO_3^-. Equation [5-63] was finite differenced using the same method used for differencing Eq. [5-39] for the non-boundary nodes for both the first and second ADI steps.

- Corner nodes at the bottom (i = L, j = 1 or M)

At the corner nodes in the bottom layer, it was assumed that the Neumann condition applied along both y- and z-axes. The boundary condition (Eq. [5-64]) and the resulting CDE (Eq. [5-65]) are:

$$\frac{\partial^2 ({}_{n}c)}{\partial z^2} = \frac{\partial^2 ({}_{n}c)}{\partial y^2} = 0 \qquad i = L, j = 1 \text{ or } M, t \geq 0 \qquad [5\text{-}64]$$

$$\frac{\partial(\theta \cdot_n c)}{\partial t} = \left(\frac{\partial(\theta \cdot_n D_z)}{\partial z} \cdot \frac{\partial(_n c)}{\partial z}\right) - \frac{\partial(q_z \cdot _n c)}{\partial z} - Q \qquad [5\text{-}65]$$

Equation [5-65] was finite differenced to obtain NO_3^- concentration at the corner nodes for both the first and second ADI steps.

- Nodes at the lateral boundaries ($j = 1$ or M, $2 \le i \le L\text{-}1$)

Again, the Neumann condition applied at the node on the lower boundary was applied. The boundary condition (Eq. [5-66]) and the resulting CDE (Eq. [5-67]) are:

$$\frac{\partial^2(_n c)}{\partial y^2} = 0 \qquad j = 1 \text{ or } M, 2 \le i \le L-1, t \ge 0 \qquad [5\text{-}66]$$

$$\frac{\partial(\theta_n c)}{\partial t} = \frac{\partial}{\partial z}\left((\theta(_n D_z))\frac{\partial(_n c)}{\partial z}\right) - \frac{\partial(q_z(_n c))}{\partial z} - Q \qquad [5\text{-}67]$$

where $_nD_z$ is the D_z for NO_3^-. Equation [5-67] was finite differenced using the same method used for differencing Eq. [5-39] for the non-boundary nodes for both the first and second ADI steps.

3. Nitrate source term

Nitrification results in depletion of NH_4^+ and production of NO_3^-. For every 18 g (1 mole) of NH_4^+ nitrified, 62 g (1 mole) of NO_3^- is produced. Hence, the NO_3^- source term was calculated as:

$$_nQ_{source} = (62/18) \cdot _aQ_{sink1} \qquad [5\text{-}68]$$

where $_nQ_{source}$ is expressed in $mg \cdot cm^{-3} \cdot h^{-1}$. The $_nQ_{source}$ was written on the right side of the CDE as a positive term for all except the boundary nodes.

4. Rate of NO_3^- removal by plants (sink term)

The sink term in the NO_3^- CDE, $_nQ_{sink}$ accounted for the rate of NO_3^-removal by the crop. Assumptions used in estimating NH_4^+ removal were also applied for calculating $_nQ_{sink}$. Hence, based on the amount of water removed by transpiration from each cell, the amount of NO_3^- from a particular cell was estimated. The sink term, $_aQ_{sink}$, was applied as a negative quantity on the right side of the CDE to all except the boundary nodes.

5. Nitrate-N loading from the root zone

Nitrate-N loading from the root zone for any time step is calculated by multiplying the moisture flux through the lowest node (i = L) at the mid-time step ($q^{k+1/2}L$) by the average NO_3^--N concentration in the lowest layer in the root zone (i = L, j = 1, …, M). Nitrate-N loading values over the individual time steps are summed to obtain NO_3^--N loading during the simulation period.

Selection of the time increment or time step (Δt)

Selection of the time step using the Courant or the Courant-Friedrichs-Lewy (CFL) criterion ensures the stability of hyperbolic equations, for example, the wave equation (Anderson, 1995). However, the CFL criterion can also be used to select Δt for parabolic equations such as the CDE (Kaluarachchi and Parker, 1988), though the presence of the convective term does not always guarantee the stability of the system. For the CDE (Eq. [5-39]), the CFL criterion is represented as (Anderson, 1995):

$$\frac{2(D_z)_{max} \cdot \Delta t}{(\Delta z)^2} \leq 1 \qquad [5\text{-}69]$$

where $(D_z)_{max}$ is the maximum D_z anywhere in the soil profile along the vertical axis (i = 1, …, L); Δt and Δz are as previously explained. Hence, the time step in the model was calculated as given below:

$$\Delta t = \frac{(\Delta z)^2}{2 \cdot \tau \cdot ({}_a D_z)_{max}} \qquad [5\text{-}70]$$

where τ, the margin of safety factor (1.25) used in Eq. [5-30] for determining Δt was introduced in Eq. [5-70] to ensure that the CFL criterion remains equal to 0.8 to ensure the stability of the CDE. Further, the D_m component in D_z varies with the N-form, with NH_4^+ having the highest value (Section 5.2). Hence, in determining Δt, D_m for NH_4^+ (${}_aD_m$) was used to obtain the smallest Δt value.

While testing the full model it was observed that, at low moisture flux values (e.g., 0.01 cm/h), use of Δt calculated using Eq. [5-30] resulted in numerical oscillations since the CFL criterion was violated. However, at higher moisture flux values (e.g., 1.0 cm/h), Δt calculated using Eq. [5-30] satisfied the CFL criterion. Hence, for the time before fertilizer application, Eq. [5-30] was used to calculate Δt for the model.

Otherwise, Δt obtained using Eq. [5-30] was compared with Δt obtained using Eq. [5-70], and the smaller of the two time steps was selected. Such an approach ensured the stability of the model and also minimized numerical oscillations.

5.2. *Model Evaluation*

The model was evaluated for a period of 325 days from 12 May 1998 through 2 April 1999 using data obtained from the field experiment. This section includes a discussion of the input data required to run the model. Moisture and N sub-models (for both pellets and granules) were evaluated for their mass conservative properties. Measured and simulated moisture and inorganic-N were compared to evaluate the ability of the model to simulate the physical process. Limited model calibration was also performed. Finally, model sensitivity to selected parameters was analyzed.

5.2.1. Input Data

While some model parameters were measured in the laboratory for the Ross soil (the soil at the field experiment site) or estimated using laboratory measurements, other parameters were obtained from the literature. The required input parameters, their sources, and selection procedures are described below. The values of the variables and parameters contained in the input files are presented in Appendix B while the input file formats are presented in Appendix C. The model code is presented in Appendix D.

1. Initial volumetric moisture content (θ)

Using moisture content estimations at 30, 45, 60, 90, and 120-cm depths using the neutron probe (Chapter 3) and an assumed value of θ at the surface (based on antecedent precipitation conditions), θ values were calculated for intermediate nodes within the root zone (120 cm). The θ values thus obtained were used to specify the initial moisture conditions.

2. Hourly weather parameters

Hourly weather parameters were obtained from multiple sources with the objective of obtaining data that could be considered to be representative of the field site (table

5.1). The data were used to calculate hourly reference ET (E_{tr}) externally using REF-ET (Allen, 1990) as well as to calculate hourly potential crop ET (E_{tc}) within the model.

Table 5.1. Sources of hourly weather parameters required by the model

Parameter	Source (duration)
Air temperature (°C) Relative humidity (%) Wind speed (km)	Roanoke Regional Airport (12 May-19 September, 1998) * Kentland Farm Weather Station (20 September 1998 - 2 April 1999)†
Soil temperature (°C)	Kentland Farm‡
Solar radiation (W/m^2)	Bluefield State College, West Virginia§
Precipitation (mm)	Field site at Kentland Farm‖

* Source: State Climatologist's Office, Charlottesville, Va.

† Located about 1 km from field site

‡ Obtained by averaging hourly temperature measured at 5 cm depth beneath a sod cover during 1993 (part), 1994, and 1995 (Source: N. Persaud, Virginia Tech, Blacksburg, Va.)

§ Source: National Renewable Energy Laboratory (1999)

‖ Collected 150 m from field site; precipitation data recorded on strip charts with a readability of 0.127 cm were digitized to obtain hourly precipitation data

3. Initial applied inorganic-N status in the soil

During the May 1998 soil sampling event, the fertilizer treatments did not have higher inorganic-N amounts than the control treatment in any layer in the root zone (Chapter 4). Hence, assuming that there was no residual inorganic-N in the soil profile from the fertilizer application made during the 1997 corn season, urea, NH_4^+, and NO_3^- concentrations were set equal to zero everywhere in the soil profile.

4. Parameters required for estimating hydraulic conductivity (K)

Pressure head was estimated from θ and the parameters θ_s, θ_r, α, m, and n using Eq. [5-9]. Hydraulic conductivity was estimated using h and the parameters K_s, α, m, n, and L (Sec. 5.1.1) using Eq. [5-8]. The parameters (Table 5.2) were estimated using soil properties in the top 10-cm of the soil profile and applied to the entire root zone.

Table 5.2. Parameters required for estimating K from θ or h

Parameter	Value used in model	Estimation method
θ_s (mL/cm^3)	0.488	Measured in the laboratory
θ_r (mL/cm^3)	0.029	Estimated from RETC.FOR using $h(\theta)$ and θ_s
K_s (cm/h)	1.00	Estimated from RETC.FOR using $h(\theta)$ and θ_s*
α (cm)	0.1302	Estimated from RETC.FOR using $h(\theta)$ and θ_s
m	0.1244	Estimated from RETC.FOR using $h(\theta)$ and θ_s
n	1.005	Estimated from RETC.FOR using $h(\theta)$ and θ_s
L	0.5	Estimated from RETC.FOR using $h(\theta)$ and θ_s

* Due to uncertainty in K_s measurement, measured K_s (0.92 cm/h) was replaced by estimated K_s value in the model as recommended by van Genuchten et al. (1991).

5. Soil water capacity (C) at saturation

At saturation (h = 0), C becomes zero (Eq. [5-12]) resulting in an indeterminate value of h in the next time step (Eq. [5-13]). By trial and error, over a simulation period of 3574 h, it was determined that the mass balance error computed using Eq. [5-29] was reduced to zero when h was set equal to – 0.0001 cm at saturation.

6. Net radiation (R_n)

Net radiation is the difference between the total upward and total downward radiation fluxes (Rosenberg et al., 1983). Net radiation is generally expressed as a linear function of solar radiation, R_s (Rosenberg et al., 1983). Using measured data, Rosenthal et al. (1977) developed the following relationship to estimate R_n as a function of R_s:

$$R_n = \begin{cases} 0.861\,(R_s) - 103.92 & \text{LAI} \le 3.0 \\ 0.848\,(R_s) - 144.49 & \text{LAI} > 3.0 \end{cases} \qquad [5\text{-}71]$$

where R_s is expressed in $cal \cdot cm^{-2} \cdot d^{-1}$ and LAI is the leaf area index. The value of R_n obtained from Eq. [5-71] in $cal \cdot cm^{-2} \cdot d^{-1}$ was converted to $MJ \cdot m^{-2} \cdot d^{-1}$ within the model.

7. Extinction coefficient (C_e)

The extinction coefficient was used to calculate R_{ns}, the net soil solar radiation (Eq. [5-25]). For corn, Farahani and Bausch (1995) estimated C_e as 0.594. Farahani and Bausch (1995) reported that the C_e value in their study had likely been underestimated, resulting in the overestimation of surface evaporation. Uchijima (1976) reported that C_e values ranged between 0.45 to 0.65 for rice. Hence, based on the observations of Uchijima (1976) and Farahani and Bausch (1995), a C_e value of 0.63 was used.

8. Corn crop coefficient (K_c)

Even though E_{tr}-based K_c values are in principle universally applicable, local calibration is desirable to account for differences in cultural practices. However, K_c values for corn are not available for Virginia; hence K_c values developed for corn grown in the San Joaquin Valley, California (fig. 5.6) were used (Allen et al., 1990).

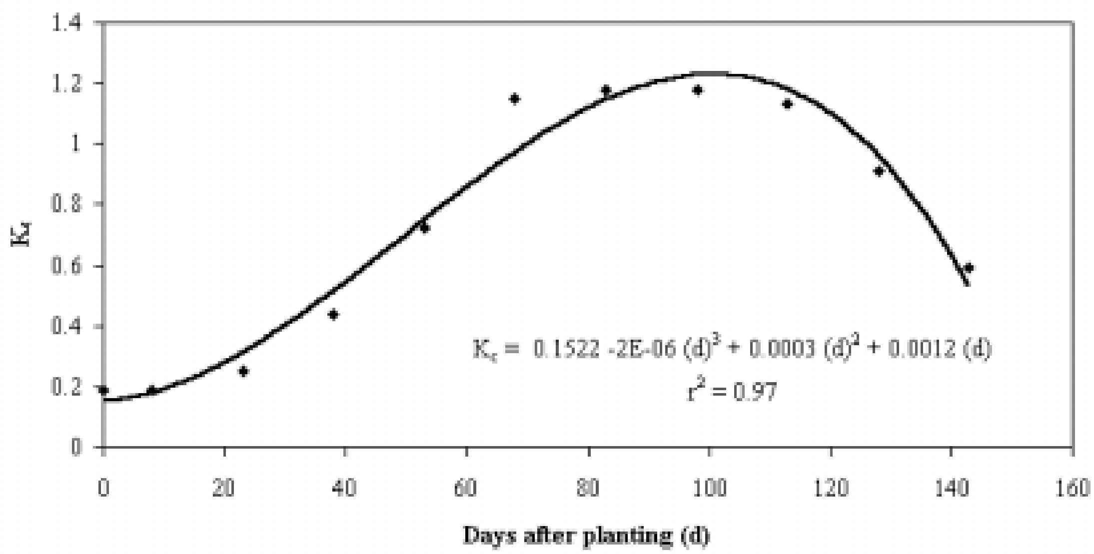

Figure 5.6. Corn crop coefficient (K_c) during the growing season in California (adapted from Allen et al., 1990)

The relationship shown in figure 5.6 was used to calculate K_c any time during the growing season. The variables in figure 5.6 had a high degree of correlation as demonstrated by the high r^2 value. Crop coefficient values were updated at 10-d intervals beginning the sixth day until 140 days after planting; for the other periods, K_c was assumed to be equal to 0.19 (Allen et al., 1990). Since corn is usually harvested within 140 days of planting, a K_c value of 0.19 was assigned for those days exceeding 140 days after planting. Further, if the crop was harvested earlier than 140 days, the model set the K_c value equal to 0.19 for those days.

9. Leaf area index (LAI)

Change in LAI of corn over the growing season was obtained from the documentation of the CREAMS model (USDA-SCS, 1984). Leaf area indices reported in portions of the growing season were calculated for days of the growing season assuming that a full corn season lasted 140 days (fig. 5.7).

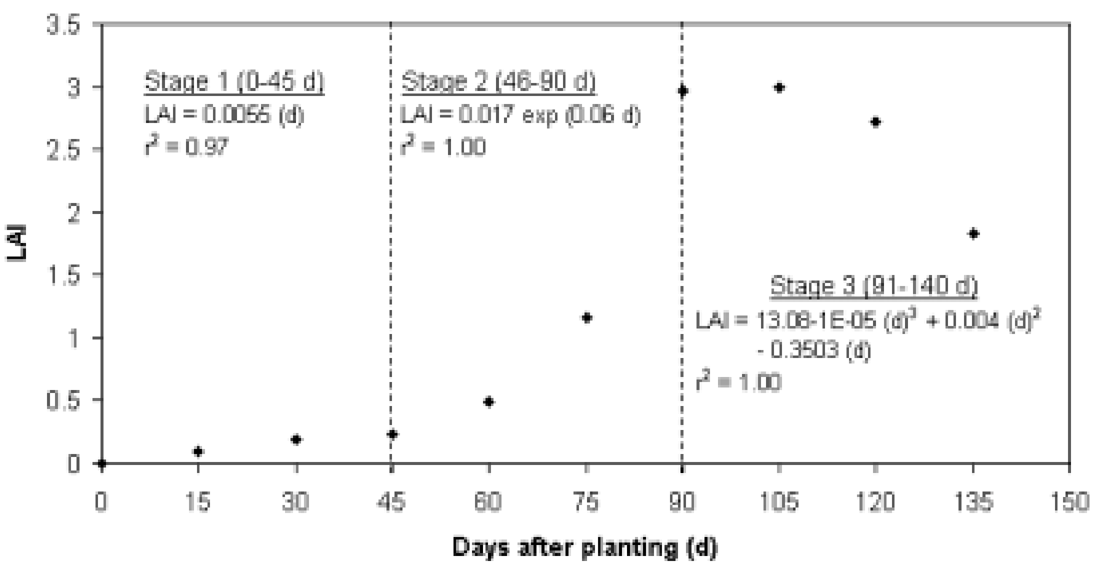

Figure 5.7. Corn LAI during the growing season (adapted from USDA-SCS, 1984)

Three regression equations were developed to express LAI as a function of time (fig. 5.7). For stage 1 (0-45 d), a linear equation was used for expressing LAI as a function of time (fig. 5.7). For second (46-90 d) and third (>90 d) stages, exponential and fourth-order polynomial relationships, respectively, were used. Correlations between the variables for all three stages were good, as indicated by the high r^2 values (fig. 5.7). Leaf area indices were updated using equations given in figure 5.7 at 10-d intervals beginning the sixth day until 140 days after planting; for the other periods, LAI was assumed to be equal to zero.

10. Root depth

Maximum root depth of the corn plant varies between 1.0 and 1.7 m (Smith, 1992). Since the Ross soil has a maximum solum thickness of 1.14m (SCS, 1985), maximum root depth of the corn crop was assumed to be 1.2 m. Based on the study by Saxton et al. (1974), an empirical relationship of root depth versus days after planting was developed (fig. 5.8).

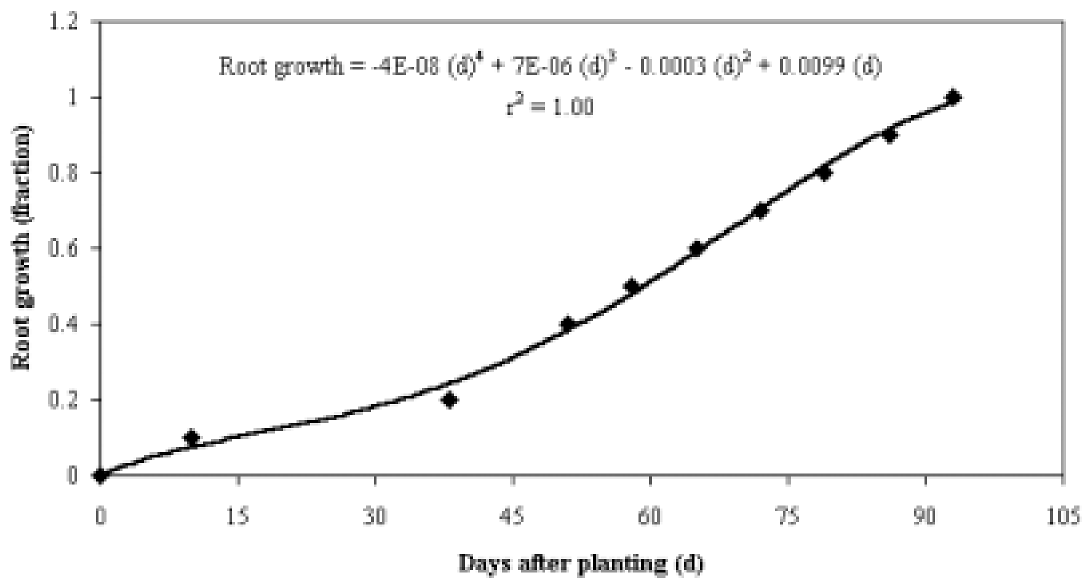

Figure 5.8. Root development as function of crop growth (adapted from Saxton et al., 1974)

The variables in figure 5.8 had a high degree of correlation as demonstrated by the r^2 value. The relationship shown in figure 5.8 was used to calculate root growth as a fraction of the maximum root depth any time during the growing season. Root depth was calculated by multiplying the root growth fraction by the maximum root depth. Root depth values were updated at 10-d intervals beginning the sixth day until 90 days after planting. Between 90 and 140 days, or the time of harvest (whichever came first), it was assumed that root depth did not change. For other periods, root depth was assumed to be zero.

11. Pressure head values at limiting ($_2h$) and wilting points ($_3h$)

In this application, $_2h$ and $_3h$ were assigned the drier-end values of –1 000.0 and –20 000.0 cm, respectively, since corn is considered to be an efficient user of water.

12. Distribution coefficient (K_d) for NH_4^+

For a sandy loam soil, Selim and Iskandar (1981) reported a K_d of 0.25 mL/g for NH_4^+. Hence, a K_d of 0.25 mL/g was used in this application because the Ross soil has a texture comparable to the sandy loam soil studied by Selim and Iskandar (1981).

13. Molecular diffusion coefficients

The aqueous diffusion coefficient (D_0) for any solute is affected by both solute concentration and temperature. Temperature effect on D_0 was not considered. However, where available, D_0 measured for high solute concentration was selected. Singh and Nye (1984) used a urea molecular diffusion coefficient ($_uD_0$) value of 0.03 cm^2/h based on a urea concentration of 480 g-urea/L-aqueous solution at 25°C. Since high solute concentrations were expected in banded-N application, $_uD_0$ value of 0.03 cm^2/h was used. For NH_4^+, a molecular diffusion coefficient ($_aD_0$) of 0.07 cm^2/h at 25°C reported by Singh and Nye (1984) was used.

Since the aqueous diffusion coefficient for NO_3^- ($_nD_0$) could not be obtained from the literature, the following relationship proposed by Nye and Tinker (1977) was used to estimate the proportionality constant K_p for urea:

$$K_p = {}_uD_0 \cdot \sqrt[3]{MW_u} \qquad [5\text{-}72]$$

where $_uD_0$ is the molecular diffusion coefficient and MW_u is the molecular weight of urea (60 amu). Using the value of K_p (0.1174) calculated using Eq. [5-72] and the molecular weight of NO_3^- (62 amu), $_nD_0$ was calculated using a modification of Eq. [5-

72]. The value of ${}_nD_0$ thus calculated, 0.03 cm^2/h, was used. In Eq. [5-72], K_p was calculated using ${}_uD_0$ because urea and NO_3^- are similar in molecular weights.

14. Longitudinal dispersivity (λ_l)

For sandy clay soil, Kaluarachchi and Parker (1988) used a value of 1.0 cm for λ_l. Brusseau (1993) reported λ_l values of 0.03 to 0.11 cm for sandy soils in Florida. In this study, λ_l was assumed to have a value of 1.0 cm.

15. Slope of mass of urea dissolved per unit square root of time as affected by urea particle size

Dissolution rate of urea particle was estimated (Eqs. [5-46, 47]) using m_g and m_p, slopes applicable to granules and pellets, respectively. The values of parameters m_g and m_p, estimated using laboratory measurements of urea particle weight loss over time (Chapter 4) used in this study were 0.3877 and 0.1345, respectively.

16. Urea hydrolysis parameters

Tabatabai (1973) reported V_{max} and K_{max} values for urea hydrolysis for seven Iowa soils that covered a wide range of textures. Based on the V_{max} values reported by Tabatabai (1973), a range of 0.02 to 0.44 mg-urea·g^{-1}-soil·h^{-1} based on soil texture, a value of 0.19 mg-urea·g^{-1}-soil·h^{-1} was selected for the Ross soil. Similarly, from a range of K_{max} values (0.08 to 0.42 mg-urea/mL), a value of 0.2 mg-urea/mL was selected.

Kumar and Wagenet (1984) determined ${}_{uh}E_a$ for a number of soils; based on comparable urease activities between Ross soil and Panoche soil, ${}_{uh}E_a$ value of 5.78 kcal/mole-urea calculated for Panoche soil by Kumar and Wagenet (1984) was used. Since ${}_{uh}f_T$ is one at 310°K (37°C) (Tabatabai, 1982), substituting the known values of ${}_{uh}E_a$, R, and T (310°K) in Eq. [5-52], the pre-exponential factor, ${}_{uh}A$ was calculated to be 11724.4. Hence, with known values of ${}_{uh}A$, ${}_{uh}E_a$ and R, ${}_{uh}f_T$ was calculated for the temperature (T) of interest.

17. Nitrification parameters

For a silty clay loam soil, Wagenet et al. (1977) reported a ${}_{nit}k_1$ value of 0.01/h; this value was used in this study. The ${}_{nit}k_0$ value of 347×10^{-6} mg-NH_4^+·mL^{-1}·h^{-1} reported by Chen et al. (1972) for lake sediment samples from Wisconsin was used in this study.

The value of ${}_{nit}E_a$ (Eq. [5-59]) used in the model was 12.64 kcal/mole-NH_4^+ (L. Ma, personal communication, 3 March 1999, Great Plains Systems Research Group, Ft. Collins, Colo.). Assuming that ${}_{nit}f_T$ is equal to one at 298°K (25°C), substituting the known values of ${}_{nit}E_a$, R, and T (298°K) in Eq. [5-59], the pre-exponential factor, ${}_{nit}A$ was calculated to be 1.806×10^9. Hence, with known values of ${}_{nit}A$, ${}_{nit}E_a$ and R, ${}_{nit}f_T$ was calculated for the temperature (T) of interest.

5.2.2. Moisture Sub-model Performance

The mass conservative property of the moisture sub-model was evaluated for two durations from 5 May to 9 October 1998 and from 5 May 1998 to 2 April 1999. After corn silage was harvested in September 1998, moisture measurements were made and soil samples were obtained to determine inorganic-N status on 9 October 1998. Moisture measurements and soil inorganic-N status were determined again on 2 April 1999, when the field experiment was concluded. In addition to 9 October 1998, simulated and measured moisture values were also compared for 6 June, 10 July, and 11 August 1998, days that had been preceded by substantial precipitation depths. Simulated total crop evapotranspiration was compared with published values of corn ET. Finally, the results of sub-model calibration are presented.

1. Mass conservative property of the moisture sub-model

While Richards' equation is based on the principle of conservation of mass (Eq. [5-1]), the nonlinearity of the K(h) and C(h) relationships, inputs to the Richards' equation, can result in errors. Also, selection of the finite differencing scheme may result in errors if the scheme does not display mass conservative properties. The index for evaluating the mass conservative property of the moisture sub-model (η_{moist}) was expressed as:

$$\eta_{moist} = \frac{(\theta_{fin} - \theta_{in})}{(q_{sur} - E_{act} - T_{act} - q_{bot})} \qquad [5\text{-}73]$$

where θ_{fin} and θ_{in} are final (simulated) and initial volumetric moisture contents in the soil profile (cm), respectively, q_{sur} is simulated surface infiltration (cm), E_{act} is simulated actual surface evaporation (cm), T_{act} is simulated actual crop transpiration (cm), and q_{bot} is simulated percolation from the root zone (cm). The components E_{act} and T_{act} are summed to obtain actual crop ET. Errors in the mass conservative property of the moisture sub-model and components of mass balance simulated by the sub-model for both durations of simulation are given in table 5.3. When η_{moist} is equal to one, the model exhibits no error in mass conservation; values greater than one indicate overestimation.

Table 5.3. Simulated moisture mass balance components for the first (5 May - 9 October 1998) and second (5 May 1998 - 2 April 1999) durations of simulation in the root zone (120 cm)

Mass balance components (cm of water)	First duration (3574 h)	Second duration (7800 h)
Final volumetric moisture content, θ_{fin}	35.2	53.0
Initial volumetric moisture content, θ_{in}	44.9	44.9
Surface infiltration, q_{sur}	35.0	61.6
Surface evaporation, E_{act}	12.8	17.4
Crop transpiration, T_{act}	31.3	31.3
Percolation, q_{bot}	0.6	5.0
η_{moist}*	1.00	1.02

* Value equal to 1.00 indicates no error in mass conservation

No error for the first duration (3574 h) (table 5.3) indicated that the model conserved mass. Unlike solution schemes that only consider boundary fluxes in calculating the time step (Feddes et al., 1978), in this sub-model, the time step was calculated using the maximum flux at any point within the root zone. Such an approach used in calculating the time step minimized numerical oscillations, improving accuracy.

There was 2% overestimation in mass conservation over the entire simulation period (7800 h), which could be considered to be acceptable given the long duration of simulation.

The simulation periods included complicated boundary conditions involving precipitation on dry soils with minimal numerical oscillations. Hence, the developed model could be considered to be robust given its capability to simulate precipitation in very dry soil for long periods of time with good mass conservative property.

2. Comparison of estimated and simulated moisture contents

The moisture sub-model was evaluated to see if it represented the physics of moisture redistribution in the field by simulating moisture redistribution accurately. Moisture content values were estimated with measured neutron counts at 30, 45, 60, 90, and 120-cm depths. Estimated and simulated moisture volumes (table 5.4) and distributions (fig. 5.9) in the root zone were compared for five dates, 6 June 1998, 10 July 1998, 11 August 1998, 9 October 1998, and 2 April 1999 (fig. 5.9).

Table 5.4. Comparison of estimated and simulated moisture volumes in the root zone (June 1998 - April 1999)

Date	Estimated (cm)*	Simulated (cm)	Error (%)†
6 June 1998	41.6	47.2	13.4
10 July 1998	36.0	45.6	26.9
11 August 1998	36.1	42.9	18.9
9 October 1998	34.6	35.2	1.7
2 April 1999	44.9	53.0	18.0

* Based on measured neutron counts

† (Simulated-estimated)×100/estimated; positive values indicate overestimation

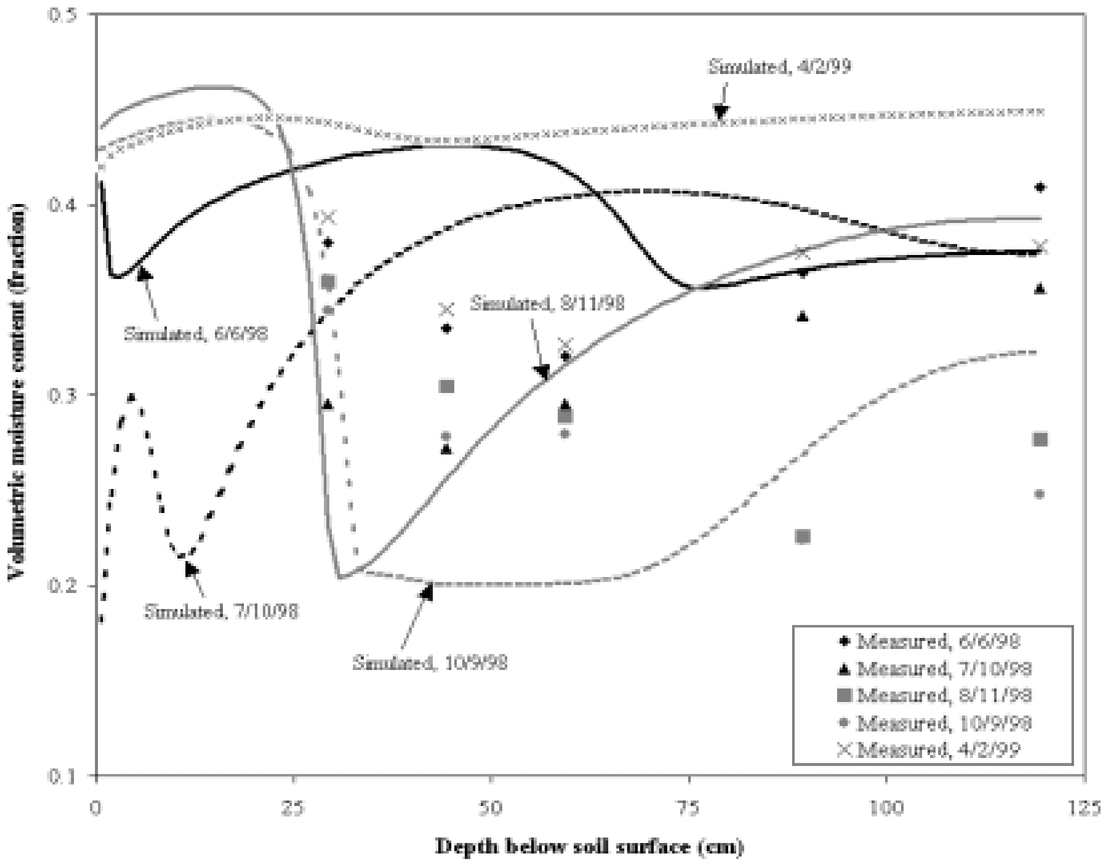

Figure 5.9. Comparison of measured and simulated moisture content values in the root zone during June 1998 through April 1999

During 2-5 June 1998, 2.4 cm of precipitation was recorded at the site with 1.7 cm falling during 2-3 June. For 6 June 1998, the model overestimated moisture volume in the root zone (table 5.4) with the distribution being overestimated in the 30-60 cm depth, correctly estimated at 90 cm and underestimated at 120 cm (fig. 5.9). During 7-8 July 1998, 1.1 cm of precipitation was recorded at the site. For 10 July 1998, the model substantially overestimated moisture volume in the root zone (table 5.4, fig. 5.9). During 8-10 August 1998, 9.5 cm of precipitation was recorded at the field site. For 11 August 1998, the model overestimated total moisture volume (table 5.4), particularly in the lower depths of the root zone (fig. 5.9). During 7-8 October 1998, 5.6 cm of precipitation was recorded at the field site. For 9 October 1998, the model overestimated total moisture volume slightly (table 5.4). However, except at the 30-cm depth, simulated and measured moisture contents in the root zone were considerably different (fig. 5.9). On 1 April 1999, 1.1 cm of precipitation was recorded at the site. For 2 April 1999, the model overestimated both total moisture volume (table 5.4) and moisture distribution (fig. 5.9) in the root zone. It is clear from table 5.4 that the error in moisture volume simulation is not cumulative in nature.

Moisture redistribution profiles in the root zone were compared during 20 - 22 May 1998 to see how the model responded to precipitation events (fig. 5.10). The profile for 21 May was developed at 1100 hours while the profiles for 22 May were developed at 0800 hours (during precipitation) and 1100 hours (after precipitation).

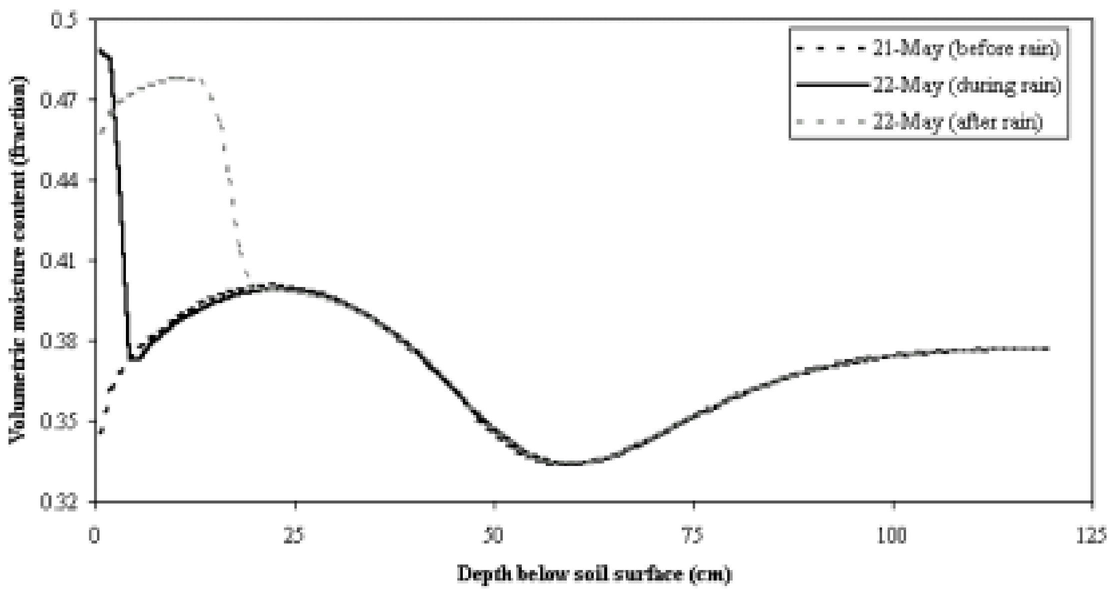

Figure 5.10. Moisture redistribution profiles before, during, and after precipitation during 21-22 May 1998

On 22 May, during 0800 through 1000 hours, 1.7 cm of precipitation was received resulting in an increase in moisture content close to soil surface compared to the previous day (fig. 5.10). Given the comparatively low antecedent moisture content near the soil surface, moisture movement was relatively rapid into the profile as indicated by the relatively high moisture content in the upper 20 cm of the root zone. Figure 5.10

indicated that the sub-model responded to evaporative and infiltration fluxes as expected.

Reasons for the inability of the sub-model to simulate moisture redistribution in the soil profile were examined in light of the sub-model's ability to respond to changing boundary conditions. Because of uncertainty of some parameter estimates, the selected parameters may not have represented conditions at the field site. The Ross soil used in this study exhibited inconsistent soil properties (table 5.1) with respect to the K-h-θ relationship. The K_S value of 1.0 cm/h selected for Ross soil (loam) by the RETC.FOR model (van Genuchten et al., 1991) was comparable to the measured value of 0.92 cm/h (table 3.3). Measured saturated θ (θ_s) value of 48.8% (tables 3.4, 5.1) seemed to be too high for a loam soil compared with published values (~43%) (van Genuchten et al., 1991). Based on the h(θ) relationship (table 3.4), the RETC.FOR model calculated the parameters required to develop the K-h-θ relationships (table 5.1). The value of the 'n' parameter determined to be 1.005 (table 5.1), representative of fine-textured soils (van Genuchten et al., 1991), may not have been representative of the loam soil used in this study. More importantly, use of one set of parameters (table 5.1) for estimating K(h) for the entire soil profile made the K(h) relationship not representative for the profile, thereby increasing errors. Use of an assumed θ value for the upper-most node in the soil profile as part of the initial condition likely affected the accuracy of simulation.

Large differences in estimated and simulated moisture volumes (table 5.4) (as well as the estimated and simulated moisture distributions, fig. 5.9) could have been affected by estimation of moisture contents using the neutron probe in the root zone. Compared to the gravimetric method, use of the neutron probe for moisture estimation increased uncertainty. Low r^2 at the 60- and 90-cm depths (table 3.2) and a smaller data set (versus the other depths) used for developing the neutron count versus θ relationship at the 120-cm depth (table 3.2) indicated that the regressions developed for those depths probably did not represent soil moisture conditions accurately. Use of Roanoke weather data for simulating ET for the early part of the simulation period could have also affected the ability of the model to simulate moisture movement in the soil profile.

3. Comparison of published and simulated crop ET

The moisture sub-model computed soil surface evaporation and crop transpiration values of 11.6 cm and 31.3 cm, respectively, with a total seasonal corn silage ET value of 42.9 cm or 0.34 cm/d. Simulated cumulative evaporation, transpiration, and ET with plant growth are shown in figure 5.11. The evaporation, transpiration, and ET trends are similar to reported trends (e.g., Rosenthal et al., 1977). As expected, with a sparse canopy cover, evaporation dominated ET; transpiration became increasingly larger as the canopy cover developed.

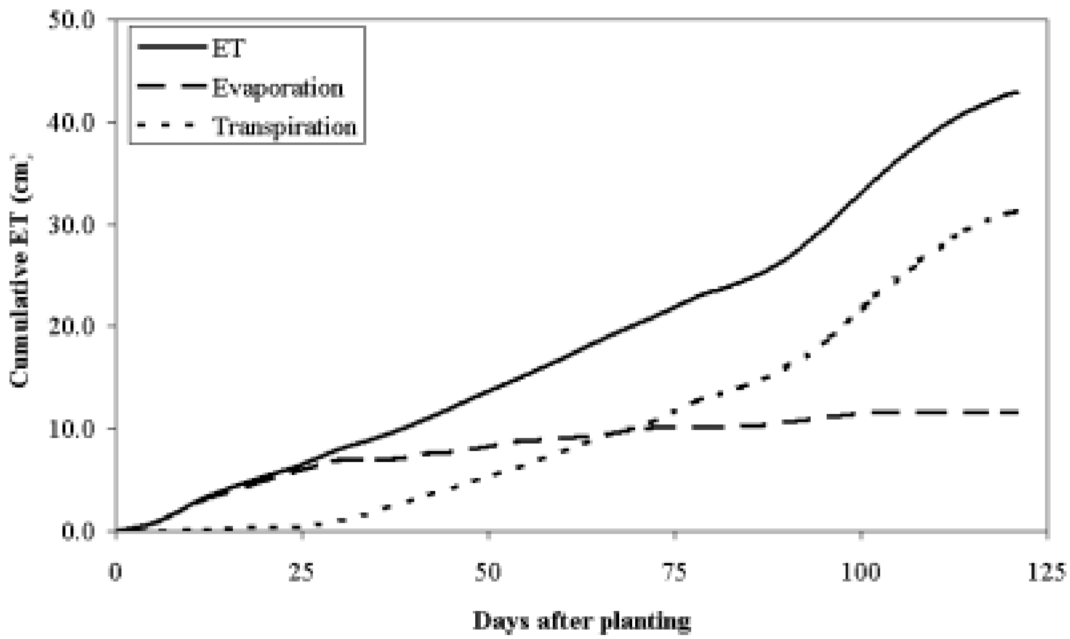

Figure 5.11. Simulated cumulative evaporation, transpiration, and evapotranspiration (ET) for corn silage grown in Blacksburg, Virginia during 1998

Doorenbos and Pruitt (1977) suggested a corn ET range of 50 to 80 cm for a wide range of environmental conditions. Using the Bowen ratio method in Colorado, Farahani and Bausch (1995) estimated that seasonal corn ET was 50.9 cm (0.41 cm/d) while Rosenthal et al. (1977) reported a value of 55.9 cm (0.39 cm/d) for Kansas. Both studies in Colorado and Kansas were performed under irrigated conditions. As expected, corn silage ET in this study was lower than published ET values for irrigated corn, not only because it was grown under rainfed conditions but also because there was a precipitation deficit of 11.5 cm (compared to normal rainfall) during the season (fig. 4.2 and fig. A(a), Appendix A).

Applying the Penman-Monteith method directly to corn (without using K_c), Farahani and Bausch (1995) estimated daily corn ET value of 0.31 cm/d. Hence, it seemed likely that the Penman-Monteith method underpredicted corn ET, particularly under partial canopy conditions, as was reported by Farahani and Bausch (1995). Further, application of K_c developed in California (Allen et al., 1990) to Virginian conditions likely affected the estimation of corn silage ET. No K_c values could be obtained for Virginia or the neighboring states.

5. Moisture sub-model calibration

At least part of the differences in estimated and simulated moisture volumes was likely due to uncertainties in model parameter selection. A representative saturated hydraulic conductivity (K_S) is difficult to estimate for a field site since K_S varies widely both laterally as well as vertically. The model was run using mean measured value of 0.92 cm/h (table 3.3) as well as the lowest K_S value (0.57 cm/h) measured in the laboratory for Ross soil. The moisture volumes for all three values of K_S on five dates during June 1998 and April 1999 are compared in table 5.5.

Except for 9 October 1998, with reductions in K_S, errors in volume estimation decreased (table 5.5). Reduction in K_S results in reduction in the amount of precipitation that infiltrates; hence when the model overestimated moisture contents in the root zone, use of a smaller K_S reduced error (table 5.5). Compared to 0.97 and 1.00 cm/h, a K_S value of 0.57 cm/h resulted in the smallest error (between simulated and estimated moisture volumes) over the entire simulation period as well as on five of six dates (table 5.5). Hence, based on the calibration of the moisture submodel, among the K_S values that were considered, K_S of 0.57 cm/h gave the least error in simulating the total moisture volume in the root zone. Moisture profiles obtained using the three K_S values on 9 October 1998 (least error) and 2 April 1999 (greatest error) are compared in figures 5.12 and 5.13, respectively.

Table 5.5. Comparison of estimated and simulated moisture volumes in the root zone on 6 June 1998 for three K_S values

Date	Estim.* (cm)	K_S (cm/h) 1.00 Sim.† (cm)	1.00 Error (%)‡	0.92 Sim. (cm)	0.92 Error (%)	0.57 Sim. (cm)	0.57 Error (%)
6 June 1998	41.6	47.2	13.4	46.8	12.4	46.2	11.1
10 July 1998	36.0	45.6	26.9	43.2	20.0	42.6	18.3
11 August 1998	36.1	42.9	18.9	41.9	16.3	40.0	10.9
9 October 1998	34.6	35.2	1.7	34.6	0.0	29.8	-13.8
2 April 1999	44.9	53.0	18.0	53.1	50.8	33.2	-5.7

* Estimated with measured neutron counts

† Simulated

‡ (Simulated-estimated)×100/estimated; positive values indicate overestimation

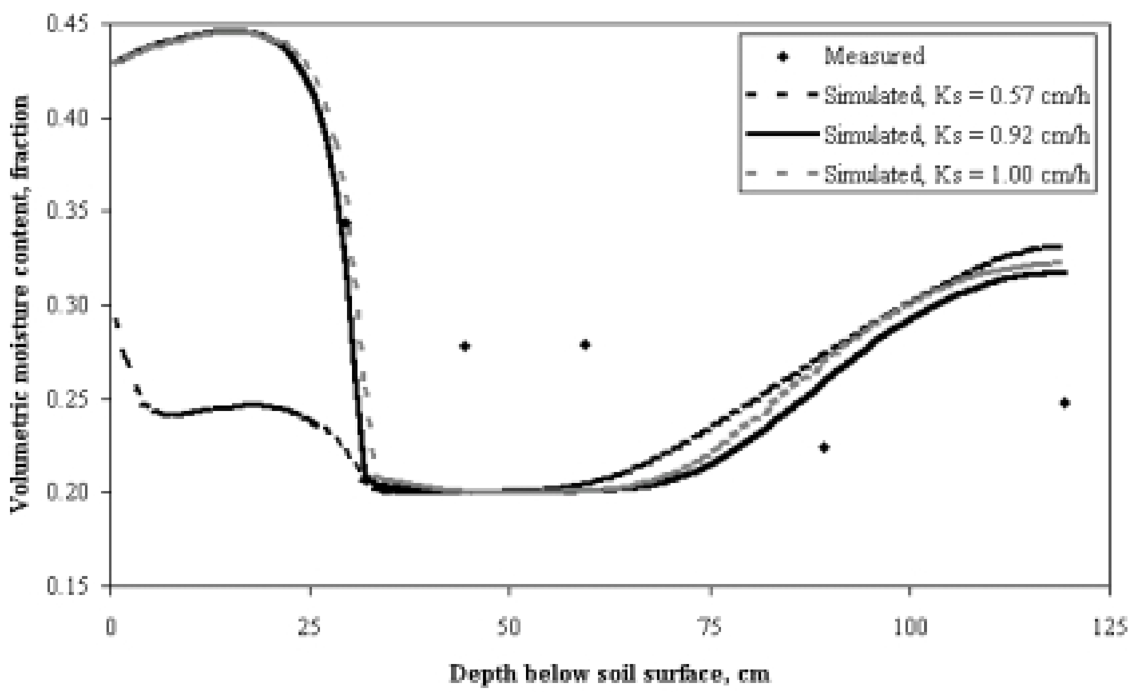

Figure 5.12. Comparison of moisture redistribution profiles for three values of saturated hydraulic conductivity (K_S) on 9 October 1998

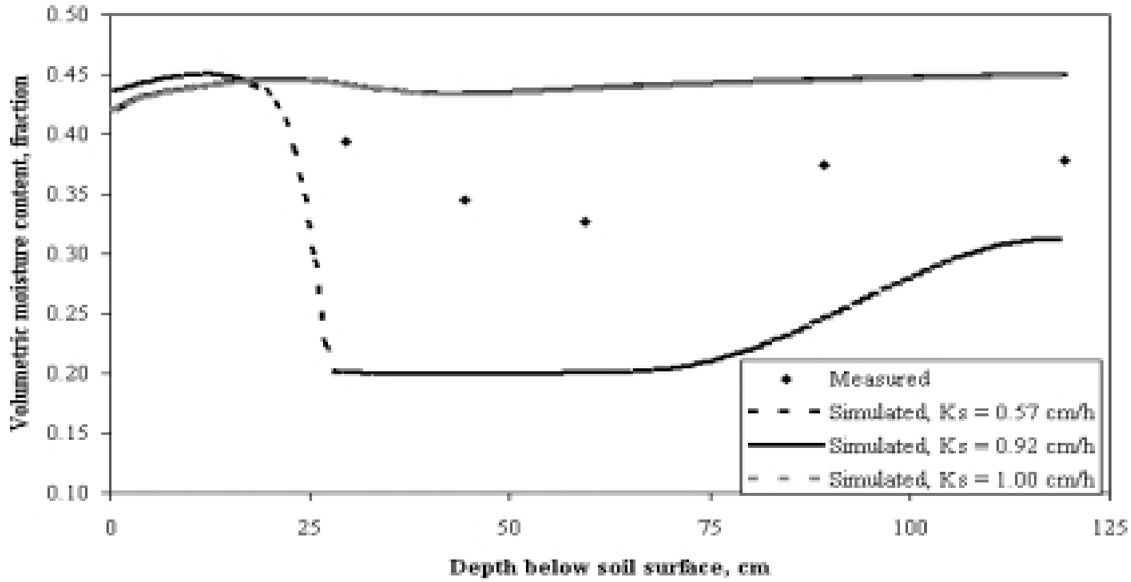

Figure 5.13. Comparison of moisture redistribution profiles for three values of saturated hydraulic conductivity (K_S) on 2 April 1999. Volumetric content values for K_s values of 0.92 and 1.00 cm/h were nearly identical.

For 9 October 1998, moisture profiles obtained with K_S values of 1.00 and 0.92 cm/h underestimated moisture contents at 45-60 cm depths, overestimated moisture contents at 90-120 cm depths, and correctly estimated the moisture content at the 30-cm depth. On 9 October 1998, the moisture profile with K_S of 0.57 cm/h underestimated moisture contents in the 30-60 cm depths while overestimating moisture contents in the 90-120 cm depths. Hence, compared to K_S value of 0.57 cm/h, use of K_S values of 1.00 and 0.92 cm/h resulted in reduced or no error in simulating the total moisture volume in the root zone; however, none of the three K_S values accurately simulated moisture contents in the profile.

For 2 April 1999, using K_S values of 1.00 and 0.92 cm/h, the model overestimated moisture contents throughout the root zone (fig. 5.13); with a K_S value of 0.57 cm/h, the model underestimated moisture contents throughout the root zone. Accounting for differences in K_S values within the entire root zone could improve the ability of the sub-model to simulate moisture redistribution in the soil profile.

5.2.3. Nitrogen Sub-model Performance

As with the moisture sub-model, the mass conservative property of the N sub-model was evaluated for two durations, 5 May - 9 October 1998 and 5 May 1998 - 2 April 1999 for the pellet and granule treatments. Simulated and measured inorganic-N concentration distributions and amounts in the root zone were also compared for the full simulation period for both treatments. Simulated and estimated applied residual inorganic-N amounts and corn N removals were also compared at the end of the simulation period for both treatments. Finally, sub-model calibration results are presented.

1. Mass conservative property of the nitrogen sub-model

The N sub-model was evaluated to determine if the convective-dispersive equation (CDE) retained its mass conservative property after finite differencing using the following index (η_{nit}):

$$\eta_{nit} = \frac{(N_{fin} - N_{in})}{(N_{fert} - N_{crop} - N_{leach})} \qquad [5\text{-}74]$$

where N_{fin} and N_{in} are final (simulated) and initial applied inorganic-N contents in the soil profile (kg/ha), respectively, N_{fert} is urea-N applied (kg/ha), N_{crop} is simulated amount of applied-N removed by the crop (kg/ha), and N_{leach} is simulated NO_3^--N leaching loss (kg/ha) from the applied-N. When η_{nit} is equal to one, the N sub-model fully satisfies the mass conservative property; a value greater than one is indicative of overestimation. Simulated N mass balance components are presented in table 5.6.

In both pellets and granules, for the first period, the N sub-model overestimated N in the profile by 2% (or applied-N removed by the crop since there was no simulated NO_3^--N leaching loss), while there was no mass balance error for the second duration. Higher mass balance error during the shorter duration (5 May - 9 October 1998) was likely due to N application as well as periods of dry and moist weather. Precipitation on dry soils probably resulted in simulated sharp wetting fronts resulting in sharp N (urea, NH_4^+, or NO_3^-) fronts causing greater mass balance error during the first period. During the second period, due to greater dispersion of N throughout the soil profile, simulated N fronts were likely less steep than during the first period resulting in lower numerical oscillations. The zero mass balance error observed at the end of the second simulation period was likely due to the compensatory nature of model error during the period of 10 October 1998 to 2 April 1999.

Table 5.6. Simulated nitrogen mass balance components for the first (5 May - 9 October 1998) and second (5 May 1998 - 2 April 1999) durations of simulation in the root zone (120 cm)

Mass balance components (kg/ha)	First duration		Second duration	
	Pellet	Granule	Pellet	Granule
Final applied-N, N_{fin}	103.9	103.9	102.0	102.0
Initial applied-N, N_{in}	0.0	0.0	0.0	0.0
N applied to crop, N_{fert}	184.0	184.0	184.0	184.0
Applied-N removed by crop, N_{crop}	81.7	81.7	81.7	81.7
Applied-NO_3^--N leaching loss, N_{leach}	0.0	0.0	0.0	0.0
Mass balance error, η_{nit}*	1.02	1.02	1.00	1.00

* Positive value indicates overestimation

Mass balance components for both pellets and granules were equal for both simulation durations (table 5.6) as expected since the only difference in pellets versus granules involved the value of the urea particle dissolution rate parameter (Eq. [5-48]). Since the impact of the urea particle dissolution rate parameter was expected to impact urea-N recovery in the short term, simulated percentages of urea-N and NH_4^+-N were compared between pellets and granules 3 d after N application (fig. 5.14).

As expected, due to the longer dissolution time of pellets, simulated urea-N percentage was slightly higher and NH_4^+-N percentage was slightly lower compared to granules. However, in the laboratory, 7 d after start of simulation (table 4.14), the pellet treatment retained 3.2% more urea-N than granules. Hence, it was likely that urea hydrolysis-related parameters such as the Michaelis-Menten maximum reaction velocity of urea hydrolysis, V_{max} (Eq. [5-50]) selected for the model was too high for the laboratory condition. The sub-model simulated no NO_3^--N percentage in either urea form, which was consistent with the results of the nitrification study in which very little NO_3^--N was recovered (in either urea form) 7 d after urea application (table 4.15).

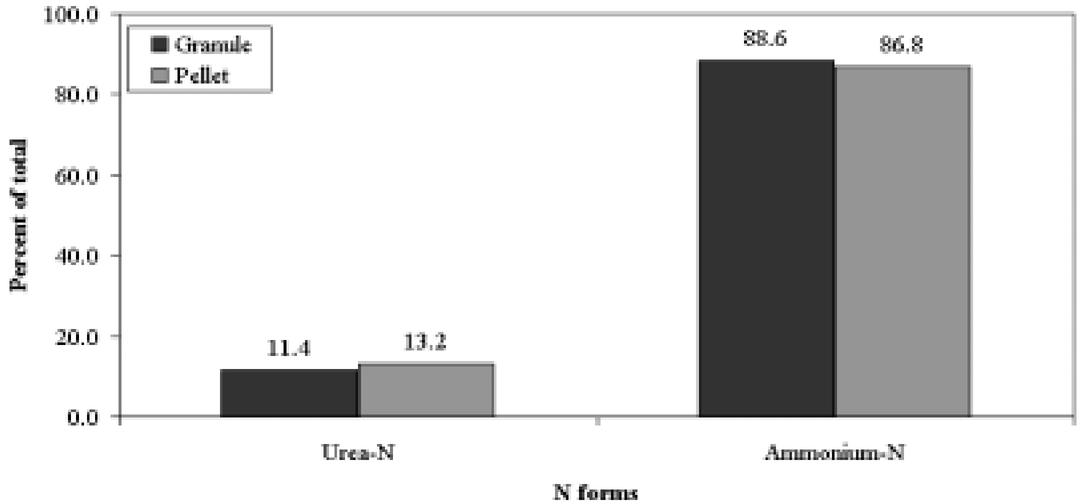

Figure 5.14. Comparison of simulated urea-N and NH_4^+-N recovery from the pellet and granule treatments three days after starter-N application

2. Comparison of measured and simulated applied residual inorganic-N results

Measured and simulated applied residual inorganic-N concentrations in different layers as well as the root zone were compared for both the pellet and granule treatments for the second duration to see if the sub-model simulated the physics of N transformation and transport in the field. Since inorganic-N amounts were measured only between rows on 9 October 1998 (Section 3.2.7), measured and simulated applied residual inorganic-N could not be compared along the y-axis for the first duration. Since inorganic-N amounts were measured at three points between crop rows for the second duration, measured and simulated inorganic-N amounts were compared along the y-axis.

Measured and simulated applied residual inorganic-N amounts in different layers and at different points in the soil profile are compared in figure 5.15. The simulated applied residual inorganic-N amounts in different layers were identical for pellets and granules.

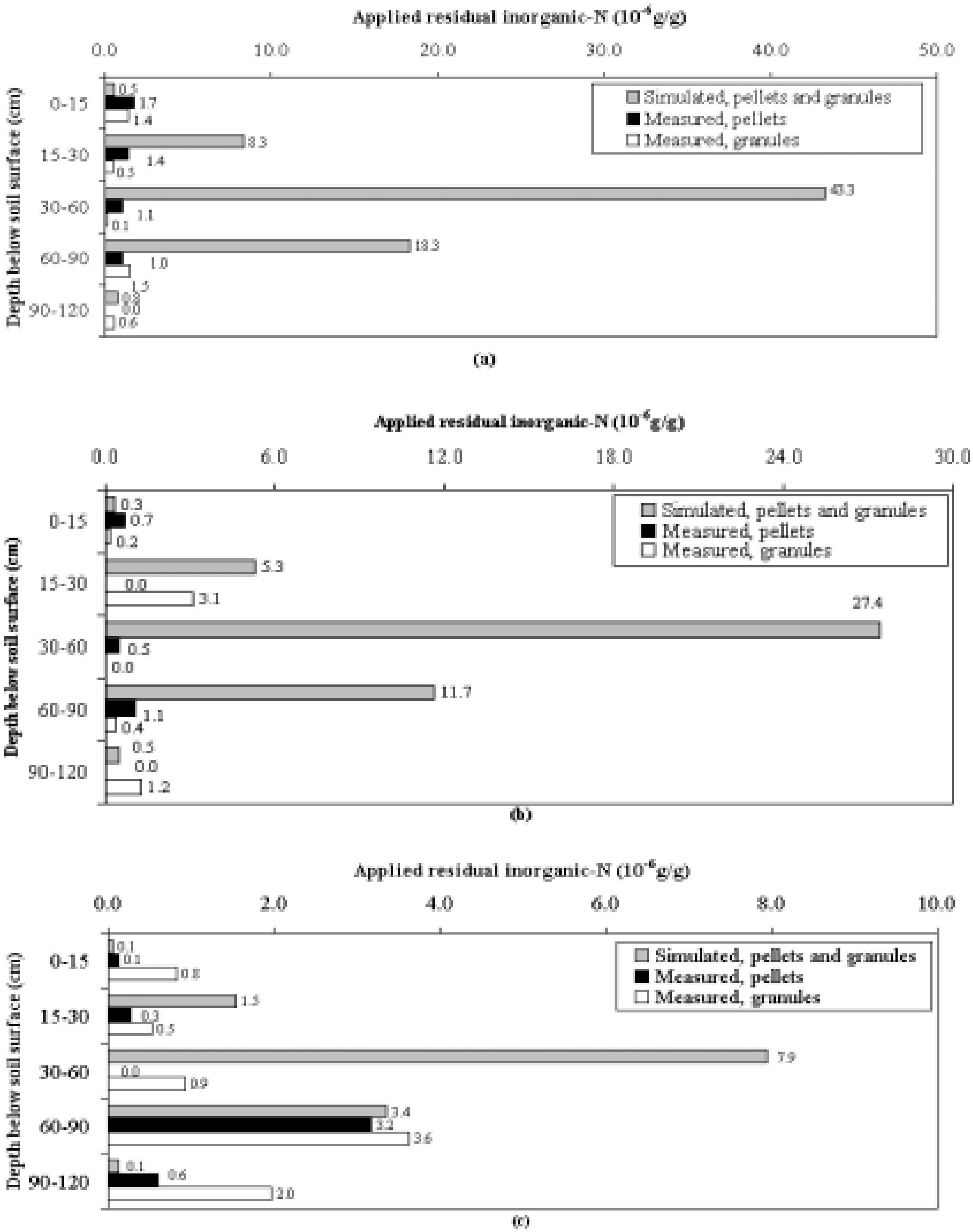

Figure 5.15. Comparison of simulated and measured applied residual inorganic-N on the (a) sidedress-N band (SS1), (b) 8.75 cm from the band (SS2), and (c) midway between the crop rows (SS3, 17.5 cm from the band) in the root zone on 2 April 1999. Scale of the x-axis on all three figures are different. Simulated applied residual inorganic-N amounts in the pellet and granule treatments were identical.

As expected, simulated inorganic-N concentrations directly below the band (fig. 5.15(a)) were higher than 8.75 cm (fig. 5.15(b)) and 17.5 cm (fig. 5.15(c)) away from the band. The model greatly overestimated inorganic-N concentrations in the upper half of the root zone at all three sampled locations (fig. 5.15 (a, b, c)).

Comparison of simulated and estimated total applied residual inorganic-N amounts recovered in the root zone from pellets and granules at the end of the simulation period as well as simulated and measured crop N removal are compared in table 5.7. Total inorganic-N in the fertilizer treatment was estimated by taking the average of inorganic-N amounts obtained by sampling at the SS1, SS2, and SS3 locations (table 4.9). Applied residual inorganic-N in the fertilizer treatment was obtained by subtracting the total inorganic-N in the control treatment from the total inorganic-N in the fertilizer treatment. Applied N amount removed by the N-fertilized crop was obtained by subtracting the N amount removed by the control treatment from the total N amount removed by the fertilized crop (fig. 4.9).

Table 5.7. Comparison of simulated and estimated applied inorganic-N amounts and crop N removal in the pellet and granule treatments for the second period (5 May 1998 - 2 April 1999) in the root zone

N mass balance components	Total applied-N (kg-N/ha)	
	Pellet	Granule
Simulated N_{fin}	102.0	102.0
Estimated N_{fin}	9.3	15.5
Error (%)*	996.8	558.1
Simulated N_{crop}	81.7	81.7
Estimated N_{crop}	105.4	76.1
Error (%)	-22.5	7.4

* (Simulated-measured)×100/measured; positive values indicate overestimation

The N sub-model greatly overestimated the final amount of applied-N remaining in the root zone at the end of the simulation period for both pellets (996.8%) and granules

(558.1%) (table 5.7). However, it may be noted that the procedure used to estimate the amount of applied-N remaining in the soil probably resulted in gross underestimation. Of the 184 kg-N/ha of fertilizer N, it was estimated that the crop removed 105.4 and 76.1 kg-N/ha from pellet and granule treatments, respectively. In the absence of substantial N losses, as discussed in Chapter 4, substantially more applied-N should have been recovered than the estimated amounts of 9.3 and 15.5 kg-N/ha from pellets and granules, respectively. While the model underestimated (22.5%) the amount of applied-N removed by the crop from the pellet treatment, the model slightly overestimated (7.4%) applied-N removed by the crop from granules (table 5.7).

Distribution of inorganic-N concentrations in the root zone from the pellet application were compared on 7 June 1999 (20 d after starter-N application), 19 July 1999 (20 d after sidedress-N application), and 2 April 1999 (end of simulation) to trace the fate of applied-N over time (fig. 5.16). Applied residual inorganic-N distribution in granules very closely resembled the distribution for pellets, and hence, is not presented.

Figure 5.16(a) shows applied inorganic-N distribution with 37 kg/ha. The solute front is concentrated close to the point of application because only 20 d had elapsed since the time of starter-N application. While all of the urea had been converted to NH_4^+, only a small fraction of the less-mobile NH_4^+ had converted to NO_3^- resulting in a compact solute plume. In figure 5.16(b), in addition to the solute plume created by the sidedress-N application (147 kg-N/ha) applied 20 d earlier, the smaller solute plume due to starter-N application 42 d earlier is clearly visible. As in figure 5.16(a), since NH_4^+ is the predominant N-form 20 d after sidedress-N application (fig. 5.16(b)), the solute plume is quite compact.

By comparison, the solute plume simulated on 2 April 1999 (fig. 5.16(c)) is more diffuse since more of the N is in the NO_3^- form compared with figures 5.16(a) and 5.16(b). Given the moisture deficit conditions during the fall-through-spring of 1998-1999, location of the plume some distance above the lower limit of the root zone was as expected. Figures 5.16(a) through 5.16(c) indicated that simulated applied-N redistribution within the root zone occurred as expected in reactive solutes, with higher N concentrations beneath the point of application accompanied by transverse and longitudinal dispersions.

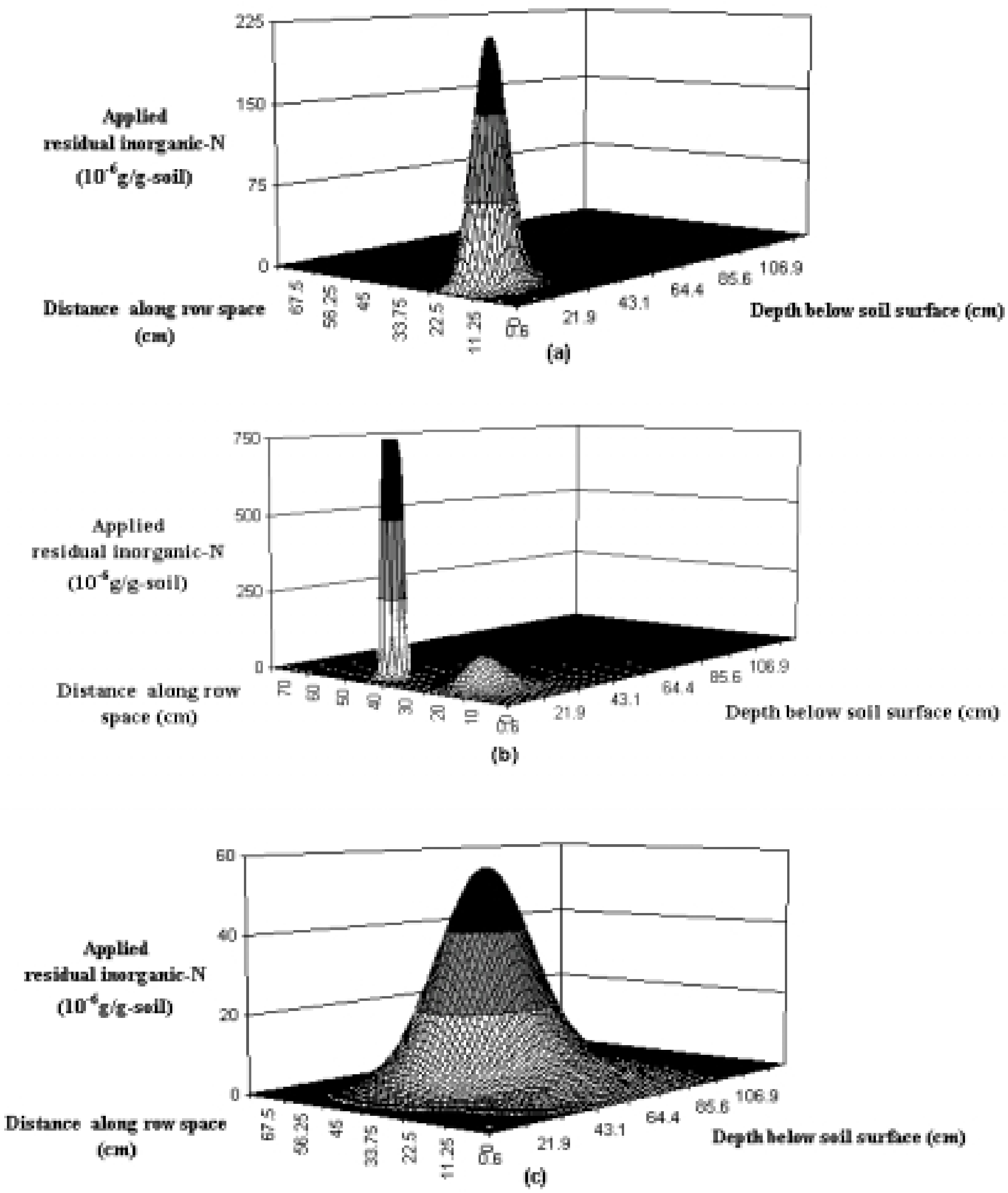

Figure 5.16. **Simulated distribution of applied residual inorganic-N in the modeling domain in pellets (a) 20 days after starter-N (37 kg/ha) application (Julian day 158), (b) 20 days after sidedress-N (147 kg/ha) application (Julian day 200), and (c) at the end of the study (Julian day 457). The starter-N and sidedress-N applications were made 20 and 45 cm, respectively from zero. Scale of the y-axis on all three figures are different. The y-axis in (b) is truncated to show the residual starter-N effect; highest N concentration due to sidedress-N application was greater than 4500 μg-N/g.**

Even though the N sub-model simulated the distribution of applied-N as expected (fig. 5.16), it greatly overestimated applied residual inorganic-N in the root zone (fig. 5.15). It was likely that one or more of the following factors affected the comparison of simulated and estimated results.

Due to uncertainty in parameter estimation, some parameters may not have represented field conditions. For example, the simulation results indicated that nearly 86% of the applied residual inorganic-N remained in the NH_4^+ form more than nine months after application. The soil sampling results for April 1999 indicated that NO_3^--N constituted 40-60% of the total inorganic-N (data not presented), depending on the depth and location of sampling (i.e., SS1). In the incubation study, more than 50% of the urea-N from the granules had undergone nitrification in 35 days (fig. 4.15). Since NO_3^--N is more mobile than NH_4^+-N, higher simulated NH_4^+-N concentrations likely resulted in slower than expected movement of applied-N in the soil profile, as indicated by figure 5.15. Some model parameters that could have affected the nitrification rate were the distribution coefficient K_d, first- and zero-order rate constants, and soil pH.

Use of a 1-D moisture sub-model could have affected model results. In the early stages of root development in row crops like corn, and when moisture movement is mainly due to capillary tension, root suction could create a significant horizontal moisture gradient. Hence, apparent dispersion of the N forms in the transverse direction (y-axis) was likely affected by transverse dispersion (D_t) which was not considered in this study since transverse moisture flux was assumed to be zero (Eq. [5-38]). As a result, the model likely underestimated the spread of the N-forms along the y-axis.

Uncertainty associated with soil sampling and the method of N analysis normally affects the determination of residual applied-N amount. Uncertainty was further increased due to the use of the control treatment to determine background inorganic-N in the fertilizer treatment. Also, due to localized high N concentrations in subsurface-N banding, the field measurement likely underestimated residual applied-N despite the implementation of a more intensive sampling scheme in April 1999 (table 4.9).

3. Nitrogen sub-model calibration

The N sub-model performance was also affected by uncertainty in parameter estimation. Since the moisture sub-model provided inputs to the N sub-model, in addition to the N-related parameters, moisture-related parameters also affected the performance of the N sub-model. Nitrogen fate was simulated with a K_S value of 0.57 cm/h, and zero- ($_nk_0$) and first-order ($_nk_1$) rate constants of nitrification that were 40% higher than the baseline values of 347×10^{-6} mg-$NH_4^+ \cdot mL^{-1} \cdot h^{-1}$ and 0.01/h, respectively. The N sub-model results obtained with the baseline and modified parameters are compared in table 5.8. Results are presented for the granule treatment only since the simulations of N fate were nearly identical for pellets and granules at 325 days.

Table 5.8. Simulated versus estimated applied-N amounts and crop N removal using baseline and modified parameters for the second period (5 May 1998 - 2 April 1999) in the root zone

N mass balance components	Total applied-N (kg-N/ha) Parameters Baseline	Modified
Simulated N_{fin}	102.0	106.7
Estimated N_{fin}	15.5	15.5
Error (%)*	558.1	588.4
Simulated N_{crop}	81.7	78.3
Estimated N_{crop}	76.1	76.1
Error (%)	7.4	2.9

* (Simulated-measured)×100/measured; positive values indicate overestimation

When K_S was decreased and $_nk_0$ and $_nk_1$ were increased, while error in estimating the amount of N removed by the crop decreased, error in estimating the total N mass in the root zone increased (table 5.8) due to the reduced crop N removal. It had been expected that by increasing $_nk_0$ and $_nk_1$ by 40%, rate of conversion of NH_4^+-N to NO_3^--N would increase proportionately, resulting in substantially greater simulated NO_3^--N recovery (as percent of total applied-N). With the baseline and modified parameters, for the 325-day simulation period, simulated NO_3^--N amount constituted 14.3 and 15.5% of the total applied-N, respectively; hence, the slight increase in simulated NO_3^--N recovery was unexpected. However, since K_S was reduced from 1.00 to 0.57 cm/h, moisture movement in the profile was much slower (fig. 5.13). Consequently, despite higher nitrification rate constants, a smaller value of K_S caused the applied-N to remain confined to a smaller region in the root zone resulting in slower nitrification due to the inhibitory effects of high NH_4^+ concentration. Distribution of applied-N directly beneath the fertilizer band is compared for the baseline and modified parameters values in figure 5.17.

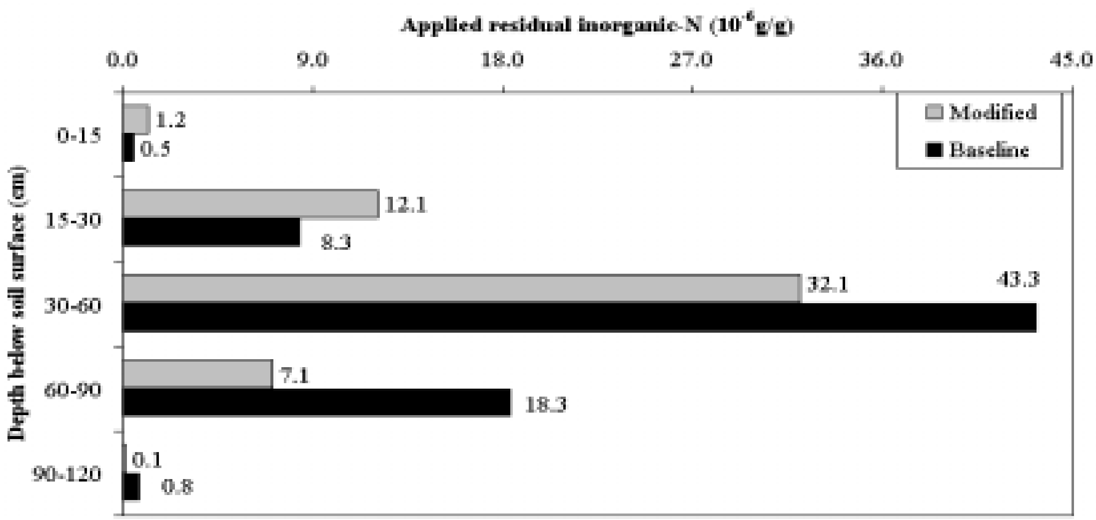

Figure 5.17. Comparison of simulated applied inorganic-N using baseline and modified parameters on the sidedress-N band (SS1) in the root zone on 2 April 1999

Despite higher nitrification rate constants which should have accelerated the downward movement of the plume, use of a K_S value of 0.57 cm/h as compared to a baseline value of 1.00 cm/h resulted in slower downward movement of the applied-N plume (fig. 5.17). Hence, this calibration exercise clearly indicated the importance of moisture-related parameters in simulating N distribution in the root zone.

5.3. Sensitivity Analysis

The concept of relative sensitivity (S_r), was used to evaluate the sensitivity of model output to selected parameters (James and Burges, 1982):

$$S_r = \frac{\left[\dfrac{O_{new} - O_{base}}{O_{base}}\right]}{\left[\dfrac{I_{new} - I_{base}}{I_{base}}\right]} \qquad [5\text{-}75]$$

where O_{new} and O_{base} are output values obtained for input parameter values I_{new} (new value) and I_{base} (baseline value), respectively. Model sensitivity to the parameters was evaluated according to the following criteria (Storm et al., 1988):

$S_r < \|0.01\|$	insensitive
$\|0.01\| \leq S_r < \|0.10\|$	slightly sensitive
$\|0.10\| \leq S_r < \|1.00\|$	moderately sensitive
$\|1.00\| \leq S_r < \|2.00\|$	sensitive
$S_r \geq \|2.00\|$	extremely sensitive

Four parameters that affected N transformation and movement were evaluated at two levels (±10%) using parameter values previously estimated to best represent the field conditions as the baseline. The simulation period considered represented the first simulation duration (3574 h) and covered the 1998 crop season.

The parameter K_D controls the amount of NH_4^+-N adsorbed to the soil versus the amount of NH_4^+-N in solution (Eq. [5-53]). Since only the dissolved NH_4^+-N undergoes nitrification, K_D impacts the ratio of NH_4^+-N/NO_3^--N. The zero-order rate constant for nitrification (Eq. [5-57]) controls the rate of NH_4^+-N to NO_3^--N transformation. Soil pH affects nitrification (Eq. [5-58]), and hence, the NH_4^+-N/NO_3^--N ratio. A higher value of longitudinal dispersivity, λ_l, allows for more rapid dispersion of solutes in the soil. In this study, since nitrification is inhibited at high NH_4^+-N concentration, more rapid dispersion of NH_4^+-N will result in more rapid nitrification. Since the ratio of NH_4^+-N/NO_3^--N affects the NO_3^--N availability for N-loss or crop removal, sensitivity of the selected parameters were also evaluated with respect to the amount of N removed by the crop in addition to the NH_4^+-N/ NO_3^--N ratio (table 5.9).

Table 5.9. Sensitivity of NH_4^+-N/NO_3^--N and N removed by crop to selected parameters

Parameter	Baseline value	Variation from baseline value (%)	NH_4^+-N/NO_3^--N			N removed by crop		
			Change in output (%)	S_r	Sensitivity	Change in output (%)	S_r	Sensitivity
Freundlich distribution coefficient, K_D	0.25 mL/g	+10.0	6.49	0.65	Moderate	-3.94	-0.39	Moderate
		-10.0	-3.24	0.32	Moderate	3.35	-0.34	Moderate
Zero-order rate constant for nitrification, $_nk_0$	347×10^{-6} $mg \cdot mL^{-1} \cdot h^{-1}$	+10.0	-5.08	-0.51	Moderate	-0.30	-0.03	Slight
		-10.0	5.87	-0.59	Moderate	-0.54	0.05	Slight
Soil pH	6.1 units	+10.0	-57.15	-5.72	Extreme	2.34	0.23	Moderate
		-10.0	29.10	-2.91	Extreme	-0.93	0.09	Slight
Longitudinal dispersivity, λ_l	1.0 cm	+10.0	-1.11	-0.11	Moderate	-0.47	-0.05	Slight
		-10.0	+1.31	-0.13	Moderate	-0.40	-0.04	Slight

The output NH_4^+-N/NO_3^--N was moderately sensitive to three of the selected parameters and extremely sensitive to the fourth, i.e., soil pH (table 5.9). The amount of N removed by the crop was moderately sensitive to K_D and slightly sensitive to the parameters, ${}_nk_0$ and λ_l (table 5.9). The amount of N removed by the crop was moderately or slightly sensitive to pH depending on whether the new parameter was increased or decreased as compared to the baseline parameter, respectively (table 5.9). Even though N removed by crop was slightly sensitive to ${}_nk_0$ and λ_l, the ratio of NH_4^+-N/NO_3^--N was at least moderately sensitive to all four parameters.

The parameter K_D could vary by more than one order of magnitude depending on soil CEC (Selim and Iskandar, 1981; Wagenet et al., 1977); however, K_D can be readily estimated. Depending on the composition of nitrifiers, ${}_nk_0$ could vary widely for soils (Schmidt and Belser, 1982), making it difficult to quantify nitrifiers. Hence, estimation of ${}_nk_0$ could involve considerable uncertainty. Even though soil pH is readily quantified, it may be important to account for soil pH variations at least in the plow layer, where most of the nitrification is likely to occur. Simulation of N fate could be improved if change in pH could be simultaneously simulated with urea hydrolysis and nitrification. While urea hydrolysis results in a localized increase in soil pH, nitrification has the opposite effect. Currently, the model accepts a single value of soil pH for the soil profile and does not simulate change in soil pH with N transformation reactions. The parameter λ_l is not readily estimated and reported values vary widely in range (Novotny and Olem, 1993; Brusseau, 1993). Simulation of N fate could be improved if all four parameters were measured or estimated for field conditions, especially since the parameters could have a multiplicative effect on N transformations.

5.4. Model Summary

A two-dimensional model was developed to simulate the fate of subsurface-banded urea. The model is comprised of a 1-D moisture sub-model and a 2-D N sub-model. The moisture sub-model uses the implicit finite difference form of the Richards' equation to simulate moisture redistribution in the root zone. The moisture sub-model uses the efficient though little-used Douglas-Jones predictor-corrector method to linearize the finite difference equations, rather than the more time-consuming iterative solution methods generally in use. The evapotranspiration component of the moisture sub-model combines the physically-based Penman-Monteith method with the empirically-tested 40-30-20-10 rule suggested by Danielson (1967). The evapotranspiration component of the moisture sub-model considers crop (canopy and root depth), soil moisture, and environmental conditions to calculate crop water use.

The N sub-model uses the 2-D convective-dispersive equation which is finite differenced using the alternating-direction-implicit (ADI) scheme. While solute movement in the transverse direction considers only molecular diffusion, movement along the vertical direction accounts for both molecular diffusion and longitudinal dispersion. The N sub-model simulates the fate of urea and its transformation products, NH_4^+ and NO_3^-; specific source and sink terms are applied as abstractions to each N-form. To better represent the physical process associated with high urea concentrations due to band applications of urea pellets or granules, particle size effects on urea dissolution and the inhibitory effects of high substrate concentrations on urea hydrolysis and nitrification are considered.

Nitrogen from subsurface-banded urea pellet will move in three directions. Hence, ideally, a three-dimensional model would be required to simulate the fate of N pellets. Use of urea particle dissolution rate as the sole parameter for distinguishing the fate of urea-N from pellets versus granules proved to be inadequate to model the fate of pellets in the 2-D model.

The model was evaluated using field data for the period of 5 May 1998 through 2 April 1999; while some model parameters were measured or estimated using field data, other parameters were selected from the literature. The model displayed good mass conservative properties for both moisture and N. The model simulated moisture and N fate under difficult conditions, i.e., precipitation into dry soils and sharp N fronts: hence, the model could be considered to be robust. Also, the model simulated moisture and N distribution profiles in the root zone as expected. Even though ET and crop N removal (for granules) estimations seemed reasonable, measured and simulated moisture and applied-N amounts as well as distributions within the root zone differed greatly. Even though the limited calibration did not improve model simulations, it underscored the importance of moisture-related parameters in simulating N fate.

Uncertainty involved in the estimation of model parameters probably accounted for part of the difference between measured and simulated values. Sensitivity analyses on four parameters indicated that the output NH_4^+-N/NO_3^--N was moderately sensitive to three and extremely sensitive to one parameter. Uncertainty involved in the estimation of these four parameters could have affected the nitrification rate substantially because of the possible multiplicative effect of these parameters on the nitrification rate. The calibration exercise demonstrated that moisture-related parameters could substantially impact the accuracy of N simulation. Uncertainty associated with both moisture and applied-N contents estimated in the field likely affected comparison between estimated and simulated values. It seemed likely that residual applied-N had been grossly underestimated.

The model requires validation using more reliable field data for both the moisture and N sub-models. For the model to be of use to planners and producers, the validated model would require incorporation into a management model.

6. SUMMARY AND CONCLUSIONS

This study evaluated the potential impacts of urea particle size on crop yield and nitrate-N (NO_3^-- N) leaching into groundwater using a field experiment, laboratory experiments, and mathematical modeling. While the field experiment was used to compare the agronomic and water quality impacts of urea pellets versus granules, the laboratory studies were used to understand the impact of urea particle size on N transformation and movement. A mathematical model was developed to simulate the transformation and fate of subsurface-banded N (urea pellets or granules). Results of the laboratory studies were used in model development and parameter estimation. The model was tested using the field data.

6.1. Summary

A two-year field study was conducted to evaluate agronomic and NO_3^--N leaching impacts of urea pellets versus urea granules in loam soil at Kentland Farm, Blacksburg, Virginia. Corn silage yield and corn N content obtained from urea pellets and granules applied at 184 kg-N/ha (sufficient) were compared. Nitrate-N leaching potential of the urea forms was evaluated at 184 kg-N/ha using soil inorganic-N (0-120 cm depth), NO_3^--N concentration in leachate (30- and 120-cm depths), and N removal by crop. Corn silage yield and corn N content obtained from pellets and granules were also compared at N application rates of 110 (deficient) and 258 (excess) kg-N/ha. A control treatment (no N) was included to evaluate the agronomic and NO_3^--N leaching impacts of background-N. All treatments were applied in triplicate.

The field experiment provided the following results.

1. In the second year of the study, corn silage yield with urea pellets was 15% higher than with urea granules at 184 kg-N/ha. No yield response was observed in the first year of the study. No urea form impact on corn silage yield was observed at other N application rates (110 and 258 kg-N/ha). Lack of yield response to urea form at 110 kg-N/ha indicated that possibly greater N losses from granules due to denitrification and NH_4^+-N fixation by clay minerals did not explain higher yield in pellets than

granules. Reduced NO_3^--N leaching was ruled out as a cause for greater yield from pellets than granules due to drier-than-normal crop season.

2. There was no corn N content response to urea form in any year.
3. In October 1997, with 39.8 cm of precipitation and irrigation over a 3.5-month period, pellets retained 9.0 and 10.3 kg/ha more inorganic-N than granules in the top 30- and 60-cm layers of the root zone, respectively.
4. Based on 27 sampling events at 120-cm depth (corn root zone depth), average NO_3^--N concentrations in the granule, pellet, and control treatments were 2.6, 2.2, and 1.6 mg/L, respectively. However, there was no significant difference in NO_3^--N leaching between pellets and granules at any sampling event. At a subsurface application rate of 184 kg-N/ha to corn silage in coarse-textured soil, NO_3^--N in leachate leaving the root zone did not pose a threat to drinking water.
5. Corn silage fertilized with urea pellets removed 19% more applied-N than the crop fertilized with urea granules in the second year. No N removal response was observed in the first year when corn silage followed soybean.

Laboratory studies were conducted to investigate urea particle size impact on dissolution rate, mechanism of movement of dissolved urea (center of mass study), mineralization (urea hydrolysis and nitrification), and NO_3^--N leaching. Treatments in the dissolution study included commercial urea granule (0.01-0.02 g), 0.5-g pellet, 1.0-g pellet, 1.5-g pellet, and 2.0-g pellet. The center of mass study considered granules and 1.5-g pellet. In the incubation study, 0.5- and 1.5-g pellets, granules, and control (no N) were considered. While the main comparison was between granule and 1.5-g pellet, the other pellets were included to obtain better information regarding the impact of urea particle size on dissolution and mineralization of urea. The leaching column study considered three treatments, 1.5-g pellets, granules, and control. All treatments were applied in triplicate.

The laboratory studies provided the following results.

1. Granules dissolved eight times faster than 1.5-g pellets.
2. Molecular diffusion was the predominant transport mechanism in both pellets and granules; however, convection was likely more important in pellets than granules.

3. Rates of urea hydrolysis and nitrification were higher in granules than in 1.5-g pellets.
4. Nitrate-N leaching between pellets and granules could not be compared in the leaching column study due to insufficient drainage resulting in excessive denitrification losses.

A two-dimensional model was developed to simulate the fate of subsurface-banded urea. The model is comprised of a 1-D moisture sub-model and a 2-D N sub-model. The moisture sub-model uses the implicit finite difference form of the Richards' equation to simulate moisture redistribution in the root zone, and simulates moisture redistribution, evapotranspiration, and percolation from the root zone. The N sub-model uses the 2-D convective-dispersive equation (CDE) which is finite differenced using the alternating-direction-implicit (ADI) scheme. The N sub-model simulates the fate of urea and its transformation products, NH_4^+ and NO_3^-, and source and sink terms such as urea dissolution and plant N removal. Particle size effects on urea dissolution and the inhibitory effects of high substrate concentrations on urea hydrolysis and nitrification are considered. Urea particle dissolution rate, the sole parameter used for distinguishing fate of urea-N from pellets versus granules was inadequate to account for difference in urea particle size.

The model was evaluated using field data for the period of 5 May 1998 through 2 April 1999. While some model parameters were measured or estimated using field data, other parameters were selected from the literature. The model displayed good mass conservative properties and robustness for both moisture and N; also, moisture and N distribution profiles in the root zone were simulated as expected. Even though ET and crop N removal (for granules) estimations seemed reasonable, measured and simulated moisture and applied-N amounts as well as distributions within the root zone differed greatly. The differences were probably due to the difficulty of selecting parameters that represent the physical situation adequately and errors in measurements of moisture and N amount in the root zone. Limited calibration did not improve model estimation. Sensitivity analyses on selected nitrification-related parameters indicated that the NH_4^+-N/NO_3^--N ratio was moderately to extremely sensitive to the parameters

6.2. Conclusions

The research described in this dissertation led to conclusions related to each of the three study objectives. The first objective was to evaluate agronomic and NO_3^--N leaching impacts of pellets versus granules on no-till corn silage. Conclusions related to this objective, for the conditions of this study, are the following:

1. Corn silage yield is improved by using urea pellets instead of urea granules.
2. Using urea pellets in place of urea granules reduces nitrate leaching in the soil profile, offering the potential of reducing nitrate leaching into groundwater.
3. Soil and leachate sampling schemes must be carefully designed to capture spatial and temporal variability when fertilizer sources are banded.

The second objective of this study was to quantify the rates of dissolution, diffusion, mineralization, and NO_3^--N movement from subsurface-applied urea pellets versus granules. The following conclusions were reached:

4. Urea particle dissolution decreases with increasing particle size.
5. Urea hydrolysis decreases with increasing particle size.
6. Nitrification rate decreases with increasing particle size.
7. Nitrification inhibition due to larger particle sizes is more important in reducing NO_3^--N availability for loss or increasing N removal by crop than urea dissolution or hydrolysis.

The third objective was to improve computer-based tools for better management of subsurface-applied urea-N. Development and testing of the 2-D N model led to the following conclusions:

8. The developed model, after validation, is appropriate for simulating N fate from subsurface-banded urea granules.
9. The developed model is not appropriate for simulating N fate from urea pellets because it does not account for three-dimensional N movement.
10. Incorporating the effects of urea hydrolysis and nitrification on soil pH will allow for more accurate simulation of nitrification, thereby, improving the model's ability to predict N fate.

The overall conclusion of the study is that use of urea pellets does increase crop yield and reduce nitrate leaching compared to granules for the crop, soil, and climatic conditions investigated in this study. The use of pellets for other crop, soil, and management conditions should be investigated.

7. RECOMMENDATIONS FOR FUTURE RESEARCH

Based on the results of this study, following are the recommendations for future research.

1. Both the agronomic and NO_3^--N leaching impacts of urea form need to be evaluated during the crop season under moist conditions. Also, longer-term studies would be useful in evaluating the agronomic and environmental impacts of urea form under changing soil-N conditions.
2. There is limited information on the impact of urea form on N-loss pathways such as NH_3 volatilization, NH_4^+-N fixation by clay minerals, denitrification, and immobilization. Such studies could lead to a better understanding of the economic and environmental impacts of urea pellets versus granules.
3. There is need to consider the prices of urea pellets and granules while considering the economics of using urea pellets versus urea granules.
4. Accounting of the applied-N fate as affected by urea form could be improved through use of labeled-N (^{15}N).
5. The potential for using phosphorus (P) pellets is recognized. Use of P pellets could result in higher localized dissolved inorganic-P concentrations leading to more efficient plant P uptake.
6. The need for developing a physically-based model to simulate solute dissolution as affected by solute particle size, soil moisture content, and soil properties is recognized. Such a model would be useful in simulating the fate of a wide variety of solutes that are applied as large particles in the soil.
7. The ability of the model developed in this study to simulate N transformations could be enhanced if pH were simulated. Such an approach could improve simulation of the nitrification process since nitrification is extremely sensitive to pH changes.
8. The need for validation of the model using multiple data sets is recognized.
9. A validated 2-D N model could enhance N management from subsurface-banded N if it were to be incorporated into a comprehensive management model.

REFERENCES

Adams, P.L., T.C. Daniel, D.R. Edwards, D.J. Nichols, D.H. Pote, and H.D. Scott. 1994. Poultry litter and manure contributions to nitrate leaching through the vadose zone. *Soil Science Society of America Journal* 58:1206-1211.

Allen, R.G. *REF-ET Reference Evapotranspiration Calculator Ver. 2.0*. Logan, Utah: Utah State Univ. Foundation.

Allen, R.G. et al. 1990. *Evapotranspiration and Irrigation Water Requirements*. ASCE Manuals and Reports on Engineering Practice No. 70, eds. M.E. Jensen, R.D. Burman, and R.G. Allen. New York: ASCE.

Anderson, J.D., Jr. 1995. *Computational Fluid Dynamics: the Basics with Applications*. New York: McGraw-Hill, Inc.

Angle, J.S, M.S. McIntosh, and R.L. Hill. 1991. Tension lysimeters for collecting soil percolate. In *Groundwater Residue Sampling Design,* eds. R.G. Nash and A.R. Leslie. Washington, D.C.: American Chemical Society.

Azevedo, A.S., R.S. Kanwar, P. Singh and, L.S. Pereira. 1996. Movement of NO_3-N and atrazine movement through soil columns as affected by lime application. *Transactions of the ASAE* 39(3):937-945.

Ballestero, T., B. Herzog, O.D. Evans, and G. Thompson. 1991. Monitoring and sampling the vadose zone. In *Practical Handbook of Ground-Water Monitoring*, ed. D.M. Nielsen, ch. 4, 97-141. Chelsea, Mich.: Lewis Publishers.

Bates, T.E. 1993. Soil handling and preparation. In *Soil Sampling and Methods of Analysis*, ed. M.R. Carter, ch. 3, 19-24. Boca Raton, Fla.: Lewis Publishers.

Blake, G.R. and K.H. Hartge. 1986a. Bulk density. In *Methods of Soil Analysis, Part 1, Physical and Mineralogical Methods* - Agronomy Monograph no. 9 (II ed.): 363-376, ed. A. Klute. Madison, WI: ASA - SSSA.

Blake, G.R. and K.H. Hartge. 1986b. Particle density. In *Methods of Soil Analysis, Part 1, Physical and Mineralogical Methods* - Agronomy Monograph no. 9 (II ed.): 377-382, ed. A. Klute. Madison, WI: ASA - SSSA.

Bohn, H.L., B.L. McNeal, and G.A. O'Connor. *Soil Chemistry, (II ed.).* New York: John Wiley & Sons.

Boswell, F.C., J.J. Meisinger, and N.L. Case. 1985. Production, marketing, and use of nitrogen fertilizers. In *Fertilizer Technology and Use (III ed.)* ed. O.P. Engelstadt, ch. 7, 229-292. Madison, Wis.: SSSA.

Bremner, J.M. 1982. Nitrogen-urea. In *Methods of Soil Analysis, Part 2, Chemical and Microbiological Properties (II ed.).* Agronomy 9:699-710, ed. A.L. Page. Madison, WI: ASA – SSSA.

Bremner, J.M. and C.S. Mulvaney. 1982. Nitrogen-total. In *Methods of Soil Analysis, Part 2, Chemical and Microbiological Properties (II ed.)*. Agronomy 9:595-624, ed. A.L. Page. Madison, WI: ASA – SSSA.

Bremner, J.M. and C.S. Mulvaney. 1978. Urease activity in soils. In *Soil Enzymes*, ed. R.G. Burns. London: Academic Press. 149-196 p.

Breve, M.A., R.W. Skaggs, J.E. Parsons, and J.W. Gilliam. 1997. DRAINMOD-N, a nitrogen model for artificially drained soils. *Transactions of the ASAE* 40(4):1067-1075.

Brusseau, M.L. 1993. In influence of solute size, pore water velocity, and intraparticle porosity on solute dispersion and transport in soil. *Water Resources Research* 29(4):1071-1080.

Campbell, G.S. 1974. A simple method for determining unsaturated conductivity from moisture retention data. *Soil Science* 117(6):311-314.

Carlo Erba Istruments. 1988. *Nitrogen Analyzer 1500 Instruction Manual.*

Carnahan, B., H.A. Luther, and J.O. Wilkes. 1969. *Applied Numerical Methods*. New York: John Wiley & Sons.

Celia, M.A., E.T. Bouloutas, and R.L. Zarba. 1990. A general mass-conservative numerical solution for the unsaturated flow equation. *Water Resources Research* 26(7):1483-1496.

Chao, G.T. 1967. *Urea, its Properties and Manufacture*. West Covina, Calif: Chao's Institute.

Chapman, H.D. 1965. Cation exchange capacity. In *Methods of Soil Analysis* Agronomy 9:981-901, ed. C.A. Black. Madison, WI: ASA.

Chen, R.L., D.R. Keeney, and J.G. Konrad. 1972. Nitrification in sediments of selected Wisconsin lakes. *Journal of Environmental Quality* 1(2):151-154.

Cuenca, R.H. 1989. *Irrigation System Design: An Engineering Approach.* Englewood Cliffs, N.J.: Prentice Hall.

Daniel, W.W. 1990. *Applied Nonparametric Statistics (II ed.)*. Boston: PWS-Kent.

Danielson, R.E. 1967. Root systems in relation to irrigation. In *Irrigation of Agricultural Lands,* Agronomy No. 11: 390-424, eds. R.M. Hagan, H.R. Haise, and T.W. Edminster. Madison, Wisc.: ASA.

de Jong, R. 1993. Unsaturated hydraulic conductivity: estimation from desorption curves. In *Soil Sampling and Methods of Analysis* ed. M.R. Carter, ch. 58. 625-631 p.

Department of Health and Safety. 1991. *Radiation Safety Handbook*. Virginia Tech Administrative Display System. Doc. No. PDS 06. Blacksburg, Va.: VPI & SU.

Donohue, S.J. and S.E. Heckendorn. 1994. *Laboratory Procedures: Virginia Tech Soil Testing and Plant Analysis Laboratory*, Pub 452-881. Blacksburg, Va.: VPI & SU.

Doorenbos, J. and W.O. Pruitt. 1977. Guidelines for predicting crop water requirements. *FAO Irrigation and Drainage Paper No. 24*, 2nd edition. Rome: FAO.

Douglas, J., Jr. and B.F. Jones, Jr. 1963. On predictor-corrector methods for nonlinear parabolic differential equations. *Journal of the Society of Industrial and Applied Mathematics* 11(1):195-204.

Durner, W. 1992. Predicting the unsaturated hydraulic conductivity using multi-porosity water retention curves. In *Proceedings of the International Workshop on Indirect Methods for Estimating the Hydraulic Properties of Unsaturated Soils, Riverside, CA, October 11-13, 1989*, eds. M.Th. van Genuchten, F.J. Leij, and L.J. Lund. Riverside, CA: U.S. Salinity Laboratory and Univ. of California. 185-202 p.

Ess, D.E. 1994. Cover crop residue effect on machine-induced soil compaction. Ph.D. diss., Agricultural Engineering Dept., VPI & SU, Blacksburg.

Farahani, H.J. and W.C. Bausch. 1995. Performance of evapotranspiration models for maize - bare soil to closed canopy. *Transactions of the ASAE* 38(4):1049-1059.

Food and Agriculture Organization (FAO). 1997. *Fertilizer Yearbook 1996 (vol. 46)*. Rome, Italy: FAO of the United Nations.

Gilliam, J.W., T.J. Logan, and F.E. Broadbent. 1985. Fertilizer use in relation to the environment. In *Fertilizer Use and Technology (III ed.),* ed. O.P. Engelstadt, ch. 16, 561-588. Madison, Wis.: SSSA.

Golden Software. 1995. *SURFER for Windows, Ver. 6 User's Guide*. Golden, Colo.: Golden Software, Inc.

Goodrich, R.D. and J.C. Meiske. 1985. Corn and sorghum silages. In *Forages The Science of Grassland Agriculture (IV ed.)*, eds. M.E. Heath, R.F. Barnes, and D. S. Metcalfe, ch. 56, 527-536. Ames, IA: Iowa State University.

Grismer, M.E., K.M. Bali, and F.E. Robinson. 1995. Field-scale neutron probe calibration and variance analysis for clay soil. *Journal of Irrigation and Drainage Engineering* 121(5):354-362.

Hansen, S., Jensen, H.E., Nielsen, N.E., Svendsen, H., 1990. *DAISY - a Soil Plant Atmosphere System Model*. NPO Research from the National Agency of Environmental Protection No. A 10. 272 pp.

Harre, E.A. and W.C. White. 1985. Fertilizer market profile. In *Fertilizer Use and Technology (III ed.),* ed. O.P. Engelstadt, ch. 1, 1-24. Madison, Wis.: SSSA.

Harris, W.G., S.S. Iyenger, L.W. Zelazny, J.C. Parker, D.A. Lietzke, and W.J. Edmonds. 1980. Mineralogy of a chronosequence formed in New River alluvium. *Soil Science Society of America Journal* 44:862-868.

Haverkamp, R., M. Vauclin, J. Touma, P.J. Wierenga, and G. Vachaud. 1977. *Soil Science Society of America Journal* 41:285-294.

Hillel, D. 1971. *Soil and Water: Physical Principles and Processes*. New York: Academic Press.

Hinkelmann, K. and O. Kempthorne. 1994. *Design and Analysis of Experiments (Vol. 1): Introduction to Experimental Design*. New York: John Wiley & Sons.

Hubbard, R.K., R.A. Leonard, and A.W. Johnson. 1991. Nitrate transport on a sandy coastal plain soil underlain by plinthite. *Transactions of the ASAE* 34(3):802-808.

James, D.L and S.J. Burges. 1982. Selection, calibration, and testing of hydrologic models. In *Hydrologic Modeling of Small Watersheds*, ed. C.T. Haan, ch. 11, 437-472. St. Joseph, Mich.: ASAE.

Jensen, J.R. and M.M. Rahman. 1987. A semi-empirical model for calculating evaporation and transpiration from wetland rice. *Agriculture and Forest Meteorology* 41:289-306.

Jones, R.D. and A.P. Schwab. 1993. Nitrate leaching and nitrite occurrence in fine-textured soil. *Soil Science* 155(4):272-282.

Kaluarachchi, J.J. and J.C. Parker. 1988. Finite element model for nitrogen species transformation and transport in the unsaturated zone. *Journal of Hydrology* 103:249-274.

Kanwar, R.S., J.L. Baker, and J.M. Laflen. 1985. Nitrate movement though the soil profile in relation to tillage system and fertilizer application method. *Transactions of the ASAE* 28(6):1802-1807.

Klute, A. 1986. Water retention: laboratory methods. In *Methods of Soil Analysis, Part 1, Physical and Mineralogical Methods* - Agronomy Monograph no. 9 (II ed.): 635-662, ed. A. Klute. Madison, WI: ASA - SSSA.

Klute, A. and C. Dirksen. 1986. Hydraulic conductivity and diffusivity: laboratory methods. In *Methods of Soil Analysis, Part 1, Physical and Mineralogical Methods (II ed.).* Agronomy 9:687-703, ed. A. Klute. Madison, WI: ASA - SSSA.

Knisel, W.G. (ed.). 1980. *CREAMS: a Field Scale Model for Chemicals, Runoff, and Erosion from Agricultural Management Systems*. Conservation Management Report No. 26. Washington, D.C.: USDA, Science and Education Administration.

Kumar, V. and R.J. Wagenet. Urease activity and kinetics of transformations in soils. *Soil Science* 137(4):263-269.

Li, Y. and M. Ghodrati. 1994. Preferential transport of nitrate through soil columns containing root channels. *Soil Science Society of America Journal* 58:653-659.

Luis, S.J. and D. McLaughlin. 1992. A stochastic approach to model validation. *Advances in Water Resources* 15(1):15-32.

Malhi, S.S. and M. Nyborg. 1979. Rate of hydrolysis of urea as influenced by thiourea and pellet size. *Plant and Soil* 51:177-186.

Marshall, T.J., J.W. Holmes, and C.W. Rose. 1996. *Soil Physics (III ed.).* Cambridge: Cambridge University Press.

McLaren, A.D. 1976. Rate constants for nitrification and denitrification in soils. *Radiation and Environmental Biophysics* 13:43-48.

McLean, E.O. 1982. Soil pH and lime requirement. In *Methods of Soil Analysis, Part 2, Chemical and Microbiological Properties (II ed.).* Agronomy 9:199-223, ed. A.L. Page. Madison, WI: ASA – SSSA.

Menelik, G., R.B. Reneau, Jr., D.C. Martens, T.W. Simpson, and G.W. Hawkins. 1990. *Effects of Tillage and Nitrogen Fertilization on Nitrogen Losses from Soils used for Corn Production.* Virginia Water Resources Center (Bull. 167). Blacksburg, Va.: VPI & SU.

Molz, F.J. and I. Remson. 1970. Extraction term models of soil moisture use by transpiring plants. *Water Resources Research* 6(5):1346-1356.

Mostaghimi, S., T.M. Younos, and U.S. Tim. 1991. The impact of fertilizer application techniques on nitrogen yield from two tillage systems. *Agriculture, Ecosystems and Environment* 36(1991):13-22.

Mualem, Y. 1976. A new model for predicting the hydraulic conductivity of unsaturated porous media. *Water Resources Research* 12(3):513-522.

National Atmospheric Deposition Program (NRSP-3)/National Trends Network. 1998. NADP/NTN Coordination Office, Illinois State Water Survey, 2204 Griffith Drive, Champaign, IL 61820. (URL: http://nadp.nrel.colostate.edu/NADP)

NWS-NOAA (National Weather Service – National Oceanic and Atmospheric Administration). 1997 –1998. Automated Flood Warning System (AFWS). National Weather Service – NWSFO Louisville, 6201 Theilor Lane, KY 40229. (URL: http://www.nws.noaa.gov/afws/raindata.htm)

Nelson, D.W. and L.E. Sommers. 1982. Total carbon, organic carbon, and organic matter. In *Methods of Soil Analysis, Part 2, Chemical and Microbiological Properties (II ed.).* Agronomy 9:539-577, ed. A.L. Page. Madison, Wisc.: ASA – SSSA.

Nommik, H. 1976. Further observations on ammonia loss from urea applied to forest soil with special reference to the effect of pellet size. *Plant Soil* 45:279-282.

Nommik, H. and K. Vahtras. 1982. Retention and fixation of ammonium and ammonia in soils. In *Nitrogen in Agricultural Soils.* Agronomy 22:123-171, ed. F.J. Stevenson et al. Madison, Wisc.: ASA, CSSA, and SSSA.

Novotny, V. and H. Olem. 1993. *Water Quality: Prevention, Identification, and Management of Diffuse Pollution.* New York: Van Nostrand Reinhold.

Nyborg, M.M. and S.S. Malhi. 1992. Effectiveness of fall- versus spring-applied urea on barley. *Fertilizer Research* 31:235-239.

Nye, P.H. and P.B. Tinker. 1977. *Solute Movement in the Soil-Root System, Studies in Ecology Vol. 4.* Berkeley, Calif.: University of California.

Ott, R. L. 1992. *An Introduction to Statistical Methods and Data Analysis (IV ed.)*. Belmont, CA: Wadsworth Publishing Company.

Poss, R., A.D. Noble, F.X. Dunin, and W. Reyenga. 1995. Evaluation of ceramic cup samplers to nitrate leaching in the field. *European Journal of Soil Science* 46:667-674.

Press, W.H., B.P. Flannery, S.A. Teukolsky, and W.T. Vetterling. 1989. *Numerical Recipes: The Art of Scientific Computing (Fortran version)*. New York: Cambridge University Press.

Prosser, J.I. 1986. Experimental and theoretical models of nitrification. In *Nitrification,* ed. J.I. Prosser, ch. 4, 63-78. Oxford, England: IRL Press.

Raynes, R.J. 1986. *Mineral Nitrogen in the Soil-Plant System*. Orlando: Academic Press.

Remson, I., G.M. Hornberger, and F.J. Molz. *Numerical Methods in Subsurface Hydrology with an Introduction to the Finite Element Method.* New York: Wiley-Interscience.

Richards, L.A. 1931. Capillary conduction through porous mediums. *Physics* 1:313-318.

Ritter, W.F., R.W. Scarborough, and E.M. Chirnside. 1993. Nitrate leaching under irrigated corn. *Journal of Irrigation Engineering* 119(3):544-553.

Roache, P.J. 1985. *Computational Fluid Dynamics*. Albuquerque, N.M.: Hermosa Publishers.

Rogers, J.S. 1994. Capacitance and initial time step effects on numerical solutions of Richards equation. *Transactions of the ASAE* 37(3):807-813.

Rosenberg, N.J., B.L. Blaad, and S.B. Verma. 1983. *Microclimate: The Biological Environment (II ed.)*. New York: John Wiley & Sons.

Rosenthal, W.D., E.T. Kanemasu, R.J. Raney, and L.R. Stone. 1977. Evaluation for an evapotranspiration model for corn. *Agronomy Journal* 69:461-464.

Ryan, P.A. and Y. Cohen. 1990. Diffusion of sorbed solutes in gas and liquid phases of low-moisture soils. *Soil Science Society of America Journal* 54:341:346.

Sadeghi, A.M., D.E. Kissel, and M.L. Cabrera. 1989. Estimating molecular diffusion coefficients of urea in unsaturated soil. *Soil Science Society of America Journal* 53:15-18.

SAS. 1996. *Selected SAS® Documentation for STAT 5615/5616: Statistics in Research (Spring 1997)*. Cary, N.C.: SAS Institute Inc.

Savant, N.K., P.S. Ongkingco, F.D. Garcia, S.S. Dhane, R.R. Khadse, S.A. Chavan, and K.S. Rao. Agronomic performance of urea briquette applicator in transplanted rice. *Fertilizer Research* 32:139142.

Saxton, K.E., H.P. Johnson, and R.H. Shaw. 1974. Modeling evapotranspiration and soil moisture. *Transactions of the ASAE* 17(4):673-677.

Scharf, P.C. and M.M. Alley. 1988. Nitrogen loss pathways and nitrogen loss inhibitors: a review. *Journal of Fertilizer Issues* 5(4):109-125.

Schmidt, E.L. and L.W. Belser. 1982. Nitrifying bacteria. In *Methods of Soil Analysis, Part 2, Chemical and Microbiological Properties (II ed.).* Agronomy 9:1027-1042, ed. A.L. Page. Madison, WI: ASA – SSSA.

Schwab, G.O. and R.K. Frevert. 1993. *Elementary Soil and Water Engineering*. Malabar, Fl.: Krieger Publishing Company.

Scotter, D.R. and P.A.C. Raats. 1970. Movement of salt and water near crystalline salt in relatively dry soil. *Soil Science* 109(3):170-178.

SCS. 1985. Soil Survey of Montgomery County, Virginia. Richmond, Va.: USDA-SCS.

Selim, H.M. 1994. Soil, chemical: movement and retention. In *Encyclopedia of Agricultural Science, Vol. 4*, 63-74. New York: Academic Press, Inc.

Selim, H.M. and I.K. Iskandar. 1981. Modeling nitrogen transport and transformations in soils: 1. theoretical considerations. *Soil Science* 131(4):233-241.

Shaffer, M.J., K. Rojas, D.G. DeCoursey, and C.S. Hebson. 1992. *Summary Documentation for OMNI, the Organic Matter/NItrogen Cycling Component of the Root Zone Water Quality Model (RZWQM).* Research Report. Ft. Collins, Colo.: USDA-ARS, Great Plains Systems Research Unit.

Shani, U., L.M. Dudley, and R.J. Hanks. 1992. Model of boron movement in soils. *Soil Science Society of America Journal* 56:1365-1370.

Short, D., W.R. Dawes, and I. White. 1995. The practicability of using Richards' equation for general purpose soil-water dynamics models. *Environment International* 21(5):723-730.

Siegel, S. 1956. *Nonparametric Statistics for the Behavioral Sciences*. New York: McGraw-Hill Book Company.

Simunek, J., M. Sejna, and M. Th. van Genuchten. 1999. *The HYDRUS-2D software Package for the Simulating Two-Dimensional Movement of Water, Heat, and Multiple Solutes in Variably-Saturated Media, Ver. 2.0.* Riverside, Calif.: U.S. Salinity Laboratory.

Singh, R and P.H. Nye. 1984. Diffusion of urea, ammonium and soil alkalinity from surface applied urea. *Journal of Soil Science* 35:529-538.

Singh, Y. and E.G. Beauchamp. 1988. Response of winter wheat to fall-applied large urea granules with dicynadiamide. *Canadian Journal of Soil Science* 68:133-142.

Singh, Y. and E.G. Beauchamp. 1987. Nitrification inhibition with large urea granules, dicyandiamide and soil temperature. *Soil Science* 144:412-419.

Singh, Y., S.S. Malhi, M.M. Nyborg, and E.G. Beauchamp. 1994. Large granules, nest or bands: methods of increasing efficiency of fall-applied urea for small cereal grains in North America. *Fertilizer Research* 38:61-87.

Skaggs, R.W. and R. Khaleel. 1982. Infiltration. In *Hydrologic Modeling of Small Watersheds,* ed. C.T. Haan, ch. 4, 121-168. St. Joseph, Mich.: ASAE.

Smith, M. 1992. *CROPWAT: a Computer Program for Irrigation Planning and Management*. Rome, Italy: FAO.

Snoeyink, V.L. and D. Jenkins. 1980. *Water Chemistry*. New York: John Wiley & Sons.

Soil Conservation Service (SCS). 1985. *Soil Survey of Montgomery County, Virginia*. Richmond: USDA - SCS.

SERCC (Southeast Regional Climate Center). 2000. South Carolina Department of Natural Resources, Water Resources Division, 1201 Main Street Suite 1100, Columbia, SC 29201. (URL: http://water.dnr.state.sc.us/climate/sercc/products/normals/440766_30yr_norm.html)

Sparks, D.L. 1989. *Kinetics of Chemical Processes in Soils.* San Diego, Calif.: Academic Press.

Storm, D.E., T.A. Dillaha, III, S. Mostaghimi, V. O. Shanholtz. 1988. Modeling phosphorus transport in surface runoff. *Transactions of the ASAE* 31(1):117-127.

Tabatabai, M.A. 1982. Soil enzymes. In *Methods of Soil Analysis, Part 2, Chemical and Microbiological Properties (II ed.)*. Agronomy 9:903-948, ed. A.L. Page. Madison, WI: ASA – SSSA.

Tabatabai, M.A. 1973. Michaelis constants of urease in soils and soil fractions. *Soil Science Society of America Proceedings* 37:707-710.

Teso, R.R., R.E. Gallavan, D.L. Sheeks, III, R.H. Neal, T. Mischke, and M.R. Peterson. 1990. *Tension Lysimeters: Monitoring of Pesticides in Soil Water*. Sacramento, Calif: Department of Food and Agriculture, State of California.

Tisdale, S.L., W.L. Nelson, J.D. Beaton, and J.L. Havlin. 1993. *Soil Fertility and Fertilizers (V ed.*). New York: Macmillan Publishing Company.

TEL. 1983. 3300 Series depth moisture gages instruction manual. Triangle Park, N.C.: Troxler Electronic Laboratories (TEL), Inc.

U.S. Census Bureau. 2000. U.S. Census Bureau - U.S. Department of Commerce, 14th and Constitution Av., Washington, D.C. 20250. (URL: http://www.census.gov)

USDA-NASS. 2000. USDA - National Agricultural Statistics Service, 14th and Independence Av. SW., Washington, D.C. 20250. (URL: http://usda.mannlib.cornell.edu/reports/nassr/field/pcp-bba/acrg006.txt)

USDA–SCS. 1984. *User's Guide for the CREAMS Computer Model*. Washington, D.C.: USDA.

USEPA. 1986. *Quality Criteria for Water 1986*. EPA 440/5-86-001. Washington, D.C.: Office of Water, USEPA.

USGS. 1999. *Ground Water Studies*. USGS Fact Sheet FS-058-95. Washington, D.C.: GPO. (URL: http://water.usgs.gov/wid/html/GW.html) van Bavel, C.H.M. and J. Ahmed. 1976. Dynamic simulation of water depletion in the root zone. *Ecological Modelling* 2:189-212.

van Genuchten, M. Th. 1980. A closed-form equation for predicting the hydraulic conductivity of unsaturated soils. *Soil Science Society of America Journal* 44:892-898.

van Genuchten, M. Th. and D. R. Nielsen. 1985. On describing and predicting the hydraulic properties of unsaturated soils. *Annales Geophysicae* 3(5):615-628.

van Genuchten, M. Th., F.J. Leij, and S.R. Yates. 1991. *The RETC Code for Quantifying the Hydraulic Functions of Unsaturated Soils*. EPA/600/2-91/065. Ada, Okla.:USEPA.

VASS. 2000. Virginia Agricultural Statistics Service (VASS), P.O. Box 1659, Richmond, Va 23218-1659. (URL: http://www.nass.usda.gov/va/pg009.htm)

VDCR. 1993. *Nutrient Management Handbook (II ed.)*. Richmond: Virginia Department of Conservation and Recreation, Division of Soil and Water Conservation.

Vomocil, J.A. 1965. Porosity. In *Methods of Soil Analysis* Agronomy 9:299-314, eds. C.A. Black, D.D. Evans, L.E. Ensminger, and F.E. Clark. Madison, WI: ASA.

Wagenet, R.J. 1981. Simulation of soil-water and nitrogen movement. In *Simulation of Nitrogen Behaviour in Soil-Plant Systems*, eds. M.J. Frissel and J.A. van Veen, ch. 4.2, 67-80. Wageningen, The Netherlands: Centre for Agricultural Publishing and Documentation.

Wagenet, R.J., J.W. Biggar, and D.R. Nielsen. 1977. Tracing the transformations of urea fertilizer during leaching. *Soil Science Society of America Journal* 41:896-902.

Wetselaar, R. 1985. Deep point-placed urea in flooded soil. In *Proceedings of Workshop on Urea Deep Placement Technology*, Spec. Pub. 6:7-14. Muscle Shoals, Ala.: International Fertilizer Development Center.

Zhang, X. 1990. Corn growth with point placed urea. M.S. Thesis. Guelph, Canada: Univ. of Guelph, microfiche.

APPENDIX A. PRECIPITATION AND AIR TEMPERATURE DATA (MAY 1999 - APRIL 1999)

Precipitation and Air Temperature Data

(May 1999 - April 1999)

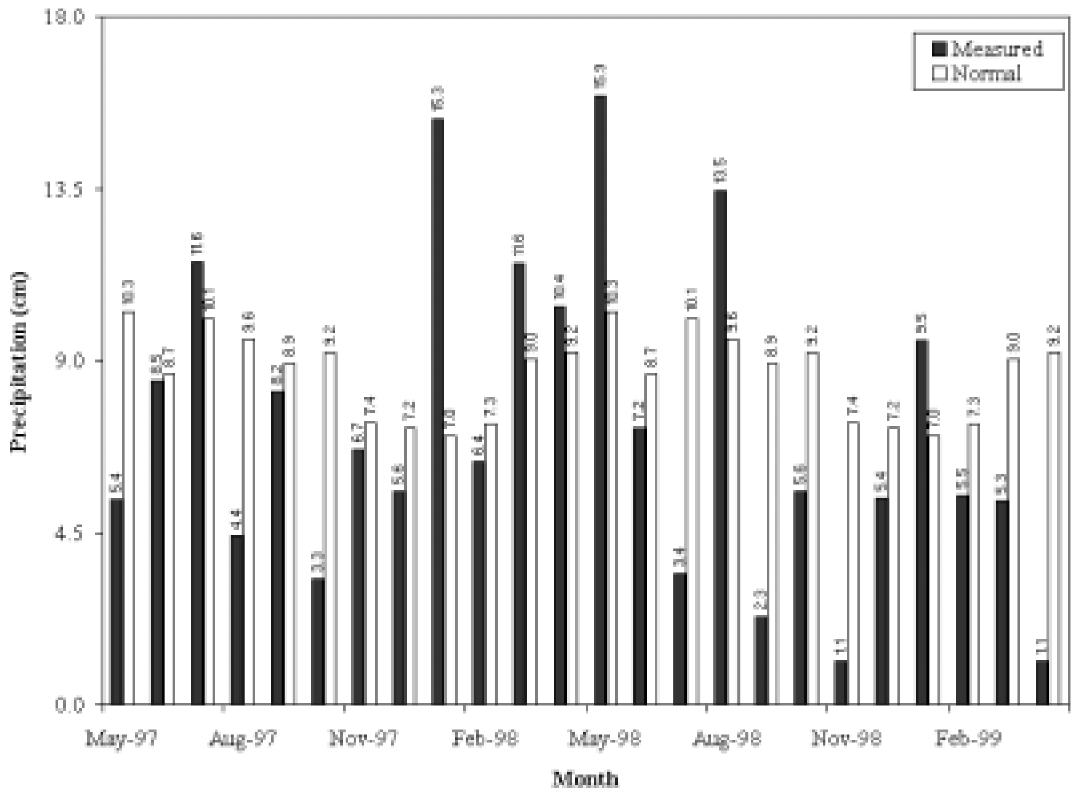

Figure A(a). Comparisons of monthly measured and 30-year normal precipitation. Precipitation was measured at the field site, with missing data filled in with Kentland Farm data. Data for April 1999 was only until April 2 when the experiment was concluded. Thirty-year normal precipitation were calculated by NWS for Blacksburg Airport (SERCC, 2000).

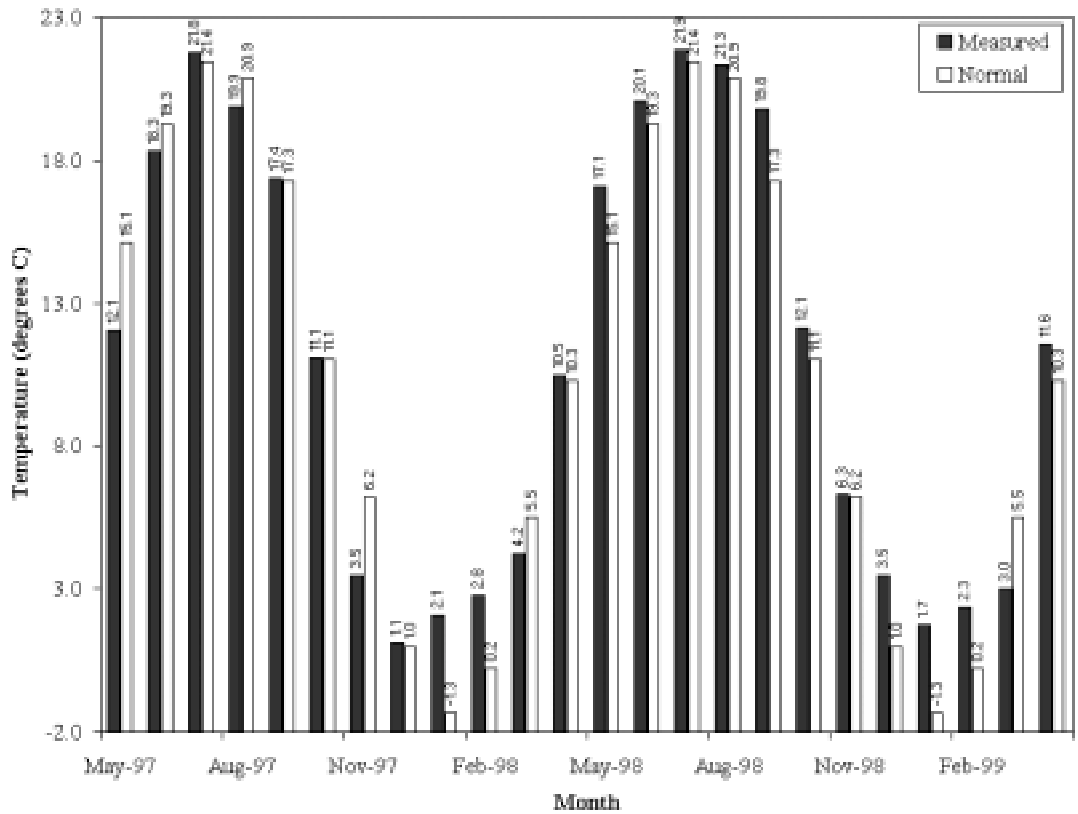

Figure A(b). Comparisons of monthly average measured and 30-year normal temperature. Temperature data were measured for Blacksburg by the National Weather Service (NWS). Thirty-year normal temperature data were calculated by NWS for Blacksburg Airport (SERCC, 2000).

APPENDIX B. INPUT REQUIREMENTS AND DEFINITION OF PARAMETERS AND VARIABLES USED IN THE MATHEMATICAL MODEL

Input Requirements and Definition of Parameters and Variables Used in the Mathematical Model

The mathematical model requires inputs from eight external text files, namely, CROPN.DAT, REFET.DAT, WEATHER.DAT, SOILPROP.DAT, UNSAT.DAT, MOIST.DAT, UREA_IN.DAT, AMMONIUM_IN.DAT, and NITRATE_IN.DAT. The inputs contained in each file along with their descriptions are given in table B.1. Other parameters that are specified in the model code (Appendix E) are described in table B.2. Finally, all the model inputs are described in table B.3.

Table B.1. Parameters and variables contained in the input files

File	Parameter/Variable	Type	Description
CROPN.DAT (contains information about the crop and N application to the crop)	PL_DATE	i*	Planting date (Julian day)
	HV_DATE	i	Harvesting date (Julian day)
	U_DATE1	i	Starter urea application date (Julian day)
	U_DATE2	i	Sidedress urea application date (Julian day)
	ROW_SPACE	dp†	Crop row spacing (cm)
	MAX_ROOTDEPTH	dp	Maximum root depth of crop (cm)
	U_RATE1	dp	Starter urea application rate (kg/ha)
	U_RATE2	dp	Sidedress urea application rate (kg/ha)
	U_DIST1	dp	Distance (cm) of starter urea application with respect to any reference point. Any distance can be selected so long as the point of application is not too close to the boundary which may make the boundary condition unrealistic.
	U_DIST2	dp	Distance (cm) of sidedress urea application with respect to any reference point
	U_DEPTH1	dp	Depth (cm) of starter urea application below the soil surface. Even though any depth may be specified, selecting a very small depth may make the boundary condition unrealistic.
	U_DEPTH2	dp	Depth (cm) of sidedress urea application below the soil surface.
	ELEV	dp	Elevation of the study plot (m above msl)
REFET.DAT	ET_REF	dp, 1d‡	Penman-Monteith hourly reference evapotranspiration (mm)
WEATHER.DAT (contains weather parameter values)	AIR_TEMP	dp, 1d	Hourly air temperature (°C)
	RH	dp, 1d	Hourly relative humidity (%)
	SOLRAD	dp, 1d	Hourly solar radiation (W/m^2)
	SOILTEMP	dp, 1d	Hourly soil temperature at the depth of urea application (°C)
	RAIN	dp, 1d	Hourly precipitation (mm)
SOILPROP.DAT (contains soil properties assumed invariant with depth)	BD	dp	Soil bulk density (g/cm^3)
	POR	dp	Soil porosity (fraction)
	LAMBDA_L	dp	Longitudinal dispersivity (cm)
	SOIL_PH	dp	Soil pH
UNSAT.DAT (contains soil properties assumed variable with depth required for the K-h-θ relationship)	KS	dp, 1d	Saturated hydraulic conductivity 9cm/h)
	THETA_S	dp, 1d	Saturated volumetric moisture content (mL/cm^3)
	THETA_R	dp, 1d	Residual volumetric moisture content (mL/cm^3)
	ALPHA_US	dp, 1d	α parameter (cm^{-1}) - Eq. [5-7]
	L_US	dp, 1d	L parameter - Eq. [5-5]
	M_US	dp, 1d	m parameter - Eq. [5-7]
	N_US	dp, 1d	n parameter - Eq. [5-7]
MOIST.DAT	THETA_IN	dp, 1d	Initial volumetric moisture content (mL/cm^3)

(Table continued)

UREA_IN.DAT	UCONC_IN	dp, 2d§	Initial urea concentration specified as mg/g-soil but converted to mg/mL-soil solution in the model
AMMONIUM_IN.DAT	ACONC_IN	dp, 2d	Initial NH_4^+ concentration specified as mg/g-soil but converted to mg/mL-soil solution in the model
NITRATE_IN.DAT	NCONC_IN	dp, 2d	Initial NO_3^- concentration specified as mg/g-soil but converted to mg/mL-soil solution in the model

* Integer
† Double precision
‡ Element in a 1-D array
§ Element in 2-D array

Table B.2. Parameters* defined in the model code

Parameter	Description
C_P	Specific heat of moist air at constant pressure ($kJ \cdot kg^{-1} \cdot °C^{-1}$)
GAS	Universal gas constant ($kcal \cdot mole^{-1} \cdot °K^{-1}$)
A_1 & B_1	Coefficients used in Eq. [5-24]
HEAD_S	Saturation pressure head (cm)
HEAD_2 & HEAD_3	Pressure heads (cm) defined as ${}_2h$ and ${}_3h$, respectively, in Eq. [5-24]
HEAD_4	Pressure head (cm) at which hydrodynamic dispersion ceases
HEAD_5	Pressure head (cm) below which surface evaporative flux is controlled by moisture movement towards the soil surface instead of environmental conditions
HEAD_MAX	Negative pressure head (cm) at which soil water capacity is calculated for saturation conditions
EXTINC_C	Extinction coefficient used in Eq. [5-25]
TAU	Margin of safety in calculating time step used in Eq. [5-
DT_MANT & DT_EXPO	Empirically developed mantissa and exponent used in time step calculation (Eq. [5-30])
UDIFF_AQ, ADIFF_AQ, & NDIFF_AQ	Molecular diffusion coefficients (cm^2/h) of urea, NH_4^+, and NO_3^-, respectively in aqueous solution
U_VMAX	Maximum reaction velocity of urea ($mg\text{-}urea \cdot g^{-1}\text{-}soil \cdot h^{-1}$) in Eq. [5-50]
U_KMAX	Michaelis constant (mg-urea/mL) in Eq. [5-50]
U_ACT_ENER	Activation energy for urea hydrolysis (kcal/mole-urea) in Eq. [5-52]
U_A	Pre-exponential factor for urea hydrolysis in Eq. [5-52]
UCONC_MM	Threshold urea concentration (${}_uc_2$) at or above which, the Michaelis-Menten equation no longer applies (Eq. [5-51])
UCONC_STOP	Urea concentration at which urea hydrolysis ceases (${}_uc_3$) (Eq. [5-51])
K_DIS	Distribution coefficient for NH_4^+ (Eq. [5-53])
ACONC_RR	Threshold NH_4^+ concentration (${}_ac_1$) above which, the zero-order equation no longer applies (Eq. [5-56])
ACONC_STOP	NH_4^+ concentration at which nitrification ceases (${}_ac_2$) (Eq. [5-56])
N_ACT_ENER	Activation energy for nitrification (kcal/mole-NH_4^+) in Eq. [5-59]
N_A	Pre-exponential factor for nitrification in Eq. [5-59]
N_K0	First-order rate constant for nitrification (h^{-1}) in Eq. [5-56]
N_K1	Zero-order rate constant for nitrification ($mg \cdot mL^{-1} \cdot h^{-1}$) in Eq. [5-56]
U_SLOPE	Slope of the mass of urea dissolved per square root of time (m_g for granule and m_p for pellet) ($mg/h^{0.5}$) in Eq. [5-47]

* All parameters are double precision

Table B.3. Variables used in the model code

Variables	Type	Description
IOS	i*	Boolean counter to check for presence of input file
I	i	Increment along z-axis
L	i	Upper bound of I
IL	i	Increment used to skip a fixed number of header lines in the input files
J	i	Increment along y-axis
M	i	Upper bound of J
N & P	i	Dummy variables (counters) used in the tridiagonal subroutines
I_FERT1 & I_FERT2	i	Increments along z-axis that receive starter and sidedress urea application, respectively
J_FERT11 & J_FERT12	i	Increments along y-axis that receive half and half of starter urea application
J_FERT21 & J_FERT22	i	Increments along z-axis that receive half and half of sidedress urea application
HR	i	Hour counter
HR_END	i	Upper bound of number of hours of simulation
TEN_D	i	Counter of tracking ten-day increments in crop growth during simulation
SIM_START	i	Date of start of simulation (Julian day)
SIM_END	i	Date of end of simulation (Julian day)
R	i, 1d†	Number of root nodes as a function of crop age
K_C	i, 1d	Crop coefficient value as a function of crop age
LAI	i, 1d	Leaf area index value as a function of crop age
DZ	dp‡	Node spacing along z-axis (cm)
DY	dp	Node spacing along y-axis (cm)
T	dp	Time (h) after start of simulation
DT	dp	Time increment (h)
T_START	dp	Hour at which simulation starts (SIM_START times 24.0)
T_END	dp	Hour at which simulation ends (SIM_END times 24.0)
T_NEW	dp	T + DT
PL_TIME	dp	Time (h) between planting date and start of simulation
HV_TIME	dp	Time (h) between harvesting date and start of simulation
U_TIME1	dp	Time (h) between starter urea application and start of simulation
U_TIME2	dp	Time (h) between sidedress urea application and start of simulation
THETA	dp, 1d	Volumetric moisture content, θ (mL/cm^3) at the nodes along z-axis used as dummy variable
THETA_M	dp, 1d	θ between the nodes along z-axis
THETA_IN	dp, 1d	θ at the nodes used as the initial (input to predictor) or the final (output from corrector) value
THETA_MID	dp, 1d	θ at the nodes received as output from the predictor and used as input to the corrector
HEAD	dp, 1d	Pressure head, h (cm) at the nodes along z-axis used as dummy variable
HEAD_IN	dp, 1d	h at the nodes along the z-axis corresponding to THETA_IN
HEAD_MID	dp, 1d	h at the nodes along the z-axis corresponding to THETA_MID
KUS	dp, 1d	Hydraulic conductivity, K (cm/h) between nodes along z-axis used as dummy variable
KUS_IN	dp, 1d	K between nodes used in the predictor
KUS_MID	dp, 1d	K between nodes used in the corrector
KUSN	dp, 1d	K at the nodes used as local variable
FLUX	dp, 1d	Moisture flux, q (cm/h) between nodes along z-axis used as dummy variable
FLUX_IN	dp, 1d	q calculated using HEAD_IN and KUS_IN
FLUX_MID	dp, 1d	q calculated using HEAD_MID and KUS_MID
SWC	dp, 1d	Soil water capacity, C(1/cm) at the nodes along z-axis used as dummy variable
SWC_IN	dp, 1d	C at the nodes used in the predictor
SWC_MID	dp, 1d	C at the nodes used in the corrector
POT_ET	dp, 1d	Hourly potential crop evapotranspiration (cm/h)
POT_EVAP	dp, 1d	Hourly potential evaporation (cm/h)
POT_TRANS	dp, 1d	Hourly potential crop transpiration (cm/h)
TRANS_LAY	dp, 1d	Hourly actual crop transpiration ($mL \cdot cm^{-3} \cdot h^{-1}$) for individual nodes along the z-axis
POT_TRANS_LAY	dp, 2d§	Potential crop transpiration (cm/h) for individual nodes along the z-axis for all specified hours
PERC_LOSS	dp	Cumulative percolation loss from the root zone (cm)
INFILT	dp	Cumulative infiltration through the soil surface (cm)
FLUX_SUR	dp	Actual surface flux due to precipitation or evaporation (cm/h)
POT_INFILT	dp	Potential infiltration at the soil surface (cm/h)
EVAP	dp	Cumulative evaporation from the soil surface (cm)
PRECIP	dp	Cumulative precipitation (cm)
TRANSPIRE	dp	Cumulative transpiration (cm)

(Table continued)

MAX_FLUX	dp	Maximum flux anywhere in the soil profile (cm/h)
N_LEACH	dp	Cumulative amount of NO_3^--N leached (kg/ha)
CROP_NREM	dp	Cumulative amount of N removed by crop (kg/ha)
UCONC_IN	dp, 2d	Urea concentration (mg/mL) used as input in the first step of ADI
UCONC_MID	dp, 2d	Urea concentration (mg/mL) used as input in the second step of ADI
ACONC_IN	dp, 2d	NH_4^+ concentration (mg/mL) used as input in the first step of ADI
ACONC_MID	dp, 2d	NH_4^+ concentration (mg/mL) used as input in the second step of ADI
NCONC_IN	dp, 2d	NO_3^- concentration (mg/mL) used as input in the first step of ADI
NCONC_MID	dp, 2d	NO_3^- concentration (mg/mL) used as input in the second step of ADI
UCONC_LO	dp, 2d	Urea concentration (mg/mL) in the downstream node in the convective component of CDE
UCONC_UP	dp, 2d	Urea concentration (mg/mL) in the upstream node in the convective component of CDE
ACONC_LO	dp, 2d	NH_4^+ concentration (mg/mL) in the downstream node in the convective component of CDE
ACONC_UP	dp, 2d	NH_4^+ concentration (mg/mL) in the upstream node in the convective component of CDE
NCONC_LO	dp, 2d	NO_3^- concentration (mg/mL) in the downstream node in the convective component of CDE
NCONC_UP	dp, 2d	NO_3^- concentration (mg/mL) in the upstream node in the convective component of CDE
UCONCMID	dp, 1d	Urea concentration (mg/mL) calculated in the first step of ADI along the y-axis
UCONCFIN	dp, 1d	Urea concentration (mg/mL) calculated in the second step of ADI along the z-axis
ACONCMID	dp, 1d	NH_4^+ concentration (mg/mL) calculated in the first step of ADI along the y-axis
ACONCFIN	dp, 1d	NH_4^+ concentration (mg/mL) calculated in the second step of ADI along the z-axis
NCONCMID	dp, 1d	NO_3^- concentration (mg/mL) calculated in the first step of ADI along the y-axis
NCONCFIN	dp, 1d	NO_3^- concentration (mg/mL) calculated in the second step of ADI along the z-axis
U_SOURCE	dp	Urea source term due to urea dissolution ($mg \cdot cm^{-3} \cdot h^{-1}$)
U_SINK	dp, 2d	Urea sink term due to urea hydrolysis ($mg \cdot cm^{-3} \cdot h^{-1}$)
U_F_TEMP	dp	Temperature factor for urea hydrolysis
U_MASS11 & U_MASS12	dp	Masses (mg) of starter urea remaining in the first and second cells, respectively, where the first and second starter urea nodes are located within the first and second cells mentioned above
U_MASS21 & U_MASS22	dp	Masses (mg) of sidedress urea remaining in the first and second cells, respectively, where the first and second sidedress urea nodes are located within the first and second cells mentioned above
U_DISS11 & U_DISS12	dp	Masses (mg) of starter urea dissolved in the first and second cells, respectively
U_DISS21 & U_DISS22	dp	Masses (mg) of sidedress urea dissolved in the first and second cells, respectively
A_SOURCE	dp, 2d	NH_4^+ source term due to urea hydrolysis ($mg \cdot cm^{-3} \cdot h^{-1}$)
A_SINK1	dp, 2d	NH_4^+ sink term due to nitrification ($mg \cdot cm^{-3} \cdot h^{-1}$); this term is also applied as the source term in the NO_3^- CDE after converting the NH_4^+ mass into the equivalent NO_3^- mass
A_SINK2	dp	NH_4^+ sink term due to plant N removal ($mg \cdot cm^{-3} \cdot h^{-1}$)
N_F_TEMP, N_F_PH, & N_F_HEAD	dp	Temperature, pH, and pressure head factors for nitrification, respectively
N_SINK	dp	NO_3^- sink term due to plant N removal ($mg \cdot cm^{-3} \cdot h^{-1}$)
U_AP_DISP	dp, 1d	Apparent dispersion (cm^2/h) of urea times θ applicable to that vertical node
A_AP_DISP	dp, 1d	Apparent dispersion (cm^2/h) of NH_4^+ times θ applicable to that vertical node
N_AP_DISP	dp, 1d	Apparent dispersion (cm^2/h) of NO_3^- times θ applicable to that vertical node
AV_ACONC	dp, 1d	Average NH_4^+-N concentration (mg/mL) for any i (2, …, L-1) in all non-boundary horizontal nodes (j = 2, …, M-1)
AV_NCONC	dp, 1d	Average NO_3^--N concentration (mg/mL) for any i (2, …, L) in all horizontal nodes (j = 1, …, M)
NA_REM_LAY	dp, 1d	N removed by crop from any vertical node ($mg \cdot cm^{-3} \cdot h^{-1}$)
X & Y	dp, 1d	Dummy variables used in the tridiagonal subroutines
A_Y, B_Y, C_Y, & K_Y	dp, 1d	Dummy variables corresponding to subdiagonal, diagonal, superdiagonal coefficients on the left side and coefficient on the right side, respectively in the tridiagonal subroutine for the moisture sub-model
A_M, B_M, C_M, & K_M	dp, 1d	Subdiagonal, diagonal, superdiagonal coefficients on the left side and coefficient on the right side, respectively in the tridiagonal subroutine for the moisture sub-model
A_X, B_X, C_X, & K_X	dp, 1d	Dummy variables corresponding to subdiagonal, diagonal, superdiagonal coefficients on the left side and coefficient on the right side, respectively in the tridiagonal subroutine for the N sub-model for the first step of the ADI
A_U, B_U, C_U, & K_U	dp, 1d	Subdiagonal, diagonal, superdiagonal coefficients on the left side and coefficient on the right side, respectively in the tridiagonal subroutine for the N sub-model for the first step of the ADI for urea
A_U2, B_U2, C_U2, & K_U2	dp, 1d	Subdiagonal, diagonal, superdiagonal coefficients on the left side and coefficient on the right side, respectively in the tridiagonal subroutine for the N sub-model for the second step of the ADI for urea
A_A, B_A, C_A, & K_A	dp, 1d	Subdiagonal, diagonal, superdiagonal coefficients on the left side and coefficient on the right side, respectively in the tridiagonal subroutine for the N sub-model for the first step of the ADI for NH_4^+

(Table continued)

A_A2, B_A2, C_A2, & K_A2	dp, 1d	Subdiagonal, diagonal, superdiagonal coefficients on the left side and coefficient on the right side, respectively in the tridiagonal subroutine for the N sub-model for the second step of the ADI for NH_4^+
A_N, B_N, C_N, & K_N	dp, 1d	Subdiagonal, diagonal, superdiagonal coefficients on the left side and coefficient on the right side, respectively in the tridiagonal subroutine for the N sub-model for the first step of the ADI for NO_3^-
A_N2, B_N2, C_N2, & K_N2	dp, 1d	Subdiagonal, diagonal, superdiagonal coefficients on the left side and coefficient on the right side, respectively in the tridiagonal subroutine for the N sub-model for the second step of the ADI for NO_3^-

* Integer
† Element in a 1-D array
‡ Double precision
§ Element in 2-D array

APPENDIX C. SAMPLE INPUT FILES REQUIRED BY THE MATHEMATICAL MODEL

SAMPLE INPUT FILES REQUIRED BY THE MATHEMATICAL MODEL

1. CROPN.DAT

```
Crop data for 1998 corn crop (modified to make boundary conditions reasonable)
 Pl. Hv. St. Sd. Row_sp.Max_Rt. St.rt. Sd.rt. St.dis. Sd.dis. St.dep. Sd.dep. Elev
 dt. dt. dt. dt. -----cm------- -urea-kg/ha- --------------cm---------------        m
 138 259 138 180 75.00  120.00  80.0   320.0  20.00   45.00   10.00   10.00   670.7
```

In the above sample file, Pl. dt. and Hv. Dt.are PL_DATE and HV_DATE, respectively; St. dt. and Sd. dt. are U_DATE1 and U_DATE2, respectively; Row_sp and Max_rt. are ROW_SPACE and MAX_ROOTDEPTH, respectively; St.rt. and Sd.rt. are U_RATE1 and U_RATE2, respectively; St.dis. and Sd.dis. are U_DIST1 and U_DIST2, respectively; St.dep. and Sd.dep. are U_DEPTH1 and U_DEPTH2, respectively, and Elev is ELEV. All variables listed above are described in table B.1.

2. REFET.DAT

```
"Trial Et calculation for Kentland Farm, May 12,1998-April 2, 1999"
       Reference Type is GRASS (Alfalfa / 1.25 )
DoY HrMn  Tmax Tmin  Rs  Wind DewP PMon KPen FcPn 63Pn Harg FRad FB-C
                 C    C  W/m2 m/s   C  mm/h mm/h mm/h mm/h mm/h mm/h mm/h
132 1100  18.5 18.5  700  2.9 11.1 0.40 0.41      0.50
132 1200  18.9 18.9  759  3.1 11.7 0.43 0.45      0.54
132 1300  19.4 19.4  320  3.1 11.2 0.24 0.24      0.29
```

The above file was generated as output by the REF-ET (Allen, 1990), the software program used to calculated reference evapotranspiration (ET). The only value in each line that is used by the mathematical model in this study in the Penman-Monteith ET value (ET_REF in table B.1.). Description of the variables in the above file may be found in Allen (1990).

3. WEATHER.DAT

```
Jday 132-262:Temp, RH,WS-Roanoke Reg. Airport; RS-Bluefield; soil temp.-
Kentland (average of 1993(part), 1994, 1995),Jday 262-92: Kentland data
    DayTime     Temp(C)   RH(%)RS(W/m2)WS(km/h)S.temp(C)Rain(mm/h)
    1321100       18.50    62.0   700.0  10.300   14.35    0.00
    1321200       18.90    63.0   759.0  11.300   14.65    0.00
    1321300       19.40    59.0   320.0  11.300   15.00    0.00
```

1321400 18.90 63.0 324.0 16.100 15.58 0.00

In the above file Temp, RS, S.temp, and Rain are AIRTEMP, SOLRAD, SOILTEMP, and RAIN, respectively, as previously defined in table B.1. Day, Time, RH, and WS are Julian days, hours, relative humidity, and wind speed which are not required by the model.

4. SOILPROP.DAT

```
Soil properties for Ross soil, Kentland Farm
BD    POR    Lambda_l Soil_pH
g/cm3 mL/cm3 cm
 1.34  0.496  0001.0  6.10
```

The variables BD, POR, lambda_l, and Soil_pH are defined as BD, POR, LAMDA_L, and SOIL_PH in table B.1.

5. UNSAT.DAT

```
Data required to calculate unsat. K by layer(1.25 cm) for Ross soil, Kentland Farm.
These are not measured but least-squares fitted values obtained from RETC3.FOR
Layer   KS(cm/h)theta_s theta_r alpha   l_us  m_us    n_us
1       1.000   0.4880  0.0286  0.1302  0.50  0.1244  1.0050
2       1.000   0.4880  0.0286  0.1302  0.50  0.1244  1.0050
3       1.000   0.4880  0.0286  0.1302  0.50  0.1244  1.0050
```

The variables Layer, KS, theta_s, theta_r, alpha, l_us, m_us, and n_us correspond to I (Table B.3.), KS, ALPHA_US, L_US, M_US, and N_US, respectively. The variables KS, ALPHA_US, L_US, M_US, and N_US are defined in Table B.1.

3. MOIST.DAT

```
Initial volumetric moisture content estimated on 5/12/98 using neutron count measurements.
Note that neutron counts were only available at 30, 45, 60, 90, and 120 cm. Intermediate values were
obtained through interpolation.
Vol. MC
0.440
0.438
0.436
0.434
0.432
```

In the above file, initial volumetric content (THETA_IN) is specified for each vertical node (I).

4. UREA_IN.DAT, AMMONIUM_IN.DAT, and NITRATE_IN.DAT

The UREA_IN.DAT, AMMONIUM_IN.DAT, and NITRATE_IN.DAT contain intial urea (UCONC_IN), NH_4^+ (ACONC_IN), and NO_3^- (NCONC_IN) concentrations for all nodes in the lateral and vertical directions. The descriptions of these variable are presented in table B.1. In this study, all initial N concentrations were set equal to zero. With the proper format (field description), the model can read intial N concentrations from a text file.

APPENDIX D. CODE OF THE TWO-DIMENSIONAL MATHEMATICAL MODEL FOR SIMULATING THE FATE OF SUBSURFACE-BANDED UREA-N (FORTRAN 90)

CODE OF THE TWO-DIMENSIONAL MATHEMATICAL MODEL FOR SIMULATING THE FATE OF SUBSURFACE-BANDED UREA-N (FORTRAN 90)

```
!*********************************************************************
! Created by Sanjay B. Shah
! July 2000
!**********************************************************************
! This model simulates the fate of urea applied in subsurface bands in
! two dimensions.  The model uses the one-dimensional Richards'
! equation to provide flux and moisture content values for running the
! N model.
!
! The moisture model simulates bare surface evaporation, transpiration,
! moisture redistribution, and percolation.  Currently, it does not
! simulate runoff.  The moisture model is capable of handling
! precipitation intensities of upto 5 cm/h.  When larger precipitation
! intensities are to be simulated, the smallest time step (10D-6 h)
! restriction will need to be removed.
!
! While the N model simulates urea dissolution, urea hydrolysis, and
! nitrification, currently, it does not simulate other N-loss pathways
! such as denitrification, ammonium fixation, and immobilization.
!
! Nitrogen fate is modeled using separate convective-dispersive
! equations (CDE) for urea, ammonium, and nitrate.  The alternating
! -direction impicit method is used to finite difference the CDE.
!
! Stability of the moisture model is checked using an empirical
! equation for calculating time step.  Stability of the CDE is tested
! with the CFL criterion set equal to 0.8.  The smaller of the two time
! steps is used depending on whether there is N applied to the soil.
!
! The model outputs three files - MOIST.OUT, NITRATE.OUT, and
! AMMONIUM.OUT.  The MOIST.OUT file contains information on all
! components of the hydrologic cycle that the model simulates.  The
! NITRATE.OUT file contains nitrate concentrations as well as amounts
! of N leached and N removed by the crop.  The AMMONIUM.OUT file
! contains ammonium concentrations.  Note that there is no file for
! urea outputs since urea does not stay in the soil for too long.
! Note that all of the above outputs are generated at 10-day intervals
! as well as at the end of simulation.  For outputs at other time
! intervals, appropriate WRITE statements will need to be inserted.
!**********************************************************************
PROGRAM MAIN
 IMPLICIT NONE
 SAVE
 ! Universal constants
 DOUBLE PRECISION,PARAMETER::C_P=1.013,GAS=8.314D+7
 ! Declared constants, measured values preferable
 DOUBLE PRECISION,PARAMETER::A_1=0.40,B_1=0.92,HEAD_S=0.0,          &
  & HEAD_2=-1000.0,HEAD_3=-20000.0,HEAD_4=-30000.0,HEAD_5=-48000.0,   &
  & HEAD_MAX=-1.0D0-4,EXTINC_C=0.63,TAU=1.25,DT_MANT=1.0D-4,         &
```

```
 & DT_EXPO=-2.4907
DOUBLE PRECISION,PARAMETER::UDIFF_AQ=0.03,ADIFF_AQ=0.07,            &
 & NDIFF_AQ=0.03,U_VMAX=0.19,U_KMAX=0.20,U_ACT_ENER=5.78,U_A=11724.4,&
 & UCONC_MM=25.0,UCONC_STOP=400.0,K_DIS=0.25,ACONC_RR=0.054,         &
 & ACONC_STOP=3.857,N_A=1.807D+9,N_ACT_ENER=12.64,N_K0=347D-6,       &
 & N_K1=0.01,U_SLOPE=0.3877
 ! The U_SLOPE value shown above applies to urea granules.  For
 ! pellets, it is 0.1345.
 ! Variable declaration
 ! Counters
 INTEGER::IOS,I,IL,J,I_FERT1,I_FERT2,J_FERT11,J_FERT12,J_FERT21,     &
  & J_FERT22,HR,TEN_D
 ! Sizes
 INTEGER::L,M,N,P,Q,HR_END,SIM_START,SIM_END
 ! Array containing number of root nodes for all growth stages
 INTEGER,DIMENSION(1:17)::R
 DOUBLE PRECISION::DY,DZ,T,DT,T_START,T_END,T_NEW
 ! Since the array dimensions are not known
 ! initially, need to usethe allocatable attribute
 DOUBLE PRECISION,ALLOCATABLE,DIMENSION(:)::THETA,THETA_IN,THETA_MID,&
  & HEAD,HEAD_IN,HEAD_MID,THETA_M
 DOUBLE PRECISION,ALLOCATABLE,DIMENSION(:)::KUS,KUS_IN,KUS_MID
 DOUBLE PRECISION,ALLOCATABLE,DIMENSION(:)::FLUX,FLUX_IN,FLUX_MID
 DOUBLE PRECISION,ALLOCATABLE,DIMENSION(:)::SWC,SWC_IN,SWC_MID
 DOUBLE PRECISION,ALLOCATABLE,DIMENSION(:)::KS,THETA_S,THETA_R,      &
  & ALPHA_US,L_US,M_US,N_US
 DOUBLE PRECISION,ALLOCATABLE,DIMENSION(:)::AIRTEMP,SOILTEMP,SOLRAD, &
  & RAIN
 DOUBLE PRECISION,ALLOCATABLE,DIMENSION(:)::ET_REF,POT_EVAP,POT_ET,  &
  & POT_TRANS
 DOUBLE PRECISION,ALLOCATABLE,DIMENSION(:,:)::POT_TRANS_LAY
 DOUBLE PRECISION,ALLOCATABLE,DIMENSION(:)::TRANS_LAY
 DOUBLE PRECISION,DIMENSION(1:17)::K_C,LAI
 DOUBLE PRECISION::BD,POR,LAMBDA_L,SOIL_PH,ELEV
 DOUBLE PRECISION::ROW_SPACE,MAX_ROOTDEPTH
 DOUBLE PRECISION::PERC_LOSS,INFILT,FLUX_SUR,POT_INFILT,EVAP,PRECIP, &
  & TRANSPIRE,MAX_FLUX,N_LEACH,CROP_NREM
 DOUBLE PRECISION,ALLOCATABLE,DIMENSION(:,:)::UCONC_IN,UCONC_MID,    &
  & ACONC_IN,ACONC_MID,NCONC_IN,NCONC_MID
 DOUBLE PRECISION,ALLOCATABLE,DIMENSION(:,:)::UCONC_UP,UCONC_LO,     &
  & ACONC_UP,ACONC_LO,NCONC_UP,NCONC_LO
 ! The uconc_up is the concentration in the upper node while uconc_lo
 ! is the concentration in the lower node and these are required to
 ! calculate the advective component.
 DOUBLE PRECISION::U_SOURCE,A_SINK2,N_SINK,U_MASS11,U_MASS12,        &
  & U_DISS11,U_DISS12,U_MASS21,U_MASS22,U_DISS21,U_DISS22
 DOUBLE PRECISION,ALLOCATABLE,DIMENSION(:)::UCONCMID,ACONCMID,       &
  & UCONCFIN,ACONCFIN
 DOUBLE PRECISION,ALLOCATABLE,DIMENSION(:)::U_AP_DISP,A_AP_DISP,     &
  & N_AP_DISP
 DOUBLE PRECISION,ALLOCATABLE,DIMENSION(:)::X,Y,Z,NCONCMID,NCONCFIN
 DOUBLE PRECISION,ALLOCATABLE,DIMENSION(:)::AV_ACONC,AV_NCONC,       &
  & NA_REM_LAY
 DOUBLE PRECISION,ALLOCATABLE,DIMENSION(:,:)::A_SINK1,U_SINK
 DOUBLE PRECISION,ALLOCATABLE,DIMENSION(:)::A_Y,B_Y,C_Y,K_Y
 DOUBLE PRECISION,ALLOCATABLE,DIMENSION(:)::A_X,B_X,C_X,K_X
 DOUBLE PRECISION,ALLOCATABLE,DIMENSION(:)::A_Z,B_Z,C_Z,K_Z
```

```
  DOUBLE PRECISION,ALLOCATABLE,DIMENSION(:)::A_M,B_M,C_M,K_M
  DOUBLE PRECISION,ALLOCATABLE,DIMENSION(:)::A_U,B_U,C_U,K_U
  DOUBLE PRECISION,ALLOCATABLE,DIMENSION(:)::A_U2,B_U2,C_U2,K_U2
  DOUBLE PRECISION,ALLOCATABLE,DIMENSION(:)::A_A,B_A,C_A,K_A
  DOUBLE PRECISION,ALLOCATABLE,DIMENSION(:)::A_A2,B_A2,C_A2,K_A2
  DOUBLE PRECISION,ALLOCATABLE,DIMENSION(:)::A_N,B_N,C_N,K_N
  DOUBLE PRECISION,ALLOCATABLE,DIMENSION(:)::A_N2,B_N2,C_N2,K_N2
  DOUBLE PRECISION::U_RATE1,U_RATE2,U_DIST1,U_DIST2,U_DEPTH1,U_DEPTH2
  DOUBLE PRECISION::U_F_TEMP,N_F_TEMP,N_F_PH,N_F_HEAD
  DOUBLE PRECISION::U_TIME1,U_TIME2
  INTEGER::U_DATE1,U_DATE2
  INTEGER::PL_DATE,PL_TIME,HV_DATE,HV_TIME
  ! All time-related declarations are made now.
  PRINT*,"Simulation should begin before or at planting and fertilizer"
  PRINT*," application and end at or after harvesting."
  PRINT*,"Specify julian day when simulation begins."
   READ*,SIM_START
   T_START=24.D0*SIM_START
  PRINT*,"Specify the julian day when simulation ends. Note that the "
  PRINT*,"simulation period cannot exceed 2 years.  For the second "
  PRINT*,"year of simulation, do not count from day 1.For example, "
  PRINT*,"if the simulation period is from May 1,1998 to Jan.7,1999, "
  PRINT*,"the date when simulation ends should be1999, the date when"
  PRINT*,"when simulation ends should be specified as 372 and not 7."
   READ *, SIM_END
   T_END=24.D0*SIM_END
   HR_END=INT(T_END-T_START)
  ! Read file containing information on the crop and fertilization
  OPEN(UNIT=1,FILE="CROPN.DAT",STATUS="OLD",IOSTAT=IOS)
   IF (IOS/=0) THEN
    PRINT*,"Unable to open file CROPN.DAT"
   ELSE
    DO IL=1,3
     READ(UNIT=1,*)
    END DO
     READ(UNIT=1,                                                     &
      & FMT='(4I4,F6.2,F8.2,F6.1,F8.1,F7.2,F8.2,F8.2,F8.2,F8.1)')     &
      & PL_DATE,HV_DATE,U_DATE1,U_DATE2,ROW_SPACE,MAX_ROOTDEPTH,      &
      & U_RATE1,U_RATE2,U_DIST1,U_DIST2,U_DEPTH1,U_DEPTH2,ELEV
   END IF
  CLOSE(UNIT=1)
  ! Note that PL_TIME and HV_TIME are specified in terms of HR, a
  ! one-hourly increment.
  PL_TIME=(PL_DATE-SIM_START)*24
  HV_TIME=(HV_DATE-SIM_START)*24
  ! Time of starter application after start of simulation (h)
  U_TIME1=(U_DATE1-SIM_START)*24.0D0
  ! Sidedress time
  U_TIME2=(U_DATE2-SIM_START)*24.0D0
!
  ALLOCATE(ET_REF(1:HR_END))
  OPEN(UNIT=2,FILE="REFET.DAT",STATUS="OLD",IOSTAT=IOS)
   IF (IOS/=0) THEN
    PRINT*,"Unable to open file REFET.DAT"
   ELSE
   ! REFET.DAT has six lines of headers and one line of dummy data
    DO IL=1,7
```

```
    READ(UNIT=2,*)
   END DO
   ! Assumed that ET is zero outside this time range
   ! This is for the Penman-Monteith method
   READ(UNIT=2,FMT='(34X,F5.2)')(ET_REF(HR),HR=1,HR_END)
    DO HR=1,HR_END
     IF (ET_REF(HR)<0.0D0) THEN
      ET_REF(HR)=0.0D0
     END IF
    END DO
    ET_REF=0.1D0*ET_REF
    ! Converts Et from mm/h to cm/h
  END IF
 CLOSE(UNIT=2)
!
 ALLOCATE(AIRTEMP(1:HR_END),SOLRAD(1:HR_END))
 ALLOCATE(SOILTEMP(1:HR_END),RAIN(1:HR_END))
 OPEN(UNIT=3,FILE="WEATHER.DAT",STATUS="OLD",IOSTAT=IOS)
  IF (IOS/=0) THEN
   PRINT*,"Unable to open file WEATHER.DAT"
  ELSE
  ! WEATHER.DAT has three lines of headers and one line of dummy data
   DO IL=1,4
    READ(UNIT=3,*)
   END DO
    READ(UNIT=3,FMT='(16X,F8.2,8X,F8.1,8X,2F8.2)')                   &
     & (AIRTEMP(HR),SOLRAD(HR),SOILTEMP(HR),RAIN(HR),HR=1,HR_END)
    RAIN=0.1D0*RAIN
  ! Converts precipitation from mm/h to cm/h
  END IF
 CLOSE(UNIT=3)
!
 ! Node spacings for both y and z axes need to be specified.
 ! The first requirement is that DY=DZ.
 PRINT*,"Both Y and Z node spacings should be equal."
 PRINT*,"Enter node spacing in cm."
  READ*,DY
  DZ=DY
 PRINT*,"Please note that row spacing should be exactly divisible by "
 PRINT*,"y axis node spacing."
 ! Note that in the vertical direction, the first and last nodes are
 ! located dz/2 below the soil surface and dz/2 above the root zone
 ! limit, respectively.  In the horizontal direction, the first and
 ! last nodes start at the modeling domain's boundaries.
 M=INT(ROW_SPACE/DZ+1)
 PRINT*,"There are ",M,"nodes along the y axis"
  L=INT(MAX_ROOTDEPTH/DZ)
 PRINT*,"There are ",L,"nodes along the z axis"
 ! Assumed that urea is applied in a single node along the z axis.
 ! Urea is equally distributed between two adjacent nodes along
 ! the y axis.
 ! Identify nodes that receive urea application.
 I_FERT1=NINT((U_DEPTH1+0.5*DZ)/DZ)
 ! The above variable identifies the depth node i that receives
 ! starter urea.
 J_FERT11=NINT(U_DIST1/DY)
 J_FERT12=J_FERT11+1
```

```
    ! J_FERT11 & J_FERT12 are the lateral nodes receiving starter urea.
    I_FERT2=NINT((U_DEPTH2+0.5*DZ)/DZ)
    J_FERT21=NINT(U_DIST2/DY)
    J_FERT22=J_FERT21+1
    ! I_FERT2, J_FERT21, and J_FERT22 pertain to sidedress urea
    ! application.
    ! U_MASS11 and U_MASS12 are equal urea amounts applied initially
    ! to J_FERT11 and J_FERT12, respectively.
    U_MASS11=(U_RATE1*ROW_SPACE*DY)*(0.01/2.0)
    U_MASS12=U_MASS11
    ! Urea application rate in kg/ha is converted to mass in mg in one
    ! node or cell by the factor (0.01/2.0)
    U_MASS21=(U_RATE2*ROW_SPACE*DZ)*(0.01/2.0)
    U_MASS22=U_MASS21
  !
    ALLOCATE(POT_EVAP(1:HR_END),POT_ET(1:HR_END),POT_TRANS(1:HR_END))
    ALLOCATE(POT_TRANS_LAY(2:L,PL_TIME+120:HV_TIME))
    CALL TRANSPIRATION(ET_REF,POT_ET,POT_EVAP,L,HR_END,TEN_D,PL_TIME,   &
     & HV_TIME,C_P,AIRTEMP,SOLRAD,ELEV,R,K_C,LAI,A_1,B_1,EXTINC_C,      &
     & MAX_ROOTDEPTH,DZ)
    ALLOCATE(TRANS_LAY(2:L))
    DEALLOCATE(ET_REF) ! This array is no longer needed
  !
    ! Read soil properties that do not vary by layer
    OPEN(UNIT=4,FILE="SOILPROP.DAT",STATUS="OLD",IOSTAT=IOS)
     IF (IOS/=0) THEN
      PRINT*,"Unable to open file SOILPROP.DAT"
     ELSE
      DO IL=1,3
       READ(UNIT=4,*)
      END DO
      READ(UNIT=4,FMT='(F5.2,F7.3,F8.1,F6.2)')BD,POR,LAMBDA_L,SOIL_PH
     END IF
    CLOSE(UNIT=4)
    ! Read soil parameters that affect unsat. K by layer
    ALLOCATE(KS(1:L),THETA_S(1:L),THETA_R(1:L),ALPHA_US(1:L),L_US(1:L), &
     & M_US(1:L),N_US(1:L))
    ALLOCATE(THETA_IN(1:L),THETA_MID(1:L),THETA_M(1:L),HEAD_IN(1:L),    &
     & HEAD_MID(1:L))
    ALLOCATE(KUS_IN(1:L),KUS_MID(1:L))
    ALLOCATE(FLUX_IN(1:L),FLUX_MID(1:L))
    ALLOCATE(SWC_IN(1:L),SWC_MID(1:L))
  !
    ALLOCATE(UCONC_IN(1:L,1:M),UCONC_MID(1:L,1:M),U_SINK(2:L-1,2:M-1),  &
     & ACONC_IN(1:L,1:M),ACONC_MID(1:L,1:M),A_SINK1(2:L-1,2:M-1),       &
     & NCONC_IN(1:L,1:M),NCONC_MID(1:L,1:M))
    ALLOCATE(UCONC_UP(1:L,1:M),UCONC_LO(1:L,1:M),ACONC_UP(1:L,1:M),     &
     & ACONC_LO(1:L,1:M),NCONC_UP(1:L,1:M),NCONC_LO(1:L,1:M))
    ALLOCATE(U_AP_DISP(1:L),A_AP_DISP(1:L),N_AP_DISP(1:L))
    ALLOCATE(UCONCMID(2:M-1),UCONCFIN(2:L-1),ACONCMID(2:M-1),           &
     & ACONCFIN(2:L-1),NCONCMID(1:M),NCONCFIN(2:L))
    ALLOCATE(AV_ACONC(2:L-1),AV_NCONC(2:L),NA_REM_LAY(2:L))
    ALLOCATE(A_M(2:L),B_M(1:L),C_M(1:L-1),K_M(1:L))
    ALLOCATE(A_U(3:M-1),B_U(2:M-1),C_U(2:M-2),K_U(2:M-1),A_U2(3:L-1),   &
     & B_U2(2:L-1),C_U2(2:L-2),K_U2(2:L-1))
    ALLOCATE(A_A(3:M-1),B_A(2:M-1),C_A(2:M-2),K_A(2:M-1),A_A2(3:L-1),   &
     & B_A2(2:L-1),C_A2(2:L-2),K_A2(2:L-1))
```

```
  ALLOCATE(A_N(3:M-1),B_N(2:M-1),C_N(2:M-2),K_N(2:M-1),A_N2(3:L),     &
   & B_N2(2:L),C_N2(2:L-1),K_N2(2:L))
!
  OPEN(UNIT=5,FILE="UNSAT.DAT",STATUS="OLD",IOSTAT=IOS)
  ! UNSAT.DAT contains for each layer: saturated K, vol. moisture
  ! content values at saturation and as residual, and van Genuchten
  ! parameters m, and L. Observe that all of the above parameters are
  ! obtained using RETC.FOR program; again, the values are least-square
  ! fitted values.  The unsaturated soil parameters must be specified
  ! by layer and layer thickness must be equal to DZ.
  IF (IOS/=0) THEN
   PRINT*,"Unable to open file UNSAT.DAT"
  ELSE
   DO IL=1,3
    READ(UNIT=5,*)
   END DO
    READ(UNIT=5,FMT='(10X,F6.3,F9.4,2F8.4,F6.2,2F8.4)')               &
     & (KS(I),THETA_S(I),THETA_R(I),ALPHA_US(I),L_US(I),M_US(I),      &
     & N_US(I),I=1,L)
  END IF
  CLOSE(UNIT=5)
  ! All of those arrays that have not already been allocated, will be
  ! allocated now.  Note that these arrays are required for the
  ! duration of the simulation and will be updated every time step.
  ! Supply initial soil moisture content values.
  OPEN(UNIT=6,FILE="MOIST.DAT",STATUS="OLD",IOSTAT=IOS)
   IF (IOS/=0) THEN
    PRINT*,"Unable to open file MOIST.DAT"
   ELSE
    DO IL=1,3
     READ(UNIT=6,*)
    END DO
    READ(UNIT=6,FMT='(F6.3)')(THETA_IN(I),I=1,L)
   END IF
  CLOSE(UNIT=6)
!
  PRINT*,"The model will search for the files for residual urea, "
  PRINT*," ammonium, and nitrate concentrations for all nodal "
  PRINT*,"points in the model domain.  If the file names are not"
  PRINT*,"found, the model will initialize the N species to zero "
  PRINT*," concentrations."
! Supply initial N species concentrations. Note that when N form
! concentrations are specified as zero in the following steps, the
! units are mg/mL.  However, residual N form concentrations are
! usually reported in mg/g-soil.  Hence, in the following files,
! if the residual N forms are non-zero, they will be converted into
! mg/mL.

  ! Urea
  OPEN(UNIT=7,FILE="UREA_IN.DAT",STATUS="OLD",IOSTAT=IOS)
   IF (IOS/=0) THEN
    PRINT*,"No residual urea file found, intializing urea "
    PRINT*,"concentrations to zero."
     UCONC_IN=0.0
   ELSE
    DO IL=1,3
     READ(UNIT=7,*)
```

```
    END DO
    READ(UNIT=7,FMT='(61F8.3)')((UCONC_IN(I,J),J=1,M),I=1,L)
    ! 61 is the number of nodes along the y-axis.
    DO I=1,L
     DO J=1,M
      UCONC_IN(I,J)=UCONC_IN(I,J)*BD/THETA_IN(I)
      ! Note that bulk density BD is assumed constant throughout
      ! the modeling domain.
     END DO
    END DO
   END IF
  CLOSE(UNIT=7)
!
  ! Ammonium
  OPEN(UNIT=8,FILE="AMMONIUM_IN.DAT",STATUS="OLD",IOSTAT=IOS)
   IF (IOS/=0) THEN
    PRINT*,"No residual ammonium file found,"
    PRINT*,"intializing concentrations to zero."
    ACONC_IN=0.0
   ELSE
    DO IL=1,3
     READ(UNIT=8,*)
    END DO
    READ(UNIT=8,FMT='(61F8.3)')((ACONC_IN(I,J),J=1,M),I=1,L)
    DO I=1,L
     DO J=1,M
      ACONC_IN(I,J)=ACONC_IN(I,J)*BD/THETA_IN(I)
     END DO
    END DO
   END IF
  CLOSE(UNIT=8)
  ! Nitrate
  OPEN(UNIT=9,FILE="NITRATE_IN.DAT",STATUS="OLD",IOSTAT=IOS)
   IF (IOS/=0) THEN
    PRINT*,"No residual nitrate file found, intializing concentration "
    PRINT*," to zero"
     NCONC_IN=0.0
   ELSE
    DO IL=1,3
     READ(UNIT=9,*)
    END DO
    READ(UNIT=9,FMT='(61F8.3)')((NCONC_IN(I,J),J=1,M),I=1,L)
    DO I=1,L
     DO J=1,M
      NCONC_IN(I,J)=NCONC_IN(I,J)*BD/THETA_IN(I)
     END DO
    END DO
   END IF
  CLOSE(UNIT=9)
!
  ! Create file to write out moisture content results
  OPEN(UNIT=11,FILE="MOIST.OUT",STATUS="REPLACE",POSITION="APPEND")
   110 FORMAT('Node-wise moisture content in the root zone',//,       &
      & 'Node thickness =  ',F4.2,' cm and the root zone depth = ',   &
    & F6.2,' cm')
   WRITE (11,110)DZ,MAX_ROOTDEPTH
  CLOSE(11)
```

```
!
  OPEN(UNIT=12,FILE="NITRATE.OUT",STATUS="REPLACE",POSITION="APPEND")
   120 FORMAT('File contains NO3-N loading,crop N removal,',          &
    & 'and node-wise nitrate, concentration data')
   WRITE(12,120)
  CLOSE(12)
!
  OPEN(UNIT=13,FILE="AMMONIUM.OUT",STATUS="REPLACE",POSITION="APPEND")
   130 FORMAT('File contains node-wise NH4 concentration data')
   WRITE(13,130)
  CLOSE(13)
!
  CALL THETA2HEAD(HEAD_IN,THETA_IN,THETA_S,THETA_R,ALPHA_US,M_US,     &
   & N_US,L)
  CALL KUNSAT(KUS_IN,HEAD_IN,HEAD_S,KS,ALPHA_US,L_US,M_US,N_US,L)
  CALL DARCY(FLUX_IN,KUS_IN,KS,HEAD_IN,HEAD_S,L,DZ)
  ! This subroutine is required to calculate theta_m since theta_in is
  ! supplied as initial condition.
  CALL HEAD2THETA(THETA_IN,THETA_M,HEAD_IN,HEAD_S,THETA_S,THETA_R,    &
   & ALPHA_US,M_US,N_US,L)
  ! The following subroutine is required to supply U_AP_DISP,.. values
  ! to the predictor for the first time step only.
  CALL AP_DISP(U_AP_DISP,A_AP_DISP,N_AP_DISP,UDIFF_AQ,ADIFF_AQ,       &
   & NDIFF_AQ,LAMBDA_L,POR,THETA_M,FLUX_IN,HEAD_IN,HEAD_4,L)
!
  ! Initialization
  T=0.0
  HR=1
  PERC_LOSS=0.0
  INFILT=0.0
  PRECIP=0.0
  EVAP=0.0
  TRANSPIRE=0.0
  CROP_NREM=0.0
  N_LEACH=0.0
  MAX_FLUX=1.0D0
  ! A maximum flux is assumed knowing that it will be compared with
  ! the surface flux in calculating the first time step in the
  ! simulation. Later in the simulation, the maximum flux anywhere
  ! in the soil profile is compared with the surface flux for the
  ! next hour in calculating time step.
!
  DO WHILE ((T_END-T_START)-T>1.0D-6)
  ! Based on soil and environmental conditions, actual infiltration
  ! or evaporation is calculated.
   IF (RAIN(HR)>0.0) THEN
    IF (HEAD_IN(1)<HEAD_S) THEN
     POT_INFILT=-((KUS_IN(1)+KS(1))*0.5)*(-1+(((0.5*(HEAD_IN(1)       &
      & +HEAD_IN(2)))-HEAD_S)/DZ))
     IF (POT_INFILT>=RAIN(HR)) THEN
      FLUX_SUR=RAIN(HR)
     ELSE
      FLUX_SUR=POT_INFILT
     END IF
    ELSE
     POT_INFILT=KS(1)
     IF (RAIN(HR)>=POT_INFILT) THEN
```

```
    FLUX_SUR=POT_INFILT
   ELSE
    FLUX_SUR=RAIN(HR)
   END IF
  END IF
   TRANS_LAY=0.0
 ELSE  ! No rain
  FLUX_SUR=-POT_EVAP(HR)
  ! If pressure head in i=1 equal or decreases below HEAD_5
  ! (-48000.0 cm), evaporative flux is controlled by upward moisture
  ! movement rather than by the environment (potential evaporation).
  IF ((HEAD_IN(1)<=HEAD_5) .AND. (FLUX_IN(1)<=0.0)) THEN
   IF (ABS(FLUX_IN(1))<POT_EVAP(HR)) THEN
    FLUX_SUR=FLUX_IN(1)
   ELSE
    FLUX_SUR=-POT_EVAP(HR)
   END IF
  END IF
 ! Transpiration is assumed non-zero 5-145 d after planting
  IF ((HR<PL_TIME+120) .OR. (HR>HV_TIME)) THEN
   TRANS_LAY=0.0
  ELSE ! The crop season
   POT_TRANS(HR)=POT_ET(HR)-ABS(FLUX_SUR)
    IF (POT_TRANS(HR)<=0.0) THEN
     TRANS_LAY=0.0
    ELSE ! Potential transpiration > zero
    ! The following statement is used to calculate potential
    ! transpiration by layer.
    ! After 145 d,transpiration = zero.
    TEN_D=INT((HR+120-PL_TIME)/240)
     DO I=2,L
      IF (I<=R(TEN_D)) THEN
       POT_TRANS_LAY(I,HR)=(((0.45*R(TEN_D))-(0.4*I)-0.1)           &
        & *POT_TRANS(HR))/(0.25*(R(TEN_D)-1)*(R(TEN_D)-2))
       IF (HEAD_IN(I)>=HEAD_2) THEN
        TRANS_LAY(I)=POT_TRANS_LAY(I,HR)/DZ
        ! For the Richards' equation to be dimensionally homogeneous,
        ! it has to be expressed in 1/hr units.  Hence POT_TRANS_LAY
        ! in the above equation as well as later are divided by DZ.
       ELSE IF(HEAD_IN(I)<HEAD_2 .AND.HEAD_IN(I)>=HEAD_3) THEN
        TRANS_LAY(I)=POT_TRANS_LAY(I,HR)*(HEAD_IN(I)-HEAD_3)        &
         &/((HEAD_2-HEAD_3)*DZ)
       ELSE  ! The layer has head < -20000.0 cm
        TRANS_LAY(I)=0.0
       END IF
      ELSE
       TRANS_LAY(I)=0.0
      END IF
     END DO
    END IF
   END IF
  END IF
  ! The maximum value of hydrodynamic dispersion is used for the CFL
  ! criterion. Ammonium'svalue is used since it has higher molecular
  ! diffusivity than the other two solutes.
  MAX_FLUX=MAXVAL(FLUX_IN(1:L))
   IF (ABS(MAX_FLUX)<ABS(FLUX_SUR)) THEN
```

```
      MAX_FLUX=FLUX_SUR
     END IF
    CALL TIMESTEP(PL_TIME,HR,A_AP_DISP,MAX_FLUX,THETA_M,TAU,DT_MANT,  &
     & DT_EXPO,DZ,DT)
    ! The following statement is needed to ensure that multiple
    ! time-steps always add up to 1 hour, the interval at for weather
    ! & ET data are available
    DT=MIN(DT,1.0-DMOD(T+0.000001D0,1.0D0))
     IF (1.0-DT<1.0D-6) THEN
      DT=1.0D0
     END IF
     ! The following step is needed for the last time-step
     IF ((T_END-T_START)-T<DT) THEN
      DT=T_END-T_START-T
     END IF
     T_NEW=T+DT
!******************Predictor for the moisture model*******************
  CALL SWCAP(SWC_IN,HEAD_IN,HEAD_S,HEAD_MAX,THETA_S,THETA_R,ALPHA_US, &
   & M_US,N_US,L)
   ! Surface layer
   I=1
    B_M(I)=(2*SWC_IN(I)/DT)+(KUS_IN(I)/(DZ**2))
    ! Note that kus(i) is actually evaluated at i+1/2
    C_M(I)=-KUS_IN(I)/(DZ**2)
    K_M(I)=(2*SWC_IN(I)*HEAD_IN(I)/DT)+((FLUX_SUR-KUS_IN(I))/DZ)
   DO I=2,L-1
    A_M(I)=-KUS_IN(I-1)/(DZ**2)
    B_M(I)=(2*SWC_IN(I)/DT)+((KUS_IN(I-1)+KUS_IN(I))/(DZ**2))
    C_M(I)=-KUS_IN(I)/(DZ**2)
    K_M(I)=(2*SWC_IN(I)*HEAD_IN(I)/DT)+((KUS_IN(I-1)-KUS_IN(I))/DZ)   &
     & -TRANS_LAY(I)
   END DO
   I=L
    A_M(I)=-1.0
    B_M(I)=1.0
    K_M(I)=0.0
   CALL TRIDIAG_M(HEAD_MID,A_M,B_M,C_M,K_M,L)
   CALL HEAD2THETA(THETA_MID,THETA_M,HEAD_MID,HEAD_S,THETA_S,THETA_R, &
    & ALPHA_US,M_US,N_US,L)
   CALL KUNSAT(KUS_MID,HEAD_MID,HEAD_S,KS,ALPHA_US,L_US,M_US,N_US,L)
   CALL DARCY(FLUX_MID,KUS_MID,KS,HEAD_MID,HEAD_S,L,DZ)
   IF (FLUX_MID(L)>0.0) THEN
    PERC_LOSS=PERC_LOSS+(FLUX_MID(L)*DT)
   END IF
!******************Predictor for the solute model*********************
! For this half of time step, for each node along the z axis, the
! solution will be marched along all y axis nodes. The initial
! conditions involve specification of N species concentration at all
! nodes in the computational domain using the relevant input files.
! Theta_mid, theta_in, and flux_in required as inputs are available
! from the moisture predictor. The following subroutine will prepare
! 2-D arrays of U_SINK and a_sink1_in.
   CALL HYDROLYSIS(UCONC_IN,UCONC_MM,UCONC_STOP,U_F_TEMP,U_A,         &
    & U_ACT_ENER,GAS,SOILTEMP,BD,U_VMAX,U_KMAX,L,M,HR,HR_END,U_SINK)
   CALL NITRIFICATION(THETA_IN,HEAD_IN,ACONC_IN,BD,HR,HR_END,L,M,     &
    & A_SINK1,SOILTEMP,N_F_TEMP,N_A,N_ACT_ENER,GAS,N_F_PH,SOIL_PH,    &
    & N_F_HEAD,ACONC_RR,ACONC_STOP,N_K1,N_K0)
```

```
    DO I=2,L
     IF (FLUX_IN(I)>=0.0) THEN
      DO J=1,M
       UCONC_LO(I,J)=UCONC_IN(I,J)
       ACONC_LO(I,J)=ACONC_IN(I,J)
       NCONC_LO(I,J)=NCONC_IN(I,J)
      END DO
     ELSE
      DO J=1,M
       UCONC_LO(I,J)=UCONC_IN(I+1,J)
       ACONC_LO(I,J)=ACONC_IN(I+1,J)
       NCONC_LO(I,J)=NCONC_IN(I+1,J)
      END DO
     END IF
    END DO
    DO I=2,L
     IF (FLUX_IN(I-1)>=0.0) THEN
      DO J=1,M
       UCONC_UP(I,J)=UCONC_IN(I-1,J)
       ACONC_UP(I,J)=ACONC_IN(I-1,J)
       NCONC_UP(I,J)=NCONC_IN(I-1,J)
      END DO
     ELSE
      DO J=1,M
       UCONC_UP(I,J)=UCONC_IN(I,J)
       ACONC_UP(I,J)=ACONC_IN(I,J)
       NCONC_UP(I,J)=NCONC_IN(I,J)
      END DO
     END IF
    END DO
   ! It is assumed that urea is not applied in the two top nodes and in
   ! the two extreme nodes, i.e., J=1 or 2 and J=M-1 or M.
!
    I=1
     DO J=1,M
      UCONC_MID(I,J)=0
      ACONC_MID(I,J)=0
      NCONC_MID(I,J)=0
     END DO
    I=2   ! There are no urea nodes in i=2
     J=1
      UCONC_MID(I,J)=0
      ACONC_MID(I,J)=0
      N_SINK=TRANS_LAY(I)*NCONC_IN(I,J)
      NCONCMID(J)=((2*THETA_IN(I)*NCONC_IN(I,J)/DT)+(N_AP_DISP(I)      &
       & *(NCONC_IN(I+1,J)-NCONC_IN(I,J))/(DZ**2))-(N_AP_DISP(I-1)     &
       & *NCONC_IN(I,J)/(DZ**2))-(NCONC_LO(I,J)*FLUX_IN(I)/DZ)-N_SINK) &
       & /(2*THETA_MID(I)/DT)
     J=2
      ! Urea
      C_U(J)=-UDIFF_AQ*(THETA_MID(I)**4.3)/(POR**2*DY**2)
      B_U(J)=2*((THETA_MID(I)/DT)-C_U(J))
      K_U(J)=(2*THETA_IN(I)*UCONC_IN(I,J)/DT)+(U_AP_DISP(I)            &
       & *(UCONC_IN(I+1,J)-UCONC_IN(I,J))/(DZ**2))-(U_AP_DISP(I-1)     &
       & *UCONC_IN(I,J)/(DZ**2))-(UCONC_LO(I,J)*FLUX_IN(I)/DZ)         &
       & -U_SINK(I,J)
      ! Ammonium
```

```
 C_A(J)=-ADIFF_AQ*(THETA_MID(I)**4.3)/(POR**2*DY**2)
 B_A(J)=2*((THETA_MID(I)/DT)-C_A(J)+(BD*K_DIS/DT))
 A_SINK2=TRANS_LAY(I)*ACONC_IN(I,J)
 K_A(J)=(2*THETA_IN(I)*ACONC_IN(I,J)/DT)+(2*BD*K_DIS*ACONC_IN(I,J)&
  & /DT)+(A_AP_DISP(I)*(ACONC_IN(I+1,J)-ACONC_IN(I,J))/(DZ**2))   &
  & -(A_AP_DISP(I-1)*ACONC_IN(I,J)/(DZ**2))-(ACONC_LO(I,J)        &
  & *FLUX_IN(I)/DZ)+(0.6*U_SINK(I,J))-A_SINK1(I,J)-A_SINK2
  ! In the above equation, the ammonium source is replaced by the
  ! urea sink times 0.6 to convert urea to ammonium.
 ! Nitrate
 C_N(J)=-NDIFF_AQ*(THETA_MID(I)**4.3)/(POR**2*DY**2)
 B_N(J)=2*((THETA_MID(I)/DT)-C_N(J))
 N_SINK=TRANS_LAY(I)*NCONC_IN(I,J)
 K_N(J)=(2*THETA_IN(I)*NCONC_IN(I,J)/DT)+(N_AP_DISP(I)            &
  & *(NCONC_IN(I+1,J)-NCONC_IN(I,J))/(DZ**2))-(N_AP_DISP(I-1)     &
  & *NCONC_IN(I,J)/(DZ**2))-(NCONC_LO(I,J)*FLUX_IN(I)/DZ)-N_SINK  &
  & -(C_N(J)*NCONCMID(J-1))+(3.4444*A_SINK1(I,J))
 ! In the above equation, the NO3- source is replaced by the NH4+
 ! sink with the 3.444 factor converting NH4+ to NO3-.
DO J=3,M-2
 ! Urea
 A_U(J)=-UDIFF_AQ*(THETA_MID(I)**4.3)/(POR**2*DY**2)
 B_U(J)=2*((THETA_MID(I)/DT)-A_U(J))
 C_U(J)=A_U(J)
 K_U(J)=(2*THETA_IN(I)*UCONC_IN(I,J)/DT)+(U_AP_DISP(I)            &
  & *(UCONC_IN(I+1,J)-UCONC_IN(I,J))/(DZ**2))-(U_AP_DISP(I-1)     &
  & *UCONC_IN(I,J)/(DZ**2))-(UCONC_LO(I,J)*FLUX_IN(I)/DZ)         &
  & -U_SINK(I,J)
 ! Ammonium
 A_A(J)=-ADIFF_AQ*(THETA_MID(I)**4.3)/(POR**2*DY**2)
 B_A(J)=2*((THETA_MID(I)/DT)-A_A(J)+(BD*K_DIS/DT))
 C_A(J)=A_A(J)
 A_SINK2=TRANS_LAY(I)*ACONC_IN(I,J)
 K_A(J)=(2*THETA_IN(I)*ACONC_IN(I,J)/DT)+(2*BD*K_DIS*ACONC_IN(I,J)&
  &/DT)+(A_AP_DISP(I)*(ACONC_IN(I+1,J)-ACONC_IN(I,J))/(DZ**2))    &
  & -(A_AP_DISP(I-1)*ACONC_IN(I,J)/(DZ**2))-(ACONC_LO(I,J)        &
  & *FLUX_IN(I)/DZ)+(0.6*U_SINK(I,J))-A_SINK1(I,J)-A_SINK2
 ! Nitrate
 A_N(J)=-NDIFF_AQ*(THETA_MID(I)**4.3)/(POR**2*DY**2)
 B_N(J)=2*((THETA_MID(I)/DT)-A_N(J))
 C_N(J)=A_N(J)
 N_SINK=TRANS_LAY(I)*NCONC_IN(I,J)
 K_N(J)=(2*THETA_IN(I)*NCONC_IN(I,J)/DT)+(N_AP_DISP(I)            &
  & *(NCONC_IN(I+1,J)-NCONC_IN(I,J))/(DZ**2))-(N_AP_DISP(I-1)     &
  & *NCONC_IN(I,J)/(DZ**2))-(NCONC_LO(I,J) *FLUX_IN(I)/DZ)-N_SINK &
  & +(3.4444*A_SINK1(I,J))
END DO
J=M
 UCONC_MID(I,J)=0
 ACONC_MID(I,J)=0
 N_SINK=TRANS_LAY(I)*NCONC_IN(I,J)
 NCONCMID(J)=((2*THETA_IN(I)*NCONC_IN(I,J)/DT)+(N_AP_DISP(I)      &
  & *(NCONC_IN(I+1,J)-NCONC_IN(I,J))/(DZ**2))-(N_AP_DISP(I-1)     &
  & *NCONC_IN(I,J)/(DZ**2))-(NCONC_LO(I,J)*FLUX_IN(I)/DZ)-N_SINK) &
  & /(2*THETA_MID(I)/DT)
J=M-1
 ! Urea
```

```
A_U(J)=-UDIFF_AQ*(THETA_MID(I)**4.3)/(POR**2*DY**2)
B_U(J)=2*((THETA_MID(I)/DT)-A_U(J))
K_U(J)=(2*THETA_IN(I)*UCONC_IN(I,J)/DT)+(U_AP_DISP(I)          &
 & *(UCONC_IN(I+1,J)-UCONC_IN(I,J))/(DZ**2))-(U_AP_DISP(I-1)     &
 & *UCONC_IN(I,J)/(DZ**2))-(UCONC_LO(I,J)*FLUX_IN(I)/DZ)         &
 & -U_SINK(I,J)
! Ammonium
A_A(J)=-ADIFF_AQ*(THETA_MID(I)**4.3)/(POR**2*DY**2)
B_A(J)=2*((THETA_MID(I)/DT)-A_A(J)+(BD*K_DIS/DT))
A_SINK2=TRANS_LAY(I)*ACONC_IN(I,J)
K_A(J)=(2*THETA_IN(I)*ACONC_IN(I,J)/DT)+(2*BD*K_DIS*ACONC_IN(I,J)&
 & /DT)+(A_AP_DISP(I)*(ACONC_IN(I+1,J)-ACONC_IN(I,J))/(DZ**2))   &
 & -(A_AP_DISP(I-1)*ACONC_IN(I,J)/(DZ**2))-(ACONC_LO(I,J)        &
 & *FLUX_IN(I)/DZ)+(0.6*U_SINK(I,J))-A_SINK1(I,J)-A_SINK2
! Nitrate
A_N(J)=-NDIFF_AQ*(THETA_MID(I)**4.3)/(POR**2*DY**2)
B_N(J)=2*((THETA_MID(I)/DT)-A_N(J))
N_SINK=TRANS_LAY(I)*NCONC_IN(I,J)
K_N(J)=(2*THETA_IN(I)*NCONC_IN(I,J)/DT)+(N_AP_DISP(I)          &
 & *(NCONC_IN(I+1,J)-NCONC_IN(I,J))/(DZ**2))-(N_AP_DISP(I-1)     &
 & *NCONC_IN(I,J)/(DZ**2))-(NCONC_LO(I,J)*FLUX_IN(I)/DZ)-N_SINK  &
 & -(A_N(J)*NCONCMID(J+1))+(3.4444*A_SINK1(I,J))
! Solve concentration values for I=2
CALL TRIDIAG(UCONCMID(2:M-1),A_U(3:M-1),B_U(2:M-1),C_U(2:M-2),   &
 & K_U(2:M-1),M)
! Data for the y nodes for a z node are inserted into a 2-D array
! in the required row
UCONC_MID(I,2:M-1)=UCONCMID(2:M-1)
CALL TRIDIAG(ACONCMID(2:M-1),A_A(3:M-1),B_A(2:M-1),C_A(2:M-2),   &
 & K_A(2:M-1),M)
ACONC_MID(I,2:M-1)=ACONCMID(2:M-1)
! The following statement averages the total NH4+ in a layer of y
! nodes(2:M-1) and converts it into NH4+-N.
AV_ACONC(I)=(SUM(ACONCMID(2:M-1))/(M-2))*0.7778
CALL TRIDIAG(NCONCMID(2:M-1),A_N(3:M-1),B_N(2:M-1),C_N(2:M-2),   &
 & K_N(2:M-1),M)
NCONC_MID(I,1:M)=NCONCMID(1:M)
AV_NCONC(I)=(SUM(NCONCMID(1:M))/M)*0.2258
! The following statement adds NH4+-N and NO3--N in each layer
! and calculates the total N removed from each layer in time DT.
NA_REM_LAY(I)=(AV_ACONC(I)+AV_NCONC(I))*DZ*TRANS_LAY(I)
DO I=3,L-2
 J=1
  UCONC_MID(I,J)=0.0
  ACONC_MID(I,J)=0.0
  N_SINK=TRANS_LAY(I)*NCONC_IN(I,J)
  NCONCMID(J)=((2*THETA_IN(I)*NCONC_IN(I,J)/DT)+(N_AP_DISP(I)    &
   & *(NCONC_IN(I+1,J)-NCONC_IN(I,J))/(DZ**2))-(N_AP_DISP(I-1)   &
   & *(NCONC_IN(I,J)-NCONC_IN(I-1,J))/(DZ**2))-((NCONC_LO(I,J)   &
   & *FLUX_IN(I)-NCONC_UP(I,J)*FLUX_IN(I-1))/DZ)-N_SINK)         &
   & /(2*THETA_MID(I)/DT)
 J=2  ! Note that there are no urea nodes in J=2
  ! Urea
  C_U(J)=-UDIFF_AQ*(THETA_MID(I)**4.3)/(POR**2*DY**2)
  B_U(J)=2*((THETA_MID(I)/DT)-C_U(J))
  K_U(J)=(2*THETA_IN(I)*UCONC_IN(I,J)/DT) +(U_AP_DISP(I)         &
   & *(UCONC_IN(I+1,J)-UCONC_IN(I,J))/(DZ**2))-(U_AP_DISP(I-1)   &
```

```
   & *(UCONC_IN(I,J)-UCONC_IN(I-1,J))/(DZ**2))-((UCONC_LO(I,J)   &
   & *FLUX_IN(I)-UCONC_UP(I,J)*FLUX_IN(I-1))/DZ)-U_SINK(I,J)
  ! Ammonium
  C_A(J)=-ADIFF_AQ*(THETA_MID(I)**4.3)/(POR**2*DY**2)
  B_A(J)=2*((THETA_MID(I)/DT)-C_A(J)+(BD*K_DIS/DT))
  A_SINK2=TRANS_LAY(I)*ACONC_IN(I,J)
  K_A(J)=(2*THETA_IN(I)*ACONC_IN(I,J)/DT)+(2*BD*K_DIS            &
   & *ACONC_IN(I,J)/DT)+(A_AP_DISP(I)*(ACONC_IN(I+1,J)           &
   & -ACONC_IN(I,J))/(DZ**2))-(A_AP_DISP(I-1)*(ACONC_IN(I,J)     &
   & -ACONC_IN(I-1,J))/(DZ**2))-((ACONC_LO(I,J)*FLUX_IN(I)       &
   & -ACONC_UP(I,J)*FLUX_IN(I-1))/DZ)+(0.6*U_SINK(I,J))          &
   & -A_SINK1(I,J)-A_SINK2
  ! Nitrate
  C_N(J)=-NDIFF_AQ*(THETA_MID(I)**4.3)/(POR**2*DY**2)
  B_N(J)=2*((THETA_MID(I)/DT)-C_N(J))
  N_SINK=TRANS_LAY(I)*NCONC_IN(I,J)
  K_N(J)=(2*THETA_IN(I)*NCONC_IN(I,J)/DT)-(C_N(J)*NCONCMID(J-1)) &
   & +(N_AP_DISP(I)*(NCONC_IN(I+1,J)-NCONC_IN(I,J))/(DZ**2))     &
   & -(N_AP_DISP(I-1)*(NCONC_IN(I,J)-NCONC_IN(I-1,J))/(DZ**2))   &
   &-((NCONC_LO(I,J)*FLUX_IN(I)-NCONC_UP(I,J)*FLUX_IN(I-1))/DZ)  &
   & +(3.4444*A_SINK1(I,J))-N_SINK
!
 DO J=3,M-2
  ! The If statements below are required to identify the time and
  ! location of urea application so that the source term in the
  ! urea equations can be quantified.
  ! For the starter:
  IF (T_NEW<U_TIME1) THEN
   U_SOURCE=0.0
  ELSE IF ((T_NEW>=U_TIME1 .AND. T_NEW<U_TIME2).AND.             &
   & (U_MASS11>0.0 .OR. U_MASS12>0.0)) THEN
   IF (I==I_FERT1 .AND. J==J_FERT11) THEN
    U_DISS11=U_SLOPE*U_MASS11*((0.5*DT)**0.5)
     IF (U_DISS11<=0.0001) THEN
      U_DISS11=0.0
     END IF
     U_SOURCE=U_DISS11/((0.5*DT)*(DZ**3))
     U_MASS11=U_MASS11-U_DISS11
     IF (U_MASS11<=0.0001) THEN
      U_MASS11=0.0
      ! Urea < 0.1 mcg, is assumed equal to zero.
     END IF
  ELSE IF (I==I_FERT1 .AND.J==J_FERT12) THEN
   U_DISS12=U_SLOPE*U_MASS12*((0.5*DT)**0.5)
   IF (U_DISS12<=0.0001) THEN
    U_DISS12=0.0
   END IF
   U_SOURCE=U_DISS12/((0.5*DT)*(DZ**3))
   U_MASS12=U_MASS12-U_DISS12
   IF (U_MASS12<=0.0001) THEN
    U_MASS12=0.0
    ! Urea < 0.1 mcg, is assumed equal to zero.
   END IF
  ELSE
   U_SOURCE=0.0
  END IF
 ELSE IF (T_NEW<U_TIME2 .AND.(U_MASS11==0.0 .AND. U_MASS12==0.0))&
```

```
 & THEN
! Assumed that all starter urea has dissolved at the time of
! sidedress application.
 U_SOURCE=0.0
ELSE IF (T_NEW>=U_TIME2 .AND.(U_MASS21>0.0 .OR. U_MASS22>0.0))  &
 & THEN
! This is for the sidedress
 IF (I==I_FERT2 .AND.J==J_FERT21) THEN
  U_DISS21=U_SLOPE*U_MASS21*((0.5*DT)**0.5)
   IF (U_DISS21<=0.0001) THEN
    U_DISS21=0.0
   END IF
   U_SOURCE=U_DISS21/((0.5*DT)*(DZ**3))
   U_MASS21=U_MASS21-U_DISS21
   IF (U_MASS21<=0.0001) THEN
    U_MASS21=0.0
   END IF
 ELSE IF (I==I_FERT2 .AND.J==J_FERT22) THEN
  U_DISS22=U_SLOPE*U_MASS22*((0.5*DT)**0.5)
  IF (U_DISS22<=0.0001) THEN
   U_DISS22=0.0
  END IF
  U_SOURCE=U_DISS22/((0.5*DT)*(DZ**3))
  U_MASS22=U_MASS22-U_DISS22
  IF (U_MASS22<=0.0001) THEN
   U_MASS22=0.0
  END IF
 ELSE
  U_SOURCE=0.0
 END IF
ELSE
 U_SOURCE=0.0
END IF
 ! Urea
 A_U(J)=-UDIFF_AQ*(THETA_MID(I)**4.3)/(POR**2*DY**2)
 B_U(J)=2*((THETA_MID(I)/DT)-A_U(J))
 C_U(J)=A_U(J)
 K_U(J)=(2*THETA_IN(I)*UCONC_IN(I,J)/DT)+(U_AP_DISP(I)          &
  & *(UCONC_IN(I+1,J)-UCONC_IN(I,J))/(DZ**2))-(U_AP_DISP(I-1)   &
  & *(UCONC_IN(I,J)-UCONC_IN(I-1,J))/(DZ**2))-((UCONC_LO(I,J)   &
  & *FLUX_IN(I)-UCONC_UP(I,J)*FLUX_IN(I-1))/DZ)+U_SOURCE        &
  & -U_SINK(I,J)
 ! Ammonium
 A_A(J)=-ADIFF_AQ*(THETA_MID(I)**4.3)/(POR**2*DY**2)
 B_A(J)=2*((THETA_MID(I)/DT)-A_A(J)+(BD*K_DIS/DT))
 C_A(J)=A_A(J)
 A_SINK2=TRANS_LAY(I)*ACONC_IN(I,J)
 K_A(J)=(2*THETA_IN(I)*ACONC_IN(I,J)/DT)+(2*BD*K_DIS            &
  & *ACONC_IN(I,J)/DT)+(A_AP_DISP(I)*(ACONC_IN(I+1,J)           &
  & -ACONC_IN(I,J))/(DZ**2))-(A_AP_DISP(I-1)*(ACONC_IN(I,J)     &
  & -ACONC_IN(I-1,J))/(DZ**2))-((ACONC_LO(I,J)*FLUX_IN(I)       &
  & -ACONC_UP(I,J)*FLUX_IN(I-1))/DZ)+(0.6*U_SINK(I,J))          &
  & -A_SINK1(I,J)-A_SINK2
 ! Nitrate
 A_N(J)=-NDIFF_AQ*(THETA_MID(I)**4.3)/(POR**2*DY**2)
 B_N(J)=2*((THETA_MID(I)/DT)-A_N(J))
 C_N(J)=A_N(J)
```

```
         N_SINK=TRANS_LAY(I)*NCONC_IN(I,J)
         K_N(J)=(2*THETA_IN(I)*NCONC_IN(I,J)/DT)+(N_AP_DISP(I)          &
          & *(NCONC_IN(I+1,J)-NCONC_IN(I,J))/(DZ**2))-(N_AP_DISP(I-1)   &
          & *(NCONC_IN(I,J)-NCONC_IN(I-1,J))/(DZ**2))-((NCONC_LO(I,J)   &
          & *FLUX_IN(I)-NCONC_UP(I,J)*FLUX_IN(I-1))/DZ)-N_SINK          &
          & +(3.4444*A_SINK1(I,J))
        END DO   ! J=3,M-2
!
        J=M
         UCONC_MID(I,J)=0.0
         ACONC_MID(I,J)=0.0
         N_SINK=TRANS_LAY(I)*NCONC_IN(I,J)
         NCONCMID(J)=((2*THETA_IN(I)*NCONC_IN(I,J)/DT)+(N_AP_DISP(I)    &
          & *(NCONC_IN(I+1,J)-NCONC_IN(I,J))/(DZ**2))-(N_AP_DISP(I-1)   &
          & *(NCONC_IN(I,J)-NCONC_IN(I-1,J))/(DZ**2))-((NCONC_LO(I,J)   &
          & *FLUX_IN(I)-NCONC_UP(I,J)*FLUX_IN(I-1))/DZ)-N_SINK)         &
          & /(2*THETA_MID(I)/DT)
!
        J=M-1
         ! Urea
         A_U(J)=-UDIFF_AQ*(THETA_MID(I)**4.3)/(POR**2*DY**2)
         B_U(J)=2*((THETA_MID(I)/DT)-A_U(J))
         K_U(J)=(2*THETA_IN(I)*UCONC_IN(I,J)/DT)+(U_AP_DISP(I)          &
          & *(UCONC_IN(I+1,J)-UCONC_IN(I,J))/(DZ**2))-(U_AP_DISP(I-1)   &
          & *(UCONC_IN(I,J)-UCONC_IN(I-1,J))/(DZ**2))-((UCONC_LO(I,J)   &
          & *FLUX_IN(I)-UCONC_UP(I,J)*FLUX_IN(I-1))/DZ)-U_SINK(I,J)
         ! Ammonium
         A_A(J)=-ADIFF_AQ*(THETA_MID(I)**4.3)/(POR**2*DY**2)
         B_A(J)=2*((THETA_MID(I)/DT)-A_A(J)+(BD*K_DIS/DT))
         A_SINK2=TRANS_LAY(I)*ACONC_IN(I,J)
         K_A(J)=(2*THETA_IN(I)*ACONC_IN(I,J)/DT)+(2*BD*K_DIS            &
          & *ACONC_IN(I,J)/DT)+(A_AP_DISP(I)*(ACONC_IN(I+1,J)           &
          & -ACONC_IN(I,J))/(DZ**2))-(A_AP_DISP(I-1)*(ACONC_IN(I,J)     &
          & -ACONC_IN(I-1,J))/(DZ**2))-((ACONC_LO(I,J)*FLUX_IN(I)       &
          & -ACONC_UP(I,J)*FLUX_IN(I-1))/DZ)+(0.6*U_SINK(I,J))          &
          & -A_SINK1(I,J)-A_SINK2
         ! Nitrate
         A_N(J)=-NDIFF_AQ*(THETA_MID(I)**4.3)/(POR**2*DY**2)
         B_N(J)=2*((THETA_MID(I)/DT)-A_N(J))
         N_SINK=TRANS_LAY(I)*NCONC_IN(I,J)
         K_N(J)=(2*THETA_IN(I)*NCONC_IN(I,J)/DT)-(A_N(J)*NCONCMID(J+1)) &
          & +(N_AP_DISP(I)*(NCONC_IN(I+1,J)-NCONC_IN(I,J))/(DZ**2))     &
          & -(N_AP_DISP(I-1)*(NCONC_IN(I,J)-NCONC_IN(I-1,J))/(DZ**2))   &
          & -((NCONC_LO(I,J)*FLUX_IN(I)-NCONC_UP(I,J)*FLUX_IN(I-1))/DZ) &
          & +(3.4444*A_SINK1(I,J))-N_SINK
        ! Need to insert CALL TRIDIAG for I=3,L-2
        CALL TRIDIAG(UCONCMID(2:M-1),A_U(3:M-1),B_U(2:M-1),C_U(2:M-2),  &
         & K_U(2:M-1),M)
         UCONC_MID(I,2:M-1)=UCONCMID(2:M-1)
        CALL TRIDIAG(ACONCMID(2:M-1),A_A(3:M-1),B_A(2:M-1),C_A(2:M-2),  &
         & K_A(2:M-1),M)
         ACONC_MID(I,2:M-1)=ACONCMID(2:M-1)
         AV_ACONC(I)=(SUM(ACONCMID(2:M-1))/(M-2))*0.7778
        CALL TRIDIAG(NCONCMID(2:M-1),A_N(3:M-1),B_N(2:M-1),C_N(2:M-2),  &
         & K_N(2:M-1),M)
         NCONC_MID(I,1:M)=NCONCMID(1:M)
         AV_NCONC(I)=(SUM(NCONCMID(1:M))/M)*0.2258
```

```
      ! The following statement adds NH4+-N and NO3--N in each layer and
      ! calculates the total N removed from each layer in time DT.
        NA_REM_LAY(I)=(AV_ACONC(I)+AV_NCONC(I))*DZ*TRANS_LAY(I)
      END DO ! I=3,L-2
!
      I=L-1
       J=1
        UCONC_MID(I,J)=0
        ACONC_MID(I,J)=0
        N_SINK=TRANS_LAY(I)*NCONC_IN(I,J)
        NCONCMID(J)=((2*THETA_IN(I)*NCONC_IN(I,J)/DT)+(N_AP_DISP(I)    &
         & *(NCONC_IN(I+1,J)-NCONC_IN(I,J))/(DZ**2))-(N_AP_DISP(I-1)   &
         & *(NCONC_IN(I,J)-NCONC_IN(I-1,J))/(DZ**2))-((NCONC_LO(I,J)   &
         & *FLUX_IN(I)-NCONC_UP(I,J)*FLUX_IN(I-1))/DZ)-N_SINK)         &
         & /(2*THETA_MID(I)/DT)
       J=2
        ! Urea
        C_U(J)=-UDIFF_AQ*(THETA_MID(I)**4.3)/(POR**2*DY**2)
        B_U(J)=2*((THETA_MID(I)/DT)-C_U(J))
        K_U(J)=(2*THETA_IN(I)*UCONC_IN(I,J)/DT)+(U_AP_DISP(I)          &
         & *(UCONC_IN(I+1,J)-UCONC_IN(I,J))/(DZ**2))-(U_AP_DISP(I-1)   &
         & *(UCONC_IN(I,J)-UCONC_IN(I-1,J))/(DZ**2))-((UCONC_LO(I,J)   &
         & *FLUX_IN(I)-UCONC_UP(I,J)*FLUX_IN(I-1))/DZ)-U_SINK(I,J)
        ! Ammonium
        C_A(J)=-ADIFF_AQ*(THETA_MID(I)**4.3)/(POR**2*DY**2)
        B_A(J)=2*((THETA_MID(I)/DT)-C_A(J)+(BD*K_DIS/DT))
        A_SINK2=TRANS_LAY(I)*ACONC_IN(I,J)
        K_A(J)=(2*THETA_IN(I)*ACONC_IN(I,J)/DT)+(2*BD*K_DIS            &
         & *ACONC_IN(I,J)/DT)+(A_AP_DISP(I)*(ACONC_IN(I+1,J)           &
         & -ACONC_IN(I,J))/(DZ**2))-(A_AP_DISP(I-1)*(ACONC_IN(I,J)     &
         & -ACONC_IN(I-1,J))/(DZ**2))-((ACONC_LO(I,J)*FLUX_IN(I)       &
         & -ACONC_UP(I,J)*FLUX_IN(I-1))/DZ)+(0.6*U_SINK(I,J))          &
         & -A_SINK1(I,J)-A_SINK2
        ! Nitrate
        C_N(J)=-NDIFF_AQ*(THETA_MID(I)**4.3)/(POR**2*DY**2)
        B_N(J)=2*((THETA_MID(I)/DT)-C_N(J))
        N_SINK=TRANS_LAY(I)*NCONC_IN(I,J)
        K_N(J)=(2*THETA_IN(I)*NCONC_IN(I,J)/DT)-(C_N(J)*NCONCMID(J-1)) &
         & +(N_AP_DISP(I)*(NCONC_IN(I+1,J)-NCONC_IN(I,J))/(DZ**2))     &
         & -(N_AP_DISP(I-1)*(NCONC_IN(I,J)-NCONC_IN(I-1,J))/(DZ**2))   &
         & -((NCONC_LO(I,J)*FLUX_IN(I)-NCONC_UP(I,J)*FLUX_IN(I-1))/DZ) &
         & -N_SINK+(3.4444*A_SINK1(I,J))
       DO J=3,M-2
        ! Urea
        A_U(J)=-UDIFF_AQ*(THETA_MID(I)**4.3)/(POR**2*DY**2)
        B_U(J)=2*((THETA_MID(I)/DT)-A_U(J))
        C_U(J)=A_U(J)
        K_U(J)=(2*THETA_IN(I)*UCONC_IN(I,J)/DT)+(U_AP_DISP(I)          &
         & *(UCONC_IN(I+1,J)-UCONC_IN(I,J))/(DZ**2))-(U_AP_DISP(I-1)   &
         & *(UCONC_IN(I,J)-UCONC_IN(I-1,J))/(DZ**2))-((UCONC_LO(I,J)   &
         & *FLUX_IN(I)-UCONC_UP(I,J)*FLUX_IN(I-1))/DZ)-U_SINK(I,J)
        ! Ammonium
        A_A(J)=-ADIFF_AQ*(THETA_MID(I)**4.3)/(POR**2*DY**2)
        B_A(J)=2*((THETA_MID(I)/DT)-A_A(J)+(BD*K_DIS/DT))
        C_A(J)=A_A(J)
        A_SINK2=TRANS_LAY(I)*ACONC_IN(I,J)
        K_A(J)=(2*THETA_IN(I)*ACONC_IN(I,J)/DT)+(2*BD*K_DIS            &
```

```
     & *ACONC_IN(I,J)/DT)+(A_AP_DISP(I)*(ACONC_IN(I+1,J)          &
     & -ACONC_IN(I,J))/(DZ**2))-(A_AP_DISP(I-1)*(ACONC_IN(I,J)     &
     & -ACONC_IN(I-1,J))/(DZ**2))-((ACONC_LO(I,J)*FLUX_IN(I)       &
     & -ACONC_UP(I,J)*FLUX_IN(I-1))/DZ)+(0.6*U_SINK(I,J))          &
     & -A_SINK1(I,J)-A_SINK2
    ! Nitrate
    A_N(J)=-NDIFF_AQ*(THETA_MID(I)**4.3)/(POR**2*DY**2)
    B_N(J)=2*((THETA_MID(I)/DT)-A_N(J))
    C_N(J)=A_N(J)
    N_SINK=TRANS_LAY(I)*NCONC_IN(I,J)
    K_N(J)=(2*THETA_IN(I)*NCONC_IN(I,J)/DT)+(N_AP_DISP(I)          &
     & *(NCONC_IN(I+1,J)-NCONC_IN(I,J))/(DZ**2))-(N_AP_DISP(I-1)   &
     & *(NCONC_IN(I,J)-NCONC_IN(I-1,J))/(DZ**2))-((NCONC_LO(I,J)   &
     & *FLUX_IN(I)-NCONC_UP(I,J)*FLUX_IN(I-1))/DZ)-N_SINK          &
     & +(3.4444*A_SINK1(I,J))
   END DO
!
   J=M
    UCONC_MID(I,J)=0
    ACONC_MID(I,J)=0
    N_SINK=TRANS_LAY(I)*NCONC_IN(I,J)
    NCONCMID(J)=((2*THETA_IN(I)*NCONC_IN(I,J)/DT)+(N_AP_DISP(I)    &
     & *(NCONC_IN(I+1,J)-NCONC_IN(I,J))/(DZ**2))-(N_AP_DISP(I-1)   &
     & *(NCONC_IN(I,J)-NCONC_IN(I-1,J))/(DZ**2))-((NCONC_LO(I,J)   &
     & *FLUX_IN(I)-NCONC_UP(I,J)*FLUX_IN(I-1))/DZ)-N_SINK)         &
     & /(2*THETA_MID(I)/DT)
   J=M-1
    ! Urea
    A_U(J)=-UDIFF_AQ*(THETA_MID(I)**4.3)/(POR**2*DY**2)
    B_U(J)=2*((THETA_MID(I)/DT)-A_U(J))
    K_U(J)=(2*THETA_IN(I)*UCONC_IN(I,J)/DT)+(U_AP_DISP(I)          &
     & *(UCONC_IN(I+1,J)-UCONC_IN(I,J))/(DZ**2))-(U_AP_DISP(I-1)   &
     & *(UCONC_IN(I,J)-UCONC_IN(I-1,J))/(DZ**2))-((UCONC_LO(I,J)   &
     & *FLUX_IN(I)-UCONC_UP(I,J)*FLUX_IN(I-1))/DZ)-U_SINK(I,J)
    ! Ammonium
    A_A(J)=-ADIFF_AQ*(THETA_MID(I)**4.3)/(POR**2*DY**2)
    B_A(J)=2*((THETA_MID(I)/DT)-A_A(J)+(BD*K_DIS/DT))
    A_SINK2=TRANS_LAY(I)*ACONC_IN(I,J)
    K_A(J)=(2*THETA_IN(I)*ACONC_IN(I,J)/DT)+(2*BD*K_DIS            &
     & *ACONC_IN(I,J)/DT)+(A_AP_DISP(I)*(ACONC_IN(I+1,J)          &
     & -ACONC_IN(I,J))/(DZ**2))-(A_AP_DISP(I-1)*(ACONC_IN(I,J)     &
     & -ACONC_IN(I-1,J))/(DZ**2))-((ACONC_LO(I,J)*FLUX_IN(I)       &
     & -ACONC_UP(I,J)*FLUX_IN(I-1))/DZ)+(0.6*U_SINK(I,J))          &
     & -A_SINK1(I,J)-A_SINK2
    ! Nitrate
    A_N(J)=-NDIFF_AQ*(THETA_MID(I)**4.3)/(POR**2*DY**2)
    B_N(J)=2*((THETA_MID(I)/DT)-A_N(J))
    N_SINK=TRANS_LAY(I)*NCONC_IN(I,J)
    K_N(J)=(2*THETA_IN(I)*NCONC_IN(I,J)/DT)-(A_N(J)*NCONCMID(J+1)) &
     & +(N_AP_DISP(I)*(NCONC_IN(I+1,J)-NCONC_IN(I,J))/(DZ**2))     &
     & -(N_AP_DISP(I-1)*(NCONC_IN(I,J)-NCONC_IN(I-1,J))/(DZ**2))   &
     & -((NCONC_LO(I,J)*FLUX_IN(I)-NCONC_UP(I,J)*FLUX_IN(I-1))/DZ) &
     & -N_SINK+(3.4444*A_SINK1(I,J))
!
   CALL TRIDIAG(UCONCMID(2:M-1),A_U(3:M-1),B_U(2:M-1),C_U(2:M-2),  &
    & K_U(2:M-1),M)
    UCONC_MID(I,2:M-1)=UCONCMID(2:M-1)
```

```
      CALL TRIDIAG(ACONCMID(2:M-1),A_A(3:M-1),B_A(2:M-1),C_A(2:M-2),  &
       &K_A(2:M-1),M)
       ACONC_MID(I,2:M-1)=ACONCMID(2:M-1)
       AV_ACONC(I)=(SUM(ACONCMID(2:M-1))/(M-2))*0.7778
      CALL TRIDIAG(NCONCMID(2:M-1),A_N(3:M-1),B_N(2:M-1),C_N(2:M-2),  &
       & K_N(2:M-1),M)
       NCONC_MID(I,1:M)=NCONCMID(1:M)
       AV_NCONC(I)=(SUM(NCONCMID(1:M))/M)*0.2258
       NA_REM_LAY(I)=(AV_ACONC(I)+AV_NCONC(I))*DZ*TRANS_LAY(I)
!
     I=L
      J=1
       UCONC_MID(I,J)=0
       ACONC_MID(I,J)=0
       N_SINK=TRANS_LAY(I)*NCONC_IN(I,J)
       NCONCMID(J)=((2*THETA_IN(I)*NCONC_IN(I,J)/DT)+((N_AP_DISP(I)   &
        & -N_AP_DISP(I-1))*(NCONC_IN(I,J)-NCONC_IN(I-1,J))/(DZ**2))   &
        & -((NCONC_IN(I,J)*FLUX_IN(I)-NCONC_IN(I-1,J)*FLUX_IN(I-1))   &
        & /DZ)-N_SINK)/(2*THETA_MID(I)/DT)
      J=2
       UCONC_MID(I,J)=0
       ACONC_MID(I,J)=0
       C_N(J)=-NDIFF_AQ*(THETA_MID(I)**4.3)/(POR**2*DY**2)
       B_N(J)=2*((THETA_MID(I)/DT)-C_N(J))
       N_SINK=TRANS_LAY(I)*NCONC_IN(I,J)
       K_N(J)=(2*THETA_IN(I)*NCONC_IN(I,J)/DT)-(C_N(J)*NCONCMID(J-1)) &
        & +((N_AP_DISP(I)-N_AP_DISP(I-1))*(NCONC_IN(I,J)              &
        & -NCONC_IN(I-1,J))/(DZ**2))-((NCONC_IN(I,J)*FLUX_IN(I)       &
        & -NCONC_IN(I-1,J)*FLUX_IN(I-1))/DZ)-N_SINK
      DO J=3,M-2
       UCONC_MID(I,J)=0
       ACONC_MID(I,J)=0
       A_N(J)=-NDIFF_AQ*(THETA_MID(I)**4.3)/(POR**2*DY**2)
       B_N(J)=2*((THETA_MID(I)/DT)-A_N(J))
       C_N(J)=A_N(J)
       N_SINK=TRANS_LAY(I)*NCONC_IN(I,J)
       K_N(J)=(2*THETA_IN(I)*NCONC_IN(I,J)/DT)+((N_AP_DISP(I)         &
        & -N_AP_DISP(I-1))*(NCONC_IN(I,J)-NCONC_IN(I-1,J))/(DZ**2))   &
        & -((NCONC_IN(I,J)*FLUX_IN(I)-NCONC_IN(I-1,J)*FLUX_IN(I-1))   &
        & /DZ)-N_SINK
      END DO
      J=M
       UCONC_MID(I,J)=0
       ACONC_MID(I,J)=0
       N_SINK=TRANS_LAY(I)*NCONC_IN(I,J)
       NCONCMID(J)=((2*THETA_IN(I)*NCONC_IN(I,J)/DT)+((N_AP_DISP(I)   &
        & -N_AP_DISP(I-1))*(NCONC_IN(I,J)-NCONC_IN(I-1,J))/(DZ**2))   &
        & -((NCONC_IN(I,J)*FLUX_IN(I)-NCONC_IN(I-1,J)*FLUX_IN(I-1))   &
        & /DZ)-N_SINK)/(2*THETA_MID(I)/DT)
      J=M-1
       UCONC_MID(I,J)=0
       ACONC_MID(I,J)=0
       A_N(J)=-NDIFF_AQ*(THETA_MID(I)**4.3)/(POR**2*DY**2)
       B_N(J)=2*((THETA_MID(I)/DT)-A_N(J))
       N_SINK=TRANS_LAY(I)*NCONC_IN(I,J)
       K_N(J)=(2*THETA_IN(I)*NCONC_IN(I,J)/DT)-(A_N(J)*NCONCMID(J+1)) &
        & +((N_AP_DISP(I)-N_AP_DISP(I-1))*(NCONC_IN(I,J)              &
```

```
        & -NCONC_IN(I-1,J))/(DZ**2))-((NCONC_IN(I,J)*FLUX_IN(I)       &
        & -NCONC_IN(I-1,J)*FLUX_IN(I-1))/DZ)-N_SINK
       ! Call TRIDIAG for nitrate only for I=L
      CALL TRIDIAG(NCONCMID(2:M-1),A_N(3:M-1),B_N(2:M-1),C_N(2:M-2),  &
       & K_N(2:M-1),M)
       NCONC_MID(L,1:M)=NCONCMID(1:M)
       AV_NCONC(L)=SUM(NCONCMID(1:M))*0.22581/M
       NA_REM_LAY(I)=AV_NCONC(L)*DZ*TRANS_LAY(L)
      ! NA_REM_LAY(I) is in mg/sq. cm-h of N removed by plant from the
      ! node i
!
      ! After exiting the I loop, N leached and removed by crop are
      ! updated.  When av_nconc (mg/mL) is multiplied with perc_vol
      ! (cm) times 100, n_leach is obtained in kg-N/ha.
      N_LEACH=N_LEACH+(AV_NCONC(L)*FLUX_MID(L)*DT*100.00)
      CROP_NREM=CROP_NREM+(SUM(NA_REM_LAY(2:L))*DT*100.00)
!*****************Corrector for the moisture model*******************
   CALL SWCAP(SWC_MID,HEAD_MID,HEAD_S,HEAD_MAX,THETA_S,THETA_R,
&
    & ALPHA_US,M_US,N_US,L)
!
     I=1
      B_M(I)=(SWC_MID(I)/DT)+(0.5*KUS_MID(I)/(DZ**2))
      C_M(I)=-0.5*KUS_MID(I)/(DZ**2)
      K_M(I)=(SWC_MID(I)*HEAD_IN(I)/DT)+(0.5*KUS_MID(I)*(HEAD_IN(I+1) &
       & -HEAD_IN(I))/(DZ**2))+((FLUX_SUR-KUS_MID(I))/DZ)
     DO I=2,L-1
      A_M(I)=-0.5*KUS_MID(I-1)/(DZ**2)
      B_M(I)=(SWC_MID(I)/DT)+(0.5*(KUS_MID(I)+KUS_MID(I-1))/(DZ**2))
      C_M(I)=-0.5*KUS_MID(I)/(DZ**2)
      K_M(I)=(SWC_MID(I)*HEAD_IN(I)/DT)+(0.5*KUS_MID(I)*(HEAD_IN(I+1) &
       & -HEAD_IN(I))/(DZ**2))-(0.5*KUS_MID(I-1)*(HEAD_IN(I)          &
       & -HEAD_IN(I-1))/(DZ**2))+((KUS_MID(I-1)-KUS_MID(I))/DZ)       &
       & -TRANS_LAY(I)
    END DO
     I=L
      A_M(I)=-1.0
      B_M(I)=1.0
      K_M(I)=0.0
!
    CALL TRIDIAG_M(HEAD_IN,A_M,B_M,C_M,K_M,L)
    CALL HEAD2THETA(THETA_IN,THETA_M,HEAD_IN,HEAD_S,THETA_S,THETA_R,  &
     & ALPHA_US,M_US,N_US,L)
    CALL KUNSAT(KUS_IN,HEAD_IN,HEAD_S,KS,ALPHA_US,L_US,M_US,N_US,L)
    CALL DARCY(FLUX_IN,KUS_IN,KS,HEAD_IN,HEAD_S,L,DZ)
!**************Corrector for solute model****************************
! For this half of time step, for each node along they axis, the
! solution will be marched along all z axis nodes. Theta_mid values
! were obtained with the moisture predictor
    CALL HYDROLYSIS(UCONC_MID,UCONC_MM,UCONC_STOP,U_F_TEMP,U_A,       &
     & U_ACT_ENER,GAS,SOILTEMP,BD,U_VMAX,U_KMAX,L,M,HR,HR_END,U_SINK)
    CALL NITRIFICATION(THETA_MID,HEAD_MID,ACONC_MID,BD,HR,HR_END,L,M, &
     & A_SINK1,SOILTEMP,N_F_TEMP,N_A,N_ACT_ENER,GAS,N_F_PH,SOIL_PH,   &
     & N_F_HEAD,ACONC_RR,ACONC_STOP,N_K1,N_K0)
    CALL AP_DISP(U_AP_DISP,A_AP_DISP,N_AP_DISP,UDIFF_AQ,ADIFF_AQ,     &
     & NDIFF_AQ,LAMBDA_L,POR,THETA_M,FLUX_IN,HEAD_IN,HEAD_4,L)
    DO I=2,L
```

```
     IF (FLUX_MID(I)>=0.0) THEN
      DO J=1,M
       UCONC_LO(I,J)=UCONC_MID(I,J)
       ACONC_LO(I,J)=ACONC_MID(I,J)
       NCONC_LO(I,J)=NCONC_MID(I,J)
      END DO
     ELSE
      DO J=1,M
       UCONC_LO(I,J)=UCONC_MID(I+1,J)
       ACONC_LO(I,J)=ACONC_MID(I+1,J)
       NCONC_LO(I,J)=NCONC_MID(I+1,J)
      END DO
     END IF
    END DO
    DO I=2,L
     IF (FLUX_MID(I-1)>=0.0) THEN
      DO J=1,M
       UCONC_UP(I,J)=UCONC_MID(I-1,J)
       ACONC_UP(I,J)=ACONC_MID(I-1,J)
       NCONC_UP(I,J)=NCONC_MID(I-1,J)
      END DO
     ELSE
      DO J=1,M
       UCONC_UP(I,J)=UCONC_MID(I,J)
       ACONC_UP(I,J)=ACONC_MID(I,J)
       NCONC_UP(I,J)=NCONC_MID(I,J)
      END DO
     END IF
    END DO
!
    ! Note that the N specie concentrations are made_in to indicate
    ! that they will be intialized for the coming time step.
    DO J=1,M
     ! Extreme lateral nodes: J=1 & M are symmetrical
     IF (J==1 .OR. J==M) THEN
      I=1
       UCONC_IN(I,J)=0
       ACONC_IN(I,J)=0
       NCONC_IN(I,J)=0
      I=2
       UCONC_IN(I,J)=0
       ACONC_IN(I,J)=0
       B_N2(I)=(2*THETA_IN(I)/DT)+((N_AP_DISP(I)+N_AP_DISP(I-1))      &
        & /(DZ**2))
       C_N2(I)=-N_AP_DISP(I)/(DZ**2)
       N_SINK=TRANS_LAY(I)*NCONC_MID(I,J)
       K_N2(I)=(2*THETA_MID(I)*NCONC_MID(I,J)/DT)-(NCONC_LO(I,J)      &
        & *FLUX_MID(I)/DZ)-N_SINK
      DO I=3,L-2
       UCONC_IN(I,J)=0
       ACONC_IN(I,J)=0
       A_N2(I)=-N_AP_DISP(I-1)/(DZ**2)
       B_N2(I)=(2*THETA_IN(I)/DT)+((N_AP_DISP(I)+N_AP_DISP(I-1))      &
        & /(DZ**2))
       C_N2(I)=-N_AP_DISP(I)/(DZ**2)
       N_SINK=TRANS_LAY(I)*NCONC_MID(I,J)
       K_N2(I)=(2*THETA_MID(I)*NCONC_MID(I,J)/DT)-((NCONC_LO(I,J)     &
```

```
          & *FLUX_MID(I)-NCONC_UP(I,J)*FLUX_MID(I-1))/DZ)-N_SINK
        END DO
        I=L-1
         UCONC_IN(I,J)=0
         ACONC_IN(I,J)=0
         A_N2(I)=-N_AP_DISP(I-1)/(DZ**2)
         B_N2(I)=(2*THETA_IN(I)/DT)+((N_AP_DISP(I)+N_AP_DISP(I-1))      &
          & /(DZ**2))
         C_N2(I)=-N_AP_DISP(I)/(DZ**2)
         N_SINK=TRANS_LAY(I)*NCONC_MID(I,J)
         K_N2(I)=(2*THETA_MID(I)*NCONC_MID(I,J)/DT)-((NCONC_LO(I,J)     &
          & *FLUX_MID(I)-NCONC_UP(I,J)*FLUX_MID(I-1))/DZ)-N_SINK
        I=L
         UCONC_IN(I,J)=0
         ACONC_IN(I,J)=0
         N_SINK=TRANS_LAY(I)*NCONC_MID(I,J)
         A_N2(I)=(N_AP_DISP(I)-N_AP_DISP(I-1))/(DZ**2)
         B_N2(I)=-A_N2(I)+(2*THETA_IN(I)/DT)
         K_N2(I)=(2*THETA_MID(I)*NCONC_MID(I,J)/DT)-((NCONC_MID(I,J)    &
          & *FLUX_MID(I)-NCONC_MID(I-1,J)*FLUX_MID(I-1))/DZ)-N_SINK
      CALL TRIDIAG_N(NCONCFIN(2:L),A_N2(3:L),B_N2(2:L),C_N2(2:L-1),     &
       & K_N2(2:L),L)
       NCONC_IN(2:L,J)=NCONCFIN(2:L)
!
       ELSE IF (J==2 .OR. J==M-1) THEN
       ! Since J=2 and M-1 nodes are not 'urea' nodes, they have to be
       ! treated separate from J=3,..,M-2
        I=1
         UCONC_IN(I,J)=0
         ACONC_IN(I,J)=0
         NCONC_IN(I,J)=0
        I=2
         ! Urea
         B_U2(I)=(2*THETA_IN(I)/DT)+((U_AP_DISP(I)+U_AP_DISP(I-1))      &
          & /(DZ**2))
         C_U2(I)=-U_AP_DISP(I)/(DZ**2)
         K_U2(I)=(2*THETA_MID(I)*UCONC_MID(I,J)/DT)+((UDIFF_AQ          &
          & /(POR**2*DY**2))*(THETA_MID(I)**4.3)*(UCONC_MID(I,J+1)      &
          & -(2*UCONC_MID(I,J))+UCONC_MID(I,J-1)))-((UCONC_LO(I,J)      &
          & *FLUX_MID(I)-UCONC_UP(I,J)*FLUX_MID(I-1))/DZ)-U_SINK(I,J)
         ! Ammonium
         B_A2(I)=(2*THETA_IN(I)/DT)+(2*BD*K_DIS/DT)+((A_AP_DISP(I)      &
          & +A_AP_DISP(I-1))/(DZ**2))
         C_A2(I)=-A_AP_DISP(I)/(DZ**2)
         A_SINK2=TRANS_LAY(I)*ACONC_MID(I,J)
         K_A2(I)=(2*THETA_MID(I)*ACONC_MID(I,J)/DT)+(2*BD*K_DIS         &
          & *ACONC_MID(I,J)/DT)+((ADIFF_AQ/(POR**2*DY**2))              &
          & *(THETA_MID(I)**4.3)*(ACONC_MID(I,J+1)-(2*ACONC_MID(I,J))   &
          & +ACONC_MID(I,J-1)))-((ACONC_LO(I,J)*FLUX_MID(I)             &
          & -ACONC_UP(I,J)*FLUX_MID(I-1))/DZ)+(0.6*U_SINK(I,J))         &
          & -A_SINK1(I,J)-A_SINK2
         ! Nitrate
         B_N2(I)=(2*THETA_IN(I)/DT)+((N_AP_DISP(I)+N_AP_DISP(I-1))      &
          & /(DZ**2))
         C_N2(I)=-N_AP_DISP(I)/(DZ**2)
         N_SINK=TRANS_LAY(I)*NCONC_MID(I,J)
         K_N2(I)=(2*THETA_MID(I)*NCONC_MID(I,J)/DT)+((NDIFF_AQ          &
```

```
     & /(POR**2*DY**2))*(THETA_MID(I)**4.3)*(NCONC_MID(I,J+1)      &
     & -(2*NCONC_MID(I,J))+NCONC_MID(I,J-1)))-((NCONC_LO(I,J)      &
     & *FLUX_MID(I)-NCONC_UP(I,J)*FLUX_MID(I-1))/DZ)-N_SINK        &
     & +(3.4444*A_SINK1(I,J))
!
      DO I=3,L-2
       ! Urea
       A_U2(I)=(-U_AP_DISP(I-1)/(DZ**2))
       B_U2(I)=(2*THETA_IN(I)/DT)+((U_AP_DISP(I)+U_AP_DISP(I-1))      &
        & /(DZ**2))
       C_U2(I)=-U_AP_DISP(I)/(DZ**2)
       K_U2(I)=(2*THETA_MID(I)*UCONC_MID(I,J)/DT)+((UDIFF_AQ          &
        & /(POR**2*DY**2))*(THETA_MID(I)**4.3)*(UCONC_MID(I,J+1)      &
        & -(2*UCONC_MID(I,J))+UCONC_MID(I,J-1)))-((UCONC_LO(I,J)      &
        & *FLUX_MID(I)-UCONC_UP(I,J)*FLUX_MID(I-1))/DZ)-U_SINK(I,J)
       ! Ammonium
       A_A2(I)=(-A_AP_DISP(I-1)/(DZ**2))
       B_A2(I)=(2*THETA_IN(I)/DT)+(2*BD*K_DIS/DT)+((A_AP_DISP(I)      &
        & +A_AP_DISP(I-1))/(DZ**2))
       C_A2(I)=-A_AP_DISP(I)/(DZ**2)
       A_SINK2=TRANS_LAY(I)*ACONC_MID(I,J)
       K_A2(I)=(2*THETA_MID(I)*ACONC_MID(I,J)/DT)+(2*BD*K_DIS         &
        & *ACONC_MID(I,J)/DT)+((ADIFF_AQ/(POR**2*DY**2))              &
        & *(THETA_MID(I)**4.3)*(ACONC_MID(I,J+1)-(2*ACONC_MID(I,J))   &
        & +ACONC_MID(I,J-1)))-((ACONC_LO(I,J)*FLUX_MID(I)             &
        & -ACONC_UP(I,J)*FLUX_MID(I-1))/DZ)+(0.6*U_SINK(I,J))         &
        & -A_SINK1(I,J)-A_SINK2
       ! Nitrate
       A_N2(I)=(-N_AP_DISP(I-1)/(DZ**2))
       B_N2(I)=(2*THETA_IN(I)/DT)+((N_AP_DISP(I)+N_AP_DISP(I-1))      &
        & /(DZ**2))
       C_N2(I)=-N_AP_DISP(I)/(DZ**2)
       N_SINK=TRANS_LAY(I)*NCONC_MID(I,J)
       K_N2(I)=(2*THETA_MID(I)*NCONC_MID(I,J)/DT)+((NDIFF_AQ          &
        & /(POR**2*DY**2))*(THETA_MID(I)**4.3)*(NCONC_MID(I,J+1)      &
        & -(2*NCONC_MID(I,J))+NCONC_MID(I,J-1)))-((NCONC_LO(I,J)      &
        & *FLUX_MID(I)-NCONC_UP(I,J)*FLUX_MID(I-1))/DZ)-N_SINK        &
        & +(3.4444*A_SINK1(I,J))
      END DO
      I=L-1
       ! Urea
       A_U2(I)=(-U_AP_DISP(I-1)/(DZ**2))
       B_U2(I)=(2*THETA_IN(I)/DT)+((U_AP_DISP(I)+U_AP_DISP(I-1))      &
        & /(DZ**2))
       K_U2(I)=(2*THETA_MID(I)*UCONC_MID(I,J)/DT)+((UDIFF_AQ          &
        & /(POR**2*DY**2))*(THETA_MID(I)**4.3)*(UCONC_MID(I,J+1)      &
        & -(2*UCONC_MID(I,J))+UCONC_MID(I,J-1)))-((UCONC_LO(I,J)      &
        & *FLUX_MID(I)-UCONC_UP(I,J)*FLUX_MID(I-1))/DZ)-U_SINK(I,J)
       ! Ammonium
       A_A2(I)=(-A_AP_DISP(I-1)/(DZ**2))
       B_A2(I)=(2*THETA_IN(I)/DT)+(2*BD*K_DIS/DT)+((A_AP_DISP(I)      &
        & +A_AP_DISP(I-1))/(DZ**2))
       A_SINK2=TRANS_LAY(I)*ACONC_MID(I,J)
       K_A2(I)=(2*THETA_MID(I)*ACONC_MID(I,J)/DT)+(2*BD*K_DIS         &
        & *ACONC_MID(I,J)/DT)+((ADIFF_AQ/(POR**2*DY**2))              &
        & *(THETA_MID(I)**4.3)*(ACONC_MID(I,J+1)-(2*ACONC_MID(I,J))   &
        & +ACONC_MID(I,J-1)))-((ACONC_LO(I,J)*FLUX_MID(I)             &
```

```
      & -ACONC_UP(I,J)*FLUX_MID(I-1))/DZ)+(U_SINK(I,J)*0.6)         &
      & -A_SINK1(I,J)-A_SINK2
     ! Nitrate
     A_N2(I)=-N_AP_DISP(I-1)/(DZ**2)
     B_N2(I)=(2*THETA_IN(I)/DT)+((N_AP_DISP(I)+N_AP_DISP(I-1))      &
      & /(DZ**2))
     C_N2(I)=-N_AP_DISP(I)/(DZ**2)
     N_SINK=TRANS_LAY(I)*NCONC_MID(I,J)
     K_N2(I)=(2*THETA_MID(I)*NCONC_MID(I,J)/DT)+((NDIFF_AQ          &
      & /(POR**2*DY**2))*(THETA_MID(I)**4.3)*(NCONC_MID(I,J+1)      &
      & -(2*NCONC_MID(I,J))+NCONC_MID(I,J-1)))-((NCONC_LO(I,J)      &
      & *FLUX_MID(I)-NCONC_UP(I,J)*FLUX_MID(I-1))/DZ)               &
      & +(3.4444*A_SINK1(I,J))-N_SINK
    I=L
     UCONC_IN(I,J)=0
     ACONC_IN(I,J)=0
     N_SINK=TRANS_LAY(I)*NCONC_MID(I,J)
     A_N2(I)=(N_AP_DISP(I)-N_AP_DISP(I-1))/(DZ**2)
     B_N2(I)=-A_N2(I)+(2*THETA_IN(I)/DT)
     K_N2(I)=(2*THETA_MID(I)*NCONC_MID(I,J)/DT)+((NDIFF_AQ          &
      & /(POR**2*DY**2))*(THETA_MID(I)**4.3)*(NCONC_MID(I,J+1)      &
      & -(2.0*NCONC_MID(I,J))+NCONC_MID(I,J-1)))-((NCONC_MID(I,J)   &
      & *FLUX_MID(I)-NCONC_MID(I-1,J)*FLUX_MID(I-1))/DZ)-N_SINK
   ! Call tridiags for all N species for J=2 & M-1
   CALL TRIDIAG(UCONCFIN(2:L-1),A_U2(3:L-1),B_U2(2:L-1),C_U2(2:L-2),&
    & K_U2(2:L-1),L)
    UCONC_IN(2:L-1,J)=UCONCFIN(2:L-1)
   CALL TRIDIAG(ACONCFIN(2:L-1),A_A2(3:L-1),B_A2(2:L-1),C_A2(2:L-2),&
    & K_A2(2:L-1),L)
    ACONC_IN(2:L-1,J)=ACONCFIN(2:L-1)
   CALL TRIDIAG_N(NCONCFIN(2:L),A_N2(3:L),B_N2(2:L),C_N2(2:L-1),    &
    & K_N2(2:L),L)
    NCONC_IN(2:L,J)=NCONCFIN(2:L)
   ELSE ! J=3,...,M-2
    I=1
     UCONC_IN(I,J)=0
     ACONC_IN(I,J)=0
     NCONC_IN(I,J)=0
    I=2
     ! Urea
     B_U2(I)=(2*THETA_IN(I)/DT)+((U_AP_DISP(I)+U_AP_DISP(I-1))      &
      & /(DZ**2))
     C_U2(I)=-U_AP_DISP(I)/(DZ**2)
     K_U2(I)=(2*THETA_MID(I)*UCONC_MID(I,J)/DT)+((UDIFF_AQ          &
      & /(POR**2*DY**2))*(THETA_MID(I)**4.3)*(UCONC_MID(I,J+1)      &
      & -(2*UCONC_MID(I,J))+UCONC_MID(I,J-1)))-(UCONC_LO(I,J)       &
      & *FLUX_MID(I)/DZ)-U_SINK(I,J)
     ! Ammonium
     B_A2(I)=(2*THETA_IN(I)/DT)+(2*BD*K_DIS/DT)+((A_AP_DISP(I)      &
      & +A_AP_DISP(I-1))/(DZ**2))
     C_A2(I)=-A_AP_DISP(I)/(DZ**2)
     A_SINK2=TRANS_LAY(I)*ACONC_MID(I,J)
     K_A2(I)=(2*THETA_MID(I)*ACONC_MID(I,J)/DT)+(2*BD*K_DIS         &
      & *ACONC_MID(I,J)/DT)+((ADIFF_AQ/(POR**2*DZ**2))              &
      & *(THETA_MID(I)**4.3)*(ACONC_MID(I,J+1)-(2*ACONC_MID(I,J))   &
      & +ACONC_MID(I,J-1)))-(ACONC_LO(I,J)*FLUX_MID(I)/DZ)          &
      & +(0.6*U_SINK(I,J))-A_SINK1(I,J)-A_SINK2
```

```
 ! Nitrate
 B_N2(I)=(2*THETA_IN(I)/DT)+((N_AP_DISP(I)+N_AP_DISP(I-1))      &
  & /(DZ**2))
 C_N2(I)=-N_AP_DISP(I)/(DZ**2)
 N_SINK=TRANS_LAY(I)*NCONC_MID(I,J)
 K_N2(I)=(2*THETA_MID(I)*NCONC_MID(I,J)/DT)+((NDIFF_AQ          &
  & /(POR**2*DY**2))*(THETA_MID(I)**4.3)*(NCONC_MID(I,J+1)      &
  & -(2*NCONC_MID(I,J))+NCONC_MID(I,J-1)))-(NCONC_LO(I,J)       &
  & *FLUX_MID(I)/DZ)-N_SINK+(3.4444*A_SINK1(I,J))
DO I=3,L-2
 IF (I==I_FERT1 .AND. J==J_FERT11) THEN
  IF (U_DISS11==0.0) THEN
   U_SOURCE=0.0
  ELSE
   U_DISS11=U_SLOPE*U_MASS11*((0.5*DT)**0.5)
   U_SOURCE=U_DISS11/((0.5*DT)*(DZ**3))
   U_MASS11=U_MASS11-U_DISS11
   IF (U_MASS11<0.0001) THEN
    U_MASS11=0.0
   END IF
  END IF
 ELSE IF (I==I_FERT1 .AND. J==J_FERT12) THEN
  IF (U_DISS12==0.0) THEN
   U_SOURCE=0.0
  ELSE
   U_DISS12=U_SLOPE*U_MASS12*((0.5*DT)**0.5)
   U_SOURCE=U_DISS12/((0.5*DT)*(DZ**3))
   U_MASS12=U_MASS12-U_DISS12
   IF (U_MASS12<0.0001) THEN
    U_MASS12=0.0
   END IF
  END IF
 ELSE IF (I==I_FERT2 .AND. J==J_FERT21) THEN
  IF (U_DISS21==0.0) THEN
   U_SOURCE=0.0
  ELSE
   U_DISS21=U_SLOPE*U_MASS21*((0.5*DT)**0.5)
   U_SOURCE=U_DISS21/((0.5*DT)*(DZ**3))
   U_MASS21=U_MASS21-U_DISS21
   IF (U_MASS21<0.0001) THEN
    U_MASS21=0.0
   END IF
  END IF
 ELSE IF (I==I_FERT2 .AND. J==J_FERT22) THEN
  IF (U_DISS22==0.0) THEN
   U_SOURCE=0.0
  ELSE
   U_DISS22=U_SLOPE*U_MASS22*((0.5*DT)**0.5)
   U_SOURCE=U_DISS22/((0.5*DT)*(DZ**3))
   U_MASS22=U_MASS22-U_DISS22
    IF (U_MASS22<0.0001) THEN
     U_MASS22=0.0
    END IF
   END IF
  ELSE
   U_SOURCE=0.0
  END IF
```

```
!
        ! Urea
        A_U2(I)=-U_AP_DISP(I-1)/(DZ**2)
        B_U2(I)=(2*THETA_IN(I)/DT)+((U_AP_DISP(I)+U_AP_DISP(I-1))      &
         & /(DZ**2))
        C_U2(I)=-U_AP_DISP(I)/(DZ**2)
        K_U2(I)=(2*THETA_MID(I)*UCONC_MID(I,J)/DT)+((UDIFF_AQ          &
         & /(POR**2*DY**2))*(THETA_MID(I)**4.3)*(UCONC_MID(I,J+1)      &
         & -(2*UCONC_MID(I,J))+UCONC_MID(I,J-1)))-((UCONC_LO(I,J)      &
         & *FLUX_MID(I)-UCONC_UP(I,J)*FLUX_MID(I-1))/DZ)+U_SOURCE      &
         & -U_SINK(I,J)
        ! Ammonium
        A_A2(I)=-A_AP_DISP(I-1)/(DZ**2)
        B_A2(I)=(2*THETA_IN(I)/DT)+(2*BD*K_DIS/DT)+((A_AP_DISP(I)      &
         & +A_AP_DISP(I-1))/(DZ**2))
        C_A2(I)=-A_AP_DISP(I)/(DZ**2)
        A_SINK2=TRANS_LAY(I)*ACONC_MID(I,J)
        K_A2(I)=(2*THETA_MID(I)*ACONC_MID(I,J)/DT)+(2*BD*K_DIS         &
         & *ACONC_MID(I,J)/DT)+((ADIFF_AQ/(POR**2*DY**2))              &
         & *(THETA_MID(I)**4.3)*(ACONC_MID(I,J+1)-(2*ACONC_MID(I,J))   &
         & +ACONC_MID(I,J-1)))-((ACONC_LO(I,J)*FLUX_MID(I)             &
         & -ACONC_UP(I,J)*FLUX_MID(I-1))/DZ)+(0.6*U_SINK(I,J))         &
         & -A_SINK1(I,J)-A_SINK2
        ! Nitrate
        A_N2(I)=-N_AP_DISP(I-1)/(DZ**2)
        B_N2(I)=(2*THETA_IN(I)/DT)+((N_AP_DISP(I)+N_AP_DISP(I-1))      &
         & /(DZ**2))
        C_N2(I)=-N_AP_DISP(I)/(DZ**2)
        N_SINK=TRANS_LAY(I)*NCONC_MID(I,J)
        K_N2(I)=(2*THETA_MID(I)*NCONC_MID(I,J)/DT)+((NDIFF_AQ          &
         & /(POR**2*DY**2))*(THETA_MID(I)**4.3)*(NCONC_MID(I,J+1)      &
         & -(2*NCONC_MID(I,J))+NCONC_MID(I,J-1)))-((NCONC_LO(I,J)      &
         & *FLUX_MID(I)-NCONC_UP(I,J)*FLUX_MID(I-1))/DZ)               &
         & +(3.4444*A_SINK1(I,J))-N_SINK
       END DO  ! I=3,L-2
       I=L-1
        ! Urea: The C_U-associated term=0
        A_U2(I)=-U_AP_DISP(I-1)/(DZ**2)
        B_U2(I)=(2*THETA_IN(I)/DT)+((U_AP_DISP(I)+U_AP_DISP(I-1))      &
         & /(DZ**2))
        K_U2(I)=(2*THETA_MID(I)*UCONC_MID(I,J)/DT)+((UDIFF_AQ          &
         & /(POR**2*DY**2))*(THETA_MID(I)**4.3)*(UCONC_MID(I,J+1)      &
         & -(2*UCONC_MID(I,J))+UCONC_MID(I,J-1)))-((UCONC_LO(I,J)      &
         & *FLUX_MID(I)-UCONC_UP(I,J)*FLUX_MID(I-1))/DZ)-U_SINK(I,J)
        ! Ammonium
        A_A2(I)=-A_AP_DISP(I-1)/(DZ**2)
        B_A2(I)=(2*THETA_IN(I)/DT)+(2*BD*K_DIS/DT)+((A_AP_DISP(I)      &
         & +A_AP_DISP(I-1))/(DZ**2))
        A_SINK2=TRANS_LAY(I)*ACONC_MID(I,J)
        K_A2(I)=(2*THETA_MID(I)*ACONC_MID(I,J)/DT)+(2*BD*K_DIS         &
         & *ACONC_MID(I,J)/DT)+((ADIFF_AQ/(POR**2*DY**2))              &
         & *(THETA_MID(I)**4.3)*(ACONC_MID(I,J+1)-(2*ACONC_MID(I,J))   &
         & +ACONC_MID(I,J-1)))-((ACONC_LO(I,J)*FLUX_MID(I)             &
         & -ACONC_UP(I,J)*FLUX_MID(I-1))/DZ)+(0.6*U_SINK(I,J))         &
         & -A_SINK1(I,J)-A_SINK2
        ! Nitrate
        A_N2(I)=-N_AP_DISP(I-1)/(DZ**2)
```

```
        B_N2(I)=(2*THETA_IN(I)/DT)+((N_AP_DISP(I)+N_AP_DISP(I-1))      &
         & /(DZ**2))
        C_N2(I)=-N_AP_DISP(I)/(DZ**2)
        N_SINK=TRANS_LAY(I)*NCONC_MID(I,J)
        K_N2(I)=((NDIFF_AQ/(POR**2*DY**2))*(THETA_MID(I)**4.3)         &
         & *(NCONC_MID(I,J+1)-(2*NCONC_MID(I,J))+NCONC_MID(I,J-1)))    &
         & +(2*THETA_MID(I)*NCONC_MID(I,J)/DT)-((NCONC_LO(I,J)         &
         & *FLUX_MID(I)-NCONC_UP(I,J)*FLUX_MID(I-1))/DZ)               &
         & +(3.4444*A_SINK1(I,J))-N_SINK
       I=L
        UCONC_IN(I,J)=0
        ACONC_IN(I,J)=0
        N_SINK=TRANS_LAY(I)*NCONC_MID(I,J)
        A_N2(I)=(N_AP_DISP(I)-N_AP_DISP(I-1))/(DZ**2)
        B_N2(I)=-A_N2(I)+(2*THETA_IN(I)/DT)
        K_N2(I)=(2*THETA_MID(I)*NCONC_MID(I,J)/DT)+((NDIFF_AQ          &
         & /(POR**2*DY**2))*(THETA_MID(I)**4.3)*(NCONC_MID(I,J+1)      &
         & -(2.0*NCONC_MID(I,J))+NCONC_MID(I,J-1)))-((NCONC_MID(I,J)   &
         & *FLUX_MID(I)-NCONC_MID(I-1,J)*FLUX_MID(I-1))/DZ)-N_SINK
       CALL TRIDIAG(UCONCFIN(2:L-1),A_U2(3:L-1),B_U2(2:L-1),           &
        & C_U2(2:L-2),K_U2(2:L-1),L)
        UCONC_IN(2:L-1,J)=UCONCFIN(2:L-1)
       CALL TRIDIAG(ACONCFIN(2:L-1),A_A2(3:L-1),B_A2(2:L-1),           &
        & C_A2(2:L-2),K_A2(2:L-1),L)
        ACONC_IN(2:L-1,J)=ACONCFIN(2:L-1)
       CALL TRIDIAG_N(NCONCFIN(2:L),A_N2(3:L),B_N2(2:L),C_N2(2:L-1),   &
        & K_N2(2:L),L)
        NCONC_IN(2:L,J)=NCONCFIN(2:L)
      END IF
     END DO
!
     IF (FLUX_SUR>0.0) THEN
      INFILT=(INFILT+(FLUX_SUR*DT))
     ELSE
      EVAP=(EVAP+(ABS(FLUX_SUR*DT)))
     END IF
     IF (SUM(TRANS_LAY(2:L))>0.0D0) THEN
      TRANSPIRE=(TRANSPIRE+(SUM(TRANS_LAY(2:L)*DZ*DT)))
     END IF
     IF (RAIN(HR)>0.0) THEN
      PRECIP=(PRECIP+(RAIN(HR)*DT))
     END IF
     IF ((DMOD((T_NEW+0.00003),240.0D0)<DT) .OR.                       &
      & ((T_END-T_START)-T_NEW<DT)) THEN
      OPEN (UNIT=11,FILE="MOIST.OUT",STATUS="OLD",POSITION="APPEND")
       WRITE(11,*)'TIME(H)=',T_NEW
       WRITE(11,*)' AMOUNT INFILTRATED=',INFILT
       WRITE(11,*)' AMOUNT PERCOLATED=',PERC_LOSS
       WRITE(11,*)' AMOUNT EVAPORATED=',EVAP
       WRITE(11,*)' TOTAL PRECIPITATION=',PRECIP
       WRITE(11,*)' AMOUNT TRANSPIRED=',TRANSPIRE
       WRITE(11,*)'HEAD_MID HEAD_FIN THETA_IN'
       113 FORMAT(F12.2,F12.2,F10.4)
       DO I=1,L
        WRITE(11,113)HEAD_MID(I),HEAD_IN(I),THETA_IN(I)
       END DO
      CLOSE(11)
```

```
     OPEN(UNIT=12,FILE="NITRATE.OUT",STATUS="OLD",POSITION="APPEND")
      121 FORMAT('Amount of fertilizer-N leached ',I4,' days after ', &
       & 'start of simulation is ',F7.2,' kg-N/ha')
      WRITE(12,121)NINT(T_NEW/24),N_LEACH
      122 FORMAT('Amount of fertilizer-N removed by the crop during ' &
       & 'this period is ',F6.2,' kg-N/ha')
      WRITE(12,122)CROP_NREM
      123 FORMAT(/,'Node-wise nitrate concentrations (mg/mL) ',I4,    &
       &' days after the start of simulation were:',/)
      WRITE(12,123) NINT(T_NEW/24)
      124 FORMAT(61F8.3)
      WRITE(12,124)((NCONC_IN(I,J),J=1,M),I=1,L)
     CLOSE(12)
     OPEN(UNIT=13,FILE="AMMONIUM.OUT",STATUS="OLD",POSITION="APPEND")
      131 FORMAT(/,'Node-wise ammonium concentrations (mg/mL) ',I4,   &
       & ' days after the start of simulation were:',/)
      WRITE(13,131) NINT(T_NEW/24)
      132 FORMAT(61F8.3)
      WRITE(13,132)((ACONC_IN(I,J),J=1,M),I=1,L)
     CLOSE(13)
    END IF
    T=T_NEW
    HR=(INT(T+0.00003)+1)
    END DO  ! The time loop goes back

!************************LIST OF SUBROUTINES*************************
 CONTAINS
SUBROUTINE TRANSPIRATION(ET_REF,POT_ET,POT_EVAP,L, HR_END,TEN_D,      &
 & PL_TIME,HV_TIME,C_P,AIRTEMP,SOLRAD,ELEV,R,K_C,LAI,A_1,B_1,EXTINC_C,&
 & MAX_ROOTDEPTH,DZ)
 IMPLICIT NONE
! In this subroutine, root depth, crop coefficient,and LAI are
! calculated and updated using empirical equations for corn. For other
! crops, crop-specific equations for root depth, kc, and LAI are
! required.  Using hourly reference ET data obtained from the
! model REF_ET and the above parameters,hourly potential transpiration
! by layer is calculated.
 INTEGER::TEN_D,I,L,HR,HR_END,PL_TIME,HV_TIME
 INTEGER,DIMENSION(1:17)::R
 DOUBLE PRECISION,DIMENSION(1:HR_END),INTENT(IN)::ET_REF,AIRTEMP,SOLRAD
 DOUBLE PRECISION,DIMENSION(1:HR_END)::POT_EVAP,POT_ET
 DOUBLE PRECISION,DIMENSION(1:17)::K_C,LAI
 DOUBLE PRECISION::C_P,A_1,B_1,EXTINC_C,ELEV,MAX_ROOTDEPTH,DZ
 ! Local variable
 DOUBLE PRECISION::PHI_NS,NET_SOLRAD,NETSOIL_SOLRAD,ROOT_DEPTH,DELTA, &
  & GAMMA,E_0,ATM_PRESS,LAT_VAP
 ! First, root growth will be calculated in 10-d stages, 10-90 d after
 ! planting.  Between 90-140 d, the maximum root depth is used.  Note
 ! that HR is an hourly interval.  Root growth at each stage (except
 ! for the last stage) is the average root growth over a 10-d period,
 ! 5 d before and after the assigned date. Crop coefficient is
 ! calculated the same way, but for 140 days. LAI is also calculated
 ! in 10-d increments upto a maximum of 140 days after planting.  It
 ! is assumed that the crop is harvested within 145 days of planting.
 ! Again, the LAI for stage 1 is for a 10-d period between 5 and
 ! 15 days.
 TEN_D=1
```

```
DO HR=PL_TIME+240,PL_TIME+4080,240
 TEN_D=MIN(TEN_D,18)
  IF (TEN_D<5) THEN
   ROOT_DEPTH=MAX_ROOTDEPTH*((-4D-8*(((HR-PL_TIME)/24)**4))          &
    & +(7D-6*(((HR-PL_TIME)/24)**3))-(0.0003*(((HR-PL_TIME)/24)**2)) &
    & +(0.0099*((HR-PL_TIME)/24)))
   R(TEN_D)=NINT(ROOT_DEPTH/DZ)
   K_C(TEN_D)=(-2D-6*(((HR-PL_TIME)/24)**3))+(0.0003                 &
    & *(((HR-PL_TIME)/24)**2))+(0.0012*((HR-PL_TIME)/24))+0.1522
   LAI(TEN_D)=0.0055*(HR-PL_TIME)/24
  ELSE IF (TEN_D>=5 .AND. TEN_D<9) THEN
   ROOT_DEPTH=MAX_ROOTDEPTH*((-4D-8*(((HR-PL_TIME)/24)**4))          &
    & +(7D-6*(((HR-PL_TIME)/24)**3))-(0.0003*(((HR-PL_TIME)/24)**2)) &
    & +(0.0099*((HR-PL_TIME)/24)))
   R(TEN_D)=NINT(ROOT_DEPTH/DZ)
   K_C(TEN_D)=(-2D-6*(((HR-PL_TIME)/24)**3))+(0.0003                 &
    & *(((HR-PL_TIME)/24)**2))+(0.0012*((HR-PL_TIME)/24))+0.1522
   LAI(TEN_D)=0.0169*EXP(0.0569*(HR-PL_TIME)/24)
  ELSE IF (TEN_D>=9 .AND. TEN_D<=14) THEN
   R(TEN_D)=NINT(MAX_ROOTDEPTH/DZ)
   K_C(TEN_D)=(-2D-6*(((HR-PL_TIME)/24)**3))+(0.0003                 &
    & *(((HR-PL_TIME)/24)**2))+(0.0012*((HR-PL_TIME)/24))+0.1522
   LAI(TEN_D)=(-1D-5*(((HR-PL_TIME)/24)**3))+(0.04                   &
    & *(((HR-PL_TIME)/24)**2))-(0.3503*(HR-PL_TIME)/24)+13.08
  ELSE
   R(TEN_D)=0.0
   K_C(TEN_D)=0.19
   LAI(TEN_D)=0.0
  END IF
 TEN_D=TEN_D+1
END DO
! Hourly potential transpiration will be calculated for the crop
! season beginning 5 d after planting.  It is assumed that
! transpiration is negligible during the remaining part of the
! simulation period.  Evaporation during that period will be
! calculated using the method suggested by Feddes et al. (1978) and
! is presented in the moisture section.
DO HR=1,HR_END
 IF ((HR>=PL_TIME+120) .AND. (HR<HV_TIME)) THEN
  TEN_D=INT((HR+120-PL_TIME)/240)
  POT_ET(HR)=ET_REF(HR)*K_C(TEN_D)
  E_0=EXP((16.78*AIRTEMP(HR)-116.9)/(AIRTEMP(HR)+237.3))
  DELTA=(4098*E_0)/((AIRTEMP(HR)+237.3)**2)
  ATM_PRESS=101.3-(0.01055*ELEV)
  LAT_VAP=(2.501-(AIRTEMP(HR)*2.361D-03))*1000.0D0
  ! Using a temperature dependent latent heat of vaporatization
  ! equation (given in Allen et al., 1992 page 169) will improve
  ! prediction.
  GAMMA=(C_P*ATM_PRESS)/(0.622*LAT_VAP)
  IF (LAI(TEN_D)<=3.0) THEN
   NET_SOLRAD=0.041855*((0.861*SOLRAD(HR)*2.0643)-103.92)
   ! Based on relationship by Rosenthal et al. (1977)
   ! The factor 2.0643 converts SOLRAD in W/sq.m into cal/sq.cm-d.
   ! The factor 0.041855 converts cal/sq.cm-d into MJ/sq.m-d
  ELSE
   NET_SOLRAD=0.041855*((0.848*SOLRAD(HR)*2.0643)-144.49)
  END IF
```

```
   IF (NET_SOLRAD<0.0D0) THEN
    NET_SOLRAD=0.0D0
   END IF
   NETSOIL_SOLRAD=11.574*(NET_SOLRAD)*(EXP(-EXTINC_C*LAI(TEN_D)))
   ! The 11.574 factor converts NETSOIL_SOLRAD back into W/sq. m
   IF (NET_SOLRAD>0.0) THEN
    PHI_NS=B_1+(A_1*(NETSOIL_SOLRAD/(NET_SOLRAD*11.574)))
   ELSE
    PHI_NS=B_1
   END IF
   IF (LAI(TEN_D)>2.7) THEN
    PHI_NS=1.0
   END IF
   ! See Allen et al. (1990) page 53
   POT_EVAP(HR)=1.457D-4*(DELTA/(DELTA+GAMMA))*PHI_NS                 &
    & *NETSOIL_SOLRAD
   ! The factor 1.457D-4 converts POT_EVAP from W/sq.m into cm/h as
   ! POT_ET is also in cm/h
  ELSE
   POT_ET(HR)=0.19*ET_REF(HR)
   POT_EVAP(HR)=POT_ET(HR)
   ! Kc = 0.19 when corn canopy is absent (Allen et al. (1990),p 127).
   ! It is better to use the above approach than using the Priestly-
   ! Taylor approach since the Priestly-Taylor method is not suitable
   ! for daily use, though it is used as in Feddes et al. (1978).
  END IF
 END DO
END SUBROUTINE TRANSPIRATION

! Calculate head from theta
SUBROUTINE THETA2HEAD(HEAD,THETA,THETA_S,THETA_R,ALPHA_US,M_US,N_US,L)
 INTEGER::I,L
 DOUBLE PRECISION,DIMENSION(1:L)::THETA,THETA_S,THETA_R,ALPHA_US,M_US,&
  & N_US
 DOUBLE PRECISION,DIMENSION(1:L),INTENT(OUT)::HEAD
 DOUBLE PRECISION::THETA_REL
  DO I=1,L
   THETA_REL=(THETA(I)-THETA_R(I))/(THETA_S(I)-THETA_R(I))
   HEAD(I)=-((((1/THETA_REL)**(1/M_US(I)))-1)**(1/N_US(I)))          &
    & /(ALPHA_US(I))
   ! HEAD(I) calculated as a positive value needs to be converted into
   ! negative value for unsaturated conditions.
  END DO
END SUBROUTINE THETA2HEAD
!
! Calculate theta from head
SUBROUTINE HEAD2THETA(THETA,THETA_M,HEAD,HEAD_S,THETA_S,THETA_R,      &
 & ALPHA_US,M_US,N_US,L)
 INTEGER::I,L
 DOUBLE PRECISION,DIMENSION(1:L),INTENT(OUT)::THETA,THETA_M
 DOUBLE PRECISION,DIMENSION(1:L),INTENT(IN)::HEAD,THETA_S,THETA_R,    &
  & ALPHA_US,M_US,N_US
 DOUBLE PRECISION::HEAD_S,HEAD_M
  DO I=1,L
   IF (HEAD(I)>=HEAD_S) THEN
    THETA(I)=THETA_S(I)
   ELSE
```

```
    THETA(I)=(THETA_R(I))+((THETA_S(I)-THETA_R(I))                    &
     &/((1+(ABS(ALPHA_US(I)*HEAD(I))**(N_US(I))))**M_US(I)))
   END IF
  END DO
  DO I=1,L-1
   HEAD_M=0.5*(HEAD(I)+HEAD(I+1))
   IF (HEAD_M>=HEAD_S) THEN
    THETA_M(I)=THETA_S(I)
   ELSE
    THETA_M(I)=(THETA_R(I))+((THETA_S(I)-THETA_R(I))                  &
     & /((1+(ABS(ALPHA_US(I)*HEAD_M)**(N_US(I))))**M_US(I)))
   END IF
  END DO
  I=L
   THETA_M(I)=THETA(I)
END SUBROUTINE HEAD2THETA
!
! Calculate unsaturated K values at the nodes and internodes
SUBROUTINE KUNSAT(KUS,HEAD,HEAD_S,KS,ALPHA_US,L_US,M_US,N_US,L)
 IMPLICIT NONE
 INTEGER::I,L
 DOUBLE PRECISION,DIMENSION(1:L),INTENT(OUT)::KUS
 DOUBLE PRECISION,DIMENSION(1:L)::KUSN
 DOUBLE PRECISION,DIMENSION(1:L),INTENT(IN)::HEAD,KS,ALPHA_US,L_US,   &
  & M_US,N_US
 DOUBLE PRECISION::HEAD_S
  DO I=1,L
   IF (HEAD(I)>=HEAD_S) THEN
    KUSN(I)=KS(I)
   ELSE
    KUSN(I)=KS(I)*(1-((ABS(ALPHA_US(I)*HEAD(I))**(M_US(I)*N_US(I)))   &
     & *((1+(ABS(ALPHA_US(I)*HEAD(I))**(N_US(I))))**(-M_US(I)))))**2  &
     & /(1+(ABS(ALPHA_US(I)*HEAD(I))**(N_US(I))))**(M_US(I)*L_US(I))
   END IF
  END DO
  DO I=1,L-1
   KUS(I)=(KUSN(I)+KUSN(I+1))*0.5
  END DO
  I=L
   KUS(I)=KUSN(I)
END SUBROUTINE KUNSAT
!
! Calculate flux at the nodes and internodes with Darcy's Law.
SUBROUTINE DARCY(FLUX,KUS,KS,HEAD,HEAD_S,L,DZ)
 IMPLICIT NONE
 INTEGER::I,L
 DOUBLE PRECISION,DIMENSION(1:L),INTENT(IN)::KUS,KS,HEAD
 DOUBLE PRECISION,DIMENSION(1:L),INTENT(OUT)::FLUX
 DOUBLE PRECISION::DZ,HEAD_S
  DO I=1,L-1
   IF ((HEAD(I+1)>HEAD_S) .AND. (HEAD(I)>HEAD_S)) THEN
    FLUX(I)=KUS(I)
   ELSE IF (HEAD(I+1)>HEAD_S) THEN
    FLUX(I)=-KUS(I)*(-1+((HEAD_S-HEAD(I))/DZ))
   ELSE IF (HEAD(I)>HEAD_S) THEN
    FLUX(I)=-KUS(I)*(-1+((HEAD(I+1)-HEAD_S)/DZ))
   ELSE
```

```
    FLUX(I)=-KUS(I)*(-1+((HEAD(I+1)-HEAD(I))/DZ))
   END IF
  END DO
  I=L
   FLUX(I)=KUS(I)
END SUBROUTINE DARCY
!
! Calculate soil water capacity
SUBROUTINE SWCAP(SWC,HEAD,HEAD_S,HEAD_MAX,THETA_S,THETA_R,ALPHA_US,   &
 & M_US,N_US,L)
 IMPLICIT NONE
 INTEGER::I,L
 DOUBLE PRECISION,DIMENSION(1:L)::HEAD,THETA_S,THETA_R,ALPHA_US,M_US, &
  & N_US
 DOUBLE PRECISION,DIMENSION(1:L)::SWC
 DOUBLE PRECISION::DENOM,NUMER,HEAD_S,HEAD_MAX
  DO I=1,L
   IF (HEAD(I)>=HEAD_S) THEN
    NUMER=-ALPHA_US(I)*M_US(I)*N_US(I)*(THETA_S(I)-THETA_R(I))        &
     & *(1.0+ABS(ALPHA_US(I)*HEAD_MAX)**N_US(I))**(M_US(I)-1)         &
     & *ABS(ALPHA_US(I)*HEAD_MAX)**(N_US(I)-1)
    DENOM=(1+ABS(ALPHA_US(I)*HEAD_MAX)**N_US(I))**(2*M_US(I))
    SWC(I)=ABS(NUMER/DENOM)
   ELSE
   ! SWC is kept positive
    NUMER=-ALPHA_US(I)*M_US(I)*N_US(I)*(THETA_S(I)-THETA_R(I))        &
     & *(1.+ABS(ALPHA_US(I)*HEAD(I))**N_US(I))**(M_US(I)-1)           &
     & *ABS(ALPHA_US(I)*HEAD(I))**(N_US(I)-1)
    DENOM=(1+ABS(ALPHA_US(I)*HEAD(I))**N_US(I))**(2*M_US(I))
    SWC(I)=ABS(NUMER/DENOM)
   END IF
  END DO
END SUBROUTINE SWCAP
!
! Calculate urea hydrolysis
SUBROUTINE HYDROLYSIS(UCONC,UCONC_MM,UCONC_STOP,U_F_TEMP,U_A,         &
 & U_ACT_ENER,GAS,SOILTEMP,BD,U_VMAX,U_KMAX,L,M,HR,HR_END,U_SINK)
 IMPLICIT NONE
 INTEGER::I,J,L,M,HR,HR_END
 DOUBLE PRECISION,DIMENSION(1:L,1:M),INTENT(IN)::UCONC
 DOUBLE PRECISION,DIMENSION(1:HR_END),INTENT(IN)::SOILTEMP
 DOUBLE PRECISION,DIMENSION(2:L-1,2:M-1),INTENT(OUT)::U_SINK
 DOUBLE PRECISION::UCONC_MM,UCONC_STOP,U_F_TEMP,U_A,U_ACT_ENER,GAS,BD
 DOUBLE PRECISION::U_VMAX,U_KMAX
 DOUBLE PRECISION::SLOPE,INTERCEPT
 ! D and W denote depth and width nodes, respectively
 U_F_TEMP=U_A*EXP(-U_ACT_ENER/(GAS*2.3935E-11*(273.0+SOILTEMP(HR))))
  IF (U_F_TEMP>1.0) THEN
   U_F_TEMP=1.0
  END IF
 ! The factor 2.3935E-11 converts the units of the universal gas
 ! constant from erg/mole-K to kcal/mole-K since U_ACT_ENER is reported
 ! in kcal and not ergs.
 ! It is assumed that soil temperature is invariant with depth. Zero
 ! hydrolysis in all boundary nodes
!
  DO I=2,L-1
```

```
   DO J=2,M-1
    IF (UCONC(I,J)<UCONC_MM) THEN
    ! Urea concentration range is suitable for using the Michaelis
    ! -Menten reaction
     U_SINK(I,J)=U_F_TEMP*(BD*U_VMAX*UCONC(I,J))/(U_KMAX+UCONC(I,J))
    ELSE IF (UCONC(I,J)>=UCONC_MM .AND.UCONC(I,J)<UCONC_STOP) THEN
     SLOPE=-(U_VMAX*BD)/(UCONC_STOP-UCONC_MM)
     INTERCEPT=(U_VMAX*BD*UCONC_STOP)/(UCONC_STOP-UCONC_MM)
     U_SINK(I,J)=U_F_TEMP*(SLOPE*UCONC(I,J)+INTERCEPT)
     ! Linear relationship (derived personally) used
    ELSE
     U_SINK(I,J)=0.0
    END IF
   END DO
  END DO
END SUBROUTINE HYDROLYSIS
!
! Calculates conversion of NH4+ to NO3-
SUBROUTINE NITRIFICATION(THETA,HEAD,ACONC,BD,HR, HR_END,L,M,A_SINK1,  &
 & SOILTEMP,N_F_TEMP,N_A,N_ACT_ENER,GAS,N_F_PH,SOIL_PH,N_F_HEAD,      &
 & ACONC_RR,ACONC_STOP,N_K1,N_K0)
 IMPLICIT NONE
 INTEGER::I,J,L,M,HR,HR_END
 DOUBLE PRECISION,DIMENSION(1:L),INTENT(IN)::THETA,HEAD
 DOUBLE PRECISION,DIMENSION(1:L,1:M),INTENT(IN)::ACONC
 DOUBLE PRECISION,DIMENSION(1:HR_END),INTENT(IN)::SOILTEMP
 DOUBLE PRECISION,DIMENSION(2:L-1,2:M-1),INTENT(OUT)::A_SINK1
 DOUBLE PRECISION::N_F_TEMP,N_A,N_ACT_ENER,GAS,N_F_PH,N_F_HEAD,       &
  & SOIL_PH,BD
 DOUBLE PRECISION::ACONC_RR,ACONC_STOP,N_K1,N_K0
 ! Temperature & pH are not varied spatially.
  ! Temperature factor
  N_F_TEMP=N_A*EXP(-N_ACT_ENER/(GAS*2.3935E-11*(273.0+SOILTEMP(HR))))
   IF (N_F_TEMP>1.0) THEN
    N_F_TEMP=1.0
   END IF
  ! pH factor
  IF (SOIL_PH<4.5 .OR. SOIL_PH>10.0) THEN
   N_F_PH=0.0
  ELSE IF (SOIL_PH>=4.5 .AND. SOIL_PH<6.0) THEN
   N_F_PH=0.12
  ELSE IF (SOIL_PH>=6.0 .AND. SOIL_PH<=8.5) THEN
   N_F_PH=0.352*(SOIL_PH-6.0)+0.12
  ELSE
   N_F_PH=-0.40*(SOIL_PH-10.0)+0.40
  END IF
  ! Moisture and NH4+ concentration factors are embedded inside the
  ! DO loop.
  DO I=2,L-1
   IF (HEAD(I)>=-100.0) THEN
    N_F_HEAD=0.01*ABS(HEAD(I))
   ELSE IF (HEAD(I)<-100.0 .AND.HEAD(I)>=-15000.0) THEN
    N_F_HEAD=-0.1673*LOG(ABS(HEAD(I)))+1.6864
   ELSE
    N_F_HEAD=0.0
   END IF
   DO J=2,M-1
```

```
    IF (ACONC(I,J)<ACONC_RR) THEN
     A_SINK1(I,J)=THETA(I)*N_K1*ACONC(I,J)
    ELSE IF (ACONC(I,J)>=ACONC_RR .AND. ACONC(I,J)<(ACONC_STOP       &
     & *(BD/THETA(I)))) THEN
     A_SINK1(I,J)=THETA(I)*N_K0
    ELSE
     A_SINK1(I,J)=0.0
    END IF
     A_SINK1(I,J)=A_SINK1(I,J)*N_F_TEMP*N_F_PH*N_F_HEAD
   END DO
  END DO
END SUBROUTINE NITRIFICATION
!
SUBROUTINE AP_DISP (U_AP_DISP,A_AP_DISP,N_AP_DISP,UDIFF_AQ,ADIFF_AQ, &
 & NDIFF_AQ,LAMBDA_L,POR,THETA_M,FLUX,HEAD,HEAD_4,L)
 INTEGER::I,L
 DOUBLE PRECISION::UDIFF_AQ,ADIFF_AQ,NDIFF_AQ,LAMBDA_L,POR
 DOUBLE PRECISION,DIMENSION(1:L),INTENT(IN)::THETA_M,FLUX,HEAD
 DOUBLE PRECISION::LONG_DISP,UMOL_DIFF,AMOL_DIFF,NMOL_DIFF,HEAD_4
 ! The longitudinal dispersion and moleculer diffusion terms already
 ! include the theta term.
 DOUBLE PRECISION,DIMENSION(1:L)::U_AP_DISP,A_AP_DISP,N_AP_DISP
  DO I=1,L
   UMOL_DIFF=UDIFF_AQ*(THETA_M(I)**4.3)/(POR**2)
   AMOL_DIFF=ADIFF_AQ*(THETA_M(I)**4.3)/(POR**2)
   NMOL_DIFF=NDIFF_AQ*(THETA_M(I)**4.3)/(POR**2)
   LONG_DISP=LAMBDA_L*FLUX(I)
   IF (HEAD(I)<=HEAD_4 .OR. FLUX(I)<=0.0) THEN
    U_AP_DISP(I)=UMOL_DIFF
    A_AP_DISP(I)=AMOL_DIFF
    N_AP_DISP(I)=NMOL_DIFF
   ELSE
    U_AP_DISP(I)=UMOL_DIFF+LONG_DISP
    A_AP_DISP(I)=AMOL_DIFF+LONG_DISP
    N_AP_DISP(I)=NMOL_DIFF+LONG_DISP
   END IF
  END DO
END SUBROUTINE AP_DISP
!
! Calculates time step as function of flux
SUBROUTINE TIMESTEP (PL_TIME,HR,A_AP_DISP,MAX_FLUX,THETA_M,TAU,       &
 & DT_MANT,DT_EXPO,DZ,DT)
 INTEGER::PL_TIME,HR
 DOUBLE PRECISION::MAX_FLUX
 DOUBLE PRECISION,DIMENSION(1:L)::A_AP_DISP,THETA_M
 DOUBLE PRECISION::TAU,DT_MANT,DT_EXPO,DZ
 DOUBLE PRECISION::DT_M,DT_N,DT,MAX_AP_DISP
 ! DT_M: time step based on moisture, DT_N: time step based on solute,
 ! i.e., CFL criteria.  MAX_AP_DISP is actually the maximum apparent
 ! dispersion for ammonium, while A_AP_DISP is the apparent dispersion
 ! for ammonium divided by the moisture content.
  DT_M=DT_MANT*((ABS(MAX_FLUX))**DT_EXPO)/TAU
  ! CFL criterion
  IF (HR<PL_TIME) THEN
   DT=DT_M
  ELSE
  I=1
```

```
    MAX_AP_DISP=(A_AP_DISP(I)/THETA_M(I))
   DO I=2,L
    IF (MAX_AP_DISP<(A_AP_DISP(I)/THETA_M(I))) THEN
     MAX_AP_DISP=A_AP_DISP(I)/THETA_M(I)
    END IF
   END DO
   DT_N=(DZ**2)/(2*MAX_AP_DISP*TAU)
   ! The CFL factor always remains at 0.8
    IF (DT_N>DT_M) THEN
     DT=DT_M
    ELSE
     DT=DT_N
    END IF
   END IF
   IF (DT<1.0D-6) THEN
    DT=1.0D-6
   ELSE IF (DT>1.0D0) THEN
    DT=1.0D0
   END IF
 END SUBROUTINE TIMESTEP
 !
 ! The following subroutine calculates concentration values
 SUBROUTINE TRIDIAG(X,A_X,B_X,C_X,K_X,N)
  ! A_X: below diagonal; B_X: diagonal; C_X: above diagonal;
  ! and K_X: right hand side coefficients
  INTEGER::CNT,N
  DOUBLE PRECISION,INTENT(IN)::A_X(3:N-1),B_X(2:N-1),C_X(2:N-2),       &
   & K_X(2:N-1)
  DOUBLE PRECISION,INTENT(OUT)::X(2:N-1)
  ! Local variables
  DOUBLE PRECISION,DIMENSION(2:N-1)::BETA,GAM
   ! To calculate beta and gamma (gam)
   CNT=2
    BETA(CNT)=B_X(CNT)
    GAM(CNT)=K_X(CNT)/BETA(CNT)
   DO CNT=3,N-1
    BETA(CNT)=B_X(CNT)-(A_X(CNT)*C_X(CNT-1)/BETA(CNT-1))
    GAM(CNT)=((K_X(CNT)-A_X(CNT)*GAM(CNT-1))/BETA(CNT))
   END DO
   ! To calculate head values
   CNT=N-1
    X(CNT)=GAM(CNT)
    DO CNT=N-2,2,-1
     X(CNT)=GAM(CNT)-(C_X(CNT)*X(CNT+1)/BETA(CNT))
    END DO
 END SUBROUTINE TRIDIAG

 ! The following subroutine calculates head values
 SUBROUTINE TRIDIAG_M(Y,A_Y,B_Y,C_Y,K_Y,P)
  IMPLICIT NONE
  ! A_Y: below diagonal; B_Y: diagonal; C_Y: above diagonal;
  ! and K_Y: right hand side coefficients
  INTEGER::CMT,P
  DOUBLE PRECISION,INTENT(IN)::A_Y(2:P),B_Y(1:P),C_Y(1:P-1),K_Y(1:P)
  DOUBLE PRECISION,INTENT(OUT)::Y(1:P)
  ! Local variables
  DOUBLE PRECISION,DIMENSION(1:P)::BETA,GAM
```

```
 ! To calculate beta and gamma (gam)
  CMT=1
   BETA(CMT)=B_Y(CMT)
   GAM(CMT)=K_Y(CMT)/BETA(CMT)
  DO CMT=2,P
   BETA(CMT)=B_Y(CMT)-(A_Y(CMT)*C_Y(CMT-1)/BETA(CMT-1))
   GAM(CMT)=((K_Y(CMT)-A_Y(CMT)*GAM(CMT-1))/BETA(CMT))
  END DO
  ! To calculate head values
  CMT=P
   Y(CMT)=GAM(CMT)
   DO CMT=P-1,1,-1
    Y(CMT)=GAM(CMT)-(C_Y(CMT)*Y(CMT+1)/BETA(CMT))
   END DO
END SUBROUTINE TRIDIAG_M
!
SUBROUTINE TRIDIAG_N(Z,A_Z,B_Z,C_Z,K_Z,Q)
 ! A_X: below diagonal; B_X: diagonal; C_X: above diagonal;
 ! and K_X: right hand side coefficients
 INTEGER::CNT,Q
 DOUBLE PRECISION,INTENT(IN)::A_Z(3:Q),B_Z(2:Q),C_Z(2:Q-1),K_Z(2:Q)
 DOUBLE PRECISION,INTENT(OUT)::Z(2:Q)
 ! Local variables
 DOUBLE PRECISION,DIMENSION(2:Q)::BETA,GAM
 ! To calculate beta and gamma (gam)
  CNT=2
   BETA(CNT)=B_Z(CNT)
   GAM(CNT)=K_Z(CNT)/BETA(CNT)
  DO CNT=3,Q
   BETA(CNT)=B_Z(CNT)-(A_Z(CNT)*C_Z(CNT-1)/BETA(CNT-1))
   GAM(CNT)=((K_Z(CNT)-A_Z(CNT)*GAM(CNT-1))/BETA(CNT))
  END DO
 ! To calculate head values
  CNT=Q
   Z(CNT)=GAM(CNT)
   DO CNT=Q-1,2,-1
    Z(CNT)=GAM(CNT)-(C_Z(CNT)*Z(CNT+1)/BETA(CNT))
   END DO
END SUBROUTINE TRIDIAG_N
END PROGRAM MAIN
```

VITA

Sanjay was born to Sushila and Kishorendra Bikram Shah on October 10, 1960 in Birganj, Nepal. He did his schooling in Patna (India) and Birganj. He did his junior college in Kathmandu, Nepal. He obtained his B. Tech. (Agric. Engineering) from Punjab Agricultural University, India in 1985. He worked for more than eight years in the area of agricultural machinery design with Agricultural Tools Factory, Birganj, Nepal. He obtained his M.S. (BAE) from LSU in the summer of 1995, before starting his PhD in Virginia Tech in the fall of 1995. While doing his PhD in Virginia Tech, Sanjay was also involved in the development of Total Maximum Daily Load for fecal coliform for a number of watersheds in Virginia. Immediately after finishing his PhD in 2000, Sanjay joined West Virginia University as extension specialist. Sanjay is married to Banu and they have two children, son Shashant (11 years) and daughter Shivani (3 years).